https://doi.org/10.15388/vu.thesis.397
https://orcid.org/0000-0001-8950-590X

VILNIUS UNIVERSITY

Rūta Zinkevičiūtė

Proteomic analysis of recombinant protein synthesis in yeast *Saccharomyces cerevisiae*

DOCTORAL DISSERTATION

Natural Sciences,
Biochemistry (N 004)

VILNIUS 2022

The dissertation was prepared between 2014 and 2018 at the Institute of Biotechnology, Vilnius University. The research was supported by EU structural funds projects (VP1-3.1-ŠMM-07-K-02-038; J05-LVPA-K-01-0128). Attendance at the 43rd FEBS Congress (2018 07 07-12) was financed by receiving the FEBS Bursary Grant.

The dissertation is defended on an external basis.

Academic consultant – Dr. Rimantas Slibinskas (Vilnius University, Natural Sciences, Biochemistry, N 004).

This doctoral dissertation will be defended in a public meeting of the Dissertation Defence Panel:

Chairman – Prof. Dr. Rolandas Meškys (Vilnius University, Natural Sciences, Biochemistry, N 004).

Members:

Dr. Rūta Gerasimaitė (Max Planck Institute, Natural Sciences, Biochemistry, N 004),

Prof. Dr. Eglė Lastauskienė (Vilnius University, Natural Sciences, Biology, N 010),

Prof. Dr. Saulius Serva (Vilnius University, Natural Sciences, Biochemistry, N 004),

Dr. Mindaugas Valius (Vilnius University, Natural Sciences, Biochemistry, N 004).

The dissertation shall be defended at a public meeting of the Dissertation Defence Panel at 14.00 / on 18th November 2022 in Room R – 401 of the Life Sciences Centre (Vilnius University).

Address: Saulėtekio av. 7, LT-10257 Vilnius, Lithuania.

The text of this dissertation can be accessed at the libraries of Vilnius University, as well as on the website of Vilnius University:

www.vu.lt/lt/naujienos/ivykiu-kalendorius

https://doi.org/10.15388/vu.thesis.397
https://orcid.org/ 0000-0001-8950-590X

VILNIAUS UNIVERSITETAS

Rūta Zinkevičiūtė

Proteominės analizės pritaikymas rekombinantinių baltymų sintezės tyrimams mielėse *Saccharomyces cerevisiae*

DAKTARO DISERTACIJA

Gamtos mokslai,
biochemija (N 004)

VILNIUS 2022

Disertacija rengta 2014–2018 metais Vilniaus universiteto Biotechnologijos institute. Mokslinius tyrimus rėmė ES struktūrinių fondų projektai (VP1-3.1-ŠMM-07-K-02-038; J05-LVPA-K-01-0128). Dalyvavimas 43-iąjame FEBS kongrese (2018 07 07-12) finansuotas FEBS stipendijų dotacija.

Disertacija ginama eksternu.

Mokslinis konsultantas – **dr. Rimantas Slibinskas** (Vilniaus universitetas, gamtos mokslai, biochemija, N 004).

Gynimo taryba:

Pirmininkas – **prof. dr. Rolandas Meškys** (Vilniaus universitetas, gamtos mokslai, biochemija, N 004).

Nariai:

dr. Rūta Gerasimaitė (Max Planck institutas, gamtos mokslai, biochemija - N 004);

prof. dr. Eglė Lastauskienė (Vilniaus universitetas, gamtos mokslai, biologija, N 010);

prof. dr. Saulius Serva (Vilniaus universitetas, gamtos mokslai, biochemija, N 004);

dr. Mindaugas Valius (Vilniaus universitetas, gamtos mokslai, biochemija, N 004).

Disertacija ginama viešame Gynimo tarybos posėdyje 2022 m. Lapkričio mėn. 18 d. 14 val. Gyvybės mokslų centro (Vilniaus universitetas) R – 401 auditorijoje.

Adresas: Saulėtekio al. 7 LT-10257 Vilnius, Lietuva.

Disertaciją galima peržiūrėti Vilniaus universiteto bibliotekoje ir VU interneto svetainėje adresu:

https://www.vu.lt/naujienos/ivykiu-kalendorius

CONTENTS

LIST OF ABBREVIATIONS

2DE	two-dimensional electrophoresis
MS	mass spectrometry
MeV	Measles virus
MeH	Measles hemagglutinin protein
MeN	Measles nucleocapsid protein
CA	carrier ampholyte
NEPHGE	non-equilibrium pH gradient electrophoresis
IPG	immobilized pH gradient
CALR	human calreticulin protein
UPR-Cyto	cytosolic unfolded protein response
IEF	isoelectric focusing
LC	liquid chromatography
LC-MSE	liquid chromatography/mass spectrometry in a data-independent acquisition mode
PTMs	posttranslational modifications
SDS	sodium dodecyl sulphate
SDS-PAGE	SDS-polyacrylamide gel electrophoresis
HPLC	high-performance liquid chromatography
DIGE	differential gel electrophoresis
SCX	strong cation exchange
SEC	size exclusion chromatography
DRC	dynamic range compression
MW	molecular weight
TCA	trichloroacetic acid
PDA	piperazine di-acrylamide
DTT	dithiothreitol
IOA	iodoacetamide
APS	ammonium persulfate
TEMED	tetramethyl ethylenediamine
MDLC	multidimensional LC
AC	affinity chromatography
IEX	ion exchange chromatography
CEX	cation exchange chromatography
AEX	anion exchange chromatography
SAX	strong anion exchange chromatography
RP	reverse phase chromatography
UPLC	ultra-performance LC
MALDI	matrix-assisted lased desorption/ionisation

ESI	electrospray ionisation
TOF	time-of-flight
RF	radio frequency
CID	collision induced dissociation
ECD	electron capture dissociation
EDT	electron transfer dissociation
Q	quadrupole
FT-ICR	Fourrier-transform ion cyclotron resonance
LIT	linear ion trap
QIT	quadrupole ion trap
PMF	peptide mass fingerprinting
FDR	false discovery rate
CCD	charge-coupled device
FC	fold change
AUC	area under the curve
GRAS	generally regarded as safe
ER	endoplasmic reticulum
UPR	unfolded protein response
ERAD	ER-associated degradation
ROS	reactive oxygen species
HSF	heat shock factor
Hsps	heat shock proteins
HSR	heat shock response
HOG	high-osmolarity glycerol pathway
MAPK	mitogen-activated protein kinase pathway
GPI	glycosylphosphatidylinositol
H	hemagglutinin protein
F	fusion protein
TRAM	translocating chain-associating membrane protein
TRAP	translocon-associated protein complex
ICD	immunogenic cell death
SNARE	N-ethylmaleimide-sensitive fusion protein-attachment protein receptor
RE	restriction endonucleases
HRP	horseradish peroxidase
ACN	acetonitrile
TFA	trifluoracetic acid
DIA	data-independent acquisition
IMS	ion mobility separation
SGD	*Saccharomyces cerevisiae* genome database

YPD	Yeast protein database
AIF	anodic isoelectric focusing
CIF	cathodic isoelectric focusing
DCW	dry cell weight
OD	optical density
CCR	carbon catabolite de-repression

INTRODUCTION

Saccharomyces cerevisiae is one of the most frequently used organisms for heterologous protein biosynthesis, as it is one of the most well studied eukaryotic organisms (Duina et al., 2014). Yeast cultivation is easy and inexpensive and there is an array of convenient molecular tools for uncomplicated genetic manipulations (Mattanovich et al., 2012; Porro et al., 2011). Important biopharmaceutical proteins like Hepatitis subunit vaccines (McAleer et al., 1984), hirudin (Bischoff et al., 1989), insulin (Thim et al., 1986), platelet-derived growth factor (Finnis et al., 1992), urate oxidase (Leplatois et al., 1992), macrophage colony-stimulating factor (Price et al., 1987) are all made in *S. cerevisiae*.

However, there are still bottlenecks, like incorrect glycosylation pattern, low protein yield and acute cellular stress (Mattanovich et al., 2004, 2012), preventing the successful production of a wider array of proteins. To troubleshoot the obstacles that stand in the way of efficient protein production a deeper analysis into the cellular proteome is needed. Unfortunately, the impact of recombinant protein synthesis on the yeast cell is scarcely studied. Such research would help us identify the reasons behind unsuccessful or, on the contrary, outstanding synthesis of recombinant proteins. This information can be used to engineer improved yeast strains or to determine the synthesis bottlenecks and overcome them. Proteomic analysis is a powerful tool to perform such research, as it directly gives us information about the fold change and abundance of the cellular proteins that are the acting molecules in the synthesis of heterologous proteins. Proteomic analysis using two-dimensional electrophoresis (2DE), is a robust, fast and inexpensive method to gain information on the major changes in the proteomes of the studied cells. Additional mass spectrometry (MS)-based analysis techniques help to enrich the data by identifying proteins with differential synthesis patterns, or by analysing the whole protein complement of the cell, to distinguish small changes in the proteomes.

The aim of this work was:

To adapt 2DE- and MS-based proteomic analysis to study the recombinant protein synthesis in yeast *S. cerevisiae*.

The objectives of this study were:

1. To choose the best-performing 2DE method for proteomic analysis of yeast *S. cerevisiae* cellular proteome in a wide pH range (pH 3–10).
2. To find yeast cell culture growth conditions that improve the translocation of Measles virus hemagglutinin (MeH) protein; identify involved cellular proteins by comparative proteomic analysis.
3. Restore the composition of carrier ampholytes (CA) for the first-dimension of non-equilibrium pH gradient electrophoresis (NEPHGE)-based 2DE and compare it to the formerly commercially available gels.
4. To analyse the impact of efficient human calreticulin (CALR) protein secretion on yeast *S. cerevisiae* cellular proteome.

Scientific novelty

In this work, for the first time Immobilized pH gradient (IPG)- and NEPHGE- based 2DE methods were compared, and NEPHGE-based method is suggested as the more suitable one for the proteomic analysis of yeast proteome. We were also able to improve the inefficient translocation of MeH protein precursors to the ER and increase the amount of glycosylated protein ~3-fold. The NEPHGE-based 2DE analysis of cells producing MeH after the heat-shock, revealed 15 cellular protein-targets for further engineering of yeast strains with improved translocation to the ER, or even reduced cytosolic Unfolded Protein Response (UPR-Cyto). Here we also present a restored CA composition for NEPHGE-based first-dimension gels that can be used instead of the no longer commercially available. The composition of commercial gels was never made public and the original recipe for NEPHGE-based isoelectric focusing (IEF) was published in 1995 by (Klose & Kobalz, 1995), with the CAs used now being discontinued. All of these obstacles made the restoration more difficult, and our published composition the more important and novel. Lastly, we report an extremely efficient secretion (140 mg/L) of human CALR protein from yeast *S. cerevisiae.* Interestingly, 2DE- and liquid chromatography/mass spectrometry in a data-independent mode (LC-MS^E)-based quantitative analysis of CALR-secreting versus control yeast cells harbouring an empty vector, revealed no induction of cellular stress or secretory pathway proteins. It is highly irregular that such an efficient secretion affects the cellular proteome so little, this suggests that it may depend on the nature of the protein itself and gives us a background for further studies on successful secretion from yeast *S. cerevisiae*.

Practical value

Since we show that NEPHGE-based 2DE is preferable for yeast proteome analysis, and the solutions for this method are commercially unavailable, our published CA mix composition is of high value for the holders of the apparatus for NEPHGE-based IEF. Our determined conditions for more efficient MeH translocation and the identified protein-targets is generally important knowledge for the production of viral surface glycoproteins that are used in subunit vaccines in recent years (Gebauer et al., 2019; Lin et al., 2012; Zhang et al., 2019). Since the secretion mechanism of human CALR from healthy mammalian cells is elusive, our results from yeast suggest that it may be easily secreted not because of a distinct mechanism, but rather because of its intrinsic properties. Our reported proteomic data on efficient secretion of CALR is also important from a biotechnological standing point, for stress-free high-level production of human proteins in yeast.

The major findings presented for defence in this thesis:

1. NEPHGE-based 2DE is the preferred method for yeast whole proteome analysis in a wide pH range (pH 3–10). IPG 3–10 (Invitrogen) 2DE method is reliable only in the analysis of acidic proteins, because in the basic side of 2D gels the results are not reproducible; meanwhile, NEPHGE method is suitable in the entire pI range and especially efficient for the analysis of basic proteins.
2. MeH glycoprotein amount and translocation efficiency increase about 3-fold when heat shock is applied at higher cell culture densities and followed by protein synthesis at 37 °C. Comparative proteomic analysis revealed 15 cellular proteins with differential synthesis that are possibly associated with the improved translocation of MeH.
3. The restored CA mix for NEPHGE-based first-dimension separation of proteins has better reproducibility and can be used instead of the no longer commercially available.
4. High-level CALR secretion has limited impact on the yeast cellular proteome, does not burden the secretory machinery and does not cause any apparent cellular stress. It only slightly impacts the biosynthesis of ribosome constituents involved in protein translation.

1. LITERATURE OVERVIEW

1.1. Proteomics

Proteomics is the systematic, large-scale analysis of proteomes. A proteome is a complete set of proteins produced by a given cell, tissue, or organism. It is described either as a complete proteome – a catalogue of all possible proteins or as a list of proteins produced under a defined set of conditions (Twyman et al., 2013). The term „proteomics“ was first proposed by Wilkins in 1994 and is derived from words *protein* and *genome* (Wilkins, 2009). The development of proteomics was dependant on the first attempts on large-scale DNA sequencing projects and the rise of „omics“ as a term for genomics and its derivatives (transcriptomics, proteomics, metabolomics, phenomics) (Twyman, 2013). Proteins are the actual function molecules of the cell and the most relevant components of a biological system. Protein PTMs and isoforms, as well as expression levels that can vary from mRNA levels, compartmentalisation of gene products, regulation of protein function by proteolysis, recycling and sequestration, protein-protein interactions and cellular structure composition – all can only be determined using proteomic analysis (Pandey & Mann, 2000). This makes proteomics one of the most important tools in modern day research.

The beginning of all protein separation methods started when Tiselius in 1930 suggested an analytical moving boundary method for protein electrophoresis (Tiselius & Uppsala universitet, 1930). In 1956, Smithies and Poulik deduced that single-dimension separations cannot resolve complex protein samples and showed a two-dimensional approach, where proteins were resolved by molecular weight and free solution mobility on starch gel (Smithies & Poulik, 1956). One dimensional protein electrophoresis became widely used by biochemists only when sodium dodecyl-sulphate (SDS) electrophoresis was introduced in the 70s (Laemmli, 1970). Nevertheless, the protein resolution was insufficient and it was clear that a second dimension was needed. At that time (and still today) it was obvious that isoelectric focusing would best complement SDS-polyacrylamide gel electrophoresis (SDS-PAGE) separation method (Rabilloud et al., 2010). There was a successful attempt in a method coupling like this, but it did not get a lot of attention due to „empty“ gels lacking spots and sample inclusion in the IEF gel, which was a complex process (MacGillivray & Rickwood, 1974). Then, in 1975 O'Farrell and independently at the same time Klose, introduced IEF and SDS-PAGE based 2DE techniques for separating cellular proteins under denaturing conditions. These techniques had detailed protocols, sample loading on top of carrier-ampholyte based IEF gels and autoradiographic

detection, which allowed to detect hundreds of spots in the same gel (Klose, 1975; O'Farrell, 1975). In 1977 Anderson & Anderson used 2DE for the analysis of human plasma and detected approximately 300 spots (Anderson & Anderson, 1977). This was the first 2DE application for clinical biology and in a short period of time, 2DE took off with applications to cell biology (Bravo & Celis, 1980; Garrels, 1979) and the creation of the predecessor of human genome project (Taylor et al., 1982). Although 2DE techniques created by O'Farrell and Klose were widely used, they were quite arduous. The IEF gels had to be cast in-laboratory, which often led to length variations and irreproducibility and the carrier-ampholytes were generally unstable and prone to cathodic drift (See chapter 1.2.1.) (Issaq & Veenstra, 2008). Then in 1982 Bjellqvist and colleagues introduced IEF gels with immobilized pH gradients, that increased reproducibility, did not have a cathodic drift and were easy to use (Bjellqvist et al., 1982). Soon after, there was a stable protocol and the method was commercialised (Görg et al., 1988), which simplified and broadened its use in science and led to interlaboratory studies (Blomberg et al., 1995; Corbett et al., 1994).

The real breakthrough for proteomics came with the emergence of mass-spectrometry based methods. Compared to Edman sequencing, MS requires a lesser amount of sample and shortens the analysis time from days to hours, provides higher sensitivity and throughput (Pandey & Mann, 2000). Combination of protein separation by 2DE and MS led to creation of various 2DE maps and databases (Büttner et al., 2001; Shaw et al., 1999). But after a substantial accumulation of data from similar strategy proteomics work, it was clear that some types of proteins are found over and over again, and some are always missing (low abundance, hydrophobic) (Corthals et al., 2000). These dynamic range (i.e., quantitative ratio between the rarest protein in the sample versus the most abundant) limitations were applicable not only to 2DE, but to MS also.

A standard proteomic analysis includes the separation of complex protein samples (See 1.2.), the identification of separate components (See 1.3.) and their systematic quantitative and/or comparative analysis (See1.4.) (Twyman, 2013).

1.2. Separation of complex protein samples

In this next chapter of literature overview, two of the most used protein separation methods – 2DE and LC will be presented. Because this work is based mainly on 2DE method, principles of 2DE will be described in greater detail. LC was used in tandem with MS only, but a short overview of the main

usages of this method will be described also. Although there are, other protein separation methods like MudPit, protein chips, capillary electrophoresis and etc., they will not be included in this dissertation, albeit are no less worthy of mention.

1.2.1. Principles of 2DE

Electrophoresis is a process when charged molecules migrate in the electric field. The migration rate depends on the ratio of molecule charge density, its mass and the strength of the electric field. Electrophoretic methods exploit the fact that differently charged molecules have different electrophoretic mobility. Proteins are charged molecules and are amphoteric in their nature – they have acidic $-COO^-$ and alkaline $-NH_3^+$ groups on their surface. Because of this property they can adsorb anions in an alkaline, or cations in an acidic pH of the solution. The pH of a solution at which protein molecules have a neutral charge is called the isoelectric point (pI). The pI value varies depending on the protein charge – the sum charge of all positively and negatively charged amino acid side chains - and the spatial form of a protein. When the pH of the solution coincides with the pI of the protein it no longer can migrate in the electric field because its charge is neutralized by ions in the solution. This property is exploited to separate proteins according to their pI and is called IEF (Dennison, 2002; Twyman et al., 2013).

The discussed properties are used to separate proteins in two dimensions in 2DE using two orthogonal separation techniques. Usually, IEF separation in the first-dimension and charge/mass ratio dependent SDS-PAGE in the second-dimension.

Electrophoretic separations that are discussed in this dissertation are all performed in polyacrylamide gels rather than in free solution. Polyacrylamide (PAA) gel electrophoresis facilitates protein separation depending on their mass by sieving through porous gel as they migrate in an electric field. Diverse pore size can be achieved by varying the concentrations of acrylamide which is a monomer gelling agent and bis-acrylamide which is the cross-linking agent, generating polyacrylamide. Other cross-linking agents can be used to improve gel properties, especially in the case of IEF gels. PDA (Piperazine di-acrylamide) increases resolution and strength of IEF gels (Gravel, 2002) and DATD (*N,N'*-diallyltartardiamine) that increases pore size in IEF gels where molecular sieving can be a problem (Kelkar et al., 1986).

1.2.2. Sample preparation for 2DE

1.2.2.1. Sample prefractionation

Protein samples from any organism contain a myriad of different proteins with different properties, so there is no universal sample preparation protocol that would fit all the proteins. Usually more abundant proteins dominate the sample and low-abundancy and hydrophobic proteins are underrepresented. One way to analyse a more specific group of proteins is to reduce the sample complexity by prefractionation. Sample prefractionation can be performed either in cellular, subcellular or protein levels. Generally, cellular fractionation is the approach to screen the whole proteome (Magdeldin et al., 2014). Subcellular fractionation is performed by density centrifugation of cell/tissue homogenate (Boisvert et al., 2010) and subsequent usage of selective solvents to dissolve ER-Golgi, mitochondrial or nuclear proteins (Cascio et al., 2011). Pre-fractionation on a protein level is usually performed based on protein physio-chemical properties, for example by their charge using strong cation exchange (SCX) chromatography (Molloy et al., 1998) or by their size using size exclusion chromatography (SEC) (Tantipaiboonwong et al., 2005). Pre-fractionation can be used to enrich samples (low abundance proteins) or to deplete samples (major high abundance proteins, for example albumin or haemoglobin in blood). Depletion of major sample proteins results in higher resolution, better separation and higher protein load (Magdeldin et al., 2014) or so called Dynamic range compression (DRC) (Griffin & Bandhakavi, 2011). In mass spectrometry high-abundant peptides mask the rarer ones, so sample depletion increases the chances of detecting very low-abundant proteins (Fountoulakis et al., 1999; Karlsson et al., 1999).

1.2.2.1.1. Sample buffer

The second important part of sample preparation for 2DE is to covert the sample to a suitable physiochemical state for IEF and retaining the charge and MW of the proteins in the sample. Usually this means that the proteins need to be solubilised, disaggregated, denatured and reduced. The procedures, of course, depend on the aim of the experiment. If there is a need to separate soluble aggregates, the sample must be prepared under non-denaturing non-reducing conditions (Shaw & Riederer, 2003). This can be achieved by using non-denaturing detergents Triton X-100 and *N*-dodecyl-β-D-maltoside (Jackowski & Pielucha, 2001). Although, the aim of most 2DE-based experiments are set to resolve as many proteins as possible, and for that it is preferable to perform IEF under denaturing and reducing conditions (Shaw & Riederer, 2003).

To properly prepare protein sample it is necessary to choose the right sample buffer that will maintain the solubility of the proteins and will not impact their pI. Usually sample buffer for IEF contains: high concentration of protein denaturing urea that disrupts noncovalent and ionic bonds among amino acid residues (Klose, 1975; O'Farrell, 1975); thiourea that increases solubility of proteins (Rabilloud et al., 1997); non-ionic (Triton X-100) or zwitterionic detergents (CHAPS, SB3-10, ASB-14, NP-40) that disrupt hydrophobic bonds and increases protein solubility, as well as maintains them in the solution during IEF (O'Farrell et al., 1977; Rabilloud, 2009); reducing agents that disrupt disulfide bonds (DTT, DTE, TBP); ampholytes that also increase protein solubility and helps to maintain the pH gradient (are chosen depending on the pH range of the gel, for example pH 3–10, pH 4–7) (Garfin, 2003). Although, the denaturing properties of most sample buffers are enough to supress proteolysis, sometimes the addition of protease inhibitors is recommended, especially during lengthy sample manipulations (Olivieri et al., 2001; Shaw & Riederer, 2003). Protease inhibitors are usually sold in cocktails and should be used according to manufacturer 's recommendations.

1.2.2.1.2. Cell/tissue disruption methods

Another part of sample preparation is the disruption of the cells or tissue. The disruption method heavily depends on the type of cells/tissue. For easily lysed cells (mammalian cell culture, blood, some microorganisms) soft lysis methods are applied: osmotic lysis (Bohring & Krause, 1999), lysis by freeze-thaw cycles, detergent (Portig et al., 1996) and enzymatic lysis (Salazar, 2008). For cells that are hard to disrupt (hard tissue, yeast, bacteria) strong lysis methods are used: disruption by sonication (Harder et al., 1999), French Pressure Cell (Cull & McHenry, 1990), grinding after freezing in liquid nitrogen (Davidsen, 1995), mechanical homogenization (Watarai et al., 2000), homogenization with glass beads (Nandakumar & Marten, 2002; Posch, 2014). Protease inhibitor cocktails are also added to the disruption buffer – if other than sample buffer is used.

1.2.2.1.3. Sample clean-up

After disruption of cells/tissues and the release of protein complement into the buffer it is important to remove any impurities that can interfere with 2DE. Impurities in the sample causes 2D gel streakiness, longer separation time, poor separation, increased electrical conductivity and protein modifications. To obtain high resolution it is necessary to remove as much of impurities as possible: perform dialysis of gel filtration for charge bearing

salts (NaCl, KCl), buffer components (Tris, PBS), nucleotides; precipitate sample with acetone or add a detergent (to a ratio of 1:5–1:8 SDS to detergent) to reduce the effect of SDS; apply DNase or disrupt sample by ultrasound to remove negatively charged DNA; centrifuge at high speed to pellet insoluble particles and aspirate purified sample. One of the most efficient ways to clean the sample from all contaminants is to precipitate proteins. This concentrates the proteins in the sample, inhibits proteases irreversibly, dismantles protein complexes, removes endogenous peptides (important for DIGE). The most common precipitation procedures are: precipitation by chloroform/methanol, acetone, TCA/acetone and TCA (Rabilloud, 1996). However, the best method for protein precipitation depends on the cell type, for example chloroform/methanol and acetone precipitation showed best protein recovery in preparing rat brain samples (Fic et al., 2010) and 20% TCA/acetone precipitation showed best results in preparing samples from liverworts (Yadav et al., 2020) as well as human plasma (Jiang et al., 2004). Commercial 2D clean-up kits are available from various manufacturers that employ the best properties of various precipitation methods and ensure high efficiency impurity removal from samples (Cytiva, Sigma-Aldrich, Bio-Rad). If precipitation was the method of choice for sample clean-up, the protein pellets need to be solubilized in sample buffer and the protein concentration determined. In the case of IPG strips (See 1.2.2.) sample buffer is usually used for strip rehydration also.

1.2.3. IEF for first dimension separation

During the process of IEF proteins are separated by their charge regardless of their mass. Electrophoresis is carried out in a pH gradient where proteins migrate to the pH value where they have no net charge – the pI. During the protein migration through the pH gradient, the charge density of the protein decreases as it moves towards its pI. When a protein reaches its pI the electrophoretic mobility stops, because net charge of the protein becomes zero. If a focused protein diffuses from its pI position, it instantly gains charge and moves back to its focus. The resolution of this separation system depends on the strength of the electrical field and the continuity of the pH gradient. That is why IEF is performed at high voltage (above 1000 V) and when the proteins are focused, then there is no ionic motion left in the system, the final current is very low (in the limits of microamperes).

There are two ways a pH gradient for IEF can be established. The original method (Klose, 1975; O'Farrell, 1975) was to form the pH gradient in a tube gel by using carrier-ampholytes – small, soluble amphoteric

molecules (synthetic peptides) characteristic for strong buffering properties at their pI. Initially, the ampholytes are evenly distributed and there is no pH gradient. With the application of electric field, the ampholytes themselves are subjected to electrophoresis – the acidic ampholytes move towards the anode, the alkaline ampholytes move towards the cathode and all the intermediate form a gradient in between, at their pI values. The system reaches equilibrium defined by a continuous gradient before the slow-moving proteins start to migrate to their pI. One of the major limitations of this approach is cathodic drift – when ampholytes migrate to the cathode due to electro-osmotic flow (bulk solvent flow towards the cathode) (Dennison, 2002; Twyman et al., 2013).

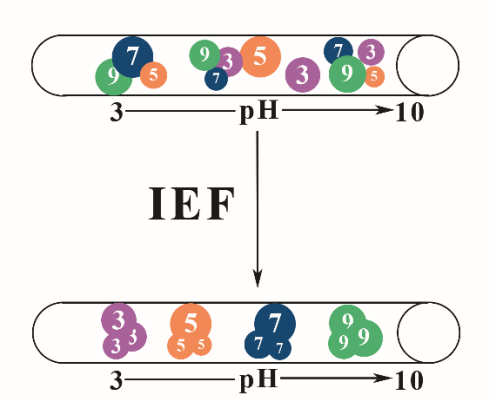

Figure 1. A schematic representation of protein separation during the process of isoelectric focusing.

1.2.3.1. NEPHGE

NEPHGE method addressed cathodic drift (O'Farrell et al., 1977) by switching the sides of sample application – applying it at the acidic end of the tube gel, rather that basic (Klose, 1975), so that all proteins in a sample are positively charged in the starting point of the run. Using this approach for IEF running time is of the essence, as if run too long the basic proteins and ampholytes would run off the end of the gel. So, the principle is to not allow the system to reach equilibrium and rather separate proteins in a rapidly forming pH gradient. The time of the electrophoresis determines the protein distribution (O'Farrell et al., 1977). NEPHGE gels are manually cast by the user in a cylindrical mold and usually are acrylamide gels cross-linked with PDA. This increases the strength of slim and frail gels. The main drawbacks of this methods are the irregular nature of ampholytes - due to their complicated manufacturing technology and the difficulty of the method itself.

This is a labour-intensive approach that needs to be mastered. Despite these disadvantages, an updated protocol for NEPHGE-based first-dimension separation was proposed (Klose & Kobalz, 1995) and later, a commercialised version of the apparatus and the solutions were manufactured and distributed by WITA GMBH called „Witavision“ (Wittmann-Liebold et al., 2006). Unfortunately, WITA GMBH has ceased their operations and left all the owners of their apparatus without the commercially available supply of solutions. Although, NEPHGE method is not broadly used, its capability to resolve basic protein spots – which poses a well-known problem for in-gel separation – made it instrumental for protein separation in broad (See Results 3.1.) as well as highly basic (Bjarnadóttir & Flengsrud, 2014; Kreipke et al., 2007) pH range.

1.2.3.2. IPG

The second manner in which a pH gradient for IEF can be established is by using IPG (Bjellqvist et al., 1982). IPG is made of an array of non-amphoteric molecules called Immobilines that on one end contain a weak acidic or basic group and an acrylic double bond on another to aid immobilization. When the gel is run, proteins migrate to their pI, but the pH gradient remain stable even if the gel is run for a long time. Carrier ampholytes are also often added to IPG gel buffer to prevent unproductive interactions between proteins and Immobilines and to increase protein solubility. If this is not addressed – proteins can form insoluble artifacts and precipitate, especially in the basic region of the gel (Twyman et al., 2013). IPG is a simple and user-friendly – pre-made dehydrated gels that are easy to use and widely available for purchase from several manufacturers differing in length and pH range (narrow (pH 4–7) or broad (pH 3–10)). High reproducibility and easy use made IPG strips one of the most used approaches for the first-dimension separation of 2DE (Görg et al., 2009).

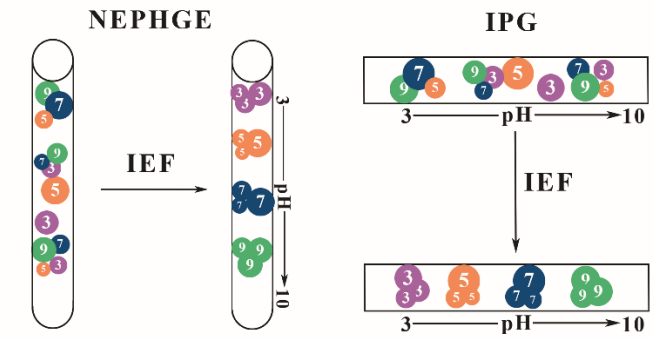

Figure 2. A schematic representation of NEPHGE and IPG isoelectric focusing methods.

1.2.3.3. Equilibration of first-dimension gels

After separating proteins in the first-dimension, the IEF gels need to be equilibrated for second-dimension. Equilibration is necessary after both IPG and NEPHGE IEF separations. The gels need to be incubated firstly in equilibration solution with 3% SDS supplemented with DTT (dithiothreitol) and secondly supplemented with IOA (iodoacetamide). This procedure not only ensures uniform charge density, but also reduces and alkylates disulphide bonds of separated proteins which ensures protein denaturation (Görg et al., 2009; Klose & Kobalz, 1995). Despite that alkylation slightly increases the molecular weight of proteins that contain a lot of disulphide bridges, it also binds to residual DTT and reduces artifact streaks that can appear when dyeing gels with silver.

1.2.4. SDS-PAGE for second-dimension separation

The second-dimension separation is usually carried out by standard SDS-PAGE (sodium dodecylsulfate polyacrylamide gel electrophoresis) where proteins are separated by their molecular mass. The principle of this technique is to denature the proteins with the anionic detergent sodium dodecylsulfate (SDS) which binds stoichiometrically to the peptide backbone (1.4 g SDS per 1 g peptide (Reynolds & Tanford, 1970)) and distributes a uniform negative charge. The presence of SDS molecules minimizes the intrinsic charge of proteins as stoichiometrically larger proteins attach more SDS molecules than smaller proteins. This ensures that proteins are separated by their mass alone, because all polypeptide/SDS complexes have the same charge density and the mass differences between proteins are maintained (Shapiro et al., 1967).

Usually, SDS-PAGE for a second-dimension separation is performed using slab PAA gels in a vertical electrophoresis system where proteins migrate from top to bottom (from cathode to anode). The separation of proteins by their molecular weight is based not only on their migration speed – smaller proteins migrate faster than bigger - but also on size-dependent sieving by the gel. The sieving depends on the pore size, and the pore size depends on the concentration of the gel (percentage of the gelling agent acrylamide, “%monomer“) and proportion to cross-linking reagent (percentage of bis-acrylamide, „%cross-linker “). Generally, the smallest pore size is achieved when %monomer is ≤ 15% and %cross-linker is 5%. Above this value of %cross-linker monomer molecules become over-linked and form

bundles mixed with large pores in-between. So, the optimal pore size is achieved by varying "%monomer "and „%cross-linker ". Usually, a mixture of monomer and cross-linker (with a ratio of 30:1–40:1) takes-up no more than 0.1% of a polyacrylamide (PAA) gel, the rest is composed of Tris-HCl (tris(hydroxymethyl)aminomethane-HCl) buffer in an aqueous solution. By adding catalysts – ammonium persulfate (APS) (1.5–2.0 mM) and tetramethyl ethylenediamine (TEMED) (0.01–0.1%) polymerization of acrylamide is initiated. For the separation of a wide variety and molecular weight of proteins, like in 2DE, 8–20% PAA concentration separating gel (pH 8.8) is used. Gels with higher PAA concentrations can be tailored to sieve very small proteins in specialised research. Additionally, a concentrating gel (2.6–4%, pH 6.6–6.8) can be used on top of the main separation gel to concentrate all migrating proteins into a single moving band. Proteins concentrate because of the lower pH and this improves protein band/spot resolution (Friedman et al., 2009; Twyman et al., 2013).

The buffering system for SDS-PAGE is usually the Tris-Glycine system described by (Laemmli, 1970). Using this buffer system, proteins are separated in the high pH, when the protein aggregation is minimal and that leads to a clear isolation of protein bands.

The gel thickness varies between 0.5 mm and 1.5 mm, thinner gels cool quicker so they can be run faster and better resolution can be obtained. Thicker gels are more structurally stable, but are harder to stain and must be run slower (Friedman et al., 2009).

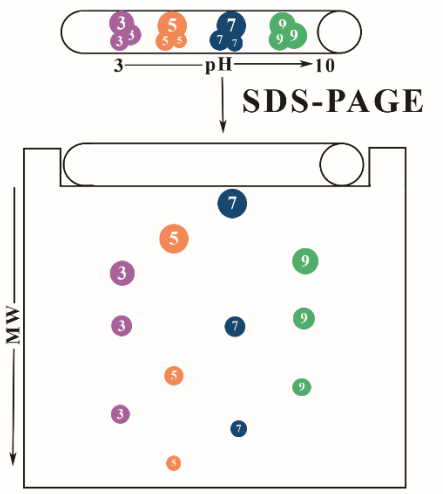

Figure 3. A representation of the second-dimension SDS-PAGE separation of 2DE.

1.2.5. 2DE gel staining

2DE gel staining procedure is an important step for visualisation and detection of resolved spot pattern that allows comparison, quantitation and depends on the further use of the gel. The main criteria for stains are a combination between: sensitivity, linear dependency between the intensity of protein spot and the amount of protein for quantitative analysis, high signal-to-noise ratio, compatibility with MS, simple use and availability and toxicity.

Proteins can be stained or marked pre-electrophoresis, for example *in vivo* marking with radioactive isotopes (^{35}S, ^{14}C, ^{3}H; ^{32}P, ^{33}P – for phosphoproteins) and visualised by autoradiography (sensitive, toxic and MS incompatible). The other pre-electrophoretic staining method is DIGE, where proteins are labelled with fluorescent tags (Sensitive, MS-compatible, expensive, special equipment needed).

Usually, proteins in the gels are stained post-electrophoresis. Coomassie blue, although suffering from low sensitivity in protein detection, is the most widely used non-covalent dye for 2DE gel staining (lower sensitivity, stains the background, MS-compatible, cheap, no special equipment needed) (Diezel et al., 1972; Neuhoff et al., 1988). Classical silver staining using silver nitrate is very sensitive, but may interfere with MS (Mortz et al., 2001). Fluorescent stains for 2DE gels (Nile red (Alba et al., 1996), SYPRO orange and SYPRO red (Steinberg et al., 1996), Deep Purple (Mackintosh et al., 2003), SYPRO Ruby (Berggren et al., 2002)) are very advantageous in comparison with other staining methods (very sensitive, MS-compatible, does not stain the background, simple to use), but are expensive and require special equipment to visualise, complicated excision from gels (Chevalier, 2010b).

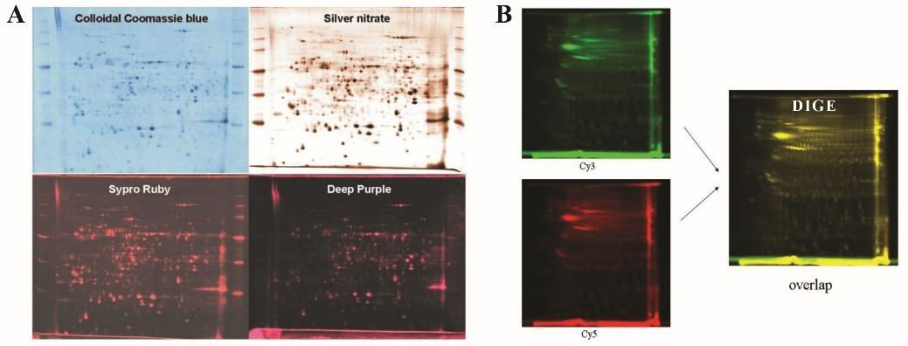

Figure 4. Examples of 2DE gel stains. A – post-electrophoretic stains; B – pre-electrophoretic DIGE fluorescent stains Cy3 and Cy5 and their overlap image. Figure adapted from (Chevalier, 2010b).

1.2.6. Liquid chromatography in proteomics

Regardless of emerging fluorescence-based methods, the problem with low abundant, hydrophobic and especially – membrane proteins, was unsolved. It was suggested that the limiting step of 2DE-gel proteomics might be the IEF due to chemical conditions prevailing at this step (low ionic strength and no ionic detergents) (Rabilloud et al., 2010). So, LC methods were implicated in addition to in-gel proteomics or without it, forming a new approach to proteomics known as multidimensional liquid chromatography (MDLC). Unlike the 2DE, LC is suitable for separation of not only proteins, but also peptides. Therefore, it can be applied upstream of 2DE to enrich, deplete or pre-fractionate samples, downstream of 2DE to separate peptide collections obtained from excised spots or instead of 2DE. In shotgun proteomics MS and LC or LC/LC is used to analyse the whole complex protein sample, quantitate differences between samples and detect an array of PTMs in a quick and sensitive manner (McDonald & Yates, 2002). LC-MS or LC-MS/MS nowadays is one of the most widely used proteomic technique. High-resolution LC-MS/MS approach was used to analyse the complete deep coverage proteome of mouse brain with 12,934 identified proteins (Sharma et al., 2015). The difference between in-gel and shotgun proteomics is shown in Figure 5.

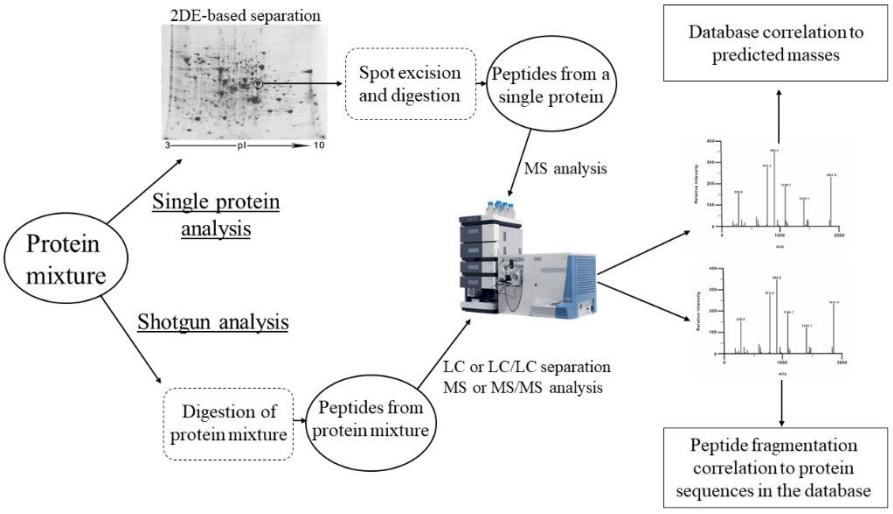

Figure 5. A comparison of in-gel 2DE-based and shotgun proteomic analysis procedures.

Like 2DE, MDLC is based on separating proteins/peptides by different principles to resolve complex mixtures. These different separation principles can include separation by size, hydrophobicity, affinity to particular ligands.

For example, affinity chromatography (AC) separates proteins and peptides on the basis of their specific ligand-binding activity. The ligands can vary from antibodies to catch specific proteins, glutathione-S-transferase (GST) affinity tags to catch fusion proteins, immobilized metal-affinity chromatography (IMAC) to isolate phosphoproteins/peptides, proteins with oligo-histidine tags (His_6) or other negatively charged proteins (Twyman, 2013). Before separation by 2DE, AC is mostly used to deplete – remove abundant protein(s) from samples (that could interfere with 2DE) or enrich samples (concentrate low-abundant proteins so they could be represented in the gel). In non-2DE approaches AC is used to simplify peptide mixtures prior to MS and is a great tool to study posttranslational modification (PTM) sites and quantitation of proteomics by using isotope-coded affinity tags. Also, affinity purification of protein complexes followed by MS is a powerful tool to map protein-protein interactions (Lee & Lee, 2004).

Size exclusion chromatography, also known as gel filtration chromatography, separates molecules on the basis of their size. An advantage of this method is that it does not require any chemical interactions between the solutes and the stationary matrix, which leads to preserving biological activity of the solutes and barely none sample loss.

Ion exchange chromatography (IEX) separates proteins/peptides according to their charge. The solute mixture is passing through a solid phase with charged chemical groups, and the target molecules reversibly adsorb to the matrix. Cationic and anionic resins may be used and they attract molecules of opposite charge. Variants of IEX chromatography include cation exchange (CEX), anion exchange (AEX) and variants with more highly charged resins - strong cation exchange (SCX) and strong anion exchange (SAX). The adsorbed target molecules are eluted in a gradient, gradually increasing ionic strength or pH of column washing buffers, resulting in a chromatogram. A chromatogram displays absorption peaks, where every peak is an individual component of the sample (Twyman, 2013). For example - 10255 different human proteins were identified in HeLa (human cervical carcinoma line) cells where the protein sample was fractionated by gel filtration, digested with three different proteases and the peptides fractionated by SAX following subsequent MS/MS analysis (Nagaraj et al., 2011).

Reverse-phase chromatography (RP) involves the separation of molecules on the basis of hydrophobicity. Like the IEX, protein/peptide mixture in aqueous solution is passing through a solid matrix and multiple fractions are produced by gradient elution with organic solvent, but in this case the reversed-phase resin consists of hydrophobic ligands, such as C_4 to C_{18} alkyl groups. Usually, reverse-phase separations are carried out using

high-performance liquid chromatography (RP-HPLC), where the solute is forced through the column under high pressure (Twyman, 2013). UPLC or ultra-performance liquid chromatography is a newer modification of HPLC and is enhanced in speed, resolution and sensitivity. The separation and quantitation is performed under even higher pressure than HPLC (Taleuzzaman M et al., 2015).

HPLC is a very powerful method to resolve complex protein/peptide mixtures for a number of reasons. Firstly, high resolution can be achieved in a wide range of different chromatographic conditions for structurally closely related or quite distant molecules. Secondly, easy to manipulate chromatographic selectivity. Thirdly, high recoveries and high productivity. And lastly, excellent reproducibility of repetitive separations. However, HPLC can cause irreversible protein denaturation, therefore reducing the possibility of recovering material in a biologically active form (Aguilar, 2004). Nevertheless, HPLC is used extensively to separate proteins/peptides followed by tryptic digestion, and the columns are often directly linked to electrospray ionization mass spectrometers to perform fully automated separation and analysis by LC-MS or LC-MS/MS (liquid chromatography-mass spectrometry or liquid chromatography-tandem mass spectrometry; See 1.2.) (Twyman, 2013).

The main disadvantage of LC methods for protein sample separation is that the visual aspect of 2DE is lost, along with pI and molecular mass, which can be determined by a spot position on the gel and that LC is a serial analysis technique, so it is difficult to run parallel experiments unless having an access to sets of identical apparatus (including the MS). Also, the buffer compatibility between separations is imperative, which can lead to arduous re-buffering in some cases.

1.3. Identification of separate components

When complex protein samples get separated either by 2DE or LC, the spots or fractions coming out of this separation are anonymous. When we select spots of interest from a 2DE gel, we get only vague information of MW and pI about the identity of that protein. So, characterization of fractions and determination which proteins are actually in the sample is essential for a proteomic experiment.

Before the emergence of mass spectrometry methods, arguably the most used ways to identify a protein were *de novo* Edman protein sequencing and antibody-based identification. Edman degradation is still one of the most used methods for protein *N*-terminal sequence identification, although it is mostly

replaced by MS techniques because of the limited speed of the method. Antibody-based techniques, can only be used to identify proteins that we know are in the sample, as there is no current antibody-based platform to identify and quantify all the proteins in the proteome of a complex organism. This is why, MS techniques are the most essential tool in proteomics.

1.3.1. Mass spectrometry

A mass spectrometer is a device that can measure the mass/charge ratio *m/z* of ions in a vacuum environment. Mass spectrometers are comprised of three main parts: an ion source, mass analyser and a detector. Initially the sample is ionized by ions produced by MALDI or ESI ion source, then they are separated in a mass analyser according to their mass-to-charge ratio. The ions are then detected by a detector and the end product is a mass spectrum – a plot of ion abundance versus *m/z* (Woods et al., 2019) (See Figure 6.). The most used soft-ionization methods that achieve ionization of large molecules without serious fragmentation are MALDI and ESI.

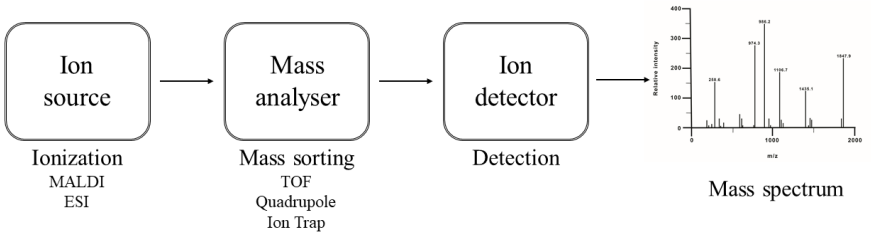

Figure 6. Schematic representation of mass spectrometry process.

1.3.1.1. Ionization sources

MALDI – matrix-assisted laser desorption/ionization is a process where the sample is co-crystallized with an excess of an aromatic UV-absorbing matrix compound, for example α-cyano-4-hydroxycinnamic acid, which absorbs energy from a nitrogen UV laser (337 nm). The mixture is then dissolved in an organic solvent and spotted on a metallic plate. When the solvent evaporates, the analyte gets embedded into matrix crystals. The plate is placed into the vacuum chamber of the MS and the sample/matrix crystals are exposed to high voltage at the same time being targeted with short laser pulses. The matrix crystals absorb the laser energy and emit it as heat (desorption), which results in proton transfer from the matrix to the analyte molecules which are being converted into gas-phase ions (See Figure 7.). The

ions then advance through the analyser towards the detector (Twyman et al., 2013; Woods et al., 2019).

ESI or electrospray ionization, is a process where the analyte is ionized in a liquid phase. The sample is dissolved and sprayed to the vacuum chamber under a high voltage. Charged droplets of liquid enter the vacuum chamber of MS where they are dried with a stream of inert gas creating gas-phase ions (See Figure 3.) that advance through the analyser towards the detector. This property of the ESI ionization source, allows its integration with upstream protein/peptide separation by LC or capillary electrophoresis. This also makes ESI-MS more suitable for complex peptide mixture analysis as in shotgun proteomics and MALDI-MS is primarily used to analyse simple peptide mixtures as in peptides obtained from a single spot of a 2D gel (Twyman et al., 2013).

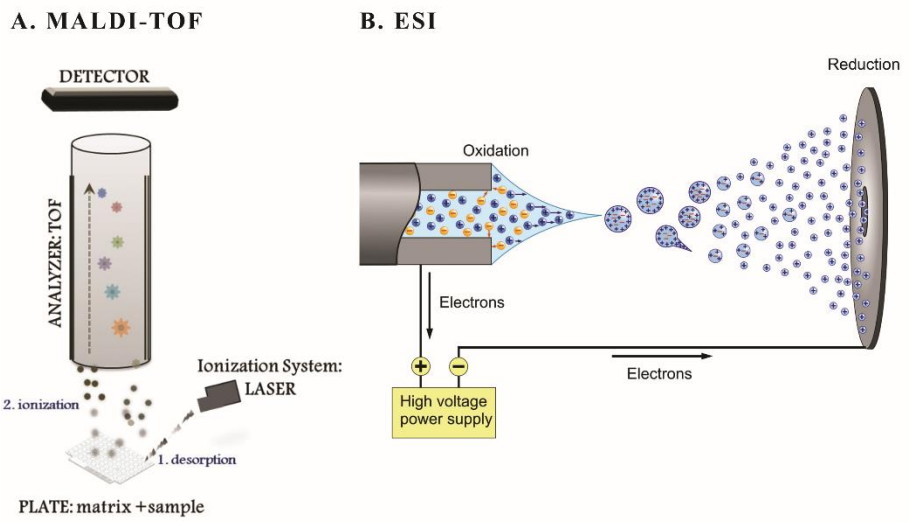

Figure 7. Schematic representation of MALDI and ESI ionization processes. A – MALDI ionization process coupled with TOF mass analyser and a detector. Figure adapted from (Torres-Sangiao et al., 2021). B – ESI ionization method. Discrimination by the size of the gas-phase ions is performed by sieving them through a reductor. Figure adapted from (Bioexcel.eu).

1.3.1.2. Mass analysers

There are several types of mass analysers, but for proteomic experiments mainly these three types are used –quadrupole (Q), time-of-flight (TOF) and trapping type instruments (Orbitrap, FT-ICR – Fourier transform ion cyclotron resonance, LIT – linear ion trap, QIT – quadrupole ion trap).

A quadrupole is a set of two pairs of charged cylindrical metal rods, which are connected to create an electrical field across the space between them. The separation of ions that enter the analyser is based on their trajectory

in the electric field. There are two modes a quadrupole can operate – RF-only mode (Radio Frequency) which lets any *m/z* ratio ions to pass through and a scanning mode that acts as a mass filter applying a potential difference which selects ions with specific *m/z* ratio and discards others. By varying the voltage, different *m/z* ratio ions can be passed over time and a mass spectrum can be obtained (Parker et al., 2010; Twyman et al., 2013; Woods et al., 2019).

A TOF mass analyser separates ions carrying the same charge by the time an ion needs to reach the detector in a field-free vacuum. Heavier ions take more time to reach the detector than lighter ones (Parker et al., 2010). Usually, TOF analysers are paired with MALDI ionization source, because it produces singly charged ions. But recently, to achieve a much higher sensitivity, MALDI sources are being paired with tandem TOF-TOF analysers or hybrid quadrupoles (Aebersold & Mann, 2003; Twyman et al., 2013; Woods et al., 2019).

Ion trapping type instruments contain a chamber with a ring electrode and two cap electrodes called an ion trap. By applying voltage to the ring electrode ions above the threshold *m/z* ratio are trapped, while others are ejected through the cap electrode. The voltage can be increased gradually so that ions with increasing *m/z* ratios will be emitted over time and a mass spectrum of intact peptides can be obtained. Generally, ion traps can be three-dimensional or linear with greater storage capacity (Parker et al., 2010).

1.3.1.3. Detectors

The detectors in mass spectrometers usually are electron multipliers, photodiode arrays, image current detectors and microchannel plates (Woods et al., 2019). Mass detectors mainly detect either the current produced or the charge induced when an ion hits or passes its surface. Because the number of ions coming from a mass analyser is usually small, the multiplication of the signal is necessary. The detector surface is called a dynode and is made out of copper-beryllium. When a charged particle strikes a dynode, it causes the release of secondary electrons in the dynode surface. This multiplication of electrons passes from one dynode to another and becomes strong enough to be detected by a cathode (Medhe, 2018). A photodiode array has a similar principle, except the charged particle hits a layer of scintillator compound and photons are emitted and registered. Image current detectors detect not a hit on a surface by a charged particle, but rather its „current image "– when a particle gets closer to a metal plate due to electrostatic attraction it induces the accumulation of opposite charge on the plate surface. This accumulation of charge is detected. Microchannel plates are closely related to an electron

multipliers and are several multipliers in an array (Medhe, 2018; Parker et al., 2010).

1.3.2. MS data interpretation

The final step of MS analysis is interpretation of gained data from produced mass spectra. The first method to identify proteins from mass spectra was peptide mass fingerprinting (PMF). This method is mainly used with 2DE and MALDI-TOF mass spectrometry when proteins are separated before digestion with trypsin. The principle of this method is that every protein has a unique signature of the masses of its constituent peptides – peptide mass fingerprint and can be identified from it. Software packages with algorithms that allowed peptide mass database searching were created specifically for this approach (Mascot (Matrix Science), MS-Fit (ProteinProspector), ProFound) (Thiede et al., 2005; Twyman et al., 2013).

The limitations of PMF are addressed by tandem MS/MS mass analysis (See 1.2. Identification of separate components). The peptide identification is performed by comparing experimental uninterpreted MS/MS spectra with the theoretical spectra derived from peptides in a database. The search is limited to peptides that correspond to analogous enzyme digestion pattern, ion mass tolerance, predicted type of ion fragments and PTMs. The similarity between experimental and theoretical spectra is defined by a search score, which can be calculated using different algorithms and programs (for example Mascot (Matrix Science), Sequest (Yates Laboratory)).

Spectral library search is a fast and accurate uninterpreted data search through spectral libraries that allows direct comparisons (SpectraST, BiblioSpec). Although, the main limitation is still the amount of MS/MS data.

Mass spectrometry-based peptide/protein identification, like all big datasets, needs to be verified using statistical significance analysis. A match can be assigned a significance measure (*p*-value) by referencing its search score to the distribution of accidental matches. The *p*-value alone is not enough to correctly identify peptides. When there are too many peptides with similarly low *p*-values, just by random chance, there can be a lot of "false" matches between all the matches called "true". Therefore, more stringent measure of significance called false-discovery rate (FDR) for multiple testing correction was introduced. The FDRs determine the expected proportion of „false positive" protein inference and are adjusted *p*-values using the Benjamini-Hochberg procedure (Benjamini & Hochberg, 1995; Choi & Nesvizhskii, 2008; The et al., 2016).

1.4. Systematic quantitative and/or comparative analysis

Comparative analysis of related samples is one of the most important approaches in proteomics. When analysing a different cell type, developmental stage or a diseased tissue it is impervious to simultaneously analyse a control sample (developmental starting point, healthy tissue). This kind of comparison can reveal proteins that are uniquely produced under given circumstances, for example - in search for biomarkers. Unfortunately, very few proteins show on/off changes. Mostly, protein differences between samples are less obvious. Thus, the quantitation of proteins is an important aspect of proteomics (Twyman et al., 2013).

1.4.1. Densitometric analysis of 2DE gels

The most straightforward protein quantitation in comparative experiments is a densitometric quantitation from 2DE gels. For this task gel images need to be digitalised by scanning with a charge-coupled device (CCD) camera, a densitometer (scanner) or a fluorescent imager, depending on the type of protein dye used.

A computer software programs (PDQuest (BioRad), ImageMaster 2D Platinum 7.0 (GE Healthcare) Z3 (Compugen), Melanie (Genebio)) are later used to detect and match spots between 2DE gels. These programs apply a set of defined parameters to interpret spot patterns. Generally, the software will enhance the image to clear the background and contrast the spots, automatically detect spots and smooth the image to subtract background noise. Some programs use edge detection filters to identify sharp changes in pixel density. Subsequently algorithms that fit, detect blobs or convert pixels into topological surface are applied.

Once the protein spots are detected the matching of all the spots in the gels is performed. This task is usually challenging because of the differences in sample preparation, gel composition, running conditions, protein mobility and spot patterns. Although, their influence can be reduced by adding landmarks (mapping the major spots that are present in all the gels) and applying a distortion mesh (warping gels to correct geometric distortions of the spot pattern (Gustafsson et al., 2002)) (Appel et al., 1997) (See Figure 8.).

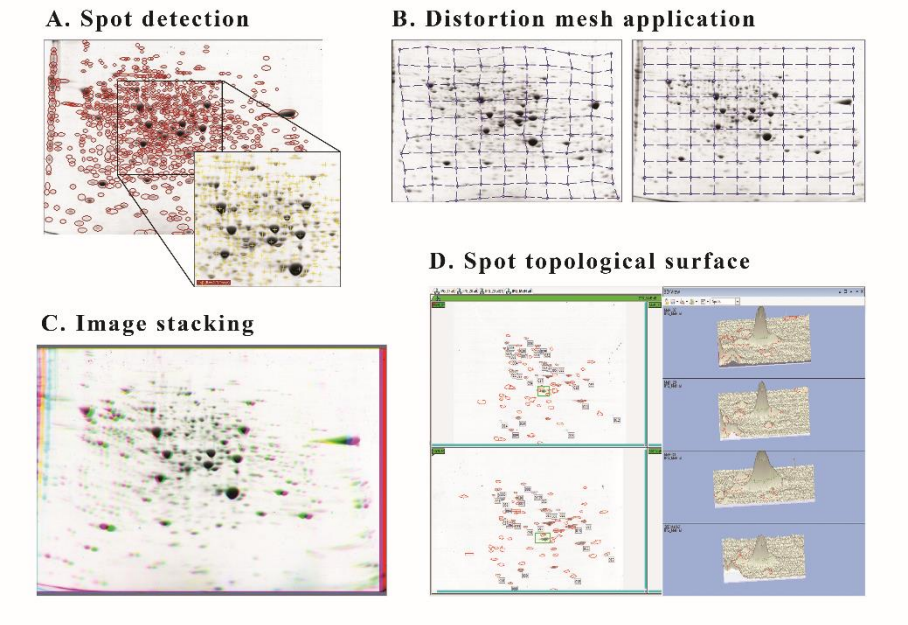

Figure 8. Examples of 2DE image analysis tools. A – image analysis with PDQuest software using spot detection tool (spots marked by crosshairs or circled). B – an example of a distortion mesh (PDQuest). C – three 2DE gel images stacked one on another (PDQuest). D – Spot pixel density converted into topological surface (ImageMaster).

The quantitation of protein spots is performed by calculating the relative volume (%Vol) of each protein spot from the total volume of all the spots in the gel. The ratio between %Vol of the same spot in different gels is called fold change (FC). So, the FC represents how many times the quantity of a given spot increased/decreased between samples analysed by 2DE (Twyman et al., 2013).

The most advantageous form of 2DE-based quantitation is Differential Gel Electrophoresis (DIGE) (Unlü et al., 1997). High sensitivity of fluorescent dyes combined with multiple sample separation in a single gel and MS-compatibility results in a robust method to detect and quantify even low-abundant proteins (Diez et al., 2010; Timms & Cramer, 2008). Although, only proteins that have free cysteines can be labelled and subsequently quantified, and that reduces the analysis to only a part of the protein complement (Chevalier, 2010a).

1.4.2. Quantitative MS

Rapid developments in MS instrumentation, demand to quantitate multiple proteins at a time and the advancement of gel-free shotgun techniques

(MudPIT) led to protein quantitation proteomics in the MS level. Quantitative mass spectrometry approaches can either bee label-free or label-based. There are two types of label-free approaches – AUC (area under the curve), or signal intensity measurement, and spectral counting. AUC is based on ion abundance measurement at each LC retention time (RT) and *m/z* ratio within defined detection limits. Measured ions represent the ionized peptides, so the quantity of ions reflects the peptide abundance. Since a peptide does not result in a single ion and can have several different charge states (especially when ionized with ESI), together with technical variations, a lot of noise is created. It is widely accepted to validate the peptides by subsequent or simultaneous LC-MS/MS identification and further computational review of the raw LC-MS data (Neilson et al., 2011; Podwojski et al., 2010).

Spectral counting is an alternative label-free quantitation approach that directly links MS/MS spectral counts and protein abundance. Spectral counts represent the number of MS/MS identifications – an abundant protein will be sampled repeatedly across a wide range of RT and identified multiple times, acquired higher abundance spectra is used to quantitate such proteins (Podwojski et al., 2010). It has been shown that the relationship between spectral counts and the protein concentrations is of linear manner of two orders of magnitude (Liu et al., 2004).

1.5. Heterologous protein synthesis in yeast

Heterologous protein synthesis is a process when a protein coding gene (or a part of it) is inserted into a host organism using recombinant DNA technology and expressed there. The host organism naturally does not have the mentioned gene and the right choice of a host organism is essential for efficient production of protein (or other molecule) products. The requirements for the heterologous protein producing system usually are – quality, quantity, yield of the produced proteins and space-time yield of the desired product, as well as price of the system, ease of cultivation, generation of properly folded and active proteins, resistance to stress, ease of genetic manipulation (Porro et al., 2011). Yeast, as host systems, are characteristic for most of these requirements. They combine the benefits of unicellular organisms (fast and easy cultivation, ease of genetic manipulation, inexpensive) with the protein processing capability of a eukaryotic organism (protein folding, assembly, PTMs) and lack of endotoxins, oncogenic or viral DNA (Mattanovich et al., 2012).

Two main groups of yeast used for recombinant protein production are non-methylotrophic and methylotrophic. Non-methylotrophic yeasts have an

advantage of familiarity to scientists working with them. *S. cerevisiae* is a particularly familiar organism to work with because starting from the 1980s the majority of recombinant proteins were produced in these yeast (Hitzeman et al., 1981). *Kluiveromyces lactis* although lesser familiar, but nevertheless widely used non-methylotrophic yeast strain with adaptations for food industry and a GRAS (Generally Regarded As Safe, approval by Federal Drug Administration USA to be used for humans) organism (van Ooyen et al., 2006). *Kluiveromyces marxianus* (Fonseca et al., 2008) is a thermotolerant sibling of *K. lactis* that has been utilized for production of endogenous or exogenous enzymes (Rocha et al., 2010). Although there are astounding improvements in yeast molecular genetics, expression levels and fermentation techniques of these yeast, large-scale processes still impose restrictions (Mattanovich et al., 2012). Other non-methylotrophic yeast species are investigated to a lesser extent. *Zygosaccharomyces* genus yeast seem promising for industrial applications due to their resistance to stressful conditions (high salt (*Z. rouxii*), sugar concentrations acidic environment and high growth temperature (*Z. bailii* (Makdesi & Beuchat, 1996; Sousa et al., 1996))). *Yarrowia lipolytica* and *Arxula adeninivorans* are dimorphic fungi that can form pseudohyfae. *Y. lipolytica* can grow on n-parafins and generate high levels of organic acids (Madzak et al., 2004). *A. adeninivorans* is a osmo- and thermotolerant yeast that assimilates nitrates (Böer et al., 2009).

Methylotrophic yeast species have gained a lot of attention recently mainly because they can grow to high cell densities in simple fermentation processes and their promoters are very strong and strictly regulated. The strict promoters are needed because of their high demand for methanol oxidizing enzymes (like alcohol oxidase). Two main species of methylotrophic yeast used for recombinant protein production are *Pichia pastoris* (Wegner, 1990) and *Hansenula polymorpha* (Sudbery et al., 1988). *P. pastoris* produces two main alcohol oxidases AOX1 and AOX2. The first generation of *P. pastoris* expression systems relied on the stronger AOX1 promoter. There are three methanol usage phenotypes in *P. pastoris* (Mut^+–wild type methanol utilization; Mut^s–slow methanol utilization; Mut^-–deleted methanol utilization) which can be applied with respect to the production process design (Mattanovich et al., 2012). In comparison to other yeast species, *P. pastoris* performs better in production of secreted recombinant proteins (Schmidt, 2004), for example it produced 8.1 g/L of extracellular recombinant xylanase (Fan et al., 2012). Although *P. pastoris* is used more and more for heterologous protein production, some limitations still exist, like high levels of proteases and risks in storing large volumes of methanol (Potvin et al., 2012). *H. polymorpha* is favourable because it utilizes a strong MOX

(methanol oxidase) promoter, is thermotolerant (48–50°C) and at high temperatures can ferment xylose to ethanol (Baghban et al., 2019; Ishchuk et al., 2008). Additionally, *Pichia methanolica* (Raymond et al., 1998) and *Candida boidinii* (Yurimoto, 2009) can be used as methylotrophic expression systems and *Ogataea minuta* (Kuroda et al., 2006) is thought to be a suitable host for glycoprotein production.

Although other yeast species can have more advantages in large-scale recombinant protein production, *S. cerevisiae* is still the most used yeast strain in research because of the massive amount of data on all aspects of this organism's biology.

1.5.1. Yeast *S. cerevisiae* as a heterologous protein production system

Yeast *S. cerevisiae* was the first and the most used host for recombinant protein synthesis (Celik & Calık, 2012). In 1996 *S. cerevisiae* (S288C strain) became the first eukaryotic organism with its genome sequenced (Goffeau et al., 1996) and because of that, it also became a model organism with the most well-studied genome organization and evolution (Duina et al., 2014). *S. cerevisiae* is also easy and inexpensive to cultivate to very high cell densities, a lot of molecular tools available for simple genetic manipulations, an array of convenient vectors, selection markers, promoters, terminators and secretion signals, there are special peptidase-deficient strains for recombinant protein production, tolerates pH changes, high ethanol and sugar concentrations and is resistant to elevated osmotic pressure, which makes it a preferred host over other yeast, bacteria and filamentous fungi (Hahn-Hägerdal et al., 2007; Mattanovich et al., 2012; Porro et al., 2011; Tesfaw & Assefa, 2014).

It is widely adopted in industrial production not only of chemicals (bioethanol), but also biopharmaceutical products such as Hepatitis vaccines (McAleer et al., 1984), hirudin (Bischoff et al., 1989), insulin (Thim et al., 1986), platelet-derived growth factor (Finnis et al., 1992), urate oxidase (Leplatois et al., 1992), macrophage colony-stimulating factor (Price et al., 1987), glucagon (Moody et al., 1987). The broad use of *S. cerevisiae* for biopharmaceuticals is also driven by the fact that it is a GRAS organism and has a history of usage in nutrition (cheese, wine, supplements).

This model organism is also the most commonly used eukaryotic organism in research and has been used to study aging (Murakami & Kaeberlein, 2009), apoptosis (Owsianowski et al., 2008), metabolism (Brocard-Masson & Dumas, 2006; López-Mirabal & Winther, 2008), signal transduction (Hohmann et al., 2007), gene expression regulation (Biddick & Young, 2009), cell cycle control (Nasheuer et al., 2002), neurodegenerative

diseases (Miller-Fleming et al., 2008), programmed cell death (Munoz et al., 2012), autophagy (Reggiori & Klionsky, 2013), secretory pathways (Celik & Calık, 2012) and countless other biological processes (Karathia et al., 2011).

Despite an array of advantages, there are still reasons why there is only a limited number or products made from *S. cerevisiae* – hypermannosylation of proteins and low protein yield (Mattanovich et al., 2012). N- and/or O-linked glycosylation is a putative PTM of a eukaryotic protein. It is a significant modification, since pharmacodynamical behaviour of 70% of therapeutic proteins depends on their glycosylation. The initial steps of N-glycosylation are similar between yeasts and mammals: in the ER, a core N-glycan (two N-acetylglucosamines and five mannose residues) is transferred to the developing polypeptide, using the Asn-X-Ser/Thr consensus sequence; after the quality control in the ER, the new proteins are transferred to the Golgi apparatus, where the N-glycan processing starts to differ between yeasts and higher eukaryotes; the glycan chains of yeast are larger, but less complex than of mammals and are limited to the addition of mannose and mannosylphosphate sugars. Attempts to prevent hypermannosylation by inactivating mannosyltransferases Och1 and Mnn1 led to acute growth defects in *S. cerevisiae* (Nakayama et al., 1992; Zhou et al., 2007), but was attainable in other yeasts (Mattanovich et al., 2012).

There are many examples how to address the low protein yield in *S. cerevisiae* such as correct selection of the expression vector and promoter systems, optimization of the fermentation process, genetic engineering of host strains (Idiris et al., 2010). But, if the right conditions do not provide good results, it is likely that the yeast cells are under some kind of metabolic or environmental stress, that usually has a strong impact on protein yield (Mattanovich et al., 2004).

1.5.2. Stress in recombinant protein producing yeast *S. cerevisiae*

Unfortunately, heterologous protein overproduction in yeast *S. cerevisiae* is almost always connected to cellular stress and one of the most common is metabolic ER stress. The ER stress is a response to the secretion of heterologous proteins - inefficient protein precursor translocation, signal sequence processing and folding in the ER, conformational stress (Gasser et al., 2008) and accumulation of unfolded proteins (Kauffman et al., 2002; Mori et al., 1992). The Unfolded protein response (UPR) is a type of ER stress and is caused by accumulation of unfolded proteins in the ER. UPR consists of three players – when BiP (*KAR2* gene product, HSP70 ER lumen molecular chaperone (Gething, 1999)) binds to an unfolded protein it is removed from a

transmembrane kinase Ire1p, and that induces the oligomerization of Ire1p; When oligomerized, Ire1p endoribonuclease activity is activated at the cytoplasmic side of the ER and Ire1p removes an intron from *HAC1* mRNA; $Hac1p^{i}$ product acts a transcription factor and upregulates UPR genes like BiP and PDI (protein disulphide isomerase, ER-localized folding catalyst (Ali Khan & Mutus, 2014)) (Sidrauski & Walter, 1997). The upregulated synthesis of BiP and PDI should alleviate the UPR in the cell and these proteins are recognised as markers of UPR. In this vein, overproduction of PDI is used to increase the secretion of various heterologous proteins in *S. cerevisiae* like, human lysozyme (Hayano et al., 1995), human platelet-derived growth factor (Robinson et al., 1994), and single-chain antibody fragments (Shusta et al., 1998). Co-synthesis of BiP with the recombinant protein also positively impacts cell growth and enhances the secretion of human erythropoietin (Robinson et al., 1996), bovine pro-chymosin (Harmsen et al., 1996) and the synthesis of antithrombic hirudin (Kim et al., 2003).

The UPR is also connected to ER associated protein degradation (ERAD) which is a process of retro-translocation of misfolded proteins from the ER to cytosol and their subsequent proteasomal degradation (Hiller et al., 1996). ERAD requires a functional UPR (Travers et al., 2000). Chaperones BiP and Lhs1p (both Hsp70 family) together with J domain proteins Jem1p and Scj1p (homologues of *E. coli* DnaJ protein (Silberstein et al., 1998)) prevent the unfolded protein aggregation in the ER and facilitate their export to the cytosol where they are conjugated to ubiquitin and directed to proteasomal degradation (Nishikawa et al., 2001). ERAD is considered to be a typical stress relief pathway and in some cases might alleviate the burden of unfolded proteins and increase the yield, but the retro-translocation of misfolded proteins is a competitive process to the translocation of proteins to the ER, thus limiting the product entering the secretory pathway (Mattanovich et al., 2004).

The UPR is not exceptional to the ER and two more types of UPR exist – UPR-M/C and UPR-Cyto (Geiler-Samerotte et al., 2011; Metzger & Michaelis, 2009). These stress responses are induced mainly by the synthesis of heterologous membrane proteins that usually suffer from low synthesis levels and protein instability and/or proteolytic degradation (Freigassner et al., 2009).

The UPR-M/C is induced by misfolded membrane proteins with lesions positioned in the membrane span or cytosol and UPR-Cyto is caused by cytosolic proteins that cannot enter the secretory pathway. Although not studied broadly, it is known that the UPR-M/C causes the impairment of proteasomal degradation machinery, and the main modulator of this stress

response is RPN4p which is a “sensor” transcription factor of proteasome function (Ju et al., 2004; Xie & Varshavsky, 2001, p. 4). RPN4p activates more proteasomes in response to their impairment caused by UPR-M/C and aids stress relief (Metzger & Michaelis, 2009).

The UPR-Cyto response is usually caused by a bottleneck in protein precursor translocation to the ER. Inefficient translocation leads to unfolded protein accumulation in the cytosol and aggregation, this invokes a broad heat-shock response that fights misfolding of proteins, altered membrane integrity, oxidative stress and decreased growth rate (Brauer et al., 2008). Most of the proteins induced by this response are regulated by *HSF1* transcription factors and are cytosolic Hsps (heat-shock chaperones, Hsp70, Hsp90, Hsp110 families) (Ciplys et al., 2011; Geiler-Samerotte et al., 2011). The eEF1A (eukaryotic translation elongation factor 1A) is also found under UPR-Cyto where it acts as a quality control chaperone (Chuang et al., 2005) and a *HSF1* activator (Shamovsky et al., 2006). In the cytosol unfolded proteins together with Hsps and eEF1A form insoluble aggregates - this and constant reinduction of chaperones, indicates that this stress is unrepairable, persistent and can’t be relieved (Ciplys et al., 2011; Metzger & Michaelis, 2009).

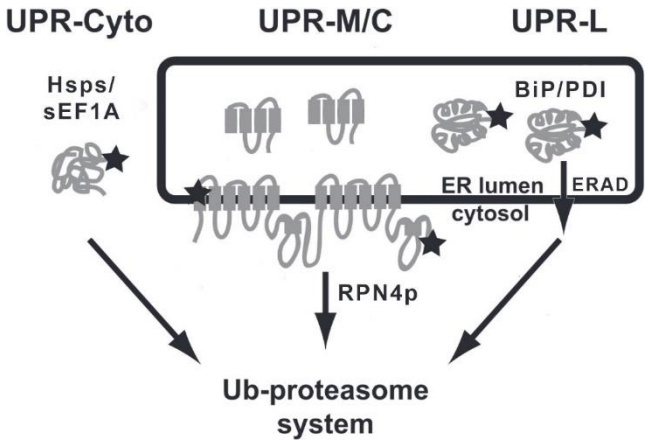

Figure 9. Graphical representation of the three UPR’s that can happen in the cell, their compartmentalization and cellular proteins that are induced to alleviate these stresses. Figure adapted from (Metzger & Michaelis, 2009).

Another yeast cell response to stress is apoptosis or programmed cell death. One of the causes of yeast apoptosis is a prolonged UPR activation when the ER becomes fragmented due to accumulation of unfolded proteins. Inefficient protein folding induces oxidative damage and subsequently cell death (Gasser et al., 2008). Environmental factors are also known to induce apoptosis, such as acetic acid (Ludovico et al., 2001), oxidative stress (Madeo

et al., 1999) and salt-stress (Huh et al., 2002). Unfortunately, no metabolic engineering approaches to inhibit apoptotic response has been proposed for yeasts (Mattanovich et al., 2004).

Yeast cells have an arsenal of environmental stress response genes (ESR genes) that are regulated by general stress transcription factors Msn2p and Man4p. There is a common regulatory program that induces genome wide transcription changes in response to diverse environmental stresses like heat shock, high osmolarity, acid, chemical substances. The gene groups that are stress induced are responsible for energy generation, carbohydrate metabolism, protein folding and degradation, fatty acid metabolism, cell stress (heat shock proteins, detoxification of reactive oxygen species (ROS), DNA damage repair) and gene groups that are repressed by stress are related to growth process, nucleotide metabolism, ribosomal proteins and RNA metabolism (Causton et al., 2001; Gasch et al., 2000). Most stress responses caused by long-term non-optimal conditions lead to the cell's adaptation to new conditions and only minor changes in gene expression. Successful adaptation to environmental stress confers an increased yeast cell resistance to other kinds of stress (Attfield, 1997). Potentially, environmental changes and stresses can be used to improve the synthesis of recombinant proteins.

Heat shock or high temperature stress has a profound impact on gene expression changes, and is regulated by heat shock factor (HSF) and Msn2p, Msn4p transcription factor control systems (Ruis & Schüller, 1995). The gene products induced by heat shock are heat shock proteins (Hsps) and a lot of them function as molecular chaperones. They are essential for heat stress relief, because not only that they guide nascent proteins towards their final conformation, but also are involved in renaturation of impaired substrates and irreparable protein targeting for degradation (Morano et al., 1998). With the increase of the temperature of the heat shock (above 37°C), the amount of insoluble protein aggregates also increases. To compensate protein loss due to aggregation and to maintain constant pool of soluble proteins the levels of stress-protective Hsps chaperones are increased. This counterbalances the increased protein turnover induced by stress temperatures and when the system is exhausted, the aggregates accumulate and the growth stops (Mühlhofer et al., 2019). Because yeasts are naturally heat sensitive, application of higher temperature for improved recombinant protein production is not generally used. Although, the heat shock response (HSR) is regulated by the transcription factor Hsf1p (heat shock factor) and most of its targets are genes that encode chaperones responsible for protein folding and preventing the accumulation of aggregated or mis-folded proteins. In this vein, the overexpression of mutant HSF1-R206S gene that constitutively activated

HSR increased the secreted heterologous α-amylase and endogenous invertase yield. This approach allowed to induce the ER and cytosolic chaperones to improve recombinant protein production (Hou et al., 2013).

Yeast cell response to cold shock is primarily triggered by changes in membrane fluidity. The signal is transduced by the usual stress pathways and transcription factors – the high-osmolarity glycerol (HOG), mitogen-activated protein kinase pathway (MAPK) and Msn2p/4p (Aguilera et al., 2007). The cold induced genes *TIP1, TIR1, TIR2* are related to cell wall organization and biogenesis (Kowalski et al., 1995), Nsr1p is involved in pre-RNA processing (Kondo et al., 1992), seripauperin (PAU) family proteins (*PAU1-PAU7*) display phospholipid-interacting activity (Homma et al., 2003; Panadero et al., 2006; Zhu et al., 2001), Tps1p and Tps2p are trehalose synthesizing enzymes (Kandror et al., 2004). After a long exposure (4–12h) to cold conditions (10°C (Sahara et al., 2002), 4°C (Murata et al., 2006), 0°C (Kandror et al., 2004), -80°C (Odani et al., 2003)) general stress response Hsps genes are induced (*HSP12, HSP26, HSP42, HSP104, SSA4, SSE2, YRO2*). Yeast cells that are under cold stress accumulate trehalose, glycerol and heat shock proteins to protect the cell from freeze injury. Other protective responses are membrane fluidification, cell wall maintenance, protein folding support, ROS detoxification (Aguilera et al., 2007). On the other hand, low cultivation temperature is known to have favourable effects on energy metabolism, protein degradation, folding, secretion, aggregation and, in this vein, increase the recombinant protein yield or activity in yeast (Cassland & Jönsson, 1999; Z. Li et al., 2001; Mattanovich et al., 2004; Zepeda et al., 2018). For example, a 16-fold higher laccase activity was achieved when *S. cerevisiae* cell were grown in 19°C instead of 28°C (Cassland & Jönsson, 1999).

A pH that is different from the optimal growth pH can also cause cellular stress (or adaptation to it) and can be used to increase recombinant protein stability (Shi et al., 2003) or decrease the protease activity (Cregg et al., 2000). In *S. cerevisiae* genes that are regulated by the pH have been identified – *PDR12* (ATP-dependant membrane transporter) (Piper et al., 2001), *ZMS1* (zinc-finger family transcription factor), *TRK2* (potassium transporter) (Ko et al., 1990), *PMA1* (plasma membrane H^+–ATPase) (Piper et al., 2001) are activated by low pH and repressed by high, and *CIT2* (peroxisomal citrate synthase), *PHO89* (sodium phosphate symporter) are repressed at low pH and activated by high (Causton et al., 2001). Both *PDR12* and *PMA1* gene products are known to be responsible for adaptation to weak acid stress (Piper et al., 2001). Low pH also induces the HOG (high osmolarity glycerol) pathway that leads to changes in cell wall organisation by activating

proteins with glycosylphosphatidylinositol (GPI) anchors (Kapteyn et al., 2001).

Accumulation of osmolytes (mainly glycerol) to increase intracellular osmolarity in accordance to external, is the main adaptation of yeast cell to osmotic shock (Mattanovich et al., 2004). Osmotic shock is caused by rise in extracellular solute concentrations. High osmolarity interferes with ion homeostasis, water availability and turgor pressure regulation (Dragosits et al., 2011). The regulatory pathway of response to osmotic shock is the HOG pathway – a MAPK cascade with Hog1p. HOG pathway also controls the Msn2p/Msn4p regulated stress response indicating that osmotic stress triggers general ESR (Schüller et al., 1994). In the case of major osmotic stress, the *GDP1* gene – the main gene involved in glycerol synthesis is induced together with other genes involved in carbohydrate metabolism. During osmotic stress, ribosomal and translation proteins are downregulated, chaperone genes induced, temporary growth arrest is observed (Rep et al., 2000). *S. cerevisiae* strains that withstand higher osmolarity and accumulate high glycerol concentrations are the ones that exhibit efficient expression of *GPD1* gene (Attfield & Kletsas, 2000).

1.6. Measles hemagglutinin protein and its production in yeast *S. cerevisiae*.

Measles virus (MeV) belongs to the family *Paramyxoviridae* and genus *Morbillivirus* of enveloped viruses with a non-infectious single-stranded (-) RNA genome (Lamb & Parks, 2007). MeV is a highly contagious viral disease that poses a great threat to unimmunized children. With the decline of vaccination (Benecke & DeYoung, 2019; Leong & Wilder-Smith, 2019; Samaraweera et al., 2020), there has been a rise in mortality rates due to MeV, with over 140000 deaths recorded in 2018 (Patel et al., 2019). MeV is serologically monotypic (Tahara et al., 2016) thus, the vaccines derived from strains isolated 50 years ago are still effective to this day against all presently circulating MeV strains (Strebel et al., 2011). MeV has two main surface spike glycoproteins that are targets of neutralizing antibodies – the hemagglutinin (H) and the fusion (F) proteins. However, because the main function of H protein is to bind to cellular receptors (Bouche et al., 2002; de Swart et al., 2005, 2009) - the humoral immune response forms mainly against it.

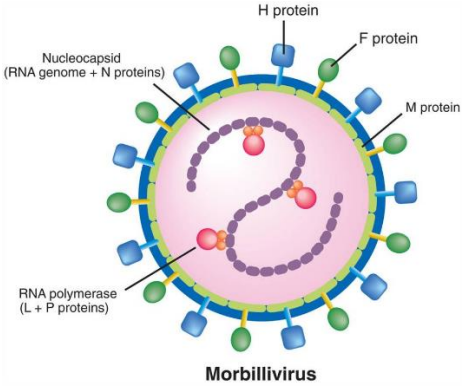

Figure 10. Graphical depiction of *Morbillivirus* genus protein structure. Figure adapted from (Sato et al., 2012).

The main receptors that the H protein binds to are SLAM (signalling lymphocyte activation molecule) and nectin-4 expressed on the surface of immune and epithelial cells respectively (Mühlebach et al., 2011; Noyce et al., 2011; Takeda et al., 2011; Tatsuo et al., 2000). Certain laboratory and vaccine MeV strains have adapted to use CD46 as a receptor in addition to SLAM and nectin-4 (Yanagi et al., 2009). Upon H protein binding to a receptor, conformational changes in the F protein are triggered which initiate the fusion between viral envelope and the plasma membrane of the host cell (Jardetzky & Lamb, 2014).

MeV H protein (MeH) is a 617 amino acid length polytopic transmembrane α-helical glycoprotein (has more than one membrane-spanning α-helix) that contains a N-terminal hydrophobic cytoplasmic tail, transmembrane region and C-terminal "head" domain that interacts with the receptors. The cytoplasmic tail acts as a signal domain that directs the nascent protein to the ER and stabilizes the protein in the lipid bilayer during its transport on the surface of membrane (Lamb & Parks, 2007). The head domain of the MeH protein is made of a six-bladed β-propeller fold (β1-β6 sheets). Looking from the top, it has a square shape with a large pocket in the centre. The pocket is shielded by an N-linked sugar at the amino acid N215 (Hashiguchi et al., 2007). There are five N-glycosylation targets in the MeH protein, with four of them always glycosylated. Because of this inherent glycosylation pattern MeH can be seen as two distinct bands in the PAA gels (Ogura et al., 1991). MeH protein forms a homodimer linked by a disulphide bridge between cysteine residues at position 154. On the surface on the host cell and the virion, MeH proteins are found further assembled to a tetrameric dimer of dimers (Hashiguchi et al., 2011).

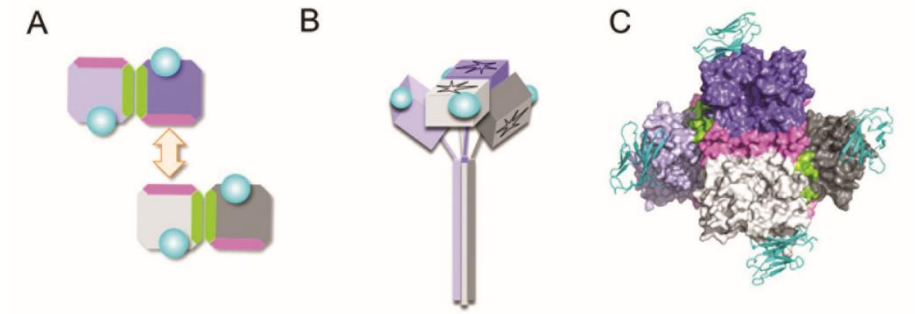

Figure 11. Tetrameric structure of MeH. Protein molecules are marked in purple, light purple, grey, light grey. Green regions mark the interface between monomers. Pink regions mark the interface between dimers in the dimer of dimers. SLAM receptor marked in cyan. A – schematic depiction of the formation of dimer of dimers. B – schematic diagram of the tetrameric dimer of dimers. C – a view from the top at the MeH tetrameric head. Models with surface representation show MeH and ribbon diagrams show SLAM. Figure adapted from (Tahara et al., 2016).

An interest in obtaining recombinant MeH protein lies in a high requirement of serological measles detection kits in areas with high infection rates. Because it is the main antigenic determinant of MeV, recombinant MeH "head" domain was also proposed for subunit vaccines (Lobanova et al., 2012), but unfortunately, no progress has been made further on. The analysis of recombinant MeH production in yeast is also important to study the aberrant viral glycoprotein processing in yeast. It has been shown that the production of such proteins results in abnormal folding and aggregate formation (Sakamoto et al., 1999; Wen et al., 1986). On the other hand, viral nucleoproteins that are not secreted and mature in the cytosol, does not form aggregates and can be efficiently purified in their native form (Juozapaitis et al., 2005, 2008; Samuel et al., 2002; Slibinskas et al., 2004). This indicates, that the problem in producing active human virus surface glycoproteins lies in the principal difference between yeast and higher eukaryote secretion pathways. Some reports highlight the possible limitations of yeast expression systems for the production of such proteins - low synthesis levels (Abdul Jabbar & Nayak, 1987; Martinet et al., 1997), insoluble aggregate formation (Sakamoto et al., 1999; Wen et al., 1986), inactivity due to hyperglycosylation (Scorer et al., 1993). However the exact mechanisms of the processes that limit the production of viral surface glycoproteins in yeast are not clear (Ciplys et al., 2011).

In the case of MeH, overproduction of protein precursors leads to inefficient SRP (Signal Recognition Particle)-dependent co-translational translocation to the ER. This way only a small part of MeH protein precursors get into the ER and are properly folded and glycosylated (Čiplys et al., 2011).

These unglycosylated and N-glycosylated forms are easily distinguished in a PAA gel as a major ~65kDa and a minor ~75kDa band, respectively. The unglycosylated MeH portion represents the precursors accumulated in the cytosol, that form insoluble aggregates and induce the UPR-Cyto response (Ciplys et al., 2011). The amount of MeH glycoprotein indicates translocation load and the translocation efficiency is indicated by the ratio of glycosylated form to total MeH protein. This makes recombinant MeH production in yeast a convenient model to study translocation into the ER.

The insoluble aggregates that accumulate in the cytosol consist of MeH protein precursors that are connected into multimers trough disulfide bonds and tightly bound eEF1A. eEF1A is thought to be involved in quality surveillance of newly synthesized proteins (Chuang et al., 2005) and is required for the activation of Hsf1p transcription factor (Shamovsky et al., 2006, p.) that induces the heat shock response or the the effects of UPR-Cyto. Also, tightly bound to the multimers are sHsps - that can only be removed at denaturing conditions - and peripherally bound large Hsps. Interestingly, during the MeH production induced stress, most of the proteins with differential synthesis patterns are all targets of Hsf1p (mostly of Hsps), with the exception of sHsps (Hsp26, Hsp42) that are regulated by Msn2/4. The synthesis of large Hsps was upregulated, whereas the synthesis of sHsps did not change or was downregulated. This proves that the biosynthesis of MeH induces a response similar to a canonical UPR-Cyto (Geiler-Samerotte et al., 2011). In yeast, Hsp26 is a strictly temperature-regulated chaperone (Haslbeck et al., 1999; Stromer et al., 2003). It can bound to unfolded polypeptides and prevent their aggregation in cooperation with large Hsps (Cashikar et al., 2005) only after the exposure to elevated temperatures (Franzmann et al., 2005). Hsp26 found tightly bound to protein precursors in aggregates at 30°C suggests that without elevated temperatures this chaperone cannot prevent precursor aggregation (Ciplys et al., 2011).

All the cellular proteins separated from the aggregates and the translocated, glycosylated MeH proteins were insoluble and inactive. The insolubility problem of glycosylated MeH can be partially solved by co-synthesizing human ER chaperone calnexin. The approach to reduce the synthesis rate of MeH resulted in complete translocation of the protein precursors into the ER, their glycosylation, but MeH proteins were still insoluble and inactive (Čiplys et al., 2011). The main bottleneck of MeH precursor translocation is caused by possible limited sufficiency of the SRP-dependent translocation pathway or lack of mammalian translocation accessory factors TRAM (translocating chain-associating membrane protein) and TRAP (translocon-associated protein complex) (Ciplys et al., 2011).

Another approach to alleviate cellular stress, or to increase recombinant protein yield, is to apply temperature stress. As was mentioned before, yeast cell adaptation to sudden temperature shock results in increased resistance to other stress factors. Also, in the case of MeH production that causes UPR-Cyto, sHsps that should prevent aggregation can be possibly activated at an elevated temperature. Additional heat shock would also induce Hsf1 regulated reintroduction of large and small Hsps that may help counter aggregate formation.

The cell culture growth phase is also important for the application of temperature shock. Yeast cell culture undergoes three main growth phases – laq, logarithmic (log) and stationary. During the log phase the cells actively multiply and perform aerobic glucose fermentation generating a by-product ethanol. When all the glucose in the media is used up, yeast cells switch their metabolism to oxidize ethanol and this switch is called diauxic shift or the Crabtree effect (De Deken, 1966). During this phenomenon an enormous change in gene expression takes place – stress-response proteins and glucose-repressed proteins are induced, glucose metabolizing enzymes are repressed, cell division speed reduces (Haurie et al., 2004). During the ethanol oxidation phase, is when the heterologous protein production is the most efficient (Ferndahl et al., 2010), especially for complex and glycosylated proteins (Liu et al., 2012; van de Laar et al., 2007). It is believed that it is so because of the stress response activation and improved protein folding and secretion (van de Laar et al., 2007).

The approach of heat shock application at a certain yeast cell growth phase has already been successful. Genetically modified *S. cerevisiae* strain, with constitutively active heat shock of various degrees (mutant *HSF1-R206S* gene), increased the α-amylase synthesis rate three times at the end of the glucose, and two times at the end of the ethanol phase. Unfortunately, the same strategy proved ineffective for the biosynthesis of human insulin precursor (Hou et al., 2013).

1.7. Human calreticulin protein and its production in yeast *S. cerevisiae*.

Calreticulin (CALR) is a multifunctional Ca^{2+} binding protein, encoded by the *CALR* gene and is present in all cells that contain ER, except yeast. It consists of 417 amino acids with highly conserved sequence between distant species and has a molecular weight of 46-kDa (Määttänen et al., 2010; Qiu & Michalak, 2009). CALR consists of three structurally and functionally distinct domains: N-globular, P-arm and C-domain. The N-domain (residues 1–180) is a globular lectin-like domain comprised of eight anti-parallel β-strands, and

a single disulfide bridge. It contains oligosaccharide- and polypeptide-binding sites, cleavable signal sequence and is responsible for interactions with DNA, α-integrins and binding of Zn^{2+} ions (Burns et al., 1994; Michalak et al., 2009; Williams, 2006). The P-arm domain is proline-rich domain located in the middle of CALR amino acid sequence (residues 181–290) that forms and extended-arm-like structure (Gelebart et al., 2005). It contains two sets of three repetitive regions that, together with the N-domain, are believed to be involved in forming lectin-like structures that ensure the protein-folding ability of CALR. It has also been shown, that P-domain can also bind Ca^{2+} with low capacity (1 mol of Ca^{2+} per 1 mol protein) and high affinity (K_d = 1μM) (Baksh & Michalak, 1991; Michalak et al., 2009). The C-domain (residues 291–400) is highly acidic and comprised mostly of negatively charged residues. At the end of this domain is the KDEL sequence responsible for CALR retrieving from the Golgi apparatus to the ER (Nakamura et al., 2001). C-domain is responsible for CALR Ca^{2+} buffering functions and can bind Ca^{2+} with high capacity (25 mol of Ca^{2+} per 1 mol protein) and low affinity (K_d = 2M), binding around 50% of all Ca^{2+} in the ER (E. F. Corbett et al., 1999; Michalak et al., 2009).

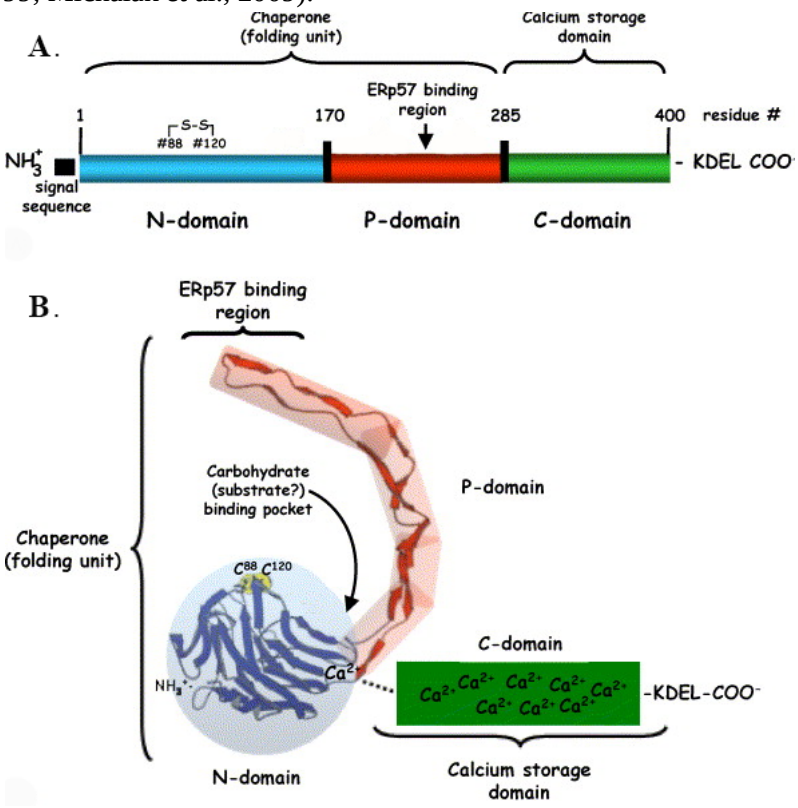

Figure 12. A schematic depiction of CALR structure. A – domain position portrayal in the CALR amino acid sequence. B – domain representation in the CALR protein structure. Figure adapted from (Gelebart et al., 2005).

CALR is best known for its role in the ER. Here, together with calnexin (an integral ER chaperone) and ERp57 (a PDI-like protein) it forms the calreticulin/calnexin cycle, which is responsible for newly synthesized glycoprotein folding and quality control (Wang et al., 2015). CALR binds Ca^{2+} with high capacity and this way regulates Ca^{2+} homeostasis and Ca^{2+}-dependent pathways in the cell (Michalak et al., 2002) and is also necessary for MHC lass I antigen processing (Gao et al., 2002). Despite having the ER-retrieval signal sequence KDEL, that should withhold this chaperone predominantly in the ER, CALR has been found in cytosol, nucleus, on the cell surface and even in the extracellular compartments (Kielbik et al., 2021). There it has even more diverse and important functions. In the cytoplasm, CALR mediates the integrin-dependent cell adhesion, transduces signals between integrins (Coppolino et al., 1997; Coppolino & Dedhar, 2000) and Ca^{2+} channels, and affects RNA stability (Nickenig et al., 2002; Totary-Jain et al., 2005). CALR in the nucleus mainly cross-talks with transcription factors, modulates the activity of nuclear receptors by affecting transcriptional regulation (Qiu & Michalak, 2009), and may even act as an import protein (Michalak et al., 2009). Cell surface and extracellular CALR has even more important functions in cellular proliferation (Nanney et al., 2008), cell adhesion (Coppolino et al., 1997; Coppolino & Dedhar, 2000), cell migration (Orr et al., 2003), phagocytosis of apoptotic cells (Gardai et al., 2005) and plays a role in the adaptive immune response, in the uptake of calreticulin-producing cancer cells by dendritic cells (Tesniere et al., 2008) and in wound healing (Greives et al., 2012; Nanney et al., 2008). It was also shown that exogenous CALR can rescue CALR-deficient cells in different CALR-dependent functions, such as cell migration, adhesion, immunoregulation and phagocytosis (Gold et al., 2010). That is why CALR protein has significant therapeutic potential for impaired diabetic wound healing, cancer therapy and many others (Chaput et al., 2007; Gold et al., 2010; Greives et al., 2012; Nanney et al., 2008; Obeid et al., 2007; Panaretakis et al., 2008).

Despite the cytoplasmic, nuclear, cell surface-bound and exogenous calreticulin involvement in a wide variety of cellular functions, the way CALR gets out of the ER remains unclear (Gold et al., 2010; Kielbik et al., 2021). It has been proposed that CALR winds-up in the cytosol when its precursor is improperly targeted to the ER, leaks out of the ER to the cytoplasm, is retrieved from ER after the removal of its signal peptide or is being released

into the cytosol due to Ca^{2+} depletion in the ER (Labriola et al., 2010). Since CALR possesses the KDEL motif, it can travel in between ER and Golgi complex and should always be retrieved into the ER. Moreover, CALR is a non-glycosylated protein and thus it lacks the usual requirements for proteins to be exposed via anterograde secretory pathways (Wiersma et al., 2015). However, it has been shown that in some mammalian cell types, the CALR exit from the cell can be induced by ER stress, which can be provoked by various stimuli like anthracyclines (Zhang & Kaufman, 2008), reduction of ER Ca^{2+} levels (Tufi et al., 2008), hypoxia, high temperature or pH imbalance (Kielbik et al., 2021). These stressors induce ER stress and the generation of ROS and condemn cells to immunogenic cell death (ICD)(a class of regulated cell death that elicits antigen-specific adaptive immune response (Kroemer et al., 2013)). The loss of ER homeostasis leads to unfolded protein accumulation in the ER and subsequently UPR. Downstream the ER stress pre-apoptotic and killer proteins are activated (BAP31, Bax, Bak). At the same time, CALR released from the ER is removed from the cell by N-ethylmaleimide-sensitive fusion protein-attachment protein receptor (SNARE)-dependent exocytosis pathway. SNAREs attached to the vesicles, interact with synaptosome associated protein 23/25 (SNAP23/25) in plasma membrane, and fuse vesicles to the membrane (Asadzadeh et al., 2020; Rufo et al., 2017). For the ER stress-induced translocation of CALR to the cell surface, co-translocation with ERp57 is essential. In the ER lumen ERp57 is tightly bound to the P-domain of CALR (Oliver et al., 1999), and the disruption of this bond inhibits CALR exocytosis to the cell surface (Coe & Michalak, 2010; Panaretakis et al., 2008). It has also been proposed that post-translationally modified CALR may be retro translocated from a properly functioning ER to the cytosol (Afshar et al., 2005) and then exposed on the cell surface, when the cells are under stress (Tarr et al., 2010). Citrullinated and arginylated isoforms of CALR has been found on the cell surface (Wiersma et al., 2015). In some cancer types, the loss of the C-terminal KDEL motif due to mutations in the CALR gene are responsible for CALR exit out of the cell (Liu et al., 2019).

Surprisingly, active, high-level secretion of mature native recombinant CALR protein was reported in yeast (Čiplys et al., 2015). When a full-length human CALR precursor with its native signal sequence was expressed in yeast *S. cerevisiae* under *PGK1* gene promoter, it resulted in secretion titer of 60–65 mg/L. The expression of the same CALR precursor under *AOX1* promoter in yeast *P. pastoris* resulted in secretion titer of 180–200 mg/L. The synthesized protein matured properly, was not retained in the ER and was almost identical to its native counterpart from human placenta, with respect to its functional activity *in vitro* and structural integrity. Interestingly, neither the

human KDEL or the yeast HDEL ER-retrieval signals did not stop CALR protein from being actively secreted in yeast. Also, the amount of secreted CALR in *S. cerevisiae* was 4- to 5-fold higher than of other human ER chaperones BiP or ERp57, under the same conditions. It is suggested, that such an efficient secretion of CALR protein is due to its intrinsic properties (Čiplys et al., 2015). In human cells the secretion of CALR can be induced by the ER Ca^{2+} depletion (Peters & Raghavan, 2011) and there is 10–100 fold less free Ca^{2+} in the lumen of the yeast ER (Strayle et al., 1999). Lack of Ca^{2+} can result in CALR conformation that reduces the accessibility of the KDEL retrieval signal and promotes protein secretion (Čiplys et al., 2015). However, the mechanism of CALR secretion in yeast, as well as in higher eukaryotes, is still unclear. It is possible that analysis of this efficient and non-detrimental secretion of CALR may hold some answers to how CALR exits human cells.

To summarize, it is mostly unknown if a recombinant protein will be successfully produced in yeast and what determines it. To further expand the variety of heterologous proteins produced in *S. cerevisiae*, it is important to identify the underlying mechanisms behind the production of these proteins. In this work we investigate how the inefficient production of an insoluble viral surface MeH protein, and an extremely efficient secretion of an ER chaperone CALR, impacts the cellular proteome. These two proteins cause a conundrum – when infected with measles virus, mammalian cells produce and expose MeH protein on the cell surface using the secretory pathway, yet in yeast, this protein is inefficiently translocated and improperly folded in the ER. CALR protein, on the other hand, is supposed to stay in the ER, but is secreted at the high-level from yeast cells. Seemingly, these two proteins should act the opposite. Our hypothesis is, that using proteomic analysis we can determine proteins involved in cellular mechanisms that could explain the inefficient MeH translocation and efficient CALR secretion. Therefore, the aim of this work was to adapt 2DE- and MS-based proteomic analysis to study the recombinant protein synthesis in yeast *S. cerevisiae*.

2. MATERIALS AND METHODS

2.1. MATERIALS

2.1.1. Plasmids

pFGG3 – empty control vector (generation of which is described in (Slibinskas et al., 2004));

pFGG3-MeH – for inducible expression of MeH protein causing UPR-Cyto stress in yeast (generation of which is described in (Ciplys et al., 2011));

pFGG3-MeN – control for inducible expression of MeN protein, which does not cause the stress response in yeast (generation of which is described in (Slibinskas et al., 2004));
pFGG3-BiP – for the inducible expression of full-length human GRP78/BiP protein was generated by subcloning of HSPA5 gene (GenBank accession no. AF216292) from the plasmid pFDC-BiP (generation of which is described in (Čiplys et al., 2014)) into BcuI site of vector pFGG3 under control of galactose inducible *S. cerevisiae GAL7* gene promoter.
pFGAL7-CRT – for inducible expression and secretion of human CALR protein. pFGAL7 vector was derived from pFGG3 vector (Slibinskas et al., 2004) by removing GAL10/PYK1 promoter using SmaI and XbaI restriction endonucleases (RE). This allows stronger expression of genes under the sole GAL7 promoter. A gene encoding full-length wild-type human CALR precursor (GenBank Acc. no. M84739 for cDNA sequence and UniProtKB acc. No. P27797 for amino acid sequence) was synthesized by GenScript. The gene was subcloned into the yeast expression vector pFGAL7 under control of galactose-inducible yeast *GAL7* gene promoter using BcuI RE. DNA manipulations were conducted according to standard procedures (Sambrook & Russell, 2001). *CALR* gene sequence in pFGAL7-CRT vector was verified by Sanger sequencing.

2.1.2. Yeast *Saccharomyces cerevisiae* strains

The strain AH22 is used in the experiments of this dissertation because of its routine use in our laboratory and the authors familiarity with it. This is a laboratory strain with its entire genome sequenced.
Strain BY4741 is used only as a control in the experiment with the knockout BY4741 ΔSOD1 strain.
AH22 (*MATa leu2-3 leu2-112 his4-519 can1 [KIL-o]*);
BY4741 (*MATa his3Δ1 leu2Δ0 met15Δ0 ura3Δ0*);
BY4741 ΔSOD1 (*MATa his3Δ1 leu2Δ0 met15Δ0 ura3Δ0 ΔSOD1*) (Yeast Knockout Collection);

2.1.3. Culture media

Solid YEPD – yeast extract 1%, peptone 2%, glucose 2%, agar-agar 2%;
YEPD – yeast extract 1%, peptone 2%, glucose 2%;
YEPG – yeast extract 1%, peptone 2%, galactose 2.5%;

2.1.4. Buffers and solutions

Disruption buffer – 50 mM sodium phosphate, pH7.2, 5 mM EDTA, 1 mM PMSF;

Glass beads – 0.5 mm diameter (BioSpec Products Inc., USA);

Bradford assay reagent („Roti-NanoQuant", Carl Roth GmbH.);

Glucose concentration determination kit (Enzytec *fluid* D-Glucose, ThermoFisher Scientific);

Ethanol concentration determination kit (Enzytec *fluid* Ethanol, ThermoFisher Scientific);

2×SDS-PAGE sample buffer – 125 mM Tris-HCl, pH 6.8, 20% glycerol, 8% sodium dodecyl sulphate (SDS), 150 mM dithiothreitol (DTT), 0.01% bromophenol blue;

Protein molecular weight marker – PageRuler unstained protein ladder (ThermoFisher Scientific, #26614), PageRuler prestained protein ladder (ThermoFisher Scientific, #26616)

4% stacking gel – 24.9% 0.5 M Tris-HCl pH 6.8, 0.1% SDS 10% (w/vol), 10% Acrylamide 40% (37.5:1), 34.9% H_2O MilliQ, 0.1% APS 10%, 0.01% TEMED.

10% separating gel (for culture medium analysis, western blots) – 24.9% 1.5 M Tris-HCl pH 8.8 (trishydroxymethylaminomethane solution with the pH brought to 8.8 with hydrogen chloride), 0.1% SDS 10% (w/vol), 24.9% acrylamide 40% (37.5:1), 50% H_2O MilliQ, 0.1% APS 10% (ammonium persulfate), 0,01% TEMED (*N*,*N*,*N*′,*N*′-tetramethylethane-1,2-diamine).

12% separating gel (for second-dimension of 2DE) – 24.9% 1.5 M Tris-HCl pH 8.8, 0.1% SDS 10% (w/vol), 30% Acrylamide 40% (37.5:1), 44.9% H_2O MilliQ, 0.1% APS 10%, 0,01% TEMED.

SDS-PAGE buffer – 25mM Tris, 190 mM glycine (pH 8.3 at 25°C), 0.1%SDS (wt/vol);

Fixation solution – 50% ethanol, 40% HPLC grade water, 10% acetic acid;

Coomassie Brilliant Blue R-250 – 50% ethanol, 10% acetic acid, 0.1% Coomassie Brilliant Blue R-250 (CBB R-250), 40% HPLC grade water;

Destaining Solution – 5% ethanol, 12.5% acetic acid in HPLC grade water;

Storage Solution – 7% acetic acid in HPLC grade water;

Cathode buffer for NEPHGE first-dimension separation – 20 g of glycerol, 216 g of urea, and 170 ml aqua dist., filled up to 380 ml; then 20 ml of ethylenediamine added; solution prepared on a 40°C heating plate;

Anode buffer for NEPHGE first-dimension separation – 72g of urea, and 300 ml aqua dist., filled up to 380 ml; with the addition of 20 ml of phosphoric acid;
Equilibration buffer – 125 mM of Tris-H3PO4 (125 mM Tris solution with the pH brought to 6.8 with phosphoric acid), 40% of glycerol, 3% of SDS;
Protein transfer buffer – 3.05 g/L Tris, 14.4 g/L glycine, 15% ethanol, MilliQ H_2O;
PBS buffer – 14.42 g/L Na_2HPO_4, 3.9 g/L $NaH_2PO_4 \times H_2O$, 5.84 g/L NaCl, MilliQ H_2O, pH 7.5;
PBS-Tween – PBS, 0.005-0.1% Tween 20.
5% Bovine serum albumin (BSA) solution – 5 g BSA, 95 ml PBS-Tween;
3,3',5,5'-Tetramethylbenzidine (TMB) Liquid Substrate System for Membranes (Sigma-Aldrich, #T0565);

2.1.5. Antibodies

Rabbit anti-Kar2 antibody (y-115, sc-33630, Santa Cruz Biotechnology);
Rabbit anti-Sis1 antibody (COP-COP-080051, Cosmo Bio Co, Japan);
Mouse anti-GAPDH Loading Control antibody (GA1R, Thermo Scientific);
Horseradish peroxidase (HRP)-labelled goat anti-rabbit conjugate (172-1019, Bio-Rad);
Horseradish peroxidase (HRP)-labelled goat anti-mouse IgG conjugate (172-1011, Bio-Rad);
Mouse monoclonal Tetra-His Antibody (QIAGEN, USA);

2.1.6. Ampholytes

Servalyt pH 2–11 (Serva), Pharmalyte pH 5–8 (SigmaAldrich), Pharmalyte pH 4–6.5 (SigmaAldrich), Ampholyte high-resolution pH 6–9 (Carl Roth), Ampholyte high-resolution pH 3–10 (Carl Roth).

2.2. METHODS

2.2.1. Yeast strain transformation

The aforementioned plasmids were used to transform *S. cerevisiae* strains using the conventional LiCl method (Sambrook & Russell, 2001).

2.2.2. Cell culture growth and temperature conditions

2.2.2.1. Growing conditions for yeast cells used in the comparative proteomic experiments

S. cerevisiae cell cultures were grown under aeration in 100 ml shake flasks with 20 ml of YEPD medium with 5 mM of formaldehyde. The synthesis of MeH, MeN, CALR was then induced with YEPG medium. Shortly, *S. cerevisiae* cells transformed with plasmid carrying measles virus H and N genes, human CALR gene, or an empty control vector, were inoculated into YEPD medium with 5 mM of formaldehyde, grown overnight and then re-inoculated into fresh YEPD medium with 5 mM of formaldehyde to 0.05 OD600. The cell culture was then grown for 21 hours, centrifugated for 5 min at 800×*g* room temperature, the old growth media discarded, fresh induction medium YEPG with 5 mM of formaldehyde added, and the cells resuspended. After change of the growth medium, cells were grown for 16–21 hours and then harvested by centrifugation and stored at –70°C.

2.2.2.2. Growing and heat shock conditions for yeast cells used in the MeH translocation improvement experiment

S. cerevisiae cell cultures were grown under aeration in 100 ml shake flasks with 20 ml of YEPD medium with 5 mM of formaldehyde. The synthesis of MeH was then induced with YEPG medium. At different time points before or after protein synthesis induction, heat shock was applied in 42 °C water bath for 2 min with following transfer to 37 °C shaker and further agitation at 220 rpm at 37 °C until the end of MeH biosynthesis. In the case of manipulations "37°C-30°C", the cultivation at 37 °C after heat shock was maintained for 3 h, and then shake flask cultures were shifted back to 30 °C until the end of MeH synthesis. In all independent experiments, at least one control variant with constant cultivation at 30 °C was included.

For the determination of growth curve, an overnight culture of MeH-transformed *S. cerevisiae* was diluted with fresh YEPD medium with formaldehyde to an OD of 0.05, and the experiment was per-formed in triplicate. Every 2 h OD_{600} was measured throughout the cultivation at 30 °C for 72 h under agitation at 220 rpm. The samples for measuring glucose and ethanol concentrations in the culture medium were taken at various time points and analysed as described below.

To evaluate heat shock impact on MeH translocation at different yeast culture densities, flasks were shifted to heat shock temperature and further incubated for 5 h at 37 °C followed by medium change to YEPG, and the synthesis of MeH was performed at 37 °C for 16 h as described above. Manipulations with controls of each OD point were the same as for 37 °C variants, except that the controls were constantly cultivated at 30 °C temperature.

2.2.3. Harvesting the cell culture medium

The culture growth medium was harvested by pelleting a portion (1ml) of the cell culture by centrifugation for 1 min at 16000×*g*, and collecting the medium.

2.2.4. Determination of glucose and ethanol concentrations in the culture medium

Harvested culture medium was divided into two equal parts and stored at –20 °C prior to analysis using enzymatic test kits from R-Biopharm AG. Enzytec fluid D-Glucose Test (E5140) and Enzytec fluid Ethanol Test (E5340) were used according to the manufacturer's instructions for determination of glucose and ethanol concentrations, respectively.

2.2.5. Cell culture medium sample preparation and SDS-PAGE

Freshly harvested culture medium was mixed in equal parts with 2×SDS-PAGE sample buffer and immediately boiled for 8–10 min. Prepared media samples were loaded onto a 10% SDS-PAGE gel, 16 µl per well, and the electrophoresis was run in SDS-PAGE buffer. PAA gels were fixed for 15 min in Fixation solution and stained for 25 min with Coomassie Brilliant Blue R-250 followed by destaining in 5% acetic acid.

Purified CALR protein (UAB Baltymas) used for densitometric quantification was prepared correspondingly, but diluted with 1×SDS-PAGE sample buffer to load different concentrations onto the PAA gel.

2.2.6. Preparation of yeast lysate samples and SDS-PAGE

10–20 mg of yeast cells were pelleted and gathered into a 1.5 ml microcentrifuge tube by centrifugation. The cell pellets were washed with distilled water and resuspended in 10 volumes (vol/wt) of disruption buffer. An approximately equal volume of glass beads (0.5 mm diameter) was added and cells were disrupted by vortexing at max speed, 8 times for 30 sec, and cooled on ice for 30 sec after each vortexing. A volume, equal to the volume of disruption buffer used, of 2×SDS-PAGE sample buffer was added, mixed and the sample was boiled for 10 min. 4 µl (up to 20 µg of protein) of the prepared whole cell lysate sample was loaded onto 10% SDS-polyacrylamide gel, then run in the SDS-PAGE buffer, fixated, stained and destained (as mentioned before).

2.2.7. Determination of protein concentration

Protein concentrations were determined by Roti-Nanoquant Protein-assay (Carl Roth Gmbh.), which is a modification of Bradford's protein assay.

2.2.8. Western blotting

For Western blotting, the protein concentrations between samples were measured and equalized by diluting the samples with 1×SDS-PAGE sample buffer. Then, an equal amount of protein in all samples was loaded onto SDS-PAGE gel and run. After SDS-PAGE the proteins from the gel were transferred to a nitrocellulose membrane Hybond™ ECL (Amersham, UK), as described in (Sambrook & Russell, 2001). The membranes were incubated over night with primary and for 2 h with secondary antibody-HRP conjugates, following the manufacturer ‘s recommendations. After the incubation, the membranes were washed and developed using TMB substrate.
Anti-GAPDH Loading Control Antibody was used in MeH translocation experiment blots to ensure that an equal amount of proteins was loaded into all lanes.

2.2.9. Cell sample preparation for 2DE

300–500 mg of cell pellets were collected into a glass test-tube by centrifugation, washed with distilled water and frozen at –80°C. After storing, the cells were placed on ice and resuspended in 3-10 volumes (v/w) (depending on the experiment) of denaturing IEF buffer containing 7 M urea, 2 M thiourea, 2% CHAPS detergent, 1% ampholytes (pH 3–10, Pharmalyte, GE Healthcare), 0.002% Bromophenol Blue and 75 mM DTT (added just before use). The cells were lysed by adding a glass bead volume twice the weight of cell pellets and vortexing at max speed 8 times for 30 sec. Samples were cooled for 10 sec on ice following 30 sec at room temperature between each vortexing. Cell debris was removed by centrifugation at 16000×*g*, for 15 min at 16°C. Cell lysate supernatants were collected and protein concentrations were measured using a modified Bradford’s protein assay (Roti-Nanoquant, Carl Roth GmbH). Samples were diluted with IEF buffer to equalize the protein concentrations. Prepared yeast cell lysates were stored frozen at –80°C.

The IEF buffer used for sample preparation was suitable for both 2DE methods used in this dissertation, according to the manufacturer’s recommendations (Invitrogen and WITA, respectively).

2.2.10. Making of NEPHGE gels

NEPHGE gels were made with a non-linear pH gradient formed by CAs. Each CA mixture was designed with narrow and broad pH range ampholytes commercially available at the time. Our restored "New mix" ampholyte blend (Mix no. 3 in the Table S1.) consists of: Servalyt pH 2–11 (Serva) – 1 part; Pharmalyte pH 5–8 (SigmaAldrich) – 2 parts; Pharmalyte pH 4–6.5 (SigmaAldrich) – 3 parts; Ampholyte high-resolution pH 6–9 (Carl Roth) – 1 part; Ampholyte high-resolution pH 3–10 (Carl Roth) – 1 part; total of 8 parts. This CA mixture was then incorporated into two essential NEPHGE gel solutions – separation gel (Sep gel) and capping gel (Cap gel) described in (Klose & Kobalz, 1995).

2.2.11. Casting NEPHGE first-dimension gels

Shortly, Sep gel and Cap gel were cast in succession in a vertical device for casting two-layered rod gels for the first dimension. The Sep gel takes-up about 2/3 and the Cap gel 1/10 to 1/20 of the glass rod mold – the rest is left for the sample. For the 8 cm length IEF gel (11 cm rod mold) 500µl of Sep gel with 12 µl 0.8% APS and 100 µl of Cap gel with 2.5 µl of 0.8% APS is required (all solutions are degassed by sonication). After casting, the initial polymerisation of the Cap gel was achieved by leaving the gel undisturbed for 30 min at room temperature. Later, the rod mold was removed from the casting device, a drop of distilled water was placed on top of the rod on the sample loading side (to prevent drying-out), ends of the rod were covered with caps or parafilm wax and left to fully polymerize for 72 hours. WITA NEPHGE gels were cast almost identically using a set of standardized materials.

2.2.12. Running the first dimension

2.2.12.1. First-dimension separation using IPG strips

Briefly, IPG strips (ZOOM strips pH 3-10NL, Invitrogen) were used for IEF in Invitrogen ZOOM IPGRunner System. 50 or 100 µg of the protein from whole cell lysate was diluted to 155 µl by IEF buffer and applied onto IPG strip following rehydration overnight. Next day the ZOOM IPGRunner Mini-Cell was assembled and IEF was performed using "PowerEase 500 Power Supply" (Invitrogen) with the following running conditions: 200 V for 20 min; 350 V for 10 min; 500 V for 4 hrs. Finally, a higher voltage step at 2000 V was performed as recommended by manufacturer (for 2 hrs, the power

supply “Consort EV233”). Focused IPG strips were stored in a sealed container at –80°C. The strips were equilibrated just before the second dimension by incubating them in the equilibration buffer supplemented with reducing (75mM DTT) and alkylating (125mM IAC) agents (treated for 15 min by both).

2.2.12.2. First-dimension separation using NEPHGE rod gels

After the full polymerization of rod gels, the first-dimension separation of proteins was performed in a vertical electrophoresis device (Klose & Kobalz, 1995). The lower chamber of the unit was filled with 400 ml of degassed cathode buffer. The rod gels were fixed in the device with their ends submerged into the cathode buffer and the water cork was removed. Sample solutions containing 80–200 μg of proteins from whole cell lysates were mixed with pre-heated (to 50°C) agarose-supplemented ampholyte phosphate buffer in a ratio of 4:1, immediately applied to the anode ends of the capillary gels leaving no trapped air bubbles, covered with 10 μl of sample-stabilizing overlay solution (O’Farrell et al., 1977) and left to set for 5–10 min. After the solidification of a sample, 400 ml of degassed anode buffer was poured into the upper chamber submerging the rod gels. The first-dimension electrophoretic separation of proteins was conducted by using the following sequence of running conditions: for small 11 cm rods – 100 V for 75 min; 200 V for 75 min; 400 V for 75 min; 600 V for 715 min; 800 V for 10 min; 1000 V for 5 min. After the electrophoresis had ended, the rod gels were carefully pushed out of the glass tube molds onto plastic rails with the help of a syringe. Then, the gels were adapted to the conditions of second-dimension by a series of three 15 min incubations in equilibration buffer and 75 mM of DTT, following three 15 min equilibrations in the same buffer with 125 mM IAC. The equilibrated gels were stored in –80°C before the application to the second-dimension separation system.

2.2.13. Second-dimension separation by SDS-PAGE

For separation in the second dimension of 2DE, standard SDS-PAGE was performed with 11% or 12% (w/v) polyacrylamide gels using a Minigel-Twin units (Biometra). Briefly, the IPG strips and rod gels of the first dimension were gently transferred from equilibration and storage rails to the top of the stacking gel zones and covered with 0.5% (w/v) agarose to fix the rod gels. The electrophoresis running conditions of the second-dimension separation were set as follows: 15 mA per gel (~100 V) for ~ 15 min (until the

dye reached resolving gel); 30 mA per gel (voltage gradually rises up to 200 V limit) for about 1 hr, until the bromophenol blue front reached the bottom of the gel.

After 2DE protein separation was complete, gels were fixed in Fixation Solution for at least 1 h under gentle agitation at room temperature (RT) and stained with Coomassie Brilliant Blue R-250 overnight under gentle agitation at RT. Next day the gels were destained in Destaining Solution for 1 hr under gentle agitation at RT followed by further destaining with Storage Solution for 4 hr (at least 2x exchange of solution) at RT.

2.2.14. Gel scanning and image analysis

2.2.14.1. Analysis of 1D SDS-PAGE gels and Western blots

All 1D gels were scanned using ImageSanner III (GE Healthcare) using blank filter, transparent mode and 300 dpi resolution. Densitometric analysis of 1D SDS-PAGE gels was performed with ImageQuant TL (GE Healthcare) using default settings.

Protein band intensity values were normalised to their respective loading control (GAPDH) or control (30°C) bands in Western blots.

To assess the amount of MeH glycoprotein, in the MeH translocation experiment, the volumes of two bands of ~75 kDa corresponding to glycosylated MeH form (indicated by dotted arrows in Figs 15, 17 and 18) in Western blots were summed up. The major ~65 kDa band (indicated by solid arrows in Figs 15 and 18) was not included into calculations of glycoprotein amount, because it represents untranslocated unglycosylated MeH precursor localized in cytosol (Ciplys et al., 2011). The volumes of glycosylated MeH in all analysed variants were compared to a volume of corresponding bands in control sample derived from cells constantly incubated at 30 °C. As the ratio of MeH glycoprotein and polypeptide precursor changed at the different conditions studied, we also calculated translocation efficiency. It is given as a percentage of glycosylated MeH from the total detected MeH in the same sample.

2.2.14.2. Analysis of 2DE gels

All 2DE gels were scanned using ImageSanner III (GE Healthcare) using blank filter, transparent mode and 300 dpi resolution.

Images of 2DE gels cast with our „New mix“ and „WITA“ solutions were analysed using BioRad PDQuest 8.0.1 2-D analysis software by following the manufacturer‘s recommendations. The coefficient of correlation

(r) was calculated by comparing each gel to another. Pearson's coefficient of correlation measures the linear association of two variables and ranges from –1 to +1, with r=1 meaning a strong linear association (Kirch, 2008).

All other 2DE images were analysed using ImageMaster 2D Platinum 7.0 software (GE Healthcare). Protein spots were detected automatically by setting the same parameters for all analysed 2D gels. Artefact spots and speckles (mostly near the boundaries of the gels) were deleted manually in every 2D gel. Then gels were matched in separate groups followed by matches between the groups according to required comparison. Cellular proteins with differential synthesis patterns were evaluated by calculating the fold change (FC) - the ratio of %Vol between spots. Our selected threshold for FC was 1.5 times (0.58 log2FC) – protein spots that show a 1.5-fold increase or decrease in volume are thought to have differential synthesis patterns, for all experiments. Various comparisons and calculations of parameters were performed as indicated in the legends of tables 1 and 2.

2.2.15. Protein identification

Protein identification MALDI-TOF/TOF and LC-MS^E methods was carried out at the Proteomics Centre in the Institute of Biochemistry, Life Sciences Center, Vilnius University (Vilnius, Lithuania).

2.2.15.1. Sample preparation and protein identification using MALDI-TOF/TOF mass spectrometry

Excised protein spots described in chapters 3.1. and 3.2. were identified using tryptic digestion (Hellman et al., 1995) - mass fingerprinting technique. Protein spots were excised from the gel and cut into 1×1 mm pieces. Gel pieces were destained with 200 µl of 25 mM ammonium bicarbonate in 50% acetonitrile (ACN), dehydrated with ACN and incubated with 40 µl 10 ng/µl of trypsin solution in 25 mM ammonium bicarbonate over night at 37°C. Next day, peptides were extracted with 2 × 100 µl 5% trifluoroacetic acid (TFA), lyophilized and dissolved in 3 µl 0.1% TFA in 50% ACN. Samples were applied to 384-well MALDI plate. 0.5 µl of sample were overlayed with 0.5 µl of matrix (alpha-cyano-4-hydroxycinnamic acid, 4 mg/ml 50% ACN with 0.1% TFA).

Proteins were identified by MALDI mass spectrometry using 4800 MALDI TOF/TOF mass spectrometer (AB/Sciex). Peptide mass spectra were acquired in reflector positive ion mode in m/z range 800–4000 Da, 400 laser shots were summed for each sample with mass accuracy ±50 ppm. MS/MS

spectra for dominating peptides were acquired in positive mode, ion collision energy was set to 1 keV, 500 laser shots were accumulated for each spectrum with mass accuracy ±0.1 Da. Proteins were identified in the TrEMBL database (3-23-10 release) using the Mascot algorithm.

2.2.15.2. Sample preparation and protein identification using LC-MS^E (Data Independent Acquisition) based protein identification

Protein spot samples excised from gels, but identified using LC-MS^E (See chapter 3.4.2.) were prepared as described by (Shevchenko et al., 2006). Whole proteome samples were digested with trypsin according to FASP protocol as described by (Wiśniewski et al., 2009). Briefly, samples were diluted in 8 M urea following two washes with urea and alkylated with 50 mM iodoacetamide (GE Healthcare Life Sciences). Protein concentrators were washed twice with urea and twice with 50 mM NH_4HCO_3. Proteins were digested overnight with TPCK Trypsin 20233 (Thermo Scientific). After overnight digestion, peptides were collected from the concentrators by centrifugation at 14000 *g* for 10 min and additionally eluted using 20% CH_3CN. The eluates were mixed, acidified with 10% CF_3COOH and lyophilized in a vacuum centrifuge. The lyophilized peptides were redissolved in 0.1% formic acid.

LC was performed using a Waters Acquity ul-tra-performance LC system (Waters Corporation). ACQUITY UPLC HSS T3 250 mm analytical column was used to perform peptide separation. Data was acquired using Synapt G2 mass spectrometer and Masslynx 4.1 software (Waters Corporation) in positive ion mode using data-independent acquisition (DIA) coupled with ion mobility separation (IMS, UDMSE) (Distler et al., 2014). For the survey scan, the mass range was set to 50–2,000 Da with a scan time set to 0.8 seconds. Raw data are available via the MassIVE repository with identifier MSV000088879. Raw data was lock mass-corrected using the doubly charged ion of [Glu1]-fibrinopeptide B (m/z 785.8426; [M+2H]2+) and a 0.25 Da tolerance window. The raw data were processed with the ProteinLynx Global SERVER (PLGS) version 3.0.1 (Waters Corporation, UK) Apex3D and Pep3D algorithms to generate precursor mass lists and associated product ion mass lists for subsequent protein identification and quantification. Peak lists were generated using the following parameters: (i) low energy threshold was set to 150 counts, (ii) elevated energy threshold was set to 50 counts, (iii) intensity threshold was set to 750 counts. Database searching was per-formed with PLGS search engine using automatic peptide tolerance and fragment tolerance, minimum fragment ion matches of 1 per peptide and 3 per protein,

FDR < 4%. Trypsin as the cleavage protease was used for data analysis, one missed cleavage was allowed, and fixed modification was set to carbamidomethylation of cysteines, the variable modification was set to oxidation of methionine. UniprotKB/SwissProt *Saccharomyces cerevisiae* databases (2020-09-24) with bovine trypsin (TRY1_BOVIN) were used for protein identification. Label-free quantification using the TOP3-approach was used for the quantification of proteins. TOP3 intensity was calculated as the average intensity of the three best ionizing peptides using ISOQuant (Kuharev et al., 2015). The maximum FDR of protein identification was set to 1%. Log2 transformation was applied to the data before computing fold-changes. The Bayes algorithm of the limma Bioconductor package was used to compute the log2 fold-changes and p-values. The calculated *p*-values are the adjusted FDRs using the Benjamini-Hochberg procedure.

3. RESULTS AND DISCUSSION

The results of this work are presented in four different chapters following the order of the research. In the first chapter the comparison of the first dimension IPG and NEPHGE techniques in two-dimensional gel electrophoresis experiment analysing the UPR-Cyto response caused by the synthesis of MeH in *S. cerevisiae* are described. Following that, the effects of heat shock on the translocation of MeH are presented. The third chapter demonstrates the results of reconstruction of the CA blend and gel solutions for NEPHGE-based 2DE method and the fourth chapter presents a comparative proteomic analysis of the high-level secretion of human CALR in *S. cerevisiae*.

3.1. Comparison of first dimension IPG and NEPHGE techniques in two-dimensional gel electrophoresis experiment with cytosolic unfolded protein response in *S. cerevisiae*

The aim of this study was to directly compare IPG- and NEPHGE-based 2DE techniques by using the same samples and identical second-dimension procedures. For IPG-based 2DE we have chosen Invitrogen "ZOOM IPGRunner" system. This mini-gel 2DE system is simple, unexpensive and both IEF gel length (7 cm) and recommended sample buffer composition is compatible with that of NEPHGE-based 2DE "WITAvision" system. It should be noted that our results represent only usage of Invitrogen IPG-based 2DE system. It was reported that commercially available IPG strips can vary considerably, leading to marked differences in subsequent protein resolution during 2DE (Taylor & Coorssen, 2006).

Earlier comparisons of IPG-based versus NEPHGE-based 2DE techniques (Nawrocki et al., 1998; Nowalk et al., 2006) were made as proteome analysis experiments. Here we performed a differential expression proteomics experiment using both methods and broad (pH 3–10) gradient range on UPR-Cyto stress in yeast *S. cerevisiae* cells. The results were compared to our previous study of the same phenomenon using Invitrogen narrow range pH 4–7 IPG strips (Ciplys et al., 2011). Our data suggest that NEPHGE-based 2DE method is a method of choice for the analysis of basic proteins. The most dramatic demonstration of this statement was identification of highly basic protein Sis1p with differential synthesis pattern by NEPHGE, but not by IPG technique. However, in the acidic pH range both techniques appeared to be similar with some specific advantages and drawbacks. We hope that this study will help others to choose the most efficient system or strategy to perform their proteomics experiments.

Note: IPG-based 2DE was performed by E. Čiplys; gel analysis was performed by R. Slibinskas and statistical analysis was performed by R. Ražanskas. NEPHGE-based 2DE was performed by the author.

3.1.1. Overview of the protocols

The same samples of whole cell lysates from yeast cells producing measles virus hemagglutinin (MeH) or nucleocapsid protein (MeN) and from the control yeast cells (transformed with empty vector pFGG3) were focused in a broad range (pH3–10) IPG strips (Invitrogen) and non-equilibrium pH gradient gels made according to manufacturers' (WITA) recommendations. After equilibration, the strips and gels were applied onto uniform SDS-polyacrylamide mini-gels and run under the same conditions in "Biometra" system. The second dimension SDS-PAGE with following gel staining, scanning and image analysis steps for IPG and NEPHGE samples were performed in parallel. Therefore, the only difference between IPG- and NEPHGE-based 2DE was the first dimension isoelectric focusing step and some deviations in equilibration protocol (IPG strips were equilibrated after, whereas NEPHGE gels before the freezing in –70°C). It allowed direct comparison of the first dimension IPG and NEPGHE techniques as other parameters, conditions and samples in both 2DE experiments were exactly the same.

Examples of 2D gel images are shown in Figures 12 and 13. We have analysed various protein spot parameters at two different experimental conditions: at standard 1x protein load (50 μg of whole cell lysate protein per gel, as recommended by manufacturer of IPG strips) and at high 2x protein

load (100 μg of total protein per gel). General quantitative analysis of IPG- and NEPHGE-based 2DE methods is presented in Tables 1 and 2 respectively, whereas their "trial" comparison with the concrete biological experiment (Ciplys et al., 2011) is summarized in Table 3.

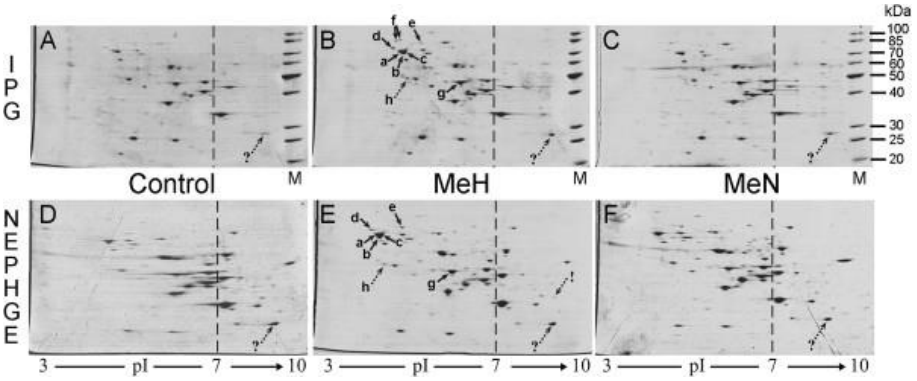

Figure 12. 2DE of yeast whole cell lysates using IPG (A-C) and NEPHGE (D-F) based methods at standard protein load. The same samples from control cells (transformed with empty vector pFGG3; A, D) and MeH (pFGG3-MeH transformant; B, E) or MeN (pFGG3-MeN; C, F) producing cells were loaded onto IPG strips (50 μg of total protein in each strip) and NEPHGE gels (30 μg of total protein in each gel). Approximate pI values are indicated below the gels (pH 3–10 gradient was used in both methods). Dashed line indicates approximate zone of neutral pI 7.0, which separates acidic (on the left, pI < 7) and basic (on the right, pI > 7) protein spots. Protein molecular weight markers (M) are loaded onto IPG-based 2D gels, their masses are indicated at the right (kDa). Arrows point to the spots described in Table 3. Solid arrows indicate protein spots that were identified in our previous work (Ciplys et al., 2011), whereas dotted arrows point to additional spots identified by MS in this study. Quantitative analysis of each indicated protein spot is presented in Table 3.

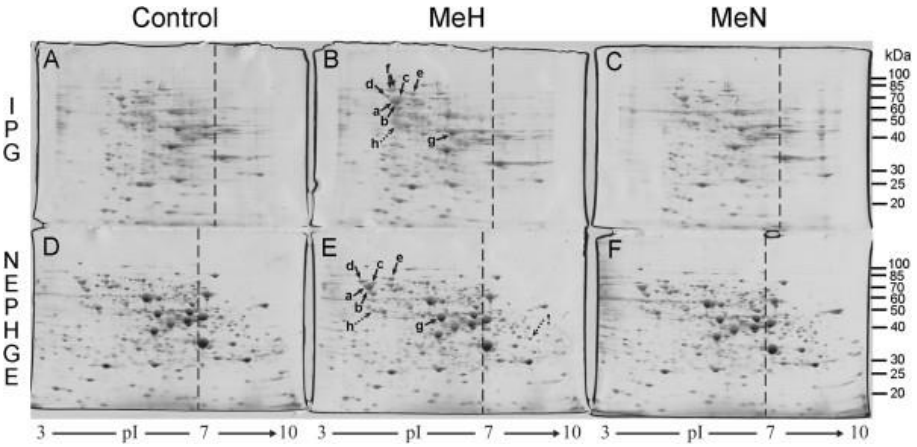

Figure 13. 2DE of yeast whole cell lysates using IPG (A-C) and NEPHGE (D-F) based methods at high protein load. The same concentrated samples from control cells (transformed with empty vector pFGG3; A, D) and MeH (pFGG3-MeH transformant; B, E) or MeN (pFGG3-MeN; C, F) producing cells were loaded onto IPG strips (100 μg of total protein in each strip) and NEPHGE gels (100 μg of total protein in each gel). Original scan of one of the replicas is shown

for comparison (six gels were being scanned in parallel at the same time). The references are the same as in Figure 12.

Table 1. Comparison of spot parameters in IPG- and NEPHGE-based 2DE at standard protein load

Method[1]	IPG[2]			NEPHGE[3]		
Parameter[4]	pI 3-10	pI <7	pI >7	pI 3-10	pI <7	pI >7
Number of detected protein spots[5]	102	79	23	110	80	30
Reproducibility of spots[6]%	75 ± 4%	82 ± 1%	44 ± 18%	76 ± 17%	72 ± 18%	87 ± 20%
Total[7] protein volume in a gel (Vol)	410302 ± 76 913	325075 ± 7 3300	85227 ± 13 613	444930 ± 7 5631	278277 ± 6 9205	166653 ± 15835
Variation of spot volume (ΔVol)[8]	(100 ± 19%)	(79 ± 4%)	(21 ± 4%)	(100 ± 17%)	(63 ± 6%)	(37 ± 6%)
	35% ± 25	36% ± 25	30% ± 25	40% ± 33	46% ± 36	27% ± 21
Variation in relative volumes of spots (Δ%Vol)[9]	30% ± 23	30% ± 23	26% ± 19	31% ± 28	31% ± 30	31% ± 25
Average saliency of protein spot[10]	2794 ± 293	2927 ± 307	2248 ± 947	2610 ± 549	2202 ± 558	3523 ± 81 0
Low quality spots (saliency <500)[11]%	15 ± 3%	14 ± 6%	21 ± 11%	27 ± 8%	30 ± 9%	20 ± 9%

[1]The same samples were analysed in IPG- and NEPHGE-based 2DE systems; ~50µg of whole cell protein was loaded onto IPG strips and ~30 µg onto NEPHGE gels (due to small space for sample application in NEPHGE tubes – see text).
[2]Immobilized pH gradient (IPG) based 2DE method (Invitrogen pH3–10 system).
[3] Non-equilibrium pH gradient gel electrophoresis (NEPHGE) based 2DE method (WITAvision pH3-10 system).
[4]Parameters were calculated from 2–3 replicas (repeating analysis of the same samples). Each parameter was calculated both for whole gel (pI 3–10, all detected proteins) and for its pI <7 and pI >7 parts (acidic and basic proteins, respectively). Neutral pI 7, separating acidic and basic protein spots, is indicated by dashed line in Figure 12.
[5]Number of detected separate protein spots in all samples (Control, MeH ir MeN), from all replicas.
[6]The same spots detected among replicas of the same sample (according to matches of the spots generated by 2D image analysis software *ImageMaster 2D Platinum 7.0*); the percentage of matched spots (±SD) is given for a whole gel (pI 3–10) and for its acidic or basic parts.
[7]Total volume (*Vol*; product of spot area and intensity) of all protein spots in one gel is calculated by 2D analysis software; here the average from whole pI3–10 gel is given as 100% (±SD), whereas pI <7 and >7 indicate acidic and basic protein portions, respectively.
[8]Variation of volumes of the same spots in separate replicas; calculation was made using all spots matched by the software and then the average of variation ΔVol ±SD was calculated.
[9]%*Vol* indicates percentage of volumes of separate spots among volume of all protein spots in a gel. In this case, all matched protein spots were evaluated in the same way as calculating variation of volumes (8), only instead *Vol* the values of %*Vol* was used (the result is average of Δ%Vol ± SD).
[10]Average saliency of detected protein spots per gel ± SD.

[11]Detected protein spots with saliency <500 were considered as low quality spots (see text). The percentage of such protein spots (±SD) was calculated for a whole gel (pI 3–10) and for its acidic or basic parts.

Table 2. Comparison of spot parameters in IPG- and NEPHGE-based 2DE at high protein load

Method[1]	**IPG[2]**			**NEPHGE[3]**		
Parameter[4]	**pI 3-10**	**pI <7**	**pI >7**	**pI 3-10**	**pI <7**	**pI >7**
Number of detected protein spots[5]	432	321	111	506	372	134
Reproducibility of spots[6]%	68 ± 1%	73 ± 4%	51 ± 13%	87 ± 5%	85 ± 6%	90 ± 4%
Total[7] protein volume in a gel (Vol)	1726878 ± 2 60176	1357575 ± 226314	369303 ± 5 9726	2618475 ± 58090	1845417 ± 54127	773057 ± 30071
Variation of spot volume (ΔVol)[8]	(100 ± 15%)	(79 ± 3%)	(21 ± 3%)	(100 ± 2%)	(70 ± 1%)	(30 ± 1%)
	49% ± 55	48% ± 54	55% ± 58	26% ± 31	28% ± 34	22% ± 23
Variation in relative volumes of spots (Δ%Vol)[9]	47% ± 51	46% ± 50	53% ± 57	25% ± 31	27% ± 34	21% ± 22
Average saliency of protein spot[10]	1931 ± 348	2028 ± 366	1419 ± 348	3210 ± 136	2947 ± 307	4189 ± 20 5
Low quality spots (saliency <500)[11]%	20±5%	18±5%	28±7%	11±4%	13±5%	6±3%

2x higher protein amounts were loaded onto 1st dimension gels, than for standard application described in Table 1. Preparation of concentrated whole cell lysates for this experiment is described in Methods section. Other procedures and all calculations were the same as for 1x protein load described in Table 1. An example of 2D gel images from a high load experiment is shown in Figure 13.

[1]The same samples were analysed in IPG- and NEPHGE-based 2DE systems; the equal amounts of ~100 μg of whole cell protein were loaded onto IPG strips and onto NEPHGE gels. [2–11]The references are the same as in Table 1 and all parameters were calculated exactly as described in Table 1 legend.

Table 3. Quantitative analysis of protein spots with differential synthesis patterns by 2DE using pH3–10 range (this study) and pH4–7 platform (previous work, ref. (Ciplys et al., 2011)).

No.[1]	Ref.[2]	Name[3]	IPG 4–7[4]	IPG 3–10[5]		NEPHGE 3–10[6]	
				Standard[5]	High load[5]	Standard[6]	High load[6]
a	1	SSA1/2	2.4 ± 0.2	1,6 ± 0,1	1,6 ± 0,4	2,6 ± 0,3	2,0 ± 0,2
b	2	SSA1/2					
c	3	SSA4					
d	4	KAR2	3.8 ± 0.4	2,7 ± 0,5	1,8 ± 0,4	9,0 ± 3,1	2,5 ± 0,2
e	5	SSE1	2.3 ± 0.2	1,4 ± 0,3	1,8 ± 0,7	2,2 ± 0,8	1,7 ± 0,1
f	6	HSC82	2.1 ± 0.3	2,0 ± 0,2	2,1 ± 1,0	- -	- -
g	6	HSP82					
	7	ENO2	1.5 ± 0.2	1,4 ± 0,3	1,1 ± 0,2	1,3 ± 0,2	1,1 ± 0,1
h	N.I.[7]	SSA1/2[7]	2.2 ± 0.3	1,5 ± 0,1	1,1 ± 0,1	1,6 ± 0,3	2,1 ± 0,4
?[8]	N.A.	GPM1	N.A.	2,2 ± 1,3	0,7 ± 0,2	1,3 ± 0,3	1,0 ± 0,1
![8]	N.A.	SIS1	N.A.	- -	- -	2,6 ± 0,4	2,2 ± 0,2

[1]Protein spots with differential synthesis in this experiment are indicated by letters (see Figures 12 and 13).

[2]The same protein spots are indicated by the numbers in the referenced article ((Ciplys et al., 2011), see Figure nine and Table one).

[3]Accepted name from the *Saccharomyces* genome database (SGD) and YPD. Spots 1 and 2 represent mixtures of similar proteins Ssa1 and Ssa2 (97% identity) at an unknown ratio (see Table one legend in (Ciplys et al., 2011)).

[4]Cellular protein synthesis fold change in MeH producing versus control cells that was determined in previous work using pH4–7 IPG-based 2DE system (Invitrogen); the values are taken from the Table one in reference (Ciplys et al., 2011).

[5]Synthesis fold changes of the same proteins determined from independent experiments in this work using pH3–10 IPG strips (Invitrogen); ~50 μg of whole cell protein was loaded onto IPG strips in "Standard" experiment, whereas ~100 μg was used in a "High load" experiment.

[6]Synthesis fold changes of the same proteins determined from independent experiments in this work using pH3-10 NEPHGE first dimension gels (WITAvision); ~30 μg of whole cell protein was loaded onto NEPHGE gels in "Standard" experiment, whereas ~100 μg was used for each gel in the "High load" analysis.

[7]Not identified (N.I.) in previous study, because increased amount of this protein was observed only in cells producing MeH, but not MuHN protein (the synthesis fold change in MeH/Control cells determined by IPG4-7 system here is given from our unpublished data).
[8]? and ! indicate basic protein spots (pI > 7) that were not analysed in previous experiment on pH4-–7 platform (N.A. – not assayed). Despite that protein spot "?" showed false change in synthesis ("artefact") in IPG-based system (unreliable changes in the biosynthesis are apparent by high error range), in this experiment it was identified as phosphoglycerate mutase 1 (Gpm1p). Protein Sis1p in this study was identified using NEPHGE-based 2DE system, whereas it was not detected by IPG-based 2DE method.

3.1.2. Spot reproducibility

We used Coomassie staining of 2D gels. It is not a very sensitive protein detection method, and in this case manufacturer of IPG strips (Invitrogen) recommends loading 20–50 μg of total protein per ZOOM strip. For "standard" loading experiment, we used maximal recommended protein amount (50 μg) per strip. It should be mentioned that smaller amount of the whole cell protein was used in parallel NEPHGE-based 2DE experiment (~30 μg versus ~50 μg in IPG). The volume of the sample is limited by the narrow tube diameter in NEPHGE procedure; therefore, it is impossible to load more protein if sample is too diluted. An example of 2D gels from this experiment is shown in Figure 12. Under these conditions, IPG- and NEPHGE-based 2DE methods were compared quantitatively in the Table 1. Similar number of protein spots (~100) was detected in 2D gels using both methods. As the study using standard protein load did not represent enough yeast proteins to make firm conclusions, we repeated the experiment by loading double amounts of protein on each gel. For this experiment, we used more concentrated whole cell lysates (see Methods). The same experimental variants were analysed by loading 100 μg of whole cell protein onto each IPG strip and NEPHGE gel. All other 2DE conditions were exactly the same. The number of detected spots at high protein load substantially increased. More than 400 different spots were detected by IPG- and over 500 spots by the NEPHGE-based 2DE (an example of 2D gels is shown in Figure 13, whereas quantitative analysis at high protein load is presented in Table 2).

A comparison of loaded and detected protein amounts suggests that more than 1/3 of total protein amount was lost using IPG strips in comparison to the total volume of protein spots detected in NEPHGE-based 2D gels (Tables 1 and 2). Analysis of the separate parts of 2D gels reveals that the loss of total protein in IPG-based 2DE method is mostly determined by the loss of basic proteins. In Tables 1 and 2 it is shown that protein amount in 2D gels is distributed unequally: in the case of NEPHGE, detected basic protein amount

is twice as large as in IPG-based 2D gels, whereas total volume of acidic protein spots is somewhat similar in both techniques.

The drawbacks of IPG method in the basic gel side are not limited to the protein amount. Different proteins are lost in separate experiments; it is obviously demonstrated by the reproducibility parameter in Tables 1 and 2. Only about a half of basic protein spots detected by IPG-based method (~44% and ~51% at standard and high protein load, respectively) are reproduced, still with large variation. Therefore, in IPG-based 2DE experiment, it is possible to quantitatively evaluate only ~50% of detected basic protein spots, and even these tend to show unreliable results (described below). In contrast, the reproducibility of NEPHGE-based method is best in the basic gel side with the reproducibility of ~90% and minimal gel-to-gel variation at high protein load (Table 2). A few spots in NEPHGE-based 2D gels at standard protein load were not evaluated due to our imperfect performance in the first dimension with a couple of the control sample replicas. Some bubbles introduced during loading of the sample or slightly shorter 1st dimension NEPHGE gel resulted in incomplete focusing or impaired spot resolution (Figure 12, D or not shown). These problems were avoided when running NEPHGE samples at high protein load.

The analysis of acidic proteins shows good reproducibility in the IPG-based method at standard protein load, because >80% spot reproducibility practically coincides with variations of total protein amount in the gel, which in our case reached almost 20% (due to loading errors or differences in gel staining intensities). Lesser amount of protein on the gel results in disappearance of weak spots, and this is the main reason of the differences among the replicas. It is evident from Figure 12 that protein pattern in 2D gels of different samples (Control, MeH, MeN) analysed by the same method is very similar. By comparing our 2D gel images obtained using IPG-based method with earlier IPG-2DE analyses of yeast proteome (Boucherie et al., 1996; Gygi et al., 1999), it could be noticed that positions and relative amounts of the vast majority of protein spots in our experiments match well with the results of previous studies. The exceptions are the protein spots with differential synthesis patterns due to different experimental conditions. Surprisingly, high protein load experiment showed better reproducibility of acidic protein spots in NEPHGE- than in IPG-based 2DE, and the difference was significant. This resulted in considerable difference of overall spot reproducibility with ~87% in NEPHGE- versus only ~68% in IPG-based 2DE (Table 2). It suggests that IPG strips were overloaded. Indeed, some areas in acidic gel zone showed incomplete focusing and loss of resolution in IPG-based 2D gels at high protein load (see Figure 13, upper panel).

3.1.3. Spot quality and protein capacity of the 1st dimension gels

Spot quality is also an important parameter in 2DE analysis. We used ImageMaster 2D Platinum 7.0 software (GE Healthcare), which calculates saliency value for every detected protein spot. This parameter is a measure based on the spot curvature. Real spots generally have high saliency values, whereas artifacts and background noise have small saliencies. The saliency is an efficient parameter for filtering and discarding spots, but it may also be used for the evaluation of the spot quality. Other 2D gel analysis software packages provide some "spot quality" values, which are also based on the spot curvature property. For example, PDQuest software (BioRad) calculates spot quality numbers, which are mainly based on Gaussian fit assessing spot shape. Absolute values of spot saliency may vary depending on brightness and contrast of 2D images. However, in our case all procedures of image processing for both IPG- and NEPHGE-based 2DE gels were the same, and therefore it was possible to compare two methods by using saliency as the spot quality parameter. We have calculated the average saliency of protein spot and the percentage of low-quality spots for every gel. This data is provided in Tables 1 and 2. Average spot saliency for a whole gel at standard protein load was similar in both methods, but again there was a difference when comparing acidic and basic gel zones. Quality of acidic protein spots was higher in IPG, whereas basic proteins were better shaped in NEPHGE-based 2DE method (Table 1). To count low quality spots, we had set an arbitrary value of saliency to 500. The saliency is highly dependent on the images, and, according to the software user manual, gels may need saliency values from 10 to 5000 for correct filtering. We have discarded all spots with a saliency <150, whereas protein spots with a saliency of <500 were defined as low-quality spots. The percentage of low-quality spots of acidic proteins at standard 1x protein load was considerably higher in NEPHGE-based method, whereas the results for spots of basic proteins were similar in both methods (Table 1). However, high protein load experiment showed substantially different results. Spot quality data confirmed that IPG strips were overloaded by 2x total protein amount. Thus, double protein load significantly decreased average spot saliency and increased percentage of low-quality spots in IPG-based 2D gels, whereas NEPHGE-based 2D gels demonstrated increased overall spot quality (see Table 2 and compare with Table 1). Especially convincing was the reduction of low-quality spots in NEPHGE gels, with only ~6% of detected basic protein spots found below saliency value of 500 (Table 2). Lower spot quality in standard protein load experiment may be at least partially explained by our imperfect performance with NEPHGE gels, which is reflected by higher error

ranges of average saliency values than at high protein load (Tables 1 and 2, respectively). Anyway, high protein load onto NEPHGE gels is preferable, because both spot quality and reproducibility are excellent. It seems that loading 100 μg of whole cell protein onto NEPHGE gel is near to optimal amount in a mini-gel format using Coomassie staining. Further attempts to increase protein amount and detect even more spots in a small gel may result in overlapping of neighbouring proteins by spots of high-abundance proteins. Experiments with loading 1x and 2x protein amount per gel revealed different protein capacity of IPG strips and NEPHGE gels. Recommendations of manufacturer to load only up to 50μg of total protein onto broad pH range IPG strip seems to be correct, because double protein amount resulted in overloading and loss of spot quality and reproducibility. Therefore, protein capacity of pH 3–10 IPG strip is limited to ~50 μg of total protein. Meanwhile, the protein capacity of NEPHGE gel is at least ~100 μg of total protein from the same sample. It should be noted that higher protein capacity of NEPHGE gels over IPG strips is not limited to ~twofold. The volume of NEPHGE gels is much smaller than volume of IPG strips of the same length. The volume of NEPHGE tubal gel (7 cm in length and 0.9 mm in diameter) is only ~45 mm3, whereas IPG gel (70 mm × 0.5 mm × 3.3 mm) has a volume of ~115 mm3. Two and half fold difference in volumes means that protein capacity of the same volume NEPHGE gel is ~5 fold higher than that of a broad range 1st dimension IPG gel.

3.1.4. Verification of proteomic results by immunoblotting

To confirm the results of 2DE study, we have done immunoblots using commercially available antibodies against two over synthesized UPR-Cyto proteins Kar2 and Sis1. Kar2p showed the highest increase in biosynthesis in UPR-Cyto stress, but determined fold change greatly varied from 1.8 to 9 depending on 2DE technique and protocol (Table 3). Sis1p was the most important protein identified in this study, because it was a new protein involved in UPR-Cyto stress and exemplified the main advantage of NEPHGE over IPG in the analysis of highly basic proteins. Representative images of Western blot analysis of Kar2p and Sis1p amounts in crude yeast lysates are shown in Figure 3. Alongside with the main Kar2p form, immunoblot has also revealed an additional Kar2p band of slightly higher molecular weight in the cells expressing MeH protein, which induces UPR-Cyto (Figure 3B). Most likely it was a precursor of Kar2 protein with uncleaved signal sequence. Therefore, we have included both bands in calculation of Kar2p synthesis fold change. The results of three independent experiments showed 3.6 ± 0.5

increase of Kar2p synthesis in yeast cells producing MeH protein. It corresponds to the fold change of Kar2p determined in our previous study using a narrow range pH 4–7 IPG-based 2DE method (Table 3). Western blotting showed 1.9 ± 0.2 increase of Sis1p in MeH producing yeast. It confirmed the overproduction of Sis1p during UPR-Cyto.

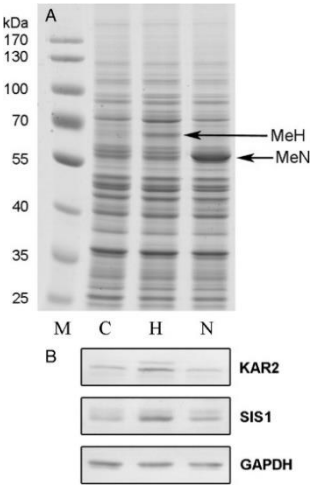

Figure 14. Verification of proteomic results by immunoblot. SDS-PAGE (A) and Western blot (B) analysis of crude yeast lysates are shown. Lysates were prepared from galactose-induced yeast cells of *S. cerevisiae* AH22 strain transformed with empty vector (control, lane C) or plasmids producing MeH (lane H) or MeN (lane N). (A) Coomassie blue-stained gel. Solid arrows indicate bands of recombinant MeH (lane H) and MeN (lane N) proteins. Lane M - prestained protein ladder with molecular weights of bands indicated at the left. (B) Western blot analysis using the same samples transferred onto nitrocellulose membrane. The blots were probed with antibodies against yeast Kar2 and Sis1 proteins. GAPDH was used as loading control.

3.1.5. General comparison of NEPHGE- and IPG-based 2DE methods

General characteristics of both methods are briefly summarized in Table 4. Considering all the data, NEPHGE-based method seems preferable in a broad range pH 3–10 gradient. The examples given above illustrate the essential differences between two methods in Tables 1 and 2: IPG 3–10 (Invitrogen) 2DE method is reliable only for the analysis of acidic proteins, whereas NEPHGE method produced acceptable results in entire pI range and was especially suitable for the analysis of basic proteins. By comparing only, the results at high protein load, we should state that NEPHGE is by far better method, because all protein spot parameters are better than parameters obtained using IPG technique, even in the acidic range (see values in $pI < 7$ columns in Table 2). The results of the differential expression proteomics experiment with UPR-Cyto stress confirmed that high sample load onto pH 3–10 IPG strips is unsuitable for studies of biological effects by 2DE. Therefore, it seems reasonable to discard from comparison high-load experiment with IPG strips and to directly compare IPG-based technique at standard 1x protein load with the NEPHGE-based method at 2x protein load. The comparison at optimal protein loading conditions (see Table 1 for IPG and Table 2 for NEPHGE) reveals very similar performance of both methods

in acidic range with almost identical spot reproducibility and quality. Overall variation of spot volume parameters is also similar in this case, as higher variation averages in IPG-based 2DE are compensated by lower SD values. The only advantage of the NEPHGE method in this case is substantially larger protein amount resolved on 2D gel. As can be seen in Tables 1 and 2, it resulted in almost five-fold higher number of separate acidic protein spots in NEPHGE (372 spots versus 79 spots detected by IPG). The parameters of detected protein spots (reproducibility, quality etc.) were nearly identical in both methods. It suggests that in the acidic zone both spot separation methods reached some optimal level, which results in similarly good parameters of resolved protein spots.

Table 4. General comparison of IPG- and NEPHGE- based 2DE methods

Method	**IPG**	**NEPHGE**
Characteristics		
Preparation of 1st dimension gels	Commercial gels; easy to prepare for IEF	Home-made gels; preparation requires skills
Procedure	Simple, easy to use	Complex, requires skills
Time for analysis	Fast, 2 days	Time-consuming, 5–6 days
Price	Cheap (Invitrogen)	Moderate (WITAvision)
Handling of 1st dimension gels	Handling of IPG strips is safe and easy	Gels are fragile, handling requires serious skills
Reproducibility	Well-reproducible in acidic, poor in a basic zone	Lower in acidic zone, but excellent in basic zone
Possible problems	Poor reproducibility of basic protein spots, protein capacity is limited	Handling difficulties, missing of some highly acidic protein spots
Protein capacity, effect of high protein load	Protein capacity is limited, quality of spots is worse at high protein load	Higher protein capacity, than in IPG gels; quality of spots is good at high load
General characteristic	Simple and easy to use method; ideal for 2-DE of acidic proteins. Drawback is poor reproducibility of basic protein spots.	Method requires skills; excellent for 2-DE of basic proteins. Analysis in acidic zone is satisfactory, but some spots are missed.

The intrinsic property of NEPHGE method is the higher protein capacity of 1st dimension gel than that of IPG gel of corresponding format. It is worth to discuss this in more detail, because it opens new opportunities. Detection of up to 500 good quality spots in a single small 2D gel by using Coomassie staining with relatively low sensitivity is a promising result. Taking into account experimental procedure and protein detection method, it seems difficult to achieve similar result using a broad range IPG strips. Thus, the main problem of pH 3–10 IPG strips seems to be limited amount of total

protein that can be resolved into good quality spots on 2D gel. Moreover, significantly larger protein amount is lost during IPG-based 2DE procedure than in NEPHGE-based method even at standard protein load. In fact, there are several specific steps where the proteins are lost during IPG-based procedure. It was earlier shown that 20–55% of loaded protein is lost due to attachment of the proteins to reswelling tray during in-gel rehydration step (Zhou et al., 2005). Additionally, only 20%–51% of total protein amount loaded onto pH 3-10 IPG strip was resolved onto 2D gel when complex protein mixture was analysed (Zhou et al., 2005). Cited study was performed using IPG strips produced by Amersham (now GE Healthcare). Therefore, it suggests that effects observed with Invitrogen strips in our study may be inherent to all pH 3–10 IPG strips in general. NEPHGE procedure does not include in-gel rehydration step (gels are casted and used fresh), and this could explain lower protein loss during 2DE. However, the most difficult thing is to explain why IPG strips are overloaded by much lower protein amounts than NEPHGE gels.

It should be noted that detection and analysis of large number of protein spots does not require the large amount of protein in the gel. Actually, we did not find any proteomic study on yeast proteins where a large number of protein spots (at least as high as in our study) was analysed by IPG-based 2DE using Coomassie staining method. For example, detection of ~1200 spots and creation of the 2D pattern as the yeast reference map was performed by using radioactive labelling (Boucherie et al., 1996). Another 2DE study using radioactive labelling of yeast proteome reported detection of ~1100 protein spots (Norbeck & Blomberg, 1997). Silver staining of large IPG-based 2D gels of yeast lysates resulted in visualisation of ~1000 spots per gel (Gygi et al., 1999). Yet another silver staining procedure was reported to visualise of ~1500 spots of yeast proteins; however, in that case a narrow range pH 4.7–5.9 IPG strip of the largest possible 25 cm length was used (Gygi et al., 2000). The use of silver staining for medium, 13 cm length, pH 3–10 IPG-based 2D gels resulted in detection and quantification of ~400 yeast protein spots per gel (Kolkman et al., 2005). Finally, the most spots in yeast proteome were detected by using fluorescent SYPRO Ruby staining method, which resulted in >2,000 protein spots on each 2D gel (Jun et al., 2012). However, the numbers of protein spots detected by IPG-based 2DE in any reported study seem small if compared to the potential of NEPHGE-based 2DE method. Over 10,000 protein spots were detected in one NEPHGE-based 2D gel using silver staining (Klose & Kobalz, 1995). It is not clear why several times more sensitive protein detection methods are necessary if it is possible to detect the same thousands of proteins by simple Coomassie staining after loading much

larger amount of protein mixture onto the 1st dimension gel. This would be convenient for both quantitative analysis and mass spectrometry protein identification. Usually, it is possible to unambiguously identify any protein spot visualised by Coomassie staining. Most likely, 2DE analysis of a whole proteome using Coomassie stain was not being used due to limited protein capacity of IPG strips. In this context, NEPHGE technique may offer an improvement in 2DE-based proteomic studies.

When comparing narrow range pH 4–7 IPG (Invitrogen) and pH 3–10 NEPHGE systems, it is more difficult to conclude which method is better. Inability to detect some less abundant acidic proteins by the NEPHGE-based method at standard protein load was easily solved by increasing the amount of total cell protein. The essential drawback of the NEPHGE-based method in acidic protein analysis is disappearance of some protein spots with differential synthesis patterns. The examples here were Hsc82 and Hsp82 protein spots. However, NEPHGE-based method enabled identification of aforementioned differentially synthesized basic Sis1 protein and this would compensate drawbacks in the acidic pI range. It should be mentioned that we have used anodic isoelectric focusing (AIF; sample applied to the anodic side of the gel) according to the NEPHGE technique developed by Klose (Klose, 1975), in contrast to cathodic isoelectric focusing (CIF; sample applied to the cathodic side of the gel) developed by O'Farrell (O'Farrell, 1975). It was reported earlier that when using CIF, a whole class of proteins (very basic proteins) is lost, whereas when using AIF, a certain amount of each protein in a protein class (very acidic proteins) do not enter the gel (Klose & Kobalz, 1995; O'Farrell et al., 1977). Our results suggest that the broad range pH 3–10 IPG-based 2DE method suffers from the same limitations (loss of the very basic proteins) as CIF technique of the NEPHGE method. Here is important to note that these specific problems are rather small if compared to the main drawback of a basic 2DE method itself. A lot of proteins do not enter any 2D gels at all. Usually, a very few membrane proteins are detected by 2DE. Moreover, there are also other protein classes that are not presented on 2D gels. Good example is recombinant viral proteins MeH and MeN with the pIs of ~6.6 and ~5.2, respectively. In this study they were overproduced in the yeast cells and are presented as strong bands in SDS-PAGE of crude yeast lysates (Figure 14A). If all proteins from whole cell lysates would enter 2D gels, MeH and MeN should be presented at microgram amounts. However, no traces of these proteins were observed in 2D gels using both 2DE methods (Figures 12 and 13). It is evident that the loss of more than a half protein amount during 2DE procedure (Zhou et al., 2005) is rather specific and a lot of proteins are totally lost from the samples. Taken together, there is no ideal technique for 2DE

method, because all techniques have some drawbacks. In our case, it seems the most efficient way to be the usage of large format NEPHGE gels for a broad range pH 3–10 analysis, whereas in the acidic range the analysis could be doubled by the narrow range IPG mini-gels (pH 4–7 or pH 4.5–5.5 etc.).

3.2. Heat shock at higher cell densities improves measles hemagglutinin translocation in *S. cerevisiae*

Although *S. cerevisiae* is a model organism that is widely used for recombinant protein production and is capable of post-translational processing, the synthesis of human virus surface glycoproteins and other complex mammalian proteins is still very troublesome. It was shown that the generation of active measles hemagglutinin (MeH) protein in *S. cerevisiae* is inefficient mostly due to a bottleneck in the translocation of viral protein precursors and, the induction of a cytosolic unfolded protein response (UPR-Cyto). The UPR-Cyto induces the expression of a subset of protein genes involved in heat-shock response (Ciplys et al., 2011). The activation of temperature-regulated chaperones suggested that temperature itself may have an impact on recombinant protein synthesis. Environmental changes, such as temperature, nutrition, oxidation, pH and osmolarity induce drastic responses in a large set of yeast genes (Causton et al., 2001). Potentially, any of these conditions could be used to change the biosynthesis efficiency of a recombinant protein. The aim of this study was to improve the translocation of MeH in *S. cerevisiae* by manipulating cell culture conditions.

Recombinant MeH is also a convenient model to assess translocation into the yeast ER. When produced in yeast, this protein is found in forms of unglycosylated precursor (~65 kDa) and N-glycosylated MeH protein (~75 kDa) that are easy to distinguish by Western blot. The unglycosylated MeH precursors are localized in the cytoplasm, where they form insoluble aggregates with cytosolic yeast proteins (Ciplys et al., 2011), whereas the glycosylated MeH represents protein translocated into the ER (Čiplys et al., 2011). Therefore, the amount of MeH glycoprotein shows translocation load, whereas the ratio of N-glycosylated form to total MeH protein indicates translocation efficiency.

In this work, we investigated the effect of heat shock and cell culture density on the translocation of recombinant MeH glycoprotein. Heat shock at higher culture densities followed by protein synthesis at 37 °C resulted in about 3-fold increase of both translocation efficiency and the amount of MeH glycoprotein. Further, we used NEPHGE-based 2DE analysis to identify high-abundance cellular proteins, changes in synthesis patterns of which correlated

with improved translocation of MeH into the yeast ER. Finally, 15 cellular proteins were selected as targets for the improvement of recombinant protein production.

3.2.1. The effect of heat shock and culture density on the translocation of recombinant MeH protein into the ER of yeast cells

Galactose-inducible expression system provides a wide window for choosing heat shock timing and duration. In our initial experiments, we incubated transformed cells for the same duration as in our previous study (Ciplys et al., 2011) and applied heat shock at various time points before or after MeH synthesis induction with subsequent temperature shift to 37 °C. The example of these experiments is provided in Fig. 15a. The largest increase of glycosylated MeH was obtained when heat shock was applied 5 h before the induction of MeH synthesis and the cells were maintained at 37 °C till the end of MeH production. Under these conditions, the amount of glycosylated MeH increased about 3-fold when compared to the usual incubation at 30 °C. Other heat shock conditions showed lesser effect on MeH translocation, whereas manipulations at 30 °C–37 °C–30 °C (see Methods) were not effective. When 20 °C instead of 37 °C temperature shift was used, the amount of glycosylated MeH decreased by 4–5-fold (to ∼20%). The relationship between heat shock conditions and glycosylated MeH amount is summarized in Methods Fig. 15b. There is a lack of data regarding effects of higher temperatures on the synthesis of heterologous recombinant proteins in yeast. It was reported that elevated biosynthesis temperature increased secretion yield of a hyperthermophilic enzyme by as much as 440% per cell in *S. cerevisiae* (Smith et al., 2005), but it may be related to specific properties of the recombinant protein. We guess that possible positive heat shock effect on recombinant protein synthesis may be simply unnoticed due to the fact that experiments in yeast are usually performed in early- or mid-log phases of glucose growth, where an increase of glycosylated MeH amount after heat shock was not observed (Fig. 16b).

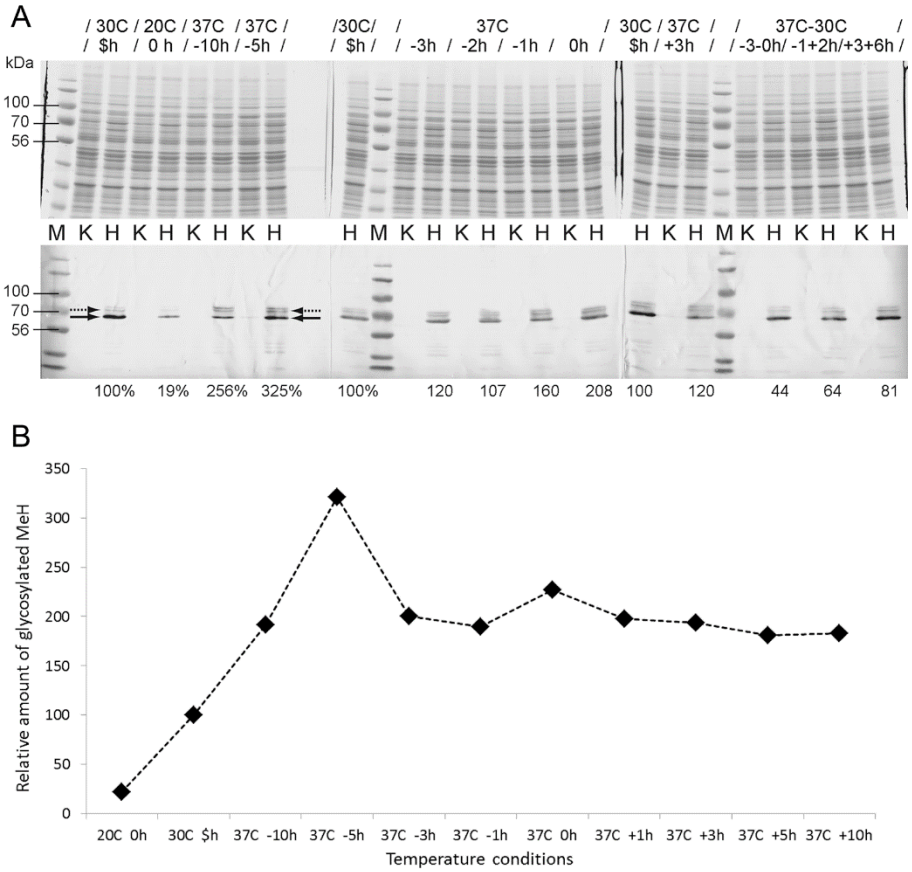

Fig. 15. MeH translocation after shift to 37°C temperature at different time points before and after protein synthesis induction. (a) Example of independent experiment. SDS-PAGE gels are shown at the top and corresponding Western blots against MeH protein—at the bottom. M—molecular weight markers; K—samples from cells with empty vector pFGG3; H—cells transformed with pFGG3-MeH. Temperature conditions are indicated above the PAA gels: 30C $h—control culture constantly incubated at 30°C temperature; 37°C-cells were heat-shocked at indicated times and transferred from 30°C to 37°C; 20C 0 h—the cells were transferred to 20°C after change of the medium to YEPG. "h" indicates hours before ("–") or after ("+") medium change to YEPG. Dotted arrows show glycosylated MeH forms, solid arrows–unglycosylated MeH polypeptides. Percentages of glycosylated MeH forms in comparison to control 30C $h samples on the same membrane are indicated below blot lanes. (b) Average relative amounts of glycosylated MeH forms at various temperature conditions from three independent experiments. The amount of MeH glycoprotein from control 30C $h sample was taken as 100%. Bars represent standard error.

However, during these experiments we noticed that increase in MeH glycoprotein amount largely depends on the culture density when heat shock is applied. This suggested that not only the duration of heat shock, but also the growth phase of yeast culture may be important. It was reported earlier that

for a successful production of yeast endogenous membrane-bound protein Fps1 it is crucial to grow cells until late-log phase in glucose medium and to harvest them prior to glucose exhaustion, i.e., just before the diauxic shift (Bonander et al., 2005). The entry into stationary phase is typically accompanied by a dramatic decrease in the overall growth rate and an increased resistance to a variety of environmental stresses, such as heat shock and oxidative stress (Herman, 2002; Jamieson, 1998). It has been shown that slowly growing yeast cells acquire heat shock resistance which can be nearly as great as that of stationary phase cells, whereas rapidly growing cells of *S. cerevisiae* are much more sensitive (Elliott & Futcher, 1993). Therefore, yeast cells in the late-log growth phase exhibit several stationary phase characteristics with similar degree of stress resistance. In general, adaptation to a stress may considerably improve recombinant protein production (Mattanovich et al., 2004). On the other hand, it has been demonstrated that secretory production of recombinant proteins is positively correlated with the specific growth rate in *S. cerevisiae* (Liu et al., 2013). Taking together, the late-log phase combines active cell growth and stress resistance that could be beneficial for recombinant protein production at elevated temperatures.

To determine the growth phases of specific yeast strain used for the protein synthesis study, we measured optical density as well as glucose and ethanol concentrations in the culture medium during a shake flask incubation of *S. cerevisiae* AH22 strain transformed with vector pFGG3-MeH (Fig. 16a). The growth phases were clearly distinguished by identifying periods with constant specific growth rates. The maximum specific growth rate of 0.41 h^{-1} was observed in the mid-log glucose phase (Methods Fig. 16a). To identify conditions at which heat shock maximally stimulates MeH translocation, the experiment was performed in a wide culture density range (Fig. 16b). According to the results obtained in the initial experiment (Fig. 15b), the induction of MeH synthesis in all culture variants was initiated 5 h after the heat shock, and cells were maintained at 37 °C till the end of MeH production in YEPG medium. The results demonstrate that heat shock improves translocation of MeH precursors at higher cell densities. Relative amounts of glycosylated MeH increased about 3-fold after heat shock in the late-log phases of both glucose and ethanol growth (Fig. 16b, columns).

The comparison of relative MeH glycoprotein amount to that of control cells grown at 30 °C does not include an evaluation of non-translocated MeH polypeptide precursor corresponding to the lower molecular weight (~65 kDa) band. Therefore, we also determined a translocation efficiency given as the ratio of glycosylated and total MeH amounts (Fig. 16b, circles). Basically, the heat shock improved MeH translocation efficiency at higher cell densities,

starting from the early-log glucose growth phase. However, the efficiency of translocation did not correlate with increased relative amount of MeH glycoprotein at all analysed points. The translocation efficiency was improved about 2-fold at the late-log glucose growth phase, whereas at the late ethanol growth phase it improved only ~25% despite the highest relative amount of MeH glycoprotein at this growth point. Interestingly, the highest increase of MeH translocation efficiency was observed after the heat shock at the late diauxic shift phase (Fig. 16b, 12–13 OD, circles), but this was determined by a decreased level of non-translocated MeH polypeptide precursor.

There was a report of a similar effect where the heat shock response (HSR) improved heterologous protein secretion in *S. cerevisiae* (Hou et al., 2013). The authors of that study overexpressed mutant HSF1 gene which can constitutively activate HSR at 30 °C, and this resulted in considerable increase of heterologous α-amylase yield. Our findings suggest that one of the reasons for improvement of protein secretion by HSR may be the increase in translocation rate. It is in agreement with previously published evidences that HSR facilitates translocation of newly synthesized polypeptides into the ER (Liu & Chang, 2008). Of course, it should be noted that heat shock with prolonged incubation of cells at 37 °C (our study) is different from constitutive activation of HSR in cells cultivated at 30 °C (Hou et al., 2013). Naturally, heat shock induces only transient synthesis changes of cellular proteins (with maximum changes 20–30 min after the shift of temperature), most of which regain previous synthesis levels after 60–120 min of incubation at 37 °C (McAlister et al., 1979; Miller et al., 1982). Despite these differences, both studies demonstrate that heat shock can be employed for improvement of recombinant protein production in *S. cerevisiae*.

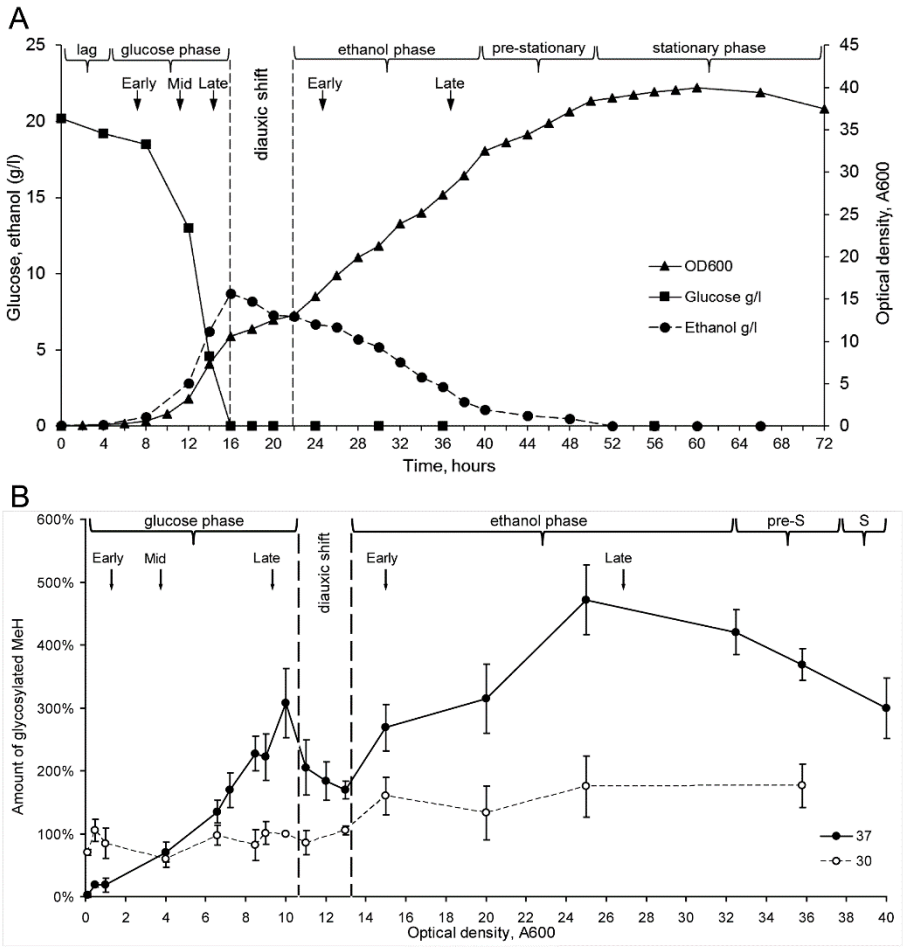

Fig. 16. Changes in MeH translocation after heat shock at different yeast culture densities. (a) Growth phases of *S. cerevisiae* AH22 strain transformed with plasmid pFGG3-MeH. Triangles indicate culture optical density, squares denote glucose, and circles—ethanol concentrations in the medium. The average value from at least three independent cultivations is shown; the standard error was less than 3%. Specific growth rates $\mu(h^{-1})$ were calculated from optical densities for separate growth stages and are given below indicated phases. (b) Cultures were heat-shocked at different densities, transferred to 37°C for 5 h, and then growth medium was changed to YEPG with subsequent incubation at 37°C. Relative MeH glycoprotein amounts in the heat-shocked cultures are shown as dark columns in comparison to MeH glycoprotein amounts in control cells incubated at 30°C (light columns). MeH glycoprotein amount in "10 OD" control variant incubated at 30°C was taken as 100%. Circles indicate translocation efficiency (percentage of MeH glycoprotein from total MeH amount in the same sample). Measurements are the average value ± standard error from at least three independent experiments.

Finally, the results were verified by independent experiments, where heat shock was performed in parallel cultures only at the two peaks with maximal MeH glycoprotein amounts. Western blot of crude lysates from yeast

cells cultivated at 37°C after the heat shock applied at 10 and 25 ODs as well as corresponding 30°C controls is shown in Fig. 17. Relative MeH glycoprotein amounts and translocation efficiencies were within the error ranges and confirmed the results of previous experiments (Fig. 16b). The observation that heat shock at the higher cell densities did not considerably affect biomass formation in MeH-producing cells may be important for production purposes. Although MeH production results in ~1.4-fold decrease in biomass accumulation (Ciplys et al., 2011), this effect is not significant when cells are grown until higher cell densities in glucose medium (YEPD), where expression of MeH gene is repressed and protein synthesis is induced at later growth stages. Moreover, yeast cells acquired resistance to heat stress at later growth phases, which correlated with the cell density of yeast culture. Therefore, the amount of final dry cell weight (DCW) was decreased in MeH expressing cells by 30–40% after heat shock at 10 OD and only up to 15–20% after heat shock at diauxic shift or ethanol growth phases in comparison to severe biomass decrease of 3–5-fold after the heat shock at early- or mid-log glucose growth stages.

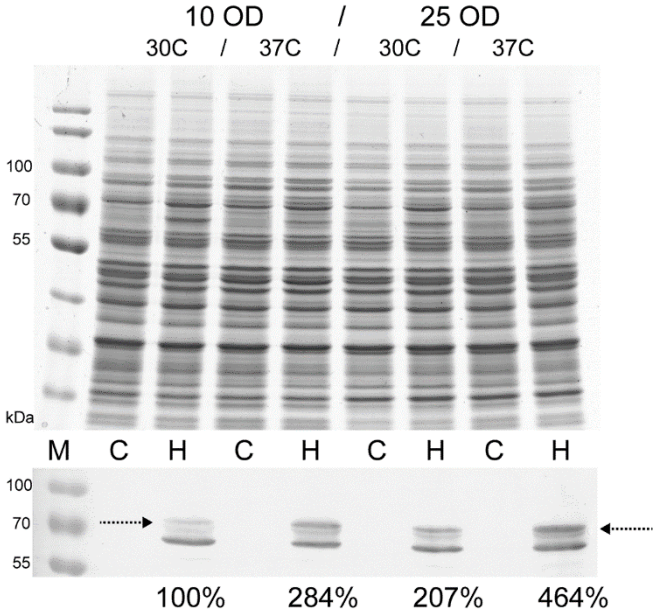

Fig. 17. Verification of the results by additional independent experiment. Crude yeast lysates from MeH producing (H) and control cells transformed with empty vector (C) were analyzed by SDS-PAGE (at the top) and Western blotting (below). Shake flasks with sub-cultures from the same initial culture were grown in parallel to the cell densities of 10 or 25 OD, and the heat shock was applied with following incubation at 37 °C as described in Fig. 16 b legend. Other references are the same as in Figs. 15 and 16.

3.2.2. Identification of cellular proteins, which biosynthesis patterns correlate with the improved translocation of MeH into the yeast ER

We performed a comparative proteomic study to identify cellular proteins, which may be involved in MeH translocation. At first, we sought for culture conditions resulting in the most drastic differences in MeH translocation. From the study of MeH production at 30 °C and 37 °C, it was still unclear whether we should choose latelog growth phases (due to the largest increase in MeH glycoprotein amount) or diauxic shift (due to the difference in MeH translocation efficiency). Therefore, we evaluated MeH translocation after a shift to 20 °C. After adaptation of cultures to lowered temperature at the late-log growth phases, relative MeH glycoprotein amounts were 20% (similarly to that shown in Fig. 15a, 20 °C) with translocation efficiences in the range of 10–15% (not shown). However, the shift of yeast culture to lower temperature at diauxic shift followed by protein production at 20 °C almost totally inhibited translocation of MeH precursors. The amount of MeH glycoprotein decreased by 50-fold when compared with production at 30 °C and constituted less than 1% of total MeH protein in yeast cells (Fig. 18b). Therefore, the difference in the amounts of MeH glycoprotein produced at 37 °C and 20 °C was about 80-fold, whereas amounts of unglycosylated MeH polypeptides were similar under both conditions. It resulted in drastic difference of MeH translocation efficiency (60-fold), and this allowed us to assess cellular proteome when MeH translocation is under ‘‘on’’ or ‘‘off’’ conditions. For internal control, we used measles virus nucleoprotein (MeN), similarly as in our previous published study. Interestingly, MeN production was also influenced by the same treatment. The synthesis at 20 °C resulted in several-fold decrease in MeN amount, whereas the shift to 37 °C slightly increased MeN synthesis (Fig. 18a and c).

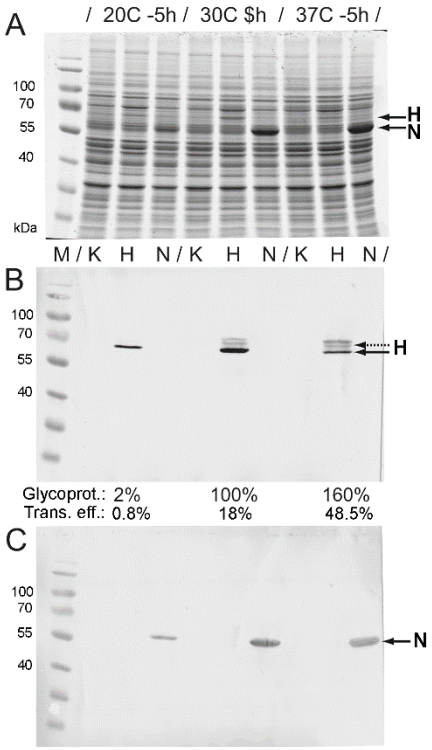

Fig. 18. Analysis of recombinant protein production in samples used for proteomic study. SDS-PAGE (a) and Western blots against MeH (b) and MeN (c). Cultures were grown till late diauxic shift phase (~12.5 OD) and shifted to 20 °C or heat-shocked and transferred to 37 °C for 5 h with subsequent change of growth medium to YEPG and incubation at the same temperatures. Control culture was cultivated in parallel at 30 °C as indicated above gel lanes. N—crude yeast lysates from MeN protein producing cells. Other references are the same as in Methods Figs. 15 and 16.

To identify proteins with differential synthesis patterns, we performed comparative proteomic analysis by two-dimensional gel electrophoresis (2DE) using both IPG- and NEPHGE-based 2DE, as described previously. In total, nine experimental variants (yeast producing MeH, MeN and transformed with empty vector, each under expression conditions at 20 °C, 30 °C and 37 °C) were analysed using both techniques. Both IPG- and NEPHGE-based 2DE showed that about 20% of high-abundance protein spots were differentially synthesized under tested conditions. NEPHGE-based technique enables to resolve more protein spots than conventional IPG-based 2DE method and provides excellent spot quality and reproducibility in the basic gel zone, therefore protein spots with differential synthesis patterns were identified from NEPHGE-2DE gels (Fig. 19 and Table 5). As we focused on MeH translocation under “on” vs. “off” conditions, most of protein spots with differential biosynthesis were identified from yeast cells producing MeH at 20 °C and 37 °C. About 40 protein spots with differential synthesis patterns were identified by tryptic peptide mass fingerprinting (Table 5). After excluding partially degraded forms of abundant cellular enzymes or their modifications and some other proteins which functionality makes them unlikely contributors to improved translocation, the remaining ~15 cellular proteins were selected as possibly involved in MeH translocation (Table 5, indicated in bold). Four of them were considered as major targets according to available data from other studies and reported protein functions.

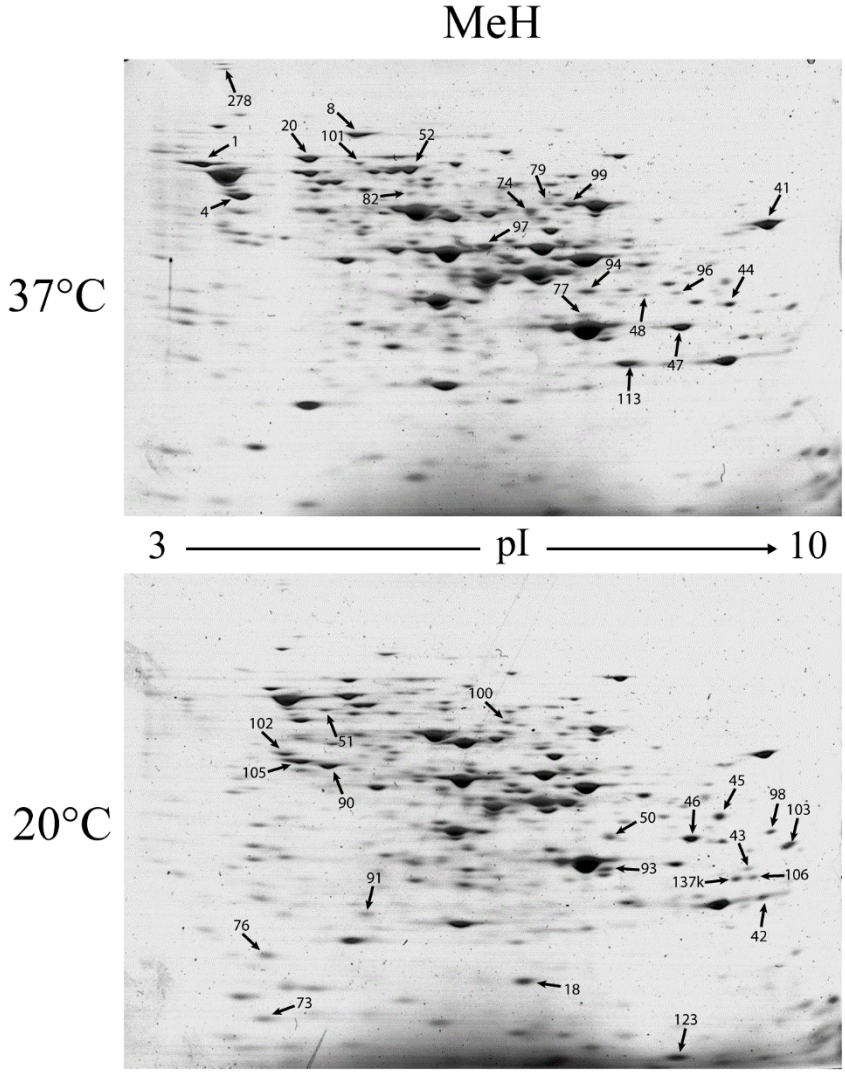

Fig. 19. Analysis of protein spots with differential synthesis patterns in whole cell lysates from yeast with efficient or switched-off MeH translocation. NEPHGE-based 2D gel electrophoresis of yeast proteins from MeH producing cells after heat shock and cultivation at 37 °C (above) or after shift to 20 °C (below). Analysis of the same samples by SDS-PAGE and Western blot are shown in Fig. 18. Numbers of identified protein spots correspond to those, given in Table 5.

Table 5. Identification of possible yeast protein targets involved in MeH translocation.

Identification of possible yeast protein targets involved in MeH translocation.

Spot No.	Protein[a]	Fold change[b] 37°C/20°C	Protein score[c] C.I.%	Function, process	Notes[d]
1	**Kar2**	3.16	100	Translocation, ER chaperone	Major protein target
4	**Hsp60**	1.62	100	Mitochondrial chaperonin	
8	**Hsp104**	2.55	100	Disaggregase, response to stress	Major protein target
18	Tdh1/2/3	0.63	100	Cytosolic enzyme, glycolysis	Minor isoform
20	**Sse1**	1.81	100	Co-chaperone, response to stress	
41	**Tef1**	1.52	100	Translation, Elongation factor	Major protein target
42	Fdh1/2	0/+	100	Cytosolic enzyme	Minor isoform
43	**Atp3**	0/+	96.5	Mitochondrial ATP synthase	
44	**Sis1**	1.50	100	Co-chaperone, response to stress	
45	**Vma1**	0.52	100	Vacuolar membrane ATPase	
46	Tef1	0.41	100	Translation, elongation factor	Minor isoform
47	Tdh1	2.05	100	Cytosolic enzyme, glycolysis	Minor isoform
48	Gal7	+/0	100	Enzyme, galactose metabolism	
50	Eno1	0.43	100	Enolase, glycolysis	Minor isoform
51	**Vma1**	0.27	100	Vacuolar membrane ATPase	
52	Gal10	5.67	100	Enzyme, galactose metabolism	
73	**Ahp1**	0/+	100	Thiol-specific peroxiredoxin	
74	Gal1	+/0	100	Enzyme, galactose metabolism	
76	Ssa1/2	0/+	100	Chaperone, response to stress	Minor isoform

Identification of possible yeast protein targets involved in MeH translocation.

Spot No.	Protein[a]	Fold change[b] 37°C/20°C	Protein score[c] C.I.%	Function, process	Notes[d]
77	**Gre3**	+/0	100	Enzyme induced by stress	
79	Cdc19	+/0	100	Pyruvate kinase, glycolysis	Minor isoform
82	Gal10	+/0	98.1	Enzyme, galactose metabolism	
90	**Atp2**	0.16	100	Mitochondrial ATP synthase	
91	Fba1	0.20	100	Cytosolic enzyme, glycolysis	Minor isoform
93	Tdh2/3	0.34	99.9	Cytosolic enzyme, glycolysis	Minor isoform
94	Gal1	2.86	100	Enzyme, galactose metabolism	
96	**Gcy1**	2.55	99.9	Enzyme induced by stress	
97	Eno1/2	2.53	100	Enolase, glycolysis	Minor isoform
98	Tef1	0.42	99.5	Translation, elongation factor	Minor isoform
99	Cdc19	2.33	100	Pyruvate kinase, glycolysis	Minor isoform
100	Pck1	0.45	100	Key enzyme in gluconeogenesis	
101	**Sti1**	2.28	100	Co-chaperone, response to stress	Major protein target
102	Ssa1/2	0.46	100	Chaperone, response to stress	Minor isoform
103	Tef1	0.47	100	Translation, elongation factor	Minor isoform
105	Ssa1	0.51	100	Chaperone, response to stress	Minor isoform
106	Tef1	0.54	100	Translation, elongation factor	Minor isoform
113	**Por1**	1.75	100	Mitochondrial porin	
123	Tdh3	0.49	100	Cytosolic enzyme, glycolysis	Minor isoform
137k	Ssa1/2	0.87	100	Chaperone, response to stress	Minor isoform
278	Ssa1/2	2.81	100	Chaperone, response to stress	Minor isoform

[a]Possible protein targets involved in MeH translocation are indicated in bold.
[b]Fold change represents ratio between the relative protein amounts (%Vol) in whole cell lysates. If spot was not detected, it is indicated by 0 vs. + (detected) at other temperature conditions.
[c]Protein score C.I.% rates the confidence level of the Protein Score for correct indentification.

[d]Major protein targets are noted according to reported protein functions and mechanisms that could be involved in MeH translocation. Minor isoforms indicate identified less abundant protein forms (modificated or partially degraded) of the same protein found in other separate major protein spot.

Our results suggest that physiological processes in early and late log phases are different with specific reaction to heat stress that influences the efficiency of protein translocation into the ER. It is difficult to predict the exact molecular mechanisms responsible for these differences, because several hundreds of genes are differentially expressed even in mid-log vs. late-log glucose growth phase (Thompson et al., 2013). Only high abundance yeast proteins were quantitatively evaluated in our proteomic study, but we suppose that highly expressed viral proteins should be assisted by a comparable amount of cellular proteins. At least, the most abundant cellular proteins may be identified as markers of specific biological processes involved in improved viral protein translocation. Indeed, functions of some protein spots with differential synthesis patterns suggest several mechanisms involved in heterologous protein translocation at both sides of the ER membrane.

The first mechanism is increased synthesis of yeast ER proteins involved in the translocation. Kar2/BiP is the most abundantly over-produced (>3-fold) protein among all identified as possibly involved in MeH translocation. It is well known that Kar2p is required for protein translocation into the yeast ER and has a critical role in facilitating protein translocation during HSR in unfolded protein response (UPR)-deficient ire1D cells (Liu & Chang, 2008). Nevertheless, the role of Kar2p should not be overestimated, because its over-production can only partially rescue the growth deficiency in UPR deficient hac1D cells and there are other components required for the observed HSR-mediated suppression of ER stress (Hou et al., 2014). Besides the KAR2, genes of the secretory pathway (SIL1, ERO1, ERV29, etc.) were significantly upregulated during HSF1 overexpression (Hou et al., 2014), and genes involved in regulating the ATPase cycle of Kar2p (SIL1, LHS1, JEM1 and SCJ1) were upregulated in yeast strain secreting higher levels of recombinant human albumin (Payne et al., 2008). Therefore, it may be expected that considerable improvement of heterologous protein translocation requires increased expression of ER-resident co-chaperones as well.

Our study revealed that cytosolic chaperones Ssa1/2, which are the most abundantly overproduced in UPR-Cyto stress during MeH synthesis (Ciplys et al., 2011), were not differentially synthesized under conditions resulting in changes of MeH translocation (except some minor partially degraded isoforms included in Table 1). In contrast, large cytosolic chaperones of Hsp90 and Hsp110 families were identified as other major proteins possibly involved in

MeH translocation. Hsp104p was highly overproduced in cells with improved MeH translocation, and this may ensure high thermotolerance with resistance to many forms of stress (Sanchez et al., 1992). Importantly, chaperone Hsp104 is required for conformational repair of heat-denatured proteins in the yeast ER (Hänninen et al., 1999). A possible role of Hsp104p in protein translocation may provide a link to the interaction of Hsp104p with the ER refolding mechanism. Another cytosolic chaperone Hsp90 was directly shown to be important for invertase secretion. Inhibition of Hsp90 using drug macbecin II dramatically reduced the amount of active invertase secreted to the media, and this effect was enhanced by the deletion of known Hsp90 co-chaperone STI1 (McClellan et al., 2007), the protein also upregulated in cells with improved translocation of MeH (Table 5). Moreover, we also identified Hsp90 chaperones Hsc/Hsp82 as overproduced proteins at 37°C vs. 30°C in MeH producing cells by using IPG-based 2DE (fold change was ~2.9). Hsc/Hsp82p is not shown in Fig. 19, because NEPHGE-2DE method failed to detect these highly acidic proteins.

The last major possible protein target is Tef1p, also known as eukaryotic translation elongation factor 1A (eEF1A), which is the first cellular protein involved in quality control of newly synthesized polypeptides after their release from ribosome (Hotokezaka et al., 2002). In our previous study, we found that eEF1A directly interacts with viral protein precursors and forms large disulfide-linked multimers with MeH (Ciplys et al., 2011). eEF1A appeared to be involved in HSR in mammalian cells where both heat shock RNA-1 (HSR1) and eEF1A were required for the activation of heat-shock transcription factor 1 (HSF1) (Shamovsky et al., 2006). Recently it was demonstrated that eEF1A participates in the entire process of the HSR in mammalian cells from transcription through translation (Vera et al., 2014). If eEF1A functions in yeast in the same way as in mammalian cells, it may support the translocation of MeH precursors both by rendering MeH polypeptides competent for translocation and coordinating the HSR. Besides the major protein targets, which could be involved in MeH translocation according to known protein functions, the role of other possible protein targets also could not be ruled out. For example, Gcy1p (spot 96, Fig. 19 and Table 5) was overproduced at 37 °C conditions in our study, whereas the gene GCY1 encoding this protein was found to be the most significant in the cells with HSF1 overexpression vs. wild-type (according to the microarray data GEO: acc. no. GSE39311 given in (Hou et al., 2014)). The identification of the same targets on both transcript and protein level in different studies suggests that such genes may have important unknown functions. On the other hand, it seems that the major protein targets act in concert during observed heat shock-

activated protein translocation. Cytosolic eEF1A possibly coordinates HSR, whereas overproduced chaperones Hsp104 and Hsp90 should provide protection from heat and support efficient biomass formation at higher cell densities. The major role of Kar2p is evident from well-explored functions of this most abundant ER protein. Possible protein targets identified in this study should be examined by genetic engineering methods.

3.3. Restoration of the NEPHGE-based 2DE method

2DE is a robust method that allows to analyse the whole intact protein complement or proteome in high resolution, including protein isoforms and post-translationally modified proteins (Rabilloud, 2009). Although NEPHGE-based 2DE is a more labour-intensive and less broadly used than IPG-based 2DE, it is still instrumental in specialized laboratories. The capability of NEPHGE-based 2DE to better resolve basic protein spots in comparison with IPG is exploited for functional proteomics experiments in a broad pH range, as well as for experiments with highly basic proteins (Bjarnadóttir & Flengsrud, 2014; Kreipke et al., 2007). While an improved protocol on NEPHGE-based 2DE was published in 1995 by Klose and Kobalz (Klose & Kobalz, 1995), it was commercialized only later by WITA GmbH (Wittmann-Liebold et al., 2006) and the „WITAvision“ 2DE system was developed. Unfortunately, this company ceased operations and left owners of the apparatus without a supply of reagents. The unavailability of pre-made gel solutions only further decreased the use of this method, so we reasoned it was important to recreate the constitution of the CA in the first-dimension gels and to make it publicly available for other operators of this 2DE system. The composition of the CA in IEF gels sold by WITA GmbH still remains unknown and recreating the original CA mixture presented by Klose and Kobalz, also posed a challenge, due to the discontinuation of production of most of the ampholytes used at that time. Despite this, here we show a restored CA composition for NEPHGE-based 2DE, which shows a high positive correlation to formerly commercially available gels.

The CA composition of our restored “New mix” NEPHGE first-dimension separation gels, is described in Methods chapter 2.2.10.

3.3.1. Comparison to the commercial “WITA” gels

We compared 2DE gels made with our re-created “New mix” and the formerly commercially available “WITA” pre-made gel solutions. We loaded the gels with the same sample of crude lysate of *S. cerevisiae* strain AH22

cells transformed with an empty pFGG3 vector. The running conditions, second-dimension SDS-PAGE, gel fixing and staining with Coomassie R-250 were identical (See Materials and Methods, Figure 22). We analysed the 2DE gels (that were triplicated each for statistical significance) using PDQuest (BioRad) 2-D analysis software and compared the six gels to each other to calculate the Pearson's coefficient of correlation (r) (See Figure 23.).

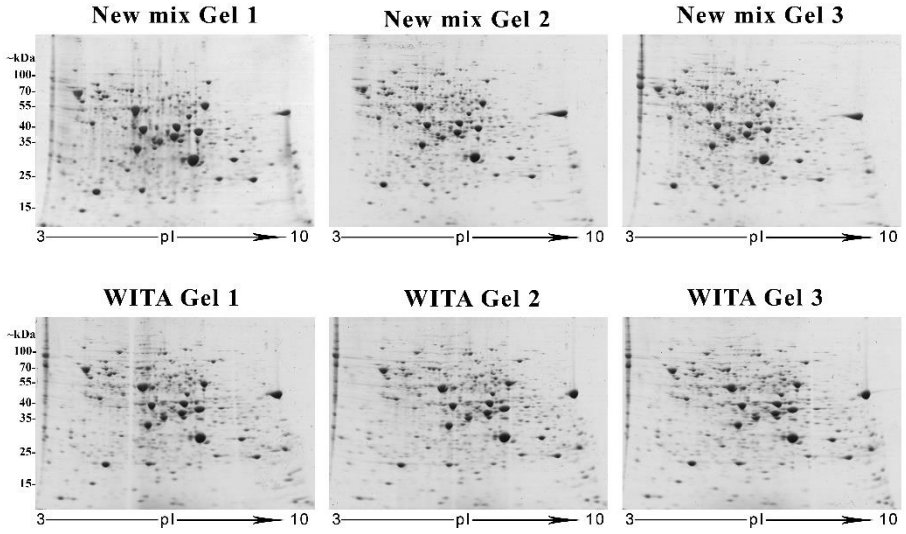

Figure 22. A triplication of 2DE separations of the same sample (80 µg of lysate of *S. cerevisiae* AH22 strain cells transformed with pFGG3 vector) using either our restored "New mix" or commercial "WITA" solutions for NEPHGE-based first-dimension IEF. The pI range of separated protein spots is marked on each gel.

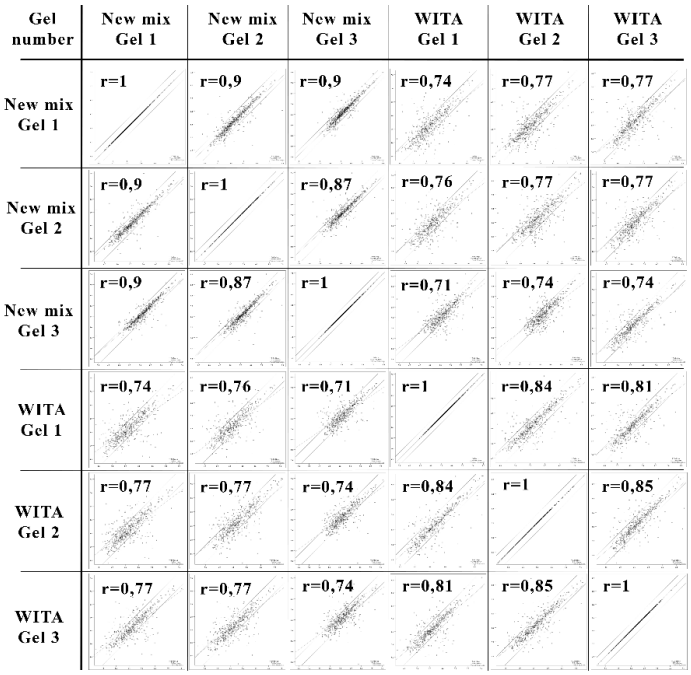

Figure 23. Scatter plot analysis and correlation coefficients (r) between 2DE gels made with the „New mix“ and commercial „WITA“ ampholyte mix. For the comparison, three runs of identical gels of each constitution („New mix “or „WITA“) were compared with each other. The correlation coefficient r=1 references the comparison of a gel with itself, which indicates strongest correlation possible. The closer r is to 1, the stronger it is.

All gels showed a strong positive correlation among them ($r > 0.7$), with small deviations. The correlation inside the gel group that was made with “WITA” solutions ranged from 0.81 to 0.85, and the correlation inside our “New mix” gel group varied between 0.87 and 0.9. When comparing our restored recipe for NEHGE-based first-dimension separation to the commercial “WITA” gels, we got a slightly lower correlation coefficient (r=0.71–0.77) than within the two gel groups (r=0.87–0.9 and r=0.81–0.85, respectively). This was to be expected, having in mind that the constitution of the CA is probably different, as the composition of “WITA” gels was never made public. A slightly better correlation between our “New mix” gels suggests better reproducibility between technical replicas. Despite the not ideal correlation between our “New mix” and “WITA” gels, they still show a strong positive correlation and our restored CA mixture and gel solutions for NEPHGE first-dimension separation can be fully used in 2DE proteomics experiments instead of the no longer commercially available ones. The number of resolved spots was very similar - about 800 spots both in our “New mix” (av. 795 spots) and “WITA” (av. 807 spots) gels.

To further test our restored NEPHGE first-dimension gel composition, we used it for our comparative proteomics experiment to analyse the secretion of human recombinant CALR protein in *S. cerevisiae* (See chapter 3.4.).

3.4. A comparative proteomic analysis of the high-level secretion of human CALR in *S. cerevisiae.*

The ER chaperone CALR also has extracellular functions and can exit the mammalian cell in response to various factors, although the mechanism by which this takes place is unknown. The yeast *Saccharomyces cerevisiae* efficiently secretes human CALR, and the analysis of this process in yeast could help to clarify how it gets out of eukaryotic cells (See Chapter 1.3.3). The aim of this study was to perform a comparative whole proteome analysis of CALR-secreting yeast *Saccharomyces cerevisiae* cells versus control cells harbouring an empty vector, using NEPHGE-based 2DE and LC-MS^{E} to try to identify cellular proteins that are likely to participate in the CALR secretion pathway.

In this comparative proteomics experiment between CALR-secreting and control cells with an empty vector, we quantified protein abundance from 2DE gels made with our restored CA mixture and also, quantified all peptides present in the whole proteome samples analysed by LC-MS^{E}, using label-free quantitation via TOP3-approach. We found that effective secretion of CALR does not induce cellular stress or the expression of any secretory pathway proteins and only results in a slightly higher demand for energy and nutrients in *S. cerevisiae*.

3.4.1. Synthesis and secretion of human recombinant CALR protein in yeast *S. cerevisiae*

In order to obtain samples for a comparative 2DE experiment, we expressed full-length human recombinant CALR protein precursor with its native signal sequence under an inducible *GAL7* promoter in *S. cerevisiae* strain AH22. The cells were grown in YEPD medium containing glucose for 21 hours before changing the culture growth medium to YEPG containing galactose. In our previous work, we determined that *S. cerevisiae* strain AH22 reaches the diauxic shift phase - when glucose is depleted in the growth medium and cells switch from glucose fermentation to the aerobic utilisation of accumulated ethanol (Galdieri et al., 2010) – in 21 hours of cell culture growth. Because *GAL* genes can only be induced to a considerable extent at a threshold glucose concentration, introducing galactose into a cell culture

during the diauxic shift, when glucose is completely depleted, results in faster GAL regulon activation (Escalante-Chong et al., 2015) and swift induction of *CALR* gene under *GAL7* promoter.

According to the data collected from densitometric analysis of SDS-PAGE gels - 18 hours after the induction of recombinant protein synthesis, the secretion yield of the mature CALR was approximately 138 mg from 1 L (in the range from 120–160 mg/L) of yeast culture medium (See Figure 24. A). To assess the growth phase, when the secretion of CALR was the most efficient, we performed densitometric evaluation of SDS-PAGE gels loaded with yeast culture medium samples taken every three hours from the start of the recombinant protein induction (See Figure 24. B). We measured relative volumes of each protein band and calculated that the biggest increase in CALR amount in the medium happened between 0 to 3 hours and between 3 to 6 hours (~2.8-fold) after the induction. We assumed, that if the secretion is the most effective at these growth points, the cellular proteins responsible for facilitating CALR secretion should be also more abundant. Three and six hours after the induction of recombinant protein synthesis was the cell culture growth points, at which we chose to take our samples for 2DE.

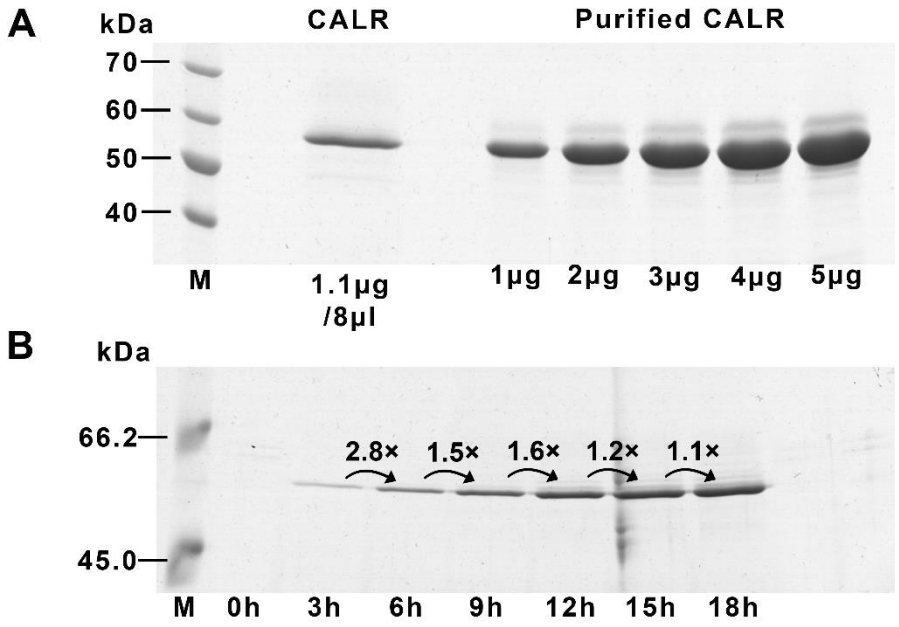

Figure 24. A – SDS-PAGE analysis of CALR-secreting yeast culture medium together with a 1-5µg of purified CALR for densitometrical quantitative calibration. 8µl of culture media containing CALR corresponds to the amount of 1.1 µg, or 139 mg/L for this specific experiment. B - SDS-PAGE analysis of the secretion efficiency of CALR measured every three

hours of 18-hour post-induction growth. Numbers above the arrows indicate how many times more of CALR was secreted into the culture medium between time points.

Our achieved secretion titer of 138 mg/L showed an about 2-fold increase in comparison with our previously published results, where human recombinant *CALR* was expressed under yeast PGK1 and pFGADH1 gene promoters in *S. cerevisiae* and yielded about 60–66 mg of protein from 1 L of culture medium (Čiplys et al., 2015, 2021). Although *CALR* was expressed under different promoters in this and our previous experiments, the yeast strain used, the cell culture medium, and the shake-flask growth conditions were identical, which allows us to directly compare the yield of the secreted CALR. This increase in the amount of secreted protein is facilitated by an inducible promoter vs constitutive, and the fact that the recombinant protein synthesis is commenced on a higher cell culture density, allowing to maximize growth before the induction of a potentially burdening biosynthesis phase (Weinhandl et al., 2014). In our previous research, we also have shown that the secretion of CALR is more efficient than that of other similarly secreted ER chaperones BiP and ERp57 due to lower intracellular retention facilitated by intrinsic properties of the protein (Čiplys et al., 2013, 2014, 2015). The other reason that could facilitate such an effective secretion of CALR in yeast is low free Ca2+ concentrations in the yeast ER lumen. It has been shown that in humans, ER calcium depletion induces CALR secretion (Peters & Raghavan, 2011), and there is 10–100 times less free Ca2+ in the yeast ER lumen (Strayle et al., 1999) compared to the ER in human cells. High secretion titer also vastly depends on the stability of the protein. Our recent study, where the secretion titer, stability and other parameters of 50 of CALR protein mutants were analysed in yeast *S. cerevisiae*, showed that single point mutants that exhibited lower secretion titers also showed decreased protein stability (Čiplys et al., 2021). In this vein, our achieved efficient 138 mg/L secretion titer of CALR asserts that the recombinant protein is highly stable and properly folded.

3.4.2. Comparative 2DE-based analysis of CALR-secreting yeast cell samples vs control

When comparing 2DE gels of CALR-secreting cell samples versus control at 3- and 6-hour growth points after the recombinant protein induction (loaded with 200μg of yeast lysates of *S. cerevisiae* strain AH22 expressing *CALR* protein gene or transformed with empty control vector (see Materials and Methods)), we found altogether 811 different protein spots with 734 of them matching throughout all gels. We evaluated protein spots with

differential synthesis patterns and found that 83 protein spots showed a fold change (FC) of 1.5 times, hence, 35 out of 811 proteins showed increased expression in CALR gels and 48 out of 811 in control gels. The Student's *t*-test analysis showed that only 35 of 811 spots had significant differential synthesis patterns with a *p*-value < 0.05 and only 8 of them with a *p*-value < 0.01 (See Figure 25.). Unfortunately, most of them were on the brinks of the gels or were extremely small and indistinct – not suitable for excision and identification.

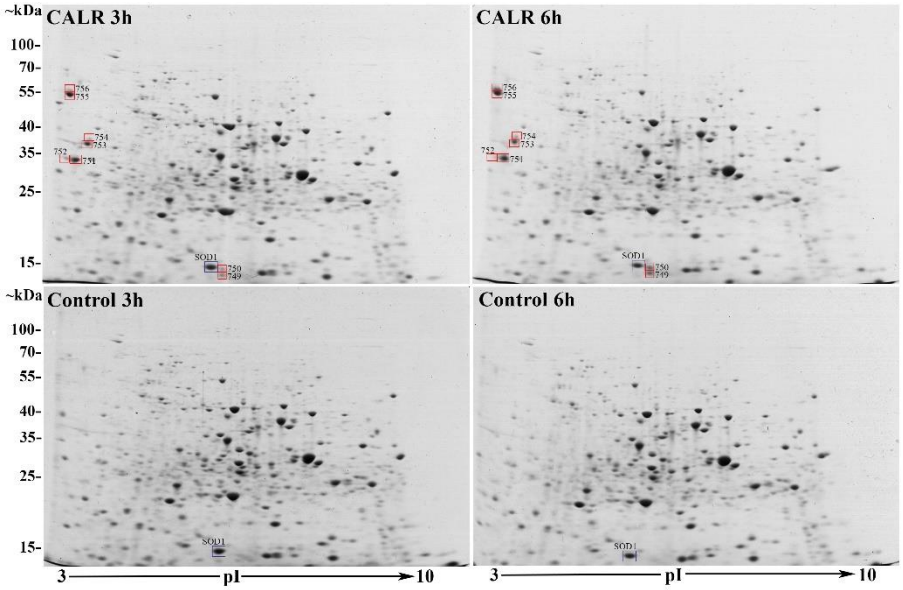

Figure 25. NEPHGE-based 2DE gels of CALR secreting and control yeast cell lysates at 3- and 6-hour growth points after the induction with galactose, when the secretion of CALR is most efficient. All gels were loaded with 200 µg of yeast *S. cerevisiae* strain AH22 cell lysates expressing *CALR* protein gene or transformed with an empty control vector (Control). Squared in red protein spots 749-756 were singled out as having the most reliable difference in the synthesis between CALR secreting yeast samples and control. Protein spots 749 and 750 were identified as SOD1, 755 and 756 as CALR and spots 751-754 were identified as degradation products of CALR. Squared in blue is also a SOD1 protein spot, but produced similarly throughout all the samples.

Additional DESeq2 analysis without a set FC threshold found 100 spots out of 811 to have a *p*-value ≤ 0.05 and 44 with a padj ≤ 0.1 value (padj – is referred as adjusted *p*-value in DESeq2 analysis, where padj < 0.1 means that the difference is highly significant (Love et al., 2014)). Out of 44 protein spots with highly significant difference in synthesis (p ≤ 0.05), only 20 met the FC threshold of 0.58 log2FC, 11 of which showed increased biosynthesis and 9 decreased biosynthesis in CALR samples. The highly significant spots (*p* ≤

0.05, padj ≤ 0.1) in the CALR samples that were above FC threshold, were the most interesting to us. The 8 spots out of 11 (marked as triangles See Figure 26A) were the spots with the highest FC that fall out of the plotting area. Not surprisingly, these spots are the same ones that were identified as highly significant using the *t*-test (749-756) and are represented in a heatmap as having the highest spot value when calculating from the average (See Figure 26B).

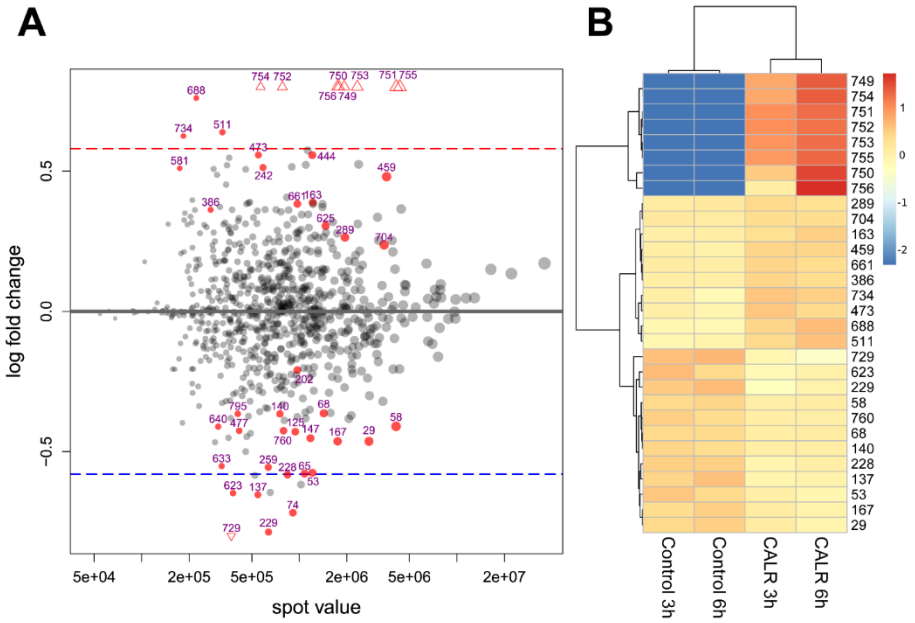

Figure 26. Representation of protein spots with differential synthesis patterns in a NEPHGE-based 2DE comparison of CALR-secreting and control yeast cultures. Protein spots 749–756 show the most significant differential synthesis. A – an MA plot (a plot of log ratio (M) and mean average (A) scales) of protein spot mean synthesis level (*x*-axis) dependence on log2FC (*y*-axis) after DeSeq2 analysis representing the strength of differential biosynthesis. Highly significant protein spots with differential synthesis patterns that had highest FC and fall out of plotting area are marked as red triangles. Dashed lines represent the 0.58 log2FC thresholds: blue line marks the threshold for decreased synthesis and red line marks the threshold for increased synthesis of proteins in CALR samples. Dots with an ID value represent proteins with *p*-value ≤ 0.05, red dots represent proteins with padj ≤ 0.1 value. B – a heatmap representation of 30 protein spots with the lowest p-value. The intensity of the colour represents how much the spot value is greater (red) or lesser (blue) than the average.

The aforementioned spots with the most significant differential synthesis patterns (749–756) were selected for LC-MS identification. Because of the close proximity, spots 753–756 were excised as single spots. The LC-MS identified spots 751-756 as human CALR protein (Accession no.: P27797, Entry CALR_HUMAN, MW 48111, pI 4.09, Calreticulin OS=Homo sapiens).

Protein spot 755 corresponds to the mature CALR protein with the pI 4.09 and MW of ~46 kDa and the spot 756 corresponds to the full-length un-translocated CALR precursor with intact signal peptide with MW of ~48 kDa. Peptide sequence analysis revealed that spots identified as CALR, but with but with different MW and pI positions in the gels are degradation products of the protein (spots 751–754). The analysed peptides covered the CALR protein sequence either at the *N*-terminus, *C*-terminus or the middle (See Figure 27), which can only happen in the case of degradation.

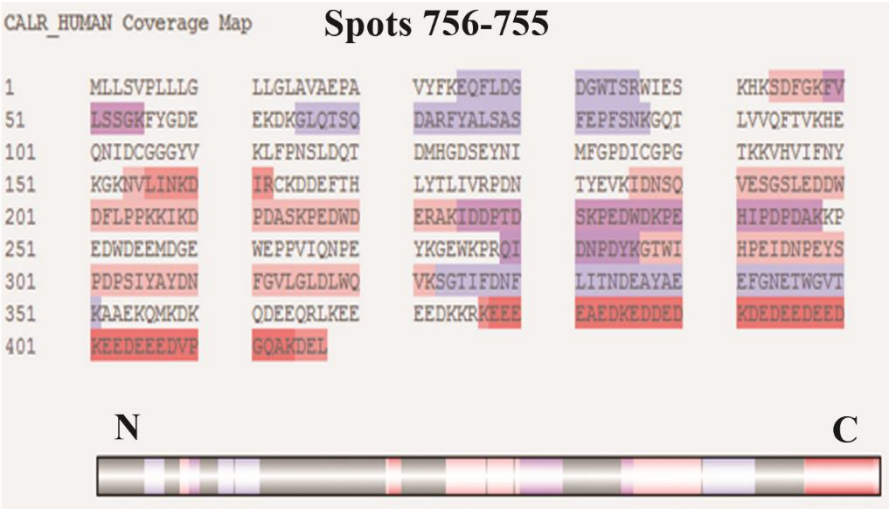

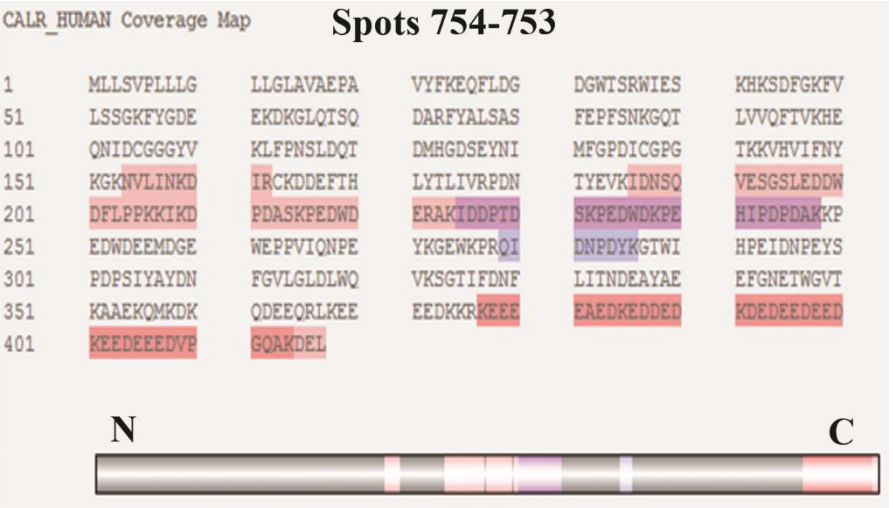

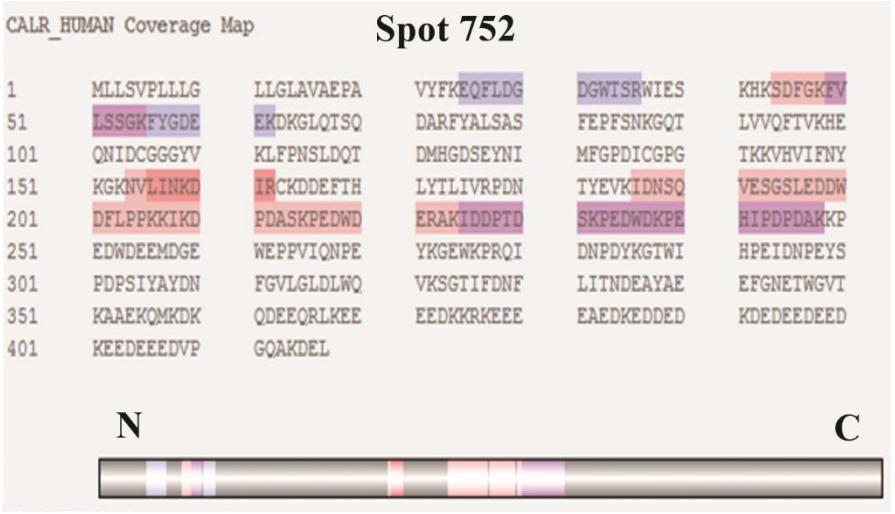

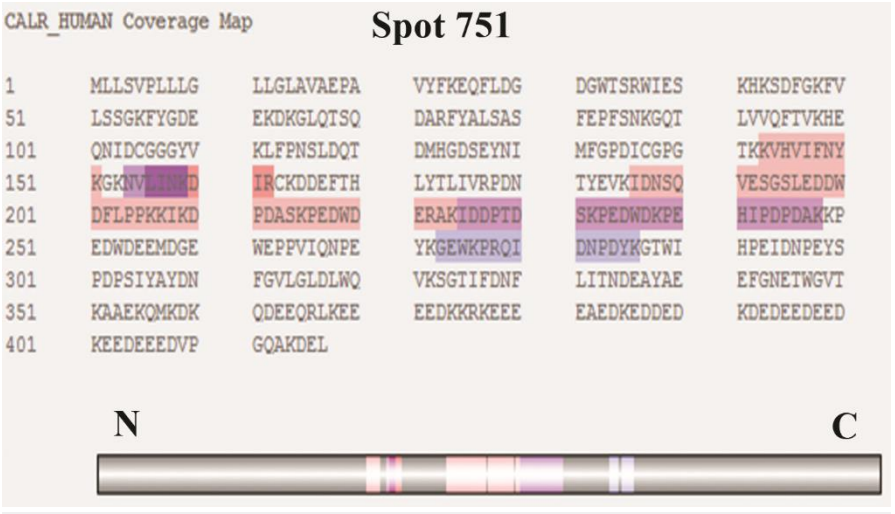

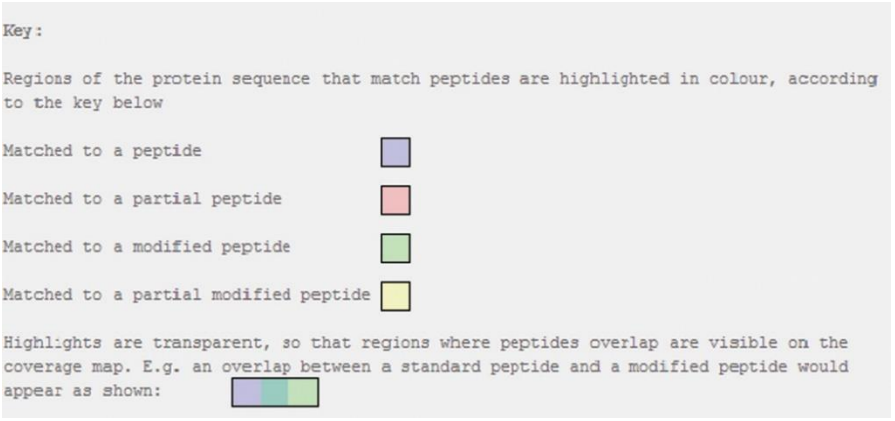

Figure 27. Sequence coverage maps depicting which parts of the CALR protein sequence did the identified peptides from excised spots 751–756 cover. The highlight colour meanings are presented in the Key, they are also transparent and can overlap or stack up. Peptides obtained

from spots 755 and 756 that correspond to the whole protein, cover parts of the CALR sequence throughout. Spots that are degradation products of CALR (spots 751–754) cover parts of the sequence either at the *N*- or *C*-terminus, or the middle of the protein sequence.

These findings suggest that despite the effective secretion of full-length CALR, there is degradation happening inside the cell. There are a few degradation pathways a protein can be sorted to undergo: ERAD is a process that retro-translocates mutated or improperly folded proteins from ER to the cytosol (Brodsky, 2012); post-Golgi sorting to vacuoles (Hou et al., 2012) or endocytosis when vesicles formed at the plasma membrane enter late endosomes and then are carried to the vacuoles (Pelham, 2002). The amount of intact and truncated CALR protein inside the yeast cell seems to be very similar, and this suggests that the degradation is notable (See Figure 25.). The truncated parts are not secreted and must be digested in the cell. We do not yet know, which degradation pathway part of CALR undergoes, but the efficient secretion indicates that it does not afflict the cell.

Spots 749 and 750 were identified as yeast Superoxide dismutase (SOD1) (Accession no.: P00445, Entry SODC_YEAST, MW 15844, pI 5.5708, Superoxide dismutase [Cu-Zn] OS=Saccharomyces cerevisiae). Because of the close proximity to the spots 749 and 750, we also identified a larger spot (See Figure 25. Blue square) that appeared to be SOD1 also, although it did not show differential synthesis patterns. In CALR samples spots 749 and 750 appear next to SOD1 and are completely absent in control samples. It is possible that these spots are isoforms of the main cytosolic SOD1 protein. How the production of CALR is related to the appearance of SOD1 isoforms, we have yet to find out. The secretion of CALR did not diminish in ΔSOD1 knock-out strain versus the BY4741 mother strain for control, which indicates that SOD1 is not essential for the secretion of CALR (See Figure 28.) in yeast.

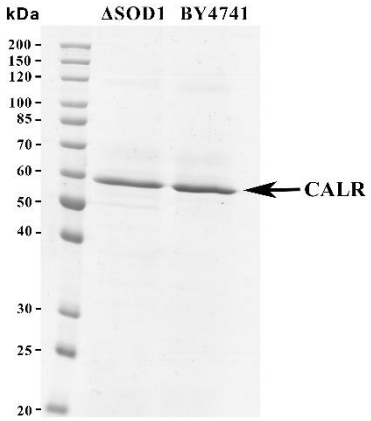

Figure 28. SDS-PAGE analysis of CALR secretion in ΔSOD1 knock-out mutant strain and its mother strain BY4741. For BY4741, 8 µl of cell culture medium was loaded. For ΔSOD1 variant the volume of cell culture medium was adjusted in accordance with cell culture optical density differences (O.D. of ΔSOD1 culture was 1/5 times lesser at the growth end-point, that is why the volume of the loaded sample was increased 1/5 times, to normalise the CALR amount).

Nevertheless, the fact that the main SOD1 spot does not show any decrease with the appearance of the isoforms may mean that the overall synthesis of SOD1 is increased. Heterologous protein overproduction in yeast generates large amounts of ROS and induces cellular oxidative stress (Martínez et al., 2016). This happens either by the assistance of chaperones in overproduced protein folding and disulphide bond formation (Tyo et al., 2012) or by mitochondria producing large quantities of ATP for the whole process (Haynes et al., 2004).

Overall, in comparative 2DE-based analysis of CALR-secreting yeast cell samples vs control, using t-test and DESeq2 analysis of the protein quantities in the gels we found altogether only 8 spots that met our criteria of FC $\geq$ 1.5 times (p-value < 0.01; padj < 0.1). Although 2DE-based analysis represents only a small part of the proteome analysed, it mostly represents high abundancy proteins, which in turn can show a high degree of change in proteomes and are the most interesting (Twyman et al., 2013). It also provides us with a visual representation of the analysed proteomes – an easy way to determine just how much the cell is affected by the production of a recombinant protein. In our case, the comparative 2DE analysis showed a very low degree of change in high abundant protein synthesis patterns between samples. The overall spot patterns and intensities varied very little between CALR secreting yeast and control, with the exception of the 8 spots mentioned (See Figure 25. and Figure 26.).

3.4.3. Comparative LC-MS^E-based analysis of CALR-secreting yeast cell samples vs control

2DE gel staining with CBB-R250 has the lowest protein detection limit of 8–10 ng (Beer & Speicher, 2002). This means that only conditionally high abundance proteins will be represented in the gel. If the NEPHGE-based 2DE analysis was limited to the most abundant cellular proteins, the LC-MS^E analysis allowed us to examine a large part of CALR-secreting and control yeast cell proteomes. We performed a comparative whole protein sample bottom-up tryptic analysis using a triplicate of the 3-hour after recombinant protein induction samples of CALR-secreting yeast versus control (6 samples total), to assess biological and methodological variations. In total, we identified 1726 unique proteins, out of which, 1574 were detected in all samples. The count of identified proteins makes up a third of the total haploid yeast proteome (de Godoy et al., 2008; Ho et al., 2018). 152 proteins were not detected in a part of samples – 83 were undetected in 33.3% of the samples (2 out of 6 samples) and another 69 undetected in ≥ 50% of samples (3 or more out of 6). Out of 1574 proteins identified in all samples, only 20 met our criteria of FC ≥ 1.5 times (0.58 log2FC), $p < 0.01$ and FDR < 0.05.

Both sample groups had underrepresented proteins. 9 proteins out of 20 were not detected at all in control samples – only in CALR-secreting yeast cell samples, and 4 were underrepresented in CALR samples. 60S ribosomal proteins L17-B, L26-A, L15-B, Ribose-phosphate pyrophosphokinase 2 (KPR2), Cytochrome c oxidase polypeptide 5B (COX5b), cAMP-dependent protein kinase type 3 (KAPC) and Hexose transporter HXT15 were all undetected in control samples. 3-hydroxy-3-methylglutaryl-coenzyme A reductase 2 (HMDH2) and Y' element ATP-dependent helicase YIL177C were undetected in CALR samples. Having in mind that all mentioned proteins are necessary for cellular housekeeping, we treated their underrepresentation in one sample and representation in another as an upregulated biosynthesis (See Table 7.).

Table 7. Function, description, log-transformed FC and FDR of the significant proteins with differential synthesis patterns identified by LC-MS^E in CALR and control samples.

Cellular proteins with upregulated biosynthesis in CALR samples

Protein name	**Description**	**Functional group**	**Log2FC**	***p*-value (<0.01)**	**FDR (<0.05)**
RL17B	60S ribosomal protein	Ribosome biogenesis	13.56	$2.38E^{-11}$	$4.1E^{-8}$

		(Bonander et al., 2009; Li et al., 2017; Slavov et al., 2015)			
RL26A	60S ribosomal protein	Ribosome biogenesis (Bonander et al., 2009; Li et al., 2017; Slavov et al., 2015)	12.45	$5.10E^{-11}$	$4.39E^{-8}$
RL15B	60S ribosomal protein	Ribosome biogenesis (Bonander et al., 2009; Li et al., 2017; Slavov et al., 2015)	11.50	$2.22E^{-10}$	$1.28E^{-7}$
KPR2	Ribose-phosphate pyrophosphokinase 2 necessary for de novo and salvage synthesis of nucleotides	Nucleotide metabolism (Moffatt & Ashihara, 2002; Yu et al., 2017)	13.15	$7.29E^{-10}$	$2.51E^{-7}$
COX5B	Hypoxia-induced Cytochrome c oxidase polypeptide 5B is a terminal oxidase of the mitochondrial respiratory chain	Energy (Allen et al., 1995; Burke et al., 1997; Siso et al., 2012)	11.06	$9.82E^{-9}$	$2.82E^{-6}$
YC21B	Transposon Ty2-C Gag-Pol polyprotein	Unknown function in the cellular processes (Curcio et al., 2015; de Godoy et al., 2008; Zaratiegui, 2017)	14.18	$2.48E^{-6}$	$3.28E^{-4}$
YD22B	Transposon Ty2-DR2 Gag-Pol polyprotein	Unknown function in the cellular processes (Curcio et al., 2015; de Godoy et al., 2008; Zaratiegui, 2017)	14.18	$2.48E^{-6}$	$3.28E^{-4}$

KAPC	cAMP-dependent protein kinase type 3 essential member of the Ras signalling pathway	Regulation of cell growth, stress resistance and metabolism (Broach, 1991; Hinnebusch & Lorsch, 2012; Kunkel et al., 2019; Lui et al., 2010; Rolland et al., 2002; Tudisca et al., 2012)	12.55	$4.67E^{-6}$	$5.76E^{-4}$
HXT15	Hexose transporter HXT15 promotes growth of non-fermentable carbon sources in case of glucose starvation	Energy/transport (Greatrix & van Vuuren, 2006; Jordan et al., 2016; Wieczorke et al., 1999)	9.38	$8.00E^{-5}$	$8.62E^{-3}$
RL7A	60S ribosomal protein	Ribosome biogenesis (Bonander et al., 2009; Li et al., 2017; Slavov et al., 2015)	0.78	$4.76E^{-4}$	0.04
IF4F2	Eukaryotic initiation factor 4F subunit p130 limiting factor of translation initiation and ribosome recruitment	Translation initiation (Clarkson et al., 2010; Costello et al., 2017; Gallie & Browning, 2001; Goyer et al., 1993; von der Haar & McCarthy, 2002)	0.58	$4.07E^{-4}$	0.04

Cellular proteins with downregulated biosynthesis in CALR samples

Protein name	**Description**	**Functional group**	**Log2FC**	***p*-value (<0.01)**	**FDR (<0.05)**
YD11A	Transposon Ty1-DR1 Gag polyprotein	Unknown function in the cellular processes	-16.37	$5.51E^{-10}$	$2.38E^{-7}$

		(Curcio et al., 2015; de Godoy et al., 2008; Zaratiegui, 2017)			
YN12B	Transposon Ty1-NL2 Gag-Pol polyprotein	Unknown function in the cellular processes (Curcio et al., 2015; de Godoy et al., 2008; Zaratiegui, 2017)	-10.18	$6.56E^{-8}$	$1.59E^{-5}$
HMDH2	Hypoxia induced 3-hydroxy-3-methylglutaryl-coenzyme A reductase 2 a rate-limiting member in sterol biosynthesis pathway	Lipid biosynthesis (Basson et al., 1986; Hampton & Garza, 2009; Wangeline & Hampton, 2018)	-13.22	$9.92E^{-8}$	$1.9E^{-5}$
YIR7	Y' element ATP-dependent helicase YIL177C	Telomerase-independent telomere maintenance (Yamada et al., 1998)	-10.72	$3.52E^{-7}$	$6.06E^{-5}$
PMA2	Plasma membrane ATPase 2 creates proton gradient for secondary nutrient transport, elevated synthesis during carbon starvation	Nutrient transport and pH homeostasis (Fernandes & Sá-Correia, 2003; Martin-Perez & Villén, 2017; Schlesser et al., 1988; Supply et al., 1993)	-2.23	$1.334E^{-6}$	$2.09E^{-4}$
RSSA1	40S ribosomal protein	Ribosome biogenesis (Bonander et al., 2009; Li et al., 2017; Slavov et al., 2015)	-1.85	$1.46E^{-5}$	$1.69E^{-3}$
RL22B	60S ribosomal protein	Ribosome biogenesis	-2.52	$2.85E^{-4}$	0.03

		(Bonander et al., 2009; Li et al., 2017; Slavov et al., 2015)			
KPR4	Ribose-phosphate pyrophosphokinase 4 necessary for de novo and salvage synthesis of nucleotides	Nucleotide metabolism (Moffatt & Ashihara, 2002; Yu et al., 2017)	-1.57	$5.16E^{-4}$	0.05

For the most part, proteins with differential synthesis patterns between CALR samples and control were responsible for protein translation, energy, nucleotide, amino acid and lipid metabolism. We did not find any differential synthesis of proteins involved in central carbon metabolism, protein folding or protein trafficking – which accounted for a large portion of proteins with differential synthesis patterns in similar experiments, where intracellular proteomes of yeast *Pichia pastoris* overproducing xylanase A (Lin et al., 2013) and *Schizosaccharomyces pombe* producing α-glucosidase maltase (Hung et al., 2016) were analysed. Together with the difference in protein functional profiles, the number of proteins with changes in their synthesis was much greater in both of the aforementioned experiments. Analysis of the proteome of *S. pombe* producing α-glucosidase maltase detected 30–40 proteins with differential synthesis. Analysis of the proteome of *Pichia pastoris* overproducing xylanase A resulted in hundreds of proteins with changes in synthesis and all the markers of the UPR. The relatively small number of proteins with differential synthesis found in this work only confirms that *CALR* gene expression and protein secretion in yeast does not induce a high-level change in the proteome.

When the yeast culture medium is switched from glucose to galactose, a process impacting the whole cell metabolism, called carbon catabolite derepression (CCR) starts. Because our CALR-secreting, as well as control cells harbouring an empty vector, were both submitted to CCR, the differential synthesis of cellular proteins must be connected to the production of recombinant CALR. Elevated transcription and translation rates in heterologous protein-producing yeast are associated with increased consumption of precursors, nutrient starvation, energy and utilization of cellular machinery, which is maintained by upregulation of relevant cellular processes (Huang et al., 2017; Kastberg et al., 2022; Mattanovich et al., 2012; Zahrl et al., 2019), and this can be recognised by looking at the functional profiles of the proteins we identified. Differential synthesis of eIF4G2 and

ribosomal proteins may be connected to elevated translation rates in CALR-secreting samples. Taking into account the high amount of the secreted recombinant protein, an involvement of cellular functions to support protein biosynthesis by the ribosomes could be anticipated. Increased synthesis of CcO5b may be induced by an elevated consumption of energy in CALR samples and reduced HMG2 levels could be the result of high flux through the sterol pathway in CALR samples due to active vesicular transport to the outer membrane. Nutrient starvation can be connected to the increased biosythesis of HXT15. Reduced PMA2 amounts may be related to a higher protein turnover in actively secreting yeast (Huang et al., 2017).

The differential synthesis of PRS2 and PRS4 isoforms are hard to explain, but they do belong to different classes of ribose-phosphate pyrophosphokinases which are essential for nucleotide metabolism. It may well be that the synthesis rates of different classes of PRSs varies in time or is dependent on the nutrient starvation, which could be higher in CALR samples due to active secretion. The functions of other identified proteins with differential synthesis between our samples are briefly presented in Table 7. While some of them can be the remnants of the recent transition to diauxic shift (Tpk3), we cannot suggest any possible connection with the secretion of CALR for others (Transposon proteins, Y' element ATP-dependent helicase). We also expected to find other considerable changes in yeast proteome related to the processing or transport of produced CALR protein to the cell surface. However, it was not the case in this study.

The most surprising fact is that we did not find any proteins with differential synthesis patterns connected to any secretory pathway. We expected that with such a high level of secretion of recombinant CALR, the machinery of at least one secretory pathway should also demonstrate upregulation. As was mentioned before, the way that CALR exits mammalian cells is still unclear. CALR exit is mainly facilitated by ER destabilization or cellular stress (Kielbik et al., 2021), which leads to UPR. However, we did not find any evidence of cellular stress caused by CALR secretion from yeast cells. Yeast cells that produce recombinant proteins usually experience some degree of stress – frequently connected with folding and secretion (Gasser et al., 2008; Mattanovich et al., 2004). Inefficient translocation to the ER leads to protein precursor accumulation in the cytosol causing UPR-Cyto and insoluble aggregate formation (Ciplys et al., 2011). Inefficient folding or misfolding causes UPR in the ER (Kauffman et al., 2002), which is directly associated with protein degradation via ERAD pathway (Hiller et al., 1996) and oxidative stress (Gasser et al., 2008). Generally, cellular stress markers associated with these responses can be used to identify the type of stress the

cell is undergoing. For example, during UPR-Cyto an elevated biosynthesis of cytosolic Hsp70, Hsp90, Hsp110 heat shock stress response chaperone family proteins is detected (Ciplys et al., 2011), and in the case of UPR, differential synthesis of BiP and PDI should be noticeable (Kauffman et al., 2002; Mattanovich et al., 2004). One of the functions of BiP is redirecting misfolded proteins to degradation by ERAD (Nishikawa et al., 2001). The fact that we did not observe changes in BiP protein synthesis suggests that there is no active UPR and the degradation of CALR is not a consequence of ERAD. Also, we did not find any differential synthesis in other ER-resident or cytosolic components of ERAD like Der1p, Der3p/Hrd1p, Hrd3p or Sec61p (Bordallo et al., 1998; Hampton et al., 1996; Knop et al., 1996; Pilon M et al., 1997). No growth impairment of CALR-secreting yeast culture - which usually is a sign of stress - was observed. Lack of cellular proteins in the cell culture medium samples indicates that apoptosis is also not prevalent.

Taken together, the high-level secretion of human recombinant CALR protein from yeast *S. cerevisiae* was mostly supported by the rearrangements of protein translation machinery in the ribosomes and limited changes in the biosynthesis of cellular proteins involved in energy and metabolism. The absence of further significant changes in the secretory pathway suggests that in a steady state, yeast secretory machinery is sufficient to maintain high-level secretion of human CALR. Such feature seems to be more characteristic to an inherently secreted protein rather than an intracellular ER chaperone. Further work is needed to compare the secretion of CALR and other naturally secreted proteins, such as human serum albumin or endogenous yeast secretory proteins. Comparative proteomic studies may help to uncover the specific mechanisms for highly efficient secretion of different proteins in eukaryotic cells and explain the dual nature of CALR being both an extracellular molecule secreted outside the cell and an intracellular chaperone residing inside the ER.

With the aim to find the best 2DE method for yeast proteome analysis, two conventional first-dimension separation methods – IPG and NEPHGE were compared, in a 2DE-based experiment studying cytosolic unfolded protein response in *S. cerevisiae*. Same whole cell lysate samples of yeast cells producing MeH, MeN and control cells harbouring an empty vector were subjected to broad pH range (pH 3–10) IPG and NEPHGE isoelectric focusing techniques and later, identical second-dimension separations were performed. Although commercially available and easy to handle, the IPG-based 2DE method turned out to be unreproducible at separating basic protein spots resulting in protein loss. Only about 50% of separated basic spots could be quantified. On the other hand, although more difficult to handle, NEPHGE-based 2DE was characteristic for high reproducibility of basic protein spots (~90%) and minimal gel-to-gel variation at high protein load. Also, the overall spot reproducibility was considerably lower when using IPG-based 2DE method at ~68%, in comparison with ~87% spot reproducibility of NEPHGE-based 2DE. It seems that the IPG-based 2DE method can only resolve a limited amount of protein into good quality spots. At the standard protein load the number of resolved spots is too low to study complex protein samples, and at high protein load the gels get overloaded and that results in protein loss. On the contrary, NEPHGE-based 2DE gel had a ~5-fold higher protein separation capacity, which resulted in better protein separation at any protein load. The results of this comparison indicate that NEPHGE-based 2DE is the preferred method for yeast whole proteome analysis. The most convincing demonstration of this, was that the NEPHGE-based method revealed the repeatable and statistically significant differential biosynthesis of low-abundant highly basic (~pI 9) protein Sis1p that is involved in UPR-Cyto, and IPG-based method did not. It is evident that the 2DE analysis of such complex protein samples as proteomes requires the most sensitive and reproducible method to provide us with the visual information about as much proteins in the protein complement as possible. And our research suggests the use of NEPHGE-based 2DE as the method of choice.

Subsequently, we continued our research on the production of MeH protein in yeast *S. cerevisiae*, including its inefficient translocation to the ER and the induction of UPR-Cyto. From our previous research we identified that the UPR-Cyto induces a group of proteins involved in the heat-shock response. The activation of temperature-regulated chaperones suggested that temperature itself may have an impact on recombinant protein biosynthesis. We investigated the effects of heat shock and cell culture density on the MeH

protein precursor translocation to the ER, and applied NEPHGE-based 2DE to identify cellular proteins involved in the process. Firstly, we studied at which cell culture growth time points and for what duration, the application of heat shock could impact the amount of translocated and glycosylated MeH protein. We found that when heat shock was applied 5 h before the MeH synthesis induction, and was maintained until the end of MeH synthesis, the amount of glycosylated MeH increased about 3-fold when compared to control cell culture grown at standard temperature. However, we noticed that the increase in glycosylated MeH amount largely depended on the cell culture density at which the heat shock was applied. This suggested that not only the duration of the heat shock, but also the growth phase of the yeast cell culture could be important. After the heat shock application at different culture growth points, we determined that it improves MeH translocation efficiency when applied at higher cell densities, starting from the early-log glucose growth phase. The highest translocation efficiency was achieved when heat shock was applied at the late diauxic shift phase of culture cell growth and was characteristic for decreased level of non-translocated MeH precursor. Although, the highest relative amount of translocated MeH was found after heat shock application at late ethanol growth phase, the translocation efficiency was only 25% at this growth point. Overall, relative amounts of glycosylated MeH increased about 3-fold after the heat shock in the late-log phases of both glucose and ethanol growth.

To find out, which cellular proteins are involved in the improved translocation of the MeH precursors, a comparative NEPHGE 2DE-based proteomic analysis was performed. We chose to investigate yeast culture growth conditions when the translocation of the MeH precursors is the most efficient, versus growth conditions when the translocation is at the lowest efficiency, to be able to detect more drastic changes in the proteome. We found that when yeast cells were transferred to 20°C at the late diauxic shift phase with subsequent induction and growth at the same temperature, the translocation of MeH was almost totally inhibited. The amount of glycosylated MeH produced at 37°C compared to 20°C was 80-fold higher and the translocation efficiency was elevated 60-fold. This drastic difference allowed us to assess cellular proteome when MeH translocation is under ‘‘on’’ or ‘‘off’’ conditions. We were able to identify 40 proteins with differential biosynthesis patterns, of which ~15 were selected as possibly involved in the MeH translocation. Although only high-abundant cellular proteins were quantitated in this study, we suppose that high synthesis rate of viral proteins should be assisted by a comparable amount of cellular proteins. At least, the most abundant cellular proteins may be identified as markers of specific

biological processes involved in improved viral protein translocation. The functions of some proteins with differential synthesis identified from NEPHGE-based 2DE gels suggest several possible mechanisms involved in heterologous protein translocation at both sides of the ER. These findings set a background for further research on viral protein translocation bottleneck in yeast *S. cerevisiae*.

Our further research came to halt when we discovered that the manufacturers of our preferred NEPHGE-2DE system ceased their operations leaving owners of the apparatus without a supply of reagents. We thought it was important to recreate the composition of NEPHGE first-dimension gels, not only for our own use, but also make it available for other operators of this system. The composition of the CA in IEF gels sold by WITA GmbH still remains unknown and recreating the original CA mixture presented by Klose and Kobalz also posed a challenge due to the discontinuation of production of most of the ampholytes used at that time. After testing 12 different CA mixtures, we found that mix no. 3 ("New mix") performed the best. To further test our "New mix" we compared it to the commercial "WITA" gel solutions. We performed a triplication of 2DE separations of the same sample using either our "New mix" or "WITA" solutions for NEPHGE-based first-dimension IEF. 2DE gel images were compared using image analysis software and Pearson's coefficient of correlation was calculated. All gels showed a strong positive correlation among them ($r > 0.7$), with small deviations. The correlation inside the gel group that was made with "WITA" solutions ranged from 0.81 to 0.85, and the correlation inside our "New mix" gel group varied between 0.87 and 0.9. When comparing our restored recipe for NEHGE-based first-dimension separation to the commercial "WITA" gels, we got a slightly lower correlation coefficient ($r=0.71–0.77$) than within the two gel groups ($r=0.87–0.9$ and $r=0.81–0.85$, respectively). A slightly better correlation between our "New mix" gels suggests better reproducibility between technical replicas. Despite the not ideal correlation between our "New mix" and "WITA" gels, they still show a strong positive correlation and our restored CA mixture and gel solutions for NEPHGE first-dimension separation can be fully used in 2DE proteomics experiments instead of the no longer commercially available ones.

After restoring the CA mix for successful NEPHGE-based 2DE, we tested it in a comparative proteomic analysis of the high-level secretion of human CALR protein in yeast *S. cerevisiae*. Human CALR protein is an ER chaperone that also has multiple extracellular functions, although the mechanism of how it exits the mammalian cell is mostly unknown. However, yeast *S. cerevisiae* efficiently secretes human CALR, and the analysis of this

process in yeast could help to clarify how it gets out of eukaryotic cells. To obtain samples for 2DE analysis, we expressed human *CALR* gene under an inducible *GAL7* promoter in *S. cerevisiae* strain AH22. We measured the amount of secreted CALR protein in the cell culture medium 18 hours after the induction of recombinant protein synthesis, and found that the yield of mature CALR protein was approximately 138 mg/L (in the range from 120–160 mg/L), which was 2-fold higher than in our previously published results (Čiplys et al., 2015, 2021). By measuring the secreted amount of CALR at different culture growth points, we determined that the most effective secretion happens between 0 to 3 hours and between 3 to 6 hours (~2.8-fold) after the induction. We reasoned that if the secretion is the most effective at these growth points, the cellular proteins responsible for facilitating CALR secretion should be also more abundant. Three and six hours after the induction of recombinant protein synthesis was the cell culture growth points, at which we chose to take our samples for 2DE.

We compared 2DE gels of CALR-producing cell samples versus control cells, harbouring an empty vector, at 3- and 6- hour growth points after the induction. The proteins in the gels were quantified using Student's *t*-test and DESeq2 analysis to assess the differential biosynthesis. We found altogether 811 distinct protein spots, with 734 of them matching throughout the gels. We searched for protein spots characteristic for statistically significant differential biosynthesis patterns with criteria of 1.5-fold change (FC) and p-value <0.01. Both statistical analyses revealed that spots that met the criteria of p-value <0.01 and the highest FC were the same 8 spots (no. 749–756). These spots were excised and subjected to LC-MS identification. Spot 755 corresponded to the mature CALR protein ~46 kDa, spot no. 756 corresponded to the full-length un-translocated CALR precursor with intact signal peptide ~48 kDa. Spots 754–751 were all identified as CALR also, but had different MW and pI. Sequence analysis revealed them to be truncated degradation products of CALR. This finding suggested that despite the effective secretion of full-length CALR, there is degradation happening inside the cell. Spots 749 and 750 were identified as yeast SOD1 and, because of the close proximity to the spots 749 and 750, we also identified a larger spot that appeared to be SOD1 also, although it did not show differential synthesis rates. In CALR samples spots 749 and 750 appear next to SOD1 and are completely absent in control samples. It is possible that these spots are isoforms of the main cytosolic SOD1 protein. How the production of CALR is related to the appearance of SOD1 isoforms, we have yet to find out. The secretion of CALR did not diminish in ΔSOD1 knock-out strain versus the BY4741 mother strain

for control, which indicates that SOD1 is not essential for the secretion of CALR in yeast.

As NEPHGE-based 2DE analysis revealed only minor changes in CALR-secreting yeast proteome, we analysed a triplicate of the same whole proteome samples of CALR-secreting and control cells, using comparative quantitative LC-MS^E, using label-free quantitation via TOP3-approach. In total, we identified and quantified 1726 unique proteins, out of which, 1574 were detected in all samples, and only 20 that met our criteria of FC $\geq$ 1.5 times (0.58log2FC), p <0.01 and FDR <0.05. For the most part, proteins that had differential synthesis rates between CALR samples and control, were responsible for protein translation, energy, nucleotide, amino acid and lipid metabolism. Surprisingly, we did not find any proteins with differential biosynthesis patterns connected to any secretory pathway or any signs of cellular stress, which is very uncommon having in mind such an effective secretion of a recombinant protein. This comparative proteomic analysis revealed, the high-level secretion of human recombinant CALR protein from yeast *S. cerevisiae* was mostly supported by the rearrangements of protein translation machinery in the ribosomes and limited changes in the biosynthesis of cellular proteins involved in energy and metabolism. The absence of further significant changes in the secretory pathway suggests that in a steady state, yeast secretory machinery is sufficient to maintain high-level stress-free secretion of human CALR.

To conclude, we have proved our hypothesis only halfway – we were able to identify some cellular proteins that are involved in improved MeH translocation and suggest possible mechanisms, but we were unsuccessful to do the same when studying the secretion of CALR. Therefore, it is obvious that the production of some heterologous proteins in yeast causes too little change in the proteome to be studied by proteomic analysis. It is also evident that although these two studied proteins both are synthesized in the cytosol and transferred to the ER, they do not induce the same responses in the cell. An interaction map of all detected differentially synthesized cellular proteins from both experiments (See Fig. 29) highlight how differently the synthesis of these proteins affected the yeast cells.

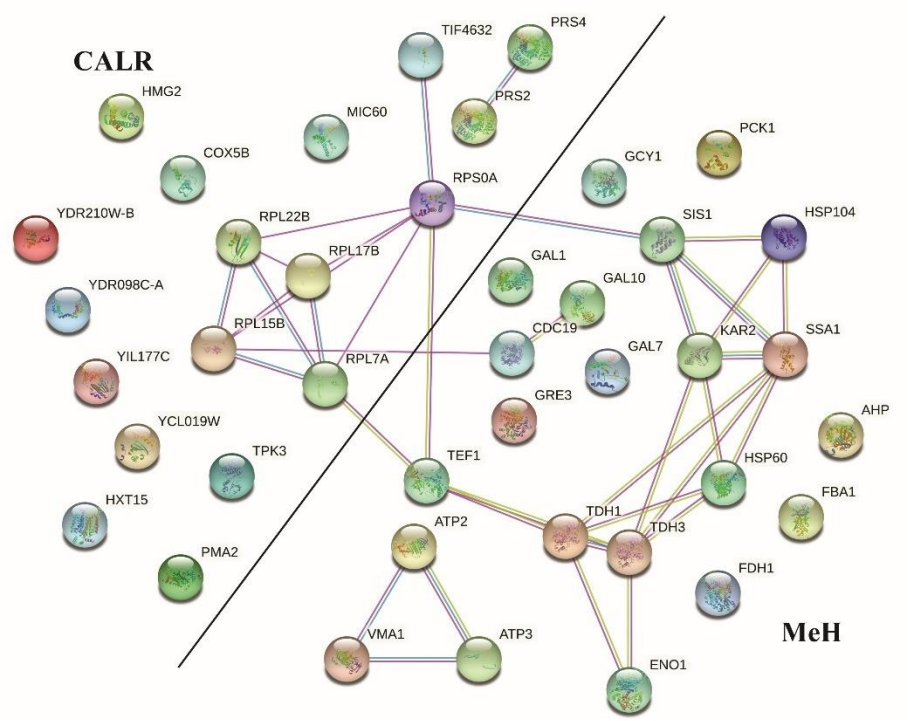

Figure 29. An interaction map of all cellular proteins with differential synthesis patterns discovered in this work. The map was composed using STRING Protein-Protein Interaction Networks Functional Enrichment Analysis tool (string-db.org). Pink marks interactions that are experimentaly determined; blue marks interactions that are found in curated databases; green marks interactions that are found via textmining.

Between these two groups of cellular proteins, the only mapped interactions are among proteins involved in translation (RPL22B, RPL17B, RPL15B, RPL7A, RPS0A, TIF4632, TEF1, CDC19, SIS1). In the CALR experiment the only proteins that interact are also involved in the translation mechanism. However, proteins identified from the MeH experiment are proved to interact a lot between themselves further suggesting their joint participation in the mechanism of improved MeH translocation and overall cellular stress.

From these results, we can predict that the translocation of viral surface glycoproteins in yeast *S. cerevisiae* can be improved by heat shock application. It is also evident that the efficient synthesis and secretion of CALR is determined by its intrinsic properties rather than some cellular mechanism, but the question why an intracellular chaperone has the properties of a secretory protein still lies unanswered. Undeniably, successful synthesis of a protein depends on its polypeptide sequence and different proteins impact the yeast cellular proteome differently. Nevertheless, by identifying two

completely different sets of cellular proteins impacted by the production of recombinant proteins, we show that 2DE- and MS-based proteomic analysis is a sufficient method to study the recombinant protein production in yeast *S. cerevisiae.*

CONCLUSIONS

1. NEPHGE-based first-dimension separation for 2DE in a wide pH 3–10 range, is the preferred method over IPG-based technique for the analysis of yeast whole proteome samples.
2. Heat shock applied at higher cell culture densities and followed by protein biosynthesis at 37 °C, results in about 3-fold increase of both translocation efficiency and the amount of MeH glycoprotein. Using NEPHGE-based 2DE, 15 cellular proteins with differential synthesis patterns, that possibly are associated with the improved translocation of MeH, were identified.
3. Our restored “New mix” CA blend and gel solutions for NEPHGE-based 2DE have better reproducibility and can be used in proteomics experiments instead of the no longer commercially available ones.
4. Efficient CALR secretion does not burden the yeast secretory machinery, only slightly impacts changes in proteome and does not cause any apparent cellular stress. The main proteins with differential synthesis include structural constituents of ribosome involved in protein translation.

REFERENCES

1. Abdul Jabbar, M., & Nayak, D. P. (1987). Signal processing, glycosylation, and secretion of mutant hemagglutinins of a human influenza virus by Saccharomyces cerevisiae. *Molecular and Cellular Biology*, *7*(4), 1476–1485. https://doi.org/10.1128/mcb.7.4.1476-1485.1987
2. Aebersold, R., & Mann, M. (2003). Mass spectrometry-based proteomics. *Nature*, *422*(6928), 198–207. https://doi.org/10.1038/nature01511
3. Afshar, N., Black, B. E., & Paschal, B. M. (2005). Retrotranslocation of the chaperone calreticulin from the endoplasmic reticulum lumen to the cytosol. *Molecular and Cellular Biology*, *25*(20), 8844–8853. https://doi.org/10.1128/MCB.25.20.8844-8853.2005
4. Aguilar, M.-I. (2004). Reversed-phase high-performance liquid chromatography. *Methods in Molecular Biology (Clifton, N.J.)*, *251*, 9–22. https://doi.org/10.1385/1-59259-742-4:9
5. Aguilera, J., Randez-Gil, F., & Prieto, J. A. (2007). Cold response in Saccharomyces cerevisiae: New functions for old mechanisms. *FEMS Microbiology Reviews*, *31*(3), 327–341. https://doi.org/10.1111/j.1574-6976.2007.00066.x
6. Alba, F. J., Bermudez, A., Bartolome, S., & Daban, J. R. (1996). Detection of five nanograms of protein by two-minute nile red staining of unfixed SDS gels. *BioTechniques*, *21*(4), 625–626. https://doi.org/10.2144/96214bm12
7. Ali Khan, H., & Mutus, B. (2014). Protein disulfide isomerase a multifunctional protein with multiple physiological roles. *Frontiers in Chemistry*, *2*, 70. https://doi.org/10.3389/fchem.2014.00070
8. Allen, L. A., Zhao, X.-J., Caughey, W., & Poyton, R. O. (1995). Isoforms of Yeast Cytochrome c Oxidase Subunit V Affect the Binuclear Reaction Center and Alter the Kinetics of Interaction with the Isoforms of Yeast Cytochrome c(∗). *Journal of Biological Chemistry*, *270*(1), 110–118. https://doi.org/10.1074/jbc.270.1.110
9. Anderson, L., & Anderson, N. G. (1977). High resolution two-dimensional electrophoresis of human plasma proteins. *Proceedings of the National Academy of Sciences of the United States of America*, *74*(12), 5421–5425. https://doi.org/10.1073/pnas.74.12.5421
10. Appel, R. D., Vargas, J. R., Palagi, P. M., Walther, D., & Hochstrasser, D. F. (1997). Melanie II – a third-generation software package for analysis of two-dimensional electrophoresis images: II. Algorithms. *ELECTROPHORESIS*, *18*(15), 2735–2748. https://doi.org/10.1002/elps.1150181507
11. Asadzadeh, Z., Safarzadeh, E., Safaei, S., Baradaran, A., Mohammadi, A., Hajiasgharzadeh, K., Derakhshani, A., Argentiero, A., Silvestris, N., & Baradaran, B. (2020). Current Approaches for Combination Therapy of Cancer: The Role of Immunogenic Cell Death. *Cancers*, *12*(4), E1047. https://doi.org/10.3390/cancers12041047
12. Attfield, P. V. (1997). Stress tolerance: The key to effective strains of industrial baker's yeast. *Nature Biotechnology*, *15*(13), 1351–1357. https://doi.org/10.1038/nbt1297-1351
13. Attfield, P. V., & Kletsas, S. (2000). Hyperosmotic stress response by strains of bakers' yeasts in high sugar concentration medium. *Letters in Applied Microbiology*, *31*(4), 323–327. https://doi.org/10.1046/j.1472-765x.2000.00825.x
14. Baghban, R., Farajnia, S., Rajabibazl, M., Ghasemi, Y., Mafi, A., Hoseinpoor, R., Rahbarnia, L., & Aria, M. (2019). Yeast Expression Systems: Overview and Recent Advances. *Molecular Biotechnology*, *61*(5), 365–384. https://doi.org/10.1007/s12033-019-00164-8
15. Baksh, S., & Michalak, M. (1991). Expression of calreticulin in Escherichia coli and identification of its Ca2+ binding domains. *The Journal of Biological Chemistry*, *266*(32), 21458–21465.
16. Basson, M. E., Thorsness, M., & Rine, J. (1986). Saccharomyces cerevisiae contains two functional genes encoding 3-hydroxy-3-methylglutaryl-coenzyme A reductase.

Proceedings of the National Academy of Sciences of the United States of America, *83*(15), 5563–5567. https://doi.org/10.1073/pnas.83.15.5563
17. Beer, L. A., & Speicher, D. W. (2002). Protein Detection in Gels Using Fixation. *Current Protocols in Protein Science*, *CHAPTER 10*, Unit-10.5. https://doi.org/10.1002/0471140864.ps1005s29
18. Benecke, O., & DeYoung, S. E. (2019). Anti-Vaccine Decision-Making and Measles Resurgence in the United States. *Global Pediatric Health*, *6*, 2333794X19862949. https://doi.org/10.1177/2333794X19862949
19. Benjamini, Y., & Hochberg, Y. (1995). Controlling the False Discovery Rate: A Practical and Powerful Approach to Multiple Testing. *Journal of the Royal Statistical Society. Series B (Methodological)*, *57*(1), 289–300.
20. Berggren, K. N., Schulenberg, B., Lopez, M. F., Steinberg, T. H., Bogdanova, A., Smejkal, G., Wang, A., & Patton, W. F. (2002). An improved formulation of SYPRO Ruby protein gel stain: Comparison with the original formulation and with a ruthenium II tris (bathophenanthroline disulfonate) formulation. *Proteomics*, *2*(5), 486–498. https://doi.org/10.1002/1615-9861(200205)2:5<486::AID-PROT486>3.0.CO;2-X
21. Biddick, R., & Young, E. T. (2009). The disorderly study of ordered recruitment. *Yeast (Chichester, England)*, *26*(4), 205–220. https://doi.org/10.1002/yea.1660
22. Bischoff, R., Clesse, D., Whitechurch, O., Lepage, P., & Roitsch, C. (1989). Isolation of recombinant hirudin by preparative high-performance liquid chromatography. *Journal of Chromatography*, *476*, 245–255. https://doi.org/10.1016/s0021-9673(01)93873-7
23. Bjarnadóttir, S. G., & Flengsrud, R. (2014). Affinity chromatography, two-dimensional electrophoresis, adapted immunodepletion and mass spectrometry used for detection of porcine and piscine heparin-binding human plasma proteins. *Journal of Chromatography. B, Analytical Technologies in the Biomedical and Life Sciences*, *944*, 107–113. https://doi.org/10.1016/j.jchromb.2013.11.004
24. Bjellqvist, B., Ek, K., Righetti, P. G., Gianazza, E., Görg, A., Westermeier, R., & Postel, W. (1982). Isoelectric focusing in immobilized pH gradients: Principle, methodology and some applications. *Journal of Biochemical and Biophysical Methods*, *6*(4), 317–339. https://doi.org/10.1016/0165-022x(82)90013-6
25. Blomberg, A., Blomberg, L., Norbeck, J., Fey, S. J., Larsen, P. M., Larsen, M., Roepstorff, P., Degand, H., Boutry, M., & Posch, A. (1995). Interlaboratory reproducibility of yeast protein patterns analyzed by immobilized pH gradient two-dimensional gel electrophoresis. *Electrophoresis*, *16*(10), 1935–1945. https://doi.org/10.1002/elps.11501601320
26. Böer, E., Piontek, M., & Kunze, G. (2009). Xplor 2—An optimized transformation/expression system for recombinant protein production in the yeast Arxula adeninivorans. *Applied Microbiology and Biotechnology*, *84*(3), 583–594. https://doi.org/10.1007/s00253-009-2167-5
27. Bohring, C., & Krause, W. (1999). The characterization of human spermatozoa membrane proteins—Surface antigens and immunological infertility. *Electrophoresis*, *20*(4–5), 971–976. https://doi.org/10.1002/(SICI)1522-2683(19990101)20:4/5<971::AID-ELPS971>3.0.CO;2-6
28. Boisvert, F.-M., Lam, Y. W., Lamont, D., & Lamond, A. I. (2010). A quantitative proteomics analysis of subcellular proteome localization and changes induced by DNA damage. *Molecular & Cellular Proteomics: MCP*, *9*(3), 457–470. https://doi.org/10.1074/mcp.M900429-MCP200
29. Bonander, N., Darby, R. A., Grgic, L., Bora, N., Wen, J., Brogna, S., Poyner, D. R., O'Neill, M. A., & Bill, R. M. (2009). Altering the ribosomal subunit ratio in yeast maximizes recombinant protein yield. *Microbial Cell Factories*, *8*, 10. https://doi.org/10.1186/1475-2859-8-10
30. Bonander, N., Hedfalk, K., Larsson, C., Mostad, P., Chang, C., Gustafsson, L., & Bill, R. M. (2005). Design of improved membrane protein production experiments: Quantitation of the host response. *Protein Science*, *14*(7), 1729–1740. https://doi.org/10.1110/ps.051435705

31. Bordallo, J., Plemper, R. K., Finger, A., & Wolf, D. H. (1998). Der3p/Hrd1p Is Required for Endoplasmic Reticulum-associated Degradation of Misfolded Lumenal and Integral Membrane Proteins. *Molecular Biology of the Cell*, *9*(1), 209–222. https://doi.org/10.1091/mbc.9.1.209
32. Bouche, F. B., Ertl, O. T., & Muller, C. P. (2002). Neutralizing B cell response in measles. *Viral Immunology*, *15*(3), 451–471. https://doi.org/10.1089/088282402760312331
33. Boucherie, H., Sagliocco, F., Joubert, R., Maillet, I., Labarre, J., & Perrot, M. (1996). Two-dimensional gel protein database of Saccharomyces cerevisiae. *Electrophoresis*, *17*(11), 1683–1699. https://doi.org/10.1002/elps.1150171106
34. Brauer, M. J., Huttenhower, C., Airoldi, E. M., Rosenstein, R., Matese, J. C., Gresham, D., Boer, V. M., Troyanskaya, O. G., & Botstein, D. (2008). Coordination of growth rate, cell cycle, stress response, and metabolic activity in yeast. *Molecular Biology of the Cell*, *19*(1), 352–367. https://doi.org/10.1091/mbc.e07-08-0779
35. Bravo, R., & Celis, J. E. (1980). A search for differential polypeptide synthesis throughout the cell cycle of HeLa cells. *The Journal of Cell Biology*, *84*(3), 795–802. https://doi.org/10.1083/jcb.84.3.795
36. Brenner, S. E. (1999). Errors in genome annotation. *Trends in Genetics: TIG*, *15*(4), 132–133. https://doi.org/10.1016/s0168-9525(99)01706-0
37. Broach, J. R. (1991). RAS genes in Saccharomyces cerevisiae: Signal transduction in search of a pathway. *Trends in Genetics*, *7*(1), 28–33. https://doi.org/10.1016/0168-9525(91)90018-L
38. Brocard-Masson, C., & Dumas, B. (2006). The fascinating world of steroids: S. cerevisiae as a model organism for the study of hydrocortisone biosynthesis. *Biotechnology & Genetic Engineering Reviews*, *22*, 213–252. https://doi.org/10.1080/02648725.2006.10648072
39. Brodsky, J. L. (2012). Cleaning Up: Endoplasmic Reticulum Associated Degradation to the Rescue. *Cell*, *151*(6), 1163–1167. https://doi.org/10.1016/j.cell.2012.11.012
40. Burke, P. V., Raitt, D. C., Allen, L. A., Kellogg, E. A., & Poyton, R. O. (1997). Effects of Oxygen Concentration on the Expression of Cytochrome c and Cytochrome c Oxidase Genes in Yeast *. *Journal of Biological Chemistry*, *272*(23), 14705–14712. https://doi.org/10.1074/jbc.272.23.14705
41. Burns, K., Duggan, B., Atkinson, E. A., Famulski, K. S., Nemer, M., Bleackley, R. C., & Michalak, M. (1994). Modulation of gene expression by calreticulin binding to the glucocorticoid receptor. *Nature*, *367*(6462), 476–480. https://doi.org/10.1038/367476a0
42. Büttner, K., Bernhardt, J., Scharf, C., Schmid, R., Mäder, U., Eymann, C., Antelmann, H., Völker, A., Völker, U., & Hecker, M. (2001). A comprehensive two-dimensional map of cytosolic proteins of Bacillus subtilis. *Electrophoresis*, *22*(14), 2908–2935. https://doi.org/10.1002/1522-2683(200108)22:14<2908::AID-ELPS2908>3.0.CO;2-M
43. Cascio, S., Zhang, L., & Finn, O. J. (2011). MUC1 protein expression in tumor cells regulates transcription of proinflammatory cytokines by forming a complex with nuclear factor-κB p65 and binding to cytokine promoters: Importance of extracellular domain. *The Journal of Biological Chemistry*, *286*(49), 42248–42256. https://doi.org/10.1074/jbc.M111.297630
44. Cashikar, A. G., Duennwald, M., & Lindquist, S. L. (2005). A chaperone pathway in protein disaggregation. Hsp26 alters the nature of protein aggregates to facilitate reactivation by Hsp104. *The Journal of Biological Chemistry*, *280*(25), 23869–23875. https://doi.org/10.1074/jbc.M502854200
45. Cassland, P., & Jönsson, L. J. (1999). Characterization of a gene encoding Trametes versicolor laccase A and improved heterologous expression in Saccharomyces cerevisiae by decreased cultivation temperature. *Applied Microbiology and Biotechnology*, *52*(3), 393–400. https://doi.org/10.1007/s002530051537
46. Causton, H. C., Ren, B., Koh, S. S., Harbison, C. T., Kanin, E., Jennings, E. G., Lee, T. I., True, H. L., Lander, E. S., & Young, R. A. (2001). Remodeling of yeast genome expression in response to environmental changes. *Molecular Biology of the Cell*, *12*(2), 323–337. https://doi.org/10.1091/mbc.12.2.323

47. Celik, E., & Calık, P. (2012). Production of recombinant proteins by yeast cells. *Biotechnology Advances*, *30*(5), 1108–1118. https://doi.org/10.1016/j.biotechadv.2011.09.011
48. Chaput, N., De Botton, S., Obeid, M., Apetoh, L., Ghiringhelli, F., Panaretakis, T., Flament, C., Zitvogel, L., & Kroemer, G. (2007). Molecular determinants of immunogenic cell death: Surface exposure of calreticulin makes the difference. *Journal of Molecular Medicine (Berlin, Germany)*, *85*(10), 1069–1076. https://doi.org/10.1007/s00109-007-0214-1
49. Chevalier, F. (2010a). Highlights on the capacities of 'Gel-based' proteomics. *Proteome Science*, *8*, 23. https://doi.org/10.1186/1477-5956-8-23
50. Chevalier, F. (2010b). Standard Dyes for Total Protein Staining in Gel-Based Proteomic Analysis. *Materials*, *3*(10), 4784–4792. https://doi.org/10.3390/ma3104784
51. Choi, H., & Nesvizhskii, A. I. (2008). False discovery rates and related statistical concepts in mass spectrometry-based proteomics. *Journal of Proteome Research*, *7*(1), 47–50. https://doi.org/10.1021/pr700747q
52. Chuang, S.-M., Chen, L., Lambertson, D., Anand, M., Kinzy, T. G., & Madura, K. (2005). Proteasome-mediated degradation of cotranslationally damaged proteins involves translation elongation factor 1A. *Molecular and Cellular Biology*, *25*(1), 403–413. https://doi.org/10.1128/MCB.25.1.403-413.2005
53. Čiplys, E., Aučynaitė, A., & Slibinskas, R. (2014). Generation of human ER chaperone BiP in yeast Saccharomyces cerevisiae. *Microbial Cell Factories*, *13*, 22. https://doi.org/10.1186/1475-2859-13-22
54. Čiplys, E., Paškevičius, T., Žitkus, E., Bielskis, J., Ražanskas, R., Šneideris, T., Smirnovas, V., Kaupinis, A., Tester, D. J., Ackerman, M. J., Højrup, P., Michalak, M., Houen, G., & Slibinskas, R. (2021). Mapping human calreticulin regions important for structural stability. *Biochimica Et Biophysica Acta. Proteins and Proteomics*, *1869*(11), 140710. https://doi.org/10.1016/j.bbapap.2021.140710
55. Ciplys, E., Samuel, D., Juozapaitis, M., Sasnauskas, K., & Slibinskas, R. (2011). Overexpression of human virus surface glycoprotein precursors induces cytosolic unfolded protein response in Saccharomyces cerevisiae. *Microbial Cell Factories*, *10*, 37. https://doi.org/10.1186/1475-2859-10-37
56. Čiplys, E., Sasnauskas, K., & Slibinskas, R. (2011). Overexpression of human calnexin in yeast improves measles surface glycoprotein solubility. *FEMS Yeast Research*, *11*(6), 514–523. https://doi.org/10.1111/j.1567-1364.2011.00742.x
57. Čiplys, E., Žitkus, E., Gold, L. I., Daubriac, J., Pavlides, S. C., Højrup, P., Houen, G., Wang, W.-A., Michalak, M., & Slibinskas, R. (2015). High-level secretion of native recombinant human calreticulin in yeast. *Microbial Cell Factories*, *14*. https://doi.org/10.1186/s12934-015-0356-8
58. Čiplys, E., Žitkus, E., & Slibinskas, R. (2013). Native signal peptide of human ERp57 disulfide isomerase mediates secretion of active native recombinant ERp57 protein in yeast Saccharomyces cerevisiae. *Protein Expression and Purification*, *89*(2), 131–135. https://doi.org/10.1016/j.pep.2013.03.003
59. Clarkson, B. K., Gilbert, W. V., & Doudna, J. A. (2010). Functional Overlap between eIF4G Isoforms in Saccharomyces cerevisiae. *PLoS ONE*, *5*(2). https://doi.org/10.1371/journal.pone.0009114
60. Coe, H., & Michalak, M. (2010). ERp57, a multifunctional endoplasmic reticulum resident oxidoreductase. *The International Journal of Biochemistry & Cell Biology*, *42*(6), 796–799. https://doi.org/10.1016/j.biocel.2010.01.009
61. Coppolino, M. G., & Dedhar, S. (2000). Bi-directional signal transduction by integrin receptors. *The International Journal of Biochemistry & Cell Biology*, *32*(2), 171–188. https://doi.org/10.1016/s1357-2725(99)00043-6
62. Coppolino, M. G., Woodside, M. J., Demaurex, N., Grinstein, S., St-Arnaud, R., & Dedhar, S. (1997). Calreticulin is essential for integrin-mediated calcium signalling and cell adhesion. *Nature*, *386*(6627), 843–847. https://doi.org/10.1038/386843a0
63. Corbett, E. F., Oikawa, K., Francois, P., Tessier, D. C., Kay, C., Bergeron, J. J., Thomas, D. Y., Krause, K. H., & Michalak, M. (1999). Ca2+ regulation of interactions between

endoplasmic reticulum chaperones. *The Journal of Biological Chemistry*, *274*(10), 6203–6211. https://doi.org/10.1074/jbc.274.10.6203
64. Corbett, J. M., Dunn, M. J., Posch, A., & Görg, A. (1994). Positional reproducibility of protein spots in two-dimensional polyacrylamide gel electrophoresis using immobilised pH gradient isoelectric focusing in the first dimension: An interlaboratory comparison. *Electrophoresis*, *15*(8–9), 1205–1211. https://doi.org/10.1002/elps.11501501182
65. Corthals, G. L., Wasinger, V. C., Hochstrasser, D. F., & Sanchez, J. C. (2000). The dynamic range of protein expression: A challenge for proteomic research. *Electrophoresis*, *21*(6), 1104–1115. https://doi.org/10.1002/(SICI)1522-2683(20000401)21:6<1104::AID-ELPS1104>3.0.CO;2-C
66. Costello, J. L., Kershaw, C. J., Castelli, L. M., Talavera, D., Rowe, W., Sims, P. F. G., Ashe, M. P., Grant, C. M., Hubbard, S. J., & Pavitt, G. D. (2017). Dynamic changes in eIF4F-mRNA interactions revealed by global analyses of environmental stress responses. *Genome Biology*, *18*. https://doi.org/10.1186/s13059-017-1338-4
67. Cregg, J. M., Cereghino, J. L., Shi, J., & Higgins, D. R. (2000). Recombinant protein expression in Pichia pastoris. *Molecular Biotechnology*, *16*(1), 23–52. https://doi.org/10.1385/MB:16:1:23
68. Cull, M., & McHenry, C. S. (1990). Preparation of extracts from prokaryotes. *Methods in Enzymology*, *182*, 147–153. https://doi.org/10.1016/0076-6879(90)82014-s
69. Curcio, M. J., Lutz, S., & Lesage, P. (2015). The Ty1 LTR-retrotransposon of budding yeast, Saccharomyces cerevisiae. *Microbiology Spectrum*, *3*(2), 1–35. https://doi.org/10.1128/microbiolspec.MDNA3-0053-2014
70. Davidsen, N. B. (1995). Two-dimensional electrophoresis of acidic proteins isolated from ozone-stressed Norway spruce needles (Picea abies L. Karst): Separation method and image processing. *Electrophoresis*, *16*(7), 1305–1311. https://doi.org/10.1002/elps.11501601214
71. De Deken, R. H. (1966). The Crabtree effect: A regulatory system in yeast. *Journal of General Microbiology*, *44*(2), 149–156. https://doi.org/10.1099/00221287-44-2-149
72. de Godoy, L. M. F., Olsen, J. V., Cox, J., Nielsen, M. L., Hubner, N. C., Fröhlich, F., Walther, T. C., & Mann, M. (2008). Comprehensive mass-spectrometry-based proteome quantification of haploid versus diploid yeast. *Nature*, *455*(7217), 1251–1254. https://doi.org/10.1038/nature07341
73. de Swart, R. L., Yüksel, S., Langerijs, C. N., Muller, C. P., & Osterhaus, A. D. M. E. (2009). Depletion of measles virus glycoprotein-specific antibodies from human sera reveals genotype-specific neutralizing antibodies. *The Journal of General Virology*, *90*(Pt 12), 2982–2989. https://doi.org/10.1099/vir.0.014944-0
74. de Swart, R. L., Yüksel, S., & Osterhaus, A. D. M. E. (2005). Relative contributions of measles virus hemagglutinin- and fusion protein-specific serum antibodies to virus neutralization. *Journal of Virology*, *79*(17), 11547–11551. https://doi.org/10.1128/JVI.79.17.11547-11551.2005
75. Dennison, C. (Ed.). (2002). Principles of Electrophoresis. In *A Guide to Protein Isolation* (pp. 115–149). Springer Netherlands. https://doi.org/10.1007/0-306-46868-9_5
76. Diez, R., Herbstreith, M., Osorio, C., & Alzate, O. (2010). 2-D Fluorescence Difference Gel Electrophoresis (DIGE) in Neuroproteomics. In O. Alzate (Ed.), *Neuroproteomics*. CRC Press/Taylor & Francis. http://www.ncbi.nlm.nih.gov/books/NBK56019/
77. Diezel, W., Kopperschläger, G., & Hofmann, E. (1972). An improved procedure for protein staining in polyacrylamide gels with a new type of Coomassie Brilliant Blue. *Analytical Biochemistry*, *48*(2), 617–620. https://doi.org/10.1016/0003-2697(72)90117-0
78. Distler, U., Kuharev, J., Navarro, P., Levin, Y., Schild, H., & Tenzer, S. (2014). Drift time-specific collision energies enable deep-coverage data-independent acquisition proteomics. *Nature Methods*, *11*(2), 167–170. https://doi.org/10.1038/nmeth.2767
79. Dragosits, M., Mattanovich, D., & Gasser, B. (2011). Induction and measurement of UPR and osmotic stress in the yeast Pichia pastoris. *Methods in Enzymology*, *489*, 165–188. https://doi.org/10.1016/B978-0-12-385116-1.00010-8

80. Duina, A. A., Miller, M. E., & Keeney, J. B. (2014). Budding yeast for budding geneticists: A primer on the Saccharomyces cerevisiae model system. *Genetics*, *197*(1), 33–48. https://doi.org/10.1534/genetics.114.163188
81. Elliott, B., & Futcher, B. (1993). Stress resistance of yeast cells is largely independent of cell cycle phase. *Yeast*, *9*(1), 33–42. https://doi.org/10.1002/yea.320090105
82. Escalante-Chong, R., Savir, Y., Carroll, S. M., Ingraham, J. B., Wang, J., Marx, C. J., & Springer, M. (2015). Galactose metabolic genes in yeast respond to a ratio of galactose and glucose. *Proceedings of the National Academy of Sciences of the United States of America*, *112*(5), 1636–1641. https://doi.org/10.1073/pnas.1418058112
83. Fan, G., Katrolia, P., Jia, H., Yang, S., Yan, Q., & Jiang, Z. (2012). High-level expression of a xylanase gene from the thermophilic fungus Paecilomyces thermophila in Pichia pastoris. *Biotechnology Letters*, *34*(11), 2043–2048. https://doi.org/10.1007/s10529-012-0995-3
84. Fernandes, A. R., & Sá-Correia, I. (2003). Transcription patterns of PMA1 and PMA2 genes and activity of plasma membrane H+-ATPase in Saccharomyces cerevisiae during diauxic growth and stationary phase. *Yeast*, *20*(3), 207–219. https://doi.org/10.1002/yea.957
85. Ferndahl, C., Bonander, N., Logez, C., Wagner, R., Gustafsson, L., Larsson, C., Hedfalk, K., Darby, R. A. J., & Bill, R. M. (2010). Increasing cell biomass in Saccharomyces cerevisiae increases recombinant protein yield: The use of a respiratory strain as a microbial cell factory. *Microbial Cell Factories*, *9*, 47. https://doi.org/10.1186/1475-2859-9-47
86. Fic, E., Kedracka-Krok, S., Jankowska, U., Pirog, A., & Dziedzicka-Wasylewska, M. (2010). Comparison of protein precipitation methods for various rat brain structures prior to proteomic analysis. *Electrophoresis*, *31*(21), 3573–3579. https://doi.org/10.1002/elps.201000197
87. Finnis, C., Goodey, A., Courtney, M., & Sleep, D. (1992). Expression of recombinant platelet-derived endothelial cell growth factor in the yeast Saccharomyces cerevisiae. *Yeast (Chichester, England)*, *8*(1), 57–60. https://doi.org/10.1002/yea.320080106
88. Fonseca, G. G., Heinzle, E., Wittmann, C., & Gombert, A. K. (2008). The yeast Kluyveromyces marxianus and its biotechnological potential. *Applied Microbiology and Biotechnology*, *79*(3), 339–354. https://doi.org/10.1007/s00253-008-1458-6
89. Fountoulakis, M., Takács, M. F., Berndt, P., Langen, H., & Takács, B. (1999). Enrichment of low abundance proteins of Escherichia coli by hydroxyapatite chromatography. *Electrophoresis*, *20*(11), 2181–2195. https://doi.org/10.1002/(SICI)1522-2683(19990801)20:11<2181::AID-ELPS2181>3.0.CO;2-Q
90. Franzmann, T. M., Wühr, M., Richter, K., Walter, S., & Buchner, J. (2005). The activation mechanism of Hsp26 does not require dissociation of the oligomer. *Journal of Molecular Biology*, *350*(5), 1083–1093. https://doi.org/10.1016/j.jmb.2005.05.034
91. Freigassner, M., Pichler, H., & Glieder, A. (2009). Tuning microbial hosts for membrane protein production. *Microbial Cell Factories*, *8*, 69. https://doi.org/10.1186/1475-2859-8-69
92. Friedman, D. B., Hoving, S., & Westermeier, R. (2009). Isoelectric focusing and two-dimensional gel electrophoresis. *Methods in Enzymology*, *463*, 515–540. https://doi.org/10.1016/S0076-6879(09)63030-5
93. Galdieri, L., Mehrotra, S., Yu, S., & Vancura, A. (2010). Transcriptional Regulation in Yeast during Diauxic Shift and Stationary Phase. *OMICS : A Journal of Integrative Biology*, *14*(6), 629–638. https://doi.org/10.1089/omi.2010.0069
94. Gallie, D. R., & Browning, K. S. (2001). EIF4G Functionally Differs from eIFiso4G in Promoting Internal Initiation, Cap-independent Translation, and Translation of Structured mRNAs *. *Journal of Biological Chemistry*, *276*(40), 36951–36960. https://doi.org/10.1074/jbc.M103869200
95. Gao, B., Adhikari, R., Howarth, M., Nakamura, K., Gold, M. C., Hill, A. B., Knee, R., Michalak, M., & Elliott, T. (2002). Assembly and Antigen-Presenting Function of MHC

Class I Molecules in Cells Lacking the ER Chaperone Calreticulin. *Immunity*, *16*(1), 99–109. https://doi.org/10.1016/S1074-7613(01)00260-6
96. Gardai, S. J., McPhillips, K. A., Frasch, S. C., Janssen, W. J., Starefeldt, A., Murphy-Ullrich, J. E., Bratton, D. L., Oldenborg, P.-A., Michalak, M., & Henson, P. M. (2005). Cell-surface calreticulin initiates clearance of viable or apoptotic cells through trans-activation of LRP on the phagocyte. *Cell*, *123*(2), 321–334. https://doi.org/10.1016/j.cell.2005.08.032
97. Garfin, D. (2003). *Two-dimensional gel electrophoresis: An overview*. https://doi.org/10.1016/S0165-9936(03)00506-5
98. Garrels, J. I. (1979). Changes in protein synthesis during myogenesis in a clonal cell line. *Developmental Biology*, *73*(1), 134–152. https://doi.org/10.1016/0012-1606(79)90143-x
99. Gasch, A. P., Spellman, P. T., Kao, C. M., Carmel-Harel, O., Eisen, M. B., Storz, G., Botstein, D., & Brown, P. O. (2000). Genomic expression programs in the response of yeast cells to environmental changes. *Molecular Biology of the Cell*, *11*(12), 4241–4257. https://doi.org/10.1091/mbc.11.12.4241
100. Gasser, B., Saloheimo, M., Rinas, U., Dragosits, M., Rodríguez-Carmona, E., Baumann, K., Giuliani, M., Parrilli, E., Branduardi, P., Lang, C., Porro, D., Ferrer, P., Tutino, M. L., Mattanovich, D., & Villaverde, A. (2008). Protein folding and conformational stress in microbial cells producing recombinant proteins: A host comparative overview. *Microbial Cell Factories*, *7*(1), 11. https://doi.org/10.1186/1475-2859-7-11
101. Gebauer, M., Hürlimann, H. C., Behrens, M., Wolff, T., & Behrens, S.-E. (2019). Subunit vaccines based on recombinant yeast protect against influenza A virus in a one-shot vaccination scheme. *Vaccine*, *37*(37), 5578–5587. https://doi.org/10.1016/j.vaccine.2019.07.094
102. Geiler-Samerotte, K. A., Dion, M. F., Budnik, B. A., Wang, S. M., Hartl, D. L., & Drummond, D. A. (2011). Misfolded proteins impose a dosage-dependent fitness cost and trigger a cytosolic unfolded protein response in yeast. *Proceedings of the National Academy of Sciences of the United States of America*, *108*(2), 680–685. https://doi.org/10.1073/pnas.1017570108
103. Gelebart, P., Opas, M., & Michalak, M. (2005). Calreticulin, a Ca2+-binding chaperone of the endoplasmic reticulum. *The International Journal of Biochemistry & Cell Biology*, *37*(2), 260–266. https://doi.org/10.1016/j.biocel.2004.02.030
104. Gething, M. J. (1999). Role and regulation of the ER chaperone BiP. *Seminars in Cell & Developmental Biology*, *10*(5), 465–472. https://doi.org/10.1006/scdb.1999.0318
105. Goffeau, A., Barrell, B. G., Bussey, H., Davis, R. W., Dujon, B., Feldmann, H., Galibert, F., Hoheisel, J. D., Jacq, C., Johnston, M., Louis, E. J., Mewes, H. W., Murakami, Y., Philippsen, P., Tettelin, H., & Oliver, S. G. (1996). Life with 6000 genes. *Science (New York, N.Y.)*, *274*(5287), 546, 563–567. https://doi.org/10.1126/science.274.5287.546
106. Gold, L. I., Eggleton, P., Sweetwyne, M. T., Van Duyn, L. B., Greives, M. R., Naylor, S.-M., Michalak, M., & Murphy-Ullrich, J. E. (2010). Calreticulin: Non-endoplasmic reticulum functions in physiology and disease. *The FASEB Journal*, *24*(3), 665–683. https://doi.org/10.1096/fj.09-145482
107. Görg, A., Drews, O., Lück, C., Weiland, F., & Weiss, W. (2009). 2-DE with IPGs. *Electrophoresis, 30 Suppl 1*, S122-132. https://doi.org/10.1002/elps.200900051
108. Görg, A., Postel, W., & Günther, S. (1988). The current state of two-dimensional electrophoresis with immobilized pH gradients. *Electrophoresis*, *9*(9), 531–546. https://doi.org/10.1002/elps.1150090913
109. Goyer, C., Altmann, M., Lee, H. S., Blanc, A., Deshmukh, M., Woolford, J. L., Trachsel, H., & Sonenberg, N. (1993). TIF4631 and TIF4632: Two yeast genes encoding the high-molecular-weight subunits of the cap-binding protein complex (eukaryotic initiation factor 4F) contain an RNA recognition motif-like sequence and carry out an essential function. *Molecular and Cellular Biology*, *13*(8), 4860–4874. https://doi.org/10.1128/mcb.13.8.4860
110. Gravel, P. (2002). Two-Dimensional Polyacrylamide Gel Electrophoresis of Proteins Using Carrier Ampholyte pH Gradients in the First Dimension. In J. M. Walker (Ed.),

The Protein Protocols Handbook (pp. 163–168). Humana Press. https://doi.org/10.1385/1-59259-169-8:163
111. Greatrix, B. W., & van Vuuren, H. J. J. (2006). Expression of the HXT13, HXT15 and HXT17 genes in Saccharomyces cerevisiae and stabilization of the HXT1 gene transcript by sugar-induced osmotic stress. *Current Genetics*, *49*(4), 205–217. https://doi.org/10.1007/s00294-005-0046-x
112. Greives, M. R., Samra, F., Pavlides, S. C., Blechman, K. M., Naylor, S.-M., Woodrell, C. D., Cadacio, C., Levine, J. P., Bancroft, T. A., Michalak, M., Warren, S. M., & Gold, L. I. (2012). Exogenous calreticulin improves diabetic wound healing. *Wound Repair and Regeneration: Official Publication of the Wound Healing Society [and] the European Tissue Repair Society*, *20*(5), 715–730. https://doi.org/10.1111/j.1524-475X.2012.00822.x
113. Griffin, T. J., & Bandhakavi, S. (2011). Dynamic range compression: A solution for proteomic biomarker discovery? *Bioanalysis*, *3*(18), 2053–2056. https://doi.org/10.4155/bio.11.206
114. Gustafsson, J. S., Blomberg, A., & Rudemo, M. (2002). Warping two-dimensional electrophoresis gel images to correct for geometric distortions of the spot pattern. *Electrophoresis*, *23*(11), 1731–1744. https://doi.org/10.1002/1522-2683(200206)23:11<1731::AID-ELPS1731>3.0.CO;2-#
115. Gygi, S. P., Corthals, G. L., Zhang, Y., Rochon, Y., & Aebersold, R. (2000). Evaluation of two-dimensional gel electrophoresis-based proteome analysis technology. *Proceedings of the National Academy of Sciences of the United States of America*, *97*(17), 9390–9395. https://doi.org/10.1073/pnas.160270797
116. Gygi, S. P., Rochon, Y., Franza, B. R., & Aebersold, R. (1999). Correlation between protein and mRNA abundance in yeast. *Molecular and Cellular Biology*, *19*(3), 1720–1730. https://doi.org/10.1128/MCB.19.3.1720
117. Hahn-Hägerdal, B., Karhumaa, K., Fonseca, C., Spencer-Martins, I., & Gorwa-Grauslund, M. F. (2007). Towards industrial pentose-fermenting yeast strains. *Applied Microbiology and Biotechnology*, *74*(5), 937–953. https://doi.org/10.1007/s00253-006-0827-2
118. Hampton, R. Y., Gardner, R. G., & Rine, J. (1996). Role of 26S proteasome and HRD genes in the degradation of 3-hydroxy-3-methylglutaryl-CoA reductase, an integral endoplasmic reticulum membrane protein. *Molecular Biology of the Cell*, *7*(12), 2029–2044. https://doi.org/10.1091/mbc.7.12.2029
119. Hampton, R. Y., & Garza, R. M. (2009). Protein quality control as a strategy for cellular regulation: Lessons from ubiquitin-mediated regulation of the sterol pathway. *Chemical Reviews*, *109*(4), 1561–1574. https://doi.org/10.1021/cr800544v
120. Hänninen, A. L., Simola, M., Saris, N., & Makarow, M. (1999). The cytoplasmic chaperone hsp104 is required for conformational repair of heat-denatured proteins in the yeast endoplasmic reticulum. *Molecular Biology of the Cell*, *10*(11), 3623–3632. https://doi.org/10.1091/mbc.10.11.3623
121. Harder, A., Wildgruber, R., Nawrocki, A., Fey, S. J., Larsen, P. M., & Görg, A. (1999). Comparison of yeast cell protein solubilization procedures for two-dimensional electrophoresis. *Electrophoresis*, *20*(4–5), 826–829. https://doi.org/10.1002/(SICI)1522-2683(19990101)20:4/5<826::AID-ELPS826>3.0.CO;2-A
122. Harmsen, M. M., Bruyne, M. I., Raué, H. A., & Maat, J. (1996). Overexpression of binding protein and disruption of the PMR1 gene synergistically stimulate secretion of bovine prochymosin but not plant thaumatin in yeast. *Applied Microbiology and Biotechnology*, *46*(4), 365–370. https://doi.org/10.1007/BF00166231
123. Hashiguchi, T., Kajikawa, M., Maita, N., Takeda, M., Kuroki, K., Sasaki, K., Kohda, D., Yanagi, Y., & Maenaka, K. (2007). Crystal structure of measles virus hemagglutinin provides insight into effective vaccines. *Proceedings of the National Academy of Sciences of the United States of America*, *104*(49), 19535–19540. https://doi.org/10.1073/pnas.0707830104
124. Hashiguchi, T., Ose, T., Kubota, M., Maita, N., Kamishikiryo, J., Maenaka, K., & Yanagi, Y. (2011). Structure of the measles virus hemagglutinin bound to its cellular receptor

SLAM. *Nature Structural & Molecular Biology*, *18*(2), 135–141. https://doi.org/10.1038/nsmb.1969
125. Haslbeck, M., Walke, S., Stromer, T., Ehrnsperger, M., White, H. E., Chen, S., Saibil, H. R., & Buchner, J. (1999). Hsp26: A temperature-regulated chaperone. *The EMBO Journal*, *18*(23), 6744–6751. https://doi.org/10.1093/emboj/18.23.6744
126. Haurie, V., Sagliocco, F., & Boucherie, H. (2004). Dissecting regulatory networks by means of two-dimensional gel electrophoresis: Application to the study of the diauxic shift in the yeast Saccharomyces cerevisiae. *Proteomics*, *4*(2), 364–373. https://doi.org/10.1002/pmic.200300564
127. Hayano, T., Hirose, M., & Kikuchi, M. (1995). Protein disulfide isomerase mutant lacking its isomerase activity accelerates protein folding in the cell. *FEBS Letters*, *377*(3), 505–511. https://doi.org/10.1016/0014-5793(95)01410-1
128. Haynes, C. M., Titus, E. A., & Cooper, A. A. (2004). Degradation of Misfolded Proteins Prevents ER-Derived Oxidative Stress and Cell Death. *Molecular Cell*, *15*(5), 767–776. https://doi.org/10.1016/j.molcel.2004.08.025
129. Hellman, U., Wernstedt, C., Góñez, J., & Heldin, C. H. (1995). Improvement of an 'In-Gel' digestion procedure for the micropreparation of internal protein fragments for amino acid sequencing. *Analytical Biochemistry*, *224*(1), 451–455. https://doi.org/10.1006/abio.1995.1070
130. Herman, P. K. (2002). Stationary phase in yeast. *Current Opinion in Microbiology*, *5*(6), 602–607. https://doi.org/10.1016/S1369-5274(02)00377-6
131. Hiller, M. M., Finger, A., Schweiger, M., & Wolf, D. H. (1996). ER Degradation of a Misfolded Luminal Protein by the Cytosolic Ubiquitin-Proteasome Pathway. *Science*, *273*(5282), 1725–1728. https://doi.org/10.1126/science.273.5282.1725
132. Hinnebusch, A. G., & Lorsch, J. R. (2012). The Mechanism of Eukaryotic Translation Initiation: New Insights and Challenges. *Cold Spring Harbor Perspectives in Biology*, *4*(10). https://doi.org/10.1101/cshperspect.a011544
133. Hitzeman, R. A., Hagie, F. E., Levine, H. L., Goeddel, D. V., Ammerer, G., & Hall, B. D. (1981). Expression of a human gene for interferon in yeast. *Nature*, *293*(5835), 717–722. https://doi.org/10.1038/293717a0
134. Ho, B., Baryshnikova, A., & Brown, G. W. (2018). Unification of Protein Abundance Datasets Yields a Quantitative Saccharomyces cerevisiae Proteome. *Cell Systems*, *6*(2), 192-205.e3. https://doi.org/10.1016/j.cels.2017.12.004
135. Hohmann, S., Krantz, M., & Nordlander, B. (2007). Yeast osmoregulation. *Methods in Enzymology*, *428*, 29–45. https://doi.org/10.1016/S0076-6879(07)28002-4
136. Homma, T., Iwahashi, H., & Komatsu, Y. (2003). Yeast gene expression during growth at low temperature. *Cryobiology*, *46*(3), 230–237. https://doi.org/10.1016/s0011-2240(03)00028-2
137. Hotokezaka, Y., Tobben, U., Hotokezaka, H., Van Leyen, K., Beatrix, B., Smith, D. H., Nakamura, T., & Wiedmann, M. (2002). Interaction of the eukaryotic elongation factor 1A with newly synthesized polypeptides. *The Journal of Biological Chemistry*, *277*(21), 18545–18551. https://doi.org/10.1074/jbc.M201022200
138. Hou, J., Österlund, T., Liu, Z., Petranovic, D., & Nielsen, J. (2013). Heat shock response improves heterologous protein secretion in Saccharomyces cerevisiae. *Applied Microbiology and Biotechnology*, *97*(8), 3559–3568. https://doi.org/10.1007/s00253-012-4596-9
139. Hou, J., Tang, H., Liu, Z., Österlund, T., Nielsen, J., & Petranovic, D. (2014). Management of the endoplasmic reticulum stress by activation of the heat shock response in yeast. *FEMS Yeast Research*, *14*(3), 481–494. https://doi.org/10.1111/1567-1364.12125
140. Hou, J., Tyo, K. E. J., Liu, Z., Petranovic, D., & Nielsen, J. (2012). Metabolic engineering of recombinant protein secretion by Saccharomyces cerevisiae. *FEMS Yeast Research*, *12*(5), 491–510. https://doi.org/10.1111/j.1567-1364.2012.00810.x
141. Huang, M., Bao, J., Hallström, B. M., Petranovic, D., & Nielsen, J. (2017). Efficient protein production by yeast requires global tuning of metabolism. *Nature Communications*, *8*(1), 1131. https://doi.org/10.1038/s41467-017-00999-2

142. Huh, G.-H., Damsz, B., Matsumoto, T. K., Reddy, M. P., Rus, A. M., Ibeas, J. I., Narasimhan, M. L., Bressan, R. A., & Hasegawa, P. M. (2002). Salt causes ion disequilibrium-induced programmed cell death in yeast and plants. *The Plant Journal: For Cell and Molecular Biology*, *29*(5), 649–659. https://doi.org/10.1046/j.0960-7412.2001.01247.x
143. Hung, C.-W., Klein, T., Cassidy, L., Linke, D., Lange, S., Anders, U., Bureik, M., Heinzle, E., Schneider, K., & Tholey, A. (2016). Comparative Proteome Analysis in Schizosaccharomyces pombe Identifies Metabolic Targets to Improve Protein Production and Secretion *. *Molecular & Cellular Proteomics*, *15*(10), 3090–3106. https://doi.org/10.1074/mcp.M115.051474
144. Idiris, A., Tohda, H., Kumagai, H., & Takegawa, K. (2010). Engineering of protein secretion in yeast: Strategies and impact on protein production. *Applied Microbiology and Biotechnology*, *86*(2), 403–417. https://doi.org/10.1007/s00253-010-2447-0
145. Ishchuk, O. P., Voronovsky, A. Y., Stasyk, O. V., Gayda, G. Z., Gonchar, M. V., Abbas, C. A., & Sibirny, A. A. (2008). Overexpression of pyruvate decarboxylase in the yeast Hansenula polymorpha results in increased ethanol yield in high-temperature fermentation of xylose. *FEMS Yeast Research*, *8*(7), 1164–1174. https://doi.org/10.1111/j.1567-1364.2008.00429.x
146. Issaq, H., & Veenstra, T. (2008). Two-dimensional polyacrylamide gel electrophoresis (2D-PAGE): Advances and perspectives. *BioTechniques*, *44*(5), 697–698, 700. https://doi.org/10.2144/000112823
147. Jackowski, G., & Pielucha, K. (2001). Heterogeneity of the main light-harvesting chlorophyll a/b-protein complex of photosystem II (LHCII) at the level of trimeric subunits. *Journal of Photochemistry and Photobiology. B, Biology*, *64*(1), 45–54. https://doi.org/10.1016/s1011-1344(01)00188-9
148. Jamieson, D. J. (1998). Oxidative stress responses of the yeast Saccharomyces cerevisiae. *Yeast*, *14*(16), 1511–1527. https://doi.org/10.1002/(SICI)1097-0061(199812)14:16<1511::AID-YEA356>3.0.CO;2-S
149. Jardetzky, T. S., & Lamb, R. A. (2014). Activation of paramyxovirus membrane fusion and virus entry. *Current Opinion in Virology*, *5*, 24–33. https://doi.org/10.1016/j.coviro.2014.01.005
150. Jiang, L., He, L., & Fountoulakis, M. (2004). Comparison of protein precipitation methods for sample preparation prior to proteomic analysis. *Journal of Chromatography. A*, *1023*(2), 317–320. https://doi.org/10.1016/j.chroma.2003.10.029
151. Jordan, P., Choe, J.-Y., Boles, E., & Oreb, M. (2016). Hxt13, Hxt15, Hxt16 and Hxt17 from Saccharomyces cerevisiae represent a novel type of polyol transporters. *Scientific Reports*, *6*(1), 23502. https://doi.org/10.1038/srep23502
152. Ju, D., Wang, L., Mao, X., & Xie, Y. (2004). Homeostatic regulation of the proteasome via an Rpn4-dependent feedback circuit. *Biochemical and Biophysical Research Communications*, *321*(1), 51–57. https://doi.org/10.1016/j.bbrc.2004.06.105
153. Jun, H., Kieselbach, T., & Jönsson, L. J. (2012). Comparative proteome analysis of Saccharomyces cerevisiae: A global overview of in vivo targets of the yeast activator protein 1. *BMC Genomics*, *13*, 230. https://doi.org/10.1186/1471-2164-13-230
154. Juozapaitis, M., Slibinskas, R., Staniulis, J., Sakaguchi, T., & Sasnauskas, K. (2005). Generation of Sendai virus nucleocapsid-like particles in yeast. *Virus Research*, *108*(1–2), 221–224. https://doi.org/10.1016/j.virusres.2004.08.003
155. Juozapaitis, M., Zvirbliene, A., Kucinskaite, I., Sezaite, I., Slibinskas, R., Coiras, M., de Ory Manchon, F., López-Huertas, M. R., Pérez-Breña, P., Staniulis, J., Narkeviciute, I., & Sasnauskas, K. (2008). Synthesis of recombinant human parainfluenza virus 1 and 3 nucleocapsid proteins in yeast Saccharomyces cerevisiae. *Virus Research*, *133*(2), 178–186. https://doi.org/10.1016/j.virusres.2007.12.016
156. Kandror, O., Bretschneider, N., Kreydin, E., Cavalieri, D., & Goldberg, A. L. (2004). Yeast adapt to near-freezing temperatures by STRE/Msn2,4-dependent induction of trehalose synthesis and certain molecular chaperones. *Molecular Cell*, *13*(6), 771–781. https://doi.org/10.1016/s1097-2765(04)00148-0

157. Kapteyn, J. C., ter Riet, B., Vink, E., Blad, S., De Nobel, H., Van Den Ende, H., & Klis, F. M. (2001). Low external pH induces HOG1-dependent changes in the organization of the Saccharomyces cerevisiae cell wall. *Molecular Microbiology*, *39*(2), 469–479. https://doi.org/10.1046/j.1365-2958.2001.02242.x
158. Karathia, H., Vilaprinyo, E., Sorribas, A., & Alves, R. (2011). Saccharomyces cerevisiae as a Model Organism: A Comparative Study. *PLoS ONE*, *6*(2), e16015. https://doi.org/10.1371/journal.pone.0016015
159. Karlsson, K., Cairns, N., Lubec, G., & Fountoulakis, M. (1999). Enrichment of human brain proteins by heparin chromatography. *Electrophoresis*, *20*(14), 2970–2976. https://doi.org/10.1002/(SICI)1522-2683(19991001)20:14<2970::AID-ELPS2970>3.0.CO;2-P
160. Kastberg, L. L. B., Ard, R., Jensen, M. K., & Workman, C. T. (2022). Burden Imposed by Heterologous Protein Production in Two Major Industrial Yeast Cell Factories: Identifying Sources and Mitigation Strategies. *Frontiers in Fungal Biology*, *3*. https://www.frontiersin.org/article/10.3389/ffunb.2022.827704
161. Kauffman, K. J., Pridgen, E. M., Doyle, F. J., Dhurjati, P. S., & Robinson, A. S. (2002). Decreased protein expression and intermittent recoveries in BiP levels result from cellular stress during heterologous protein expression in Saccharomyces cerevisiae. *Biotechnology Progress*, *18*(5), 942–950. https://doi.org/10.1021/bp025518g
162. Kelkar, R. S., Mahen, A., Saoji, A. M., & Kelkar, S. S. (1986). N-N' diallyltartardiamide (DATD) as a cross-linking agent for polyacrylamide gel disc electrophoresis of human serum proteins. *Journal of Postgraduate Medicine*, *32*(1), 27–31.
163. Kielbik, M., Szulc-Kielbik, I., & Klink, M. (2021). Calreticulin—Multifunctional Chaperone in Immunogenic Cell Death: Potential Significance as a Prognostic Biomarker in Ovarian Cancer Patients. *Cells*, *10*(1), 130. https://doi.org/10.3390/cells10010130
164. Kim, M.-D., Han, K.-C., Kang, H.-A., Rhee, S.-K., & Seo, J.-H. (2003). Coexpression of BiP increased antithrombotic hirudin production in recombinant Saccharomyces cerevisiae. *Journal of Biotechnology*, *101*(1), 81–87. https://doi.org/10.1016/s0168-1656(02)00288-2
165. Kirch, W. (Ed.). (2008). Pearson's Correlation Coefficient. In *Encyclopedia of Public Health* (pp. 1090–1091). Springer Netherlands. https://doi.org/10.1007/978-1-4020-5614-7_2569
166. Klose, J. (1975). Protein mapping by combined isoelectric focusing and electrophoresis of mouse tissues. *Humangenetik*, *26*(3), 231–243. https://doi.org/10.1007/BF00281458
167. Klose, J., & Kobalz, U. (1995). Two-dimensional electrophoresis of proteins: An updated protocol and implications for a functional analysis of the genome. *Electrophoresis*, *16*(6), 1034–1059. https://doi.org/10.1002/elps.11501601175
168. Knop, M., Finger, A., Braun, T., Hellmuth, K., & Wolf, D. H. (1996). Der1, a novel protein specifically required for endoplasmic reticulum degradation in yeast. *The EMBO Journal*, *15*(4), 753–763.
169. Ko, C. H., Buckley, A. M., & Gaber, R. F. (1990). TRK2 is required for low affinity K+ transport in Saccharomyces cerevisiae. *Genetics*, *125*(2), 305–312. https://doi.org/10.1093/genetics/125.2.305
170. Kolkman, A., Olsthoorn, M. M. A., Heeremans, C. E. M., Heck, A. J. R., & Slijper, M. (2005). Comparative proteome analysis of Saccharomyces cerevisiae grown in chemostat cultures limited for glucose or ethanol. *Molecular & Cellular Proteomics: MCP*, *4*(1), 1–11. https://doi.org/10.1074/mcp.M400087-MCP200
171. Kondo, K., Kowalski, L. R., & Inouye, M. (1992). Cold shock induction of yeast NSR1 protein and its role in pre-rRNA processing. *The Journal of Biological Chemistry*, *267*(23), 16259–16265.
172. Kowalski, L. R., Kondo, K., & Inouye, M. (1995). Cold-shock induction of a family of TIP1-related proteins associated with the membrane in Saccharomyces cerevisiae. *Molecular Microbiology*, *15*(2), 341–353. https://doi.org/10.1111/j.1365-2958.1995.tb02248.x
173. Kreipke, C. W., Morgan, R., Roberts, G., Bagchi, M., & Rafols, J. A. (2007). Calponin phosphorylation in cerebral cortex microvessels mediates sustained vasoconstriction after

brain trauma. *Neurological Research*, *29*(4), 369–374. https://doi.org/10.1179/016164107X204684
174. Kroemer, G., Galluzzi, L., Kepp, O., & Zitvogel, L. (2013). Immunogenic cell death in cancer therapy. *Annual Review of Immunology*, *31*, 51–72. https://doi.org/10.1146/annurev-immunol-032712-100008
175. Kuharev, J., Navarro, P., Distler, U., Jahn, O., & Tenzer, S. (2015). In-depth evaluation of software tools for data-independent acquisition based label-free quantification. *PROTEOMICS*, *15*(18), 3140–3151. https://doi.org/10.1002/pmic.201400396
176. Kunkel, J., Luo, X., & Capaldi, A. P. (2019). Integrated TORC1 and PKA signaling control the temporal activation of glucose-induced gene expression in yeast. *Nature Communications*, *10*(1), 3558. https://doi.org/10.1038/s41467-019-11540-y
177. Kuroda, K., Kobayashi, K., Tsumura, H., Komeda, T., Chiba, Y., & Jigami, Y. (2006). Production of Man5GlcNAc2-type sugar chain by the methylotrophic yeast Ogataea minuta. *FEMS Yeast Research*, *6*(7), 1052–1062. https://doi.org/10.1111/j.1567-1364.2006.00116.x
178. Labriola, C. A., Conte, I. L., López Medus, M., Parodi, A. J., & Caramelo, J. J. (2010). Endoplasmic reticulum calcium regulates the retrotranslocation of Trypanosoma cruzi calreticulin to the cytosol. *PloS One*, *5*(10), e13141. https://doi.org/10.1371/journal.pone.0013141
179. Laemmli, U. K. (1970). Cleavage of structural proteins during the assembly of the head of bacteriophage T4. *Nature*, *227*(5259), 680–685. https://doi.org/10.1038/227680a0
180. Lamb, R. A., & Parks, G. D. (2007). Paramyxoviridae: The viruses and their replication. In B. N. Fields, D. N. Knipe, & P. M. Howley (Eds.), *Fields virology* (5th ed., pp. 1449–1496). Lippincott, Williams, and Wilkins.
181. Lee, W.-C., & Lee, K. H. (2004). Applications of affinity chromatography in proteomics. *Analytical Biochemistry*, *324*(1), 1–10. https://doi.org/10.1016/j.ab.2003.08.031
182. Leong, W.-Y., & Wilder-Smith, A. B. (2019). Measles Resurgence in Europe: Migrants and Travellers are not the Main Drivers. *Journal of Epidemiology and Global Health*, *9*(4), 294–299. https://doi.org/10.2991/jegh.k.191007.001
183. Leplatois, P., Le Douarin, B., & Loison, G. (1992). High-level production of a peroxisomal enzyme: Aspergillus flavus uricase accumulates intracellularly and is active in Saccharomyces cerevisiae. *Gene*, *122*(1), 139–145. https://doi.org/10.1016/0378-1119(92)90041-m
184. Li, X., Chen, G., Fongang, B., Homouz, D., Rowicka, M., & Kudlicki, A. (2017). *The High-resolution Timeline of Expression of Ribosomal Protein Genes in Yeast*. https://doi.org/10.1101/170399
185. Li, Z., Xiong, F., Lin, Q., d'Anjou, M., Daugulis, A. J., Yang, D. S., & Hew, C. L. (2001). Low-temperature increases the yield of biologically active herring antifreeze protein in Pichia pastoris. *Protein Expression and Purification*, *21*(3), 438–445. https://doi.org/10.1006/prep.2001.1395
186. Lin, G.-J., Deng, M.-C., Chen, Z.-W., Liu, T.-Y., Wu, C.-W., Cheng, C.-Y., Chien, M.-S., & Huang, C. (2012). Yeast expressed classical swine fever E2 subunit vaccine candidate provides complete protection against lethal challenge infection and prevents horizontal virus transmission. *Vaccine*, *30*(13), 2336–2341. https://doi.org/10.1016/j.vaccine.2012.01.051
187. Lin, X., Liang, S., Han, S., Zheng, S., Ye, Y., & Lin, Y. (2013). Quantitative iTRAQ LC–MS/MS proteomics reveals the cellular response to heterologous protein overexpression and the regulation of HAC1 in Pichia pastoris. *Journal of Proteomics*, *91*, 58–72. https://doi.org/10.1016/j.jprot.2013.06.031
188. Liu, H., Sadygov, R. G., & Yates, J. R. (2004). A model for random sampling and estimation of relative protein abundance in shotgun proteomics. *Analytical Chemistry*, *76*(14), 4193–4201. https://doi.org/10.1021/ac0498563
189. Liu, P., Zhao, L., Kroemer, G., & Kepp, O. (2019). Secreted calreticulin mutants subvert anticancer immunosurveillance. *Oncoimmunology*, *9*(1), 1708126. https://doi.org/10.1080/2162402X.2019.1708126

190. Liu, Y., & Chang, A. (2008). Heat shock response relieves ER stress. *The EMBO Journal*, *27*(7), 1049–1059. https://doi.org/10.1038/emboj.2008.42
191. Liu, Z., Hou, J., Martínez, J. L., Petranovic, D., & Nielsen, J. (2013). Correlation of cell growth and heterologous protein production by Saccharomyces cerevisiae. *Applied Microbiology and Biotechnology*, *97*(20), 8955–8962. https://doi.org/10.1007/s00253-013-4715-2
192. Liu, Z., Tyo, K. E. J., Martínez, J. L., Petranovic, D., & Nielsen, J. (2012). Different expression systems for production of recombinant proteins in Saccharomyces cerevisiae. *Biotechnology and Bioengineering*, *109*(5), 1259–1268. https://doi.org/10.1002/bit.24409
193. Lobanova, L. M., Eng, N. F., Satkunarajah, M., Mutwiri, G. K., Rini, J. M., & Zakhartchouk, A. N. (2012). The recombinant globular head domain of the measles virus hemagglutinin protein as a subunit vaccine against measles. *Vaccine*, *30*(20), 3061–3067. https://doi.org/10.1016/j.vaccine.2012.02.067
194. López-Mirabal, H. R., & Winther, J. R. (2008). Redox characteristics of the eukaryotic cytosol. *Redox Regulation of Protein Folding*, *1783*(4), 629–640. https://doi.org/10.1016/j.bbamcr.2007.10.013
195. Love, M. I., Huber, W., & Anders, S. (2014). Moderated estimation of fold change and dispersion for RNA-seq data with DESeq2. *Genome Biology*, *15*(12), 550. https://doi.org/10.1186/s13059-014-0550-8
196. Ludovico, P., Sousa, M. J., Silva, M. T., Leão, C. L., & Côrte-Real, M. (2001). Saccharomyces cerevisiae commits to a programmed cell death process in response to acetic acid. *Microbiology (Reading, England)*, *147*(Pt 9), 2409–2415. https://doi.org/10.1099/00221287-147-9-2409
197. Lui, J., Campbell, S. G., & Ashe, M. P. (2010). Inhibition of translation initiation following glucose depletion in yeast facilitates a rationalization of mRNA content. *Biochemical Society Transactions*, *38*(4), 1131–1136. https://doi.org/10.1042/BST0381131
198. Määttänen, P., Gehring, K., Bergeron, J. J. M., & Thomas, D. Y. (2010). Protein quality control in the ER: The recognition of misfolded proteins. *Seminars in Cell & Developmental Biology*, *21*(5), 500–511. https://doi.org/10.1016/j.semcdb.2010.03.006
199. MacGillivray, A. J., & Rickwood, D. (1974). The heterogeneity of mouse-chromatin nonhistone proteins as evidenced by two-dimensional polyacrylamide-gel electrophoresis and ion-exchange chromatography. *European Journal of Biochemistry*, *41*(1), 181–190. https://doi.org/10.1111/j.1432-1033.1974.tb03258.x
200. Mackintosh, J. A., Choi, H.-Y., Bae, S.-H., Veal, D. A., Bell, P. J., Ferrari, B. C., Van Dyk, D. D., Verrills, N. M., Paik, Y.-K., & Karuso, P. (2003). A fluorescent natural product for ultra sensitive detection of proteins in one-dimensional and two-dimensional gel electrophoresis. *Proteomics*, *3*(12), 2273–2288. https://doi.org/10.1002/pmic.200300578
201. Madeo, F., Fröhlich, E., Ligr, M., Grey, M., Sigrist, S. J., Wolf, D. H., & Fröhlich, K. U. (1999). Oxygen stress: A regulator of apoptosis in yeast. *The Journal of Cell Biology*, *145*(4), 757–767. https://doi.org/10.1083/jcb.145.4.757
202. Madzak, C., Gaillardin, C., & Beckerich, J.-M. (2004). Heterologous protein expression and secretion in the non-conventional yeast Yarrowia lipolytica: A review. *Journal of Biotechnology*, *109*(1–2), 63–81. https://doi.org/10.1016/j.jbiotec.2003.10.027
203. Magdeldin, S., Enany, S., Yoshida, Y., Xu, B., Zhang, Y., Zureena, Z., Lokamani, I., Yaoita, E., & Yamamoto, T. (2014). Basics and recent advances of two dimensional-polyacrylamide gel electrophoresis. *Clinical Proteomics*, *11*(1), 16. https://doi.org/10.1186/1559-0275-11-16
204. Makdesi, A. K., & Beuchat, L. R. (1996). Evaluation of media for enumerating heat-stressed, benzoate-resistant Zygosaccharomyces bailii. *International Journal of Food Microbiology*, *33*(2–3), 169–181. https://doi.org/10.1016/0168-1605(96)01124-5
205. Martinet, W., Saelens, X., Deroo, T., Neirynck, S., Contreras, R., Min Jou, W., & Fiers, W. (1997). Protection of mice against a lethal influenza challenge by immunization with

yeast-derived recombinant influenza neuraminidase. *European Journal of Biochemistry*, *247*(1), 332–338. https://doi.org/10.1111/j.1432-1033.1997.00332.x
206. Martínez, J. L., Meza, E., Petranovic, D., & Nielsen, J. (2016). The impact of respiration and oxidative stress response on recombinant α-amylase production by Saccharomyces cerevisiae. *Metabolic Engineering Communications*, *3*, 205–210. https://doi.org/10.1016/j.meteno.2016.06.003
207. Martin-Perez, M., & Villén, J. (2017). Determinants and Regulation of Protein Turnover in Yeast. *Cell Systems*, *5*(3), 283-294.e5. https://doi.org/10.1016/j.cels.2017.08.008
208. Mattanovich, D., Branduardi, P., Dato, L., Gasser, B., Sauer, M., & Porro, D. (2012). Recombinant protein production in yeasts. *Methods in Molecular Biology (Clifton, N.J.)*, *824*, 329–358. https://doi.org/10.1007/978-1-61779-433-9_17
209. Mattanovich, D., Gasser, B., Hohenblum, H., & Sauer, M. (2004). Stress in recombinant protein producing yeasts. *Journal of Biotechnology*, *113*(1), 121–135. https://doi.org/10.1016/j.jbiotec.2004.04.035
210. McAlister, L., Strausberg, S., Kulaga, A., & Finkelstein, D. B. (1979). Altered patterns of protein synthesis induced by heat shock of yeast. *Current Genetics*, *1*(1), 63–74. https://doi.org/10.1007/BF00413307
211. McClellan, A. J., Xia, Y., Deutschbauer, A. M., Davis, R. W., Gerstein, M., & Frydman, J. (2007). Diverse cellular functions of the Hsp90 molecular chaperone uncovered using systems approaches. *Cell*, *131*(1), 121–135. https://doi.org/10.1016/j.cell.2007.07.036
212. McDonald, W. H., & Yates, J. R. (2002). Shotgun proteomics and biomarker discovery. *Disease Markers*, *18*(2), 99–105. https://doi.org/10.1155/2002/505397
213. Medhe, S. (2018). Mass Spectrometry: Detectors Review. *Annual Review of Chemical and Biomolecular Engineering*, *3*, 51–58. https://doi.org/10.11648/j.cbe.20180304.11
214. Metzger, M. B., & Michaelis, S. (2009). Analysis of Quality Control Substrates in Distinct Cellular Compartments Reveals a Unique Role for Rpn4p in Tolerating Misfolded Membrane Proteins. *Molecular Biology of the Cell*, *20*(3), 1006–1019. https://doi.org/10.1091/mbc.E08-02-0140
215. Michalak, M., Groenendyk, J., Szabo, E., Gold, L. I., & Opas, M. (2009). Calreticulin, a multi-process calcium-buffering chaperone of the endoplasmic reticulum. *The Biochemical Journal*, *417*(3), 651–666. https://doi.org/10.1042/BJ20081847
216. Michalak, M., Robert Parker, J. M., & Opas, M. (2002). Ca2+ signaling and calcium binding chaperones of the endoplasmic reticulum. *Cell Calcium*, *32*(5–6), 269–278. https://doi.org/10.1016/s0143416002001884
217. Miller, M. J., Xuong, N. H., & Geiduschek, E. P. (1982). Quantitative analysis of the heat shock response of Saccharomyces cerevisiae. *Journal of Bacteriology*, *151*(1), 311–327. https://doi.org/10.1128/jb.151.1.311-327.1982
218. Miller-Fleming, L., Giorgini, F., & Outeiro, T. F. (2008). Yeast as a model for studying human neurodegenerative disorders. *Biotechnology Journal*, *3*(3), 325–338. https://doi.org/10.1002/biot.200700217
219. Moffatt, B. A., & Ashihara, H. (2002). Purine and Pyrimidine Nucleotide Synthesis and Metabolism. *The Arabidopsis Book / American Society of Plant Biologists*, *1*. https://doi.org/10.1199/tab.0018
220. Molloy, M. P., Herbert, B. R., Walsh, B. J., Tyler, M. I., Traini, M., Sanchez, J. C., Hochstrasser, D. F., Williams, K. L., & Gooley, A. A. (1998). Extraction of membrane proteins by differential solubilization for separation using two-dimensional gel electrophoresis. *Electrophoresis*, *19*(5), 837–844. https://doi.org/10.1002/elps.1150190539
221. Moody, A. J., Norris, F., Norris, K., Hansen, M. T., & Thim, L. (1987). The secretion of glucagon by transformed yeast strains. *FEBS Letters*, *212*(2), 302–306. https://doi.org/10.1016/0014-5793(87)81365-0
222. Morano, K. A., Liu, P. C., & Thiele, D. J. (1998). Protein chaperones and the heat shock response in Saccharomyces cerevisiae. *Current Opinion in Microbiology*, *1*(2), 197–203. https://doi.org/10.1016/s1369-5274(98)80011-8

223. Mori, K., Sant, A., Kohno, K., Normington, K., Gething, M. J., & Sambrook, J. F. (1992). A 22 bp cis-acting element is necessary and sufficient for the induction of the yeast KAR2 (BiP) gene by unfolded proteins. *The EMBO Journal*, *11*(7), 2583–2593.
224. Mortz, E., Krogh, T. N., Vorum, H., & Görg, A. (2001). Improved silver staining protocols for high sensitivity protein identification using matrix-assisted laser desorption/ionization-time of flight analysis. *Proteomics*, *1*(11), 1359–1363. https://doi.org/10.1002/1615-9861(200111)1:11<1359::AID-PROT1359>3.0.CO;2-Q
225. Mühlebach, M. D., Mateo, M., Sinn, P. L., Prüfer, S., Uhlig, K. M., Leonard, V. H. J., Navaratnarajah, C. K., Frenzke, M., Wong, X. X., Sawatsky, B., Ramachandran, S., McCray, P. B., Cichutek, K., von Messling, V., Lopez, M., & Cattaneo, R. (2011). Adherens junction protein nectin-4 is the epithelial receptor for measles virus. *Nature*, *480*(7378), 530–533. https://doi.org/10.1038/nature10639
226. Mühlhofer, M., Berchtold, E., Stratil, C. G., Csaba, G., Kunold, E., Bach, N. C., Sieber, S. A., Haslbeck, M., Zimmer, R., & Buchner, J. (2019). The Heat Shock Response in Yeast Maintains Protein Homeostasis by Chaperoning and Replenishing Proteins. *Cell Reports*, *29*(13), 4593-4607.e8. https://doi.org/10.1016/j.celrep.2019.11.109
227. Munoz, A. J., Wanichthanarak, K., Meza, E., & Petranovic, D. (2012). Systems biology of yeast cell death. *FEMS Yeast Research*, *12*(2), 249–265. https://doi.org/10.1111/j.1567-1364.2011.00781.x
228. Murakami, C., & Kaeberlein, M. (2009). Quantifying Yeast Chronological Life Span by Outgrowth of Aged Cells. *Journal of Visualized Experiments : JoVE*, *27*, 1156. https://doi.org/10.3791/1156
229. Murata, Y., Homma, T., Kitagawa, E., Momose, Y., Sato, M. S., Odani, M., Shimizu, H., Hasegawa-Mizusawa, M., Matsumoto, R., Mizukami, S., Fujita, K., Parveen, M., Komatsu, Y., & Iwahashi, H. (2006). Genome-wide expression analysis of yeast response during exposure to 4 degrees C. *Extremophiles: Life Under Extreme Conditions*, *10*(2), 117–128. https://doi.org/10.1007/s00792-005-0480-1
230. Nagaraj, N., Wisniewski, J. R., Geiger, T., Cox, J., Kircher, M., Kelso, J., Pääbo, S., & Mann, M. (2011). Deep proteome and transcriptome mapping of a human cancer cell line. *Molecular Systems Biology*, *7*, 548. https://doi.org/10.1038/msb.2011.81
231. Nakamura, K., Zuppini, A., Arnaudeau, S., Lynch, J., Ahsan, I., Krause, R., Papp, S., De Smedt, H., Parys, J. B., Muller-Esterl, W., Lew, D. P., Krause, K. H., Demaurex, N., Opas, M., & Michalak, M. (2001). Functional specialization of calreticulin domains. *The Journal of Cell Biology*, *154*(5), 961–972. https://doi.org/10.1083/jcb.200102073
232. Nakayama, K., Nagasu, T., Shimma, Y., Kuromitsu, J., & Jigami, Y. (1992). OCH1 encodes a novel membrane bound mannosyltransferase: Outer chain elongation of asparagine-linked oligosaccharides. *The EMBO Journal*, *11*(7), 2511–2519.
233. Nandakumar, M. P., & Marten, M. R. (2002). Comparison of lysis methods and preparation protocols for one- and two-dimensional electrophoresis of Aspergillus oryzae intracellular proteins. *Electrophoresis*, *23*(14), 2216–2222. https://doi.org/10.1002/1522-2683(200207)23:14<2216::AID-ELPS2216>3.0.CO;2-Y
234. Nanney, L. B., Woodrell, C. D., Greives, M. R., Cardwell, N. L., Pollins, A. C., Bancroft, T. A., Chesser, A., Michalak, M., Rahman, M., Siebert, J. W., & Gold, L. I. (2008). Calreticulin Enhances Porcine Wound Repair by Diverse Biological Effects. *The American Journal of Pathology*, *173*(3), 610–630. https://doi.org/10.2353/ajpath.2008.071027
235. Nasheuer, H.-P., Smith, R., Bauerschmidt, C., Grosse, F., & Weisshart, K. (2002). Initiation of eukaryotic DNA replication: Regulation and mechanisms. *Progress in Nucleic Acid Research and Molecular Biology*, *72*, 41–94. https://doi.org/10.1016/s0079-6603(02)72067-9
236. Nawrocki, A., Larsen, M. R., Podtelejnikov, A. V., Jensen, O. N., Mann, M., Roepstorff, P., Görg, A., Fey, S. J., & Larsen, P. M. (1998). Correlation of acidic and basic carrier ampholyte and immobilized pH gradient two-dimensional gel electrophoresis patterns based on mass spectrometric protein identification. *Electrophoresis*, *19*(6), 1024–1035. https://doi.org/10.1002/elps.1150190618

237. Neilson, K., Ali, N., Muralidharan, S., Mirzaei, M., Mariani, M., Assadourian, G., Lee, A., Van sluyter, S., & Haynes, P. (2011). Less label, more free: Approaches in label-free quantitative mass spectrometry. *Proteomics*, *11*, 535–553. https://doi.org/10.1002/pmic.201000553
238. Nesvizhskii, A. I. (2007). Protein identification by tandem mass spectrometry and sequence database searching. *Methods in Molecular Biology (Clifton, N.J.)*, *367*, 87–119. https://doi.org/10.1385/1-59745-275-0:87
239. Neuhoff, V., Arold, N., Taube, D., & Ehrhardt, W. (1988). Improved staining of proteins in polyacrylamide gels including isoelectric focusing gels with clear background at nanogram sensitivity using Coomassie Brilliant Blue G-250 and R-250. *Electrophoresis*, *9*(6), 255–262. https://doi.org/10.1002/elps.1150090603
240. Nickenig, G., Michaelsen, F., Müller, C., Berger, A., Vogel, T., Sachinidis, A., Vetter, H., & Böhm, M. (2002). Destabilization of AT(1) receptor mRNA by calreticulin. *Circulation Research*, *90*(1), 53–58. https://doi.org/10.1161/hh0102.102503
241. Nishikawa, S. I., Fewell, S. W., Kato, Y., Brodsky, J. L., & Endo, T. (2001). Molecular chaperones in the yeast endoplasmic reticulum maintain the solubility of proteins for retrotranslocation and degradation. *The Journal of Cell Biology*, *153*(5), 1061–1070. https://doi.org/10.1083/jcb.153.5.1061
242. Norbeck, J., & Blomberg, A. (1997). Two-dimensional electrophoretic separation of yeast proteins using a non-linear wide range (pH 3-10) immobilized pH gradient in the first dimension; reproducibility and evidence for isoelectric focusing of alkaline (pI > 7) proteins. *Yeast (Chichester, England)*, *13*(16), 1519–1534. https://doi.org/10.1002/(SICI)1097-0061(199712)13:16<1519::AID-YEA211>3.0.CO;2-U
243. Nowalk, A. J., Nolder, C., Clifton, D. R., & Carroll, J. A. (2006). Comparative proteome analysis of subcellular fractions from Borrelia burgdorferi by NEPHGE and IPG. *Proteomics*, *6*(7), 2121–2134. https://doi.org/10.1002/pmic.200500187
244. Noyce, R. S., Bondre, D. G., Ha, M. N., Lin, L.-T., Sisson, G., Tsao, M.-S., & Richardson, C. D. (2011). Tumor cell marker PVRL4 (nectin 4) is an epithelial cell receptor for measles virus. *PLoS Pathogens*, *7*(8), e1002240. https://doi.org/10.1371/journal.ppat.1002240
245. Obeid, M., Tesniere, A., Ghiringhelli, F., Fimia, G. M., Apetoh, L., Perfettini, J.-L., Castedo, M., Mignot, G., Panaretakis, T., Casares, N., Métivier, D., Larochette, N., van Endert, P., Ciccosanti, F., Piacentini, M., Zitvogel, L., & Kroemer, G. (2007). Calreticulin exposure dictates the immunogenicity of cancer cell death. *Nature Medicine*, *13*(1), 54–61. https://doi.org/10.1038/nm1523
246. Odani, M., Komatsu, Y., Oka, S., & Iwahashi, H. (2003). Screening of genes that respond to cryopreservation stress using yeast DNA microarray. *Cryobiology*, *47*(2), 155–164. https://doi.org/10.1016/j.cryobiol.2003.09.001
247. O'Farrell, P. H. (1975). High resolution two-dimensional electrophoresis of proteins. *The Journal of Biological Chemistry*, *250*(10), 4007–4021.
248. O'Farrell, P. Z., Goodman, H. M., & O'Farrell, P. H. (1977). High resolution two-dimensional electrophoresis of basic as well as acidic proteins. *Cell*, *12*(4), 1133–1141. https://doi.org/10.1016/0092-8674(77)90176-3
249. Ogura, H., Sato, H., Kamiya, S., & Nakamura, S. (1991). Glycosylation of measles virus haemagglutinin protein in infected cells. *The Journal of General Virology*, *72 (Pt 11)*, 2679–2684. https://doi.org/10.1099/0022-1317-72-11-2679
250. Oliver, J. D., Roderick, H. L., Llewellyn, D. H., & High, S. (1999). ERp57 functions as a subunit of specific complexes formed with the ER lectins calreticulin and calnexin. *Molecular Biology of the Cell*, *10*(8), 2573–2582. https://doi.org/10.1091/mbc.10.8.2573
251. Olivieri, E., Herbert, B., & Righetti, P. G. (2001). The effect of protease inhibitors on the two-dimensional electrophoresis pattern of red blood cell membranes. *Electrophoresis*, *22*(3), 560–565. https://doi.org/10.1002/1522-2683(200102)22:3<560::AID-ELPS560>3.0.CO;2-G
252. Orr, A. W., Elzie, C. A., Kucik, D. F., & Murphy-Ullrich, J. E. (2003). Thrombospondin signaling through the calreticulin/LDL receptor-related protein co-complex stimulates

random and directed cell migration. *Journal of Cell Science*, *116*(Pt 14), 2917–2927. https://doi.org/10.1242/jcs.00600
253. Owsianowski, E., Walter, D., & Fahrenkrog, B. (2008). Negative regulation of apoptosis in yeast. *Biochimica et Biophysica Acta (BBA) - Molecular Cell Research*, *1783*(7), 1303–1310. https://doi.org/10.1016/j.bbamcr.2008.03.006
254. Panadero, J., Pallotti, C., Rodríguez-Vargas, S., Randez-Gil, F., & Prieto, J. A. (2006). A downshift in temperature activates the high osmolarity glycerol (HOG) pathway, which determines freeze tolerance in Saccharomyces cerevisiae. *The Journal of Biological Chemistry*, *281*(8), 4638–4645. https://doi.org/10.1074/jbc.M512736200
255. Panaretakis, T., Joza, N., Modjtahedi, N., Tesniere, A., Vitale, I., Durchschlag, M., Fimia, G. M., Kepp, O., Piacentini, M., Froehlich, K.-U., van Endert, P., Zitvogel, L., Madeo, F., & Kroemer, G. (2008). The co-translocation of ERp57 and calreticulin determines the immunogenicity of cell death. *Cell Death and Differentiation*, *15*(9), 1499–1509. https://doi.org/10.1038/cdd.2008.67
256. Pandey, A., & Mann, M. (2000). Proteomics to study genes and genomes. *Nature*, *405*(6788), 837–846. https://doi.org/10.1038/35015709
257. Parker, C. E., Warren, M. R., & Mocanu, V. (2010). Mass Spectrometry for Proteomics. In O. Alzate (Ed.), *Neuroproteomics*. CRC Press/Taylor & Francis. http://www.ncbi.nlm.nih.gov/books/NBK56011/
258. Patel, M. K., Dumolard, L., Nedelec, Y., Sodha, S. V., Steulet, C., Gacic-Dobo, M., Kretsinger, K., McFarland, J., Rota, P. A., & Goodson, J. L. (2019). Progress Toward Regional Measles Elimination—Worldwide, 2000-2018. *MMWR. Morbidity and Mortality Weekly Report*, *68*(48), 1105–1111. https://doi.org/10.15585/mmwr.mm6848a1
259. Payne, T., Finnis, C., Evans, L. R., Mead, D. J., Avery, S. V., Archer, D. B., & Sleep, D. (2008). Modulation of chaperone gene expression in mutagenized Saccharomyces cerevisiae strains developed for recombinant human albumin production results in increased production of multiple heterologous proteins. *Applied and Environmental Microbiology*, *74*(24), 7759–7766. https://doi.org/10.1128/AEM.01178-08
260. Pelham, H. R. B. (2002). Insights from yeast endosomes. *Current Opinion in Cell Biology*, *14*(4), 454–462. https://doi.org/10.1016/s0955-0674(02)00352-6
261. Peters, L. R., & Raghavan, M. (2011). Endoplasmic reticulum calcium depletion impacts chaperone secretion, innate immunity, and phagocytic uptake of cells. *Journal of Immunology (Baltimore, Md.: 1950)*, *187*(2), 919–931. https://doi.org/10.4049/jimmunol.1100690
262. Pilon M, Schekman R, & Romisch K. (1997). Sec61p mediates export of a misfolded secretory protein from the endoplasmic reticulum to the cytosol for degradation. *The EMBO Journal*, *16*(15), 4540–4548. https://doi.org/10.1093/emboj/16.15.4540
263. Piper, P., Calderon, C. O., Hatzixanthis, K., & Mollapour, M. (2001). Weak acid adaptation: The stress response that confers yeasts with resistance to organic acid food preservatives. *Microbiology (Reading, England)*, *147*(Pt 10), 2635–2642. https://doi.org/10.1099/00221287-147-10-2635
264. Podwojski, K., Eisenacher, M., Kohl, M., Turewicz, M., Meyer, H. E., Rahnenführer, J., & Stephan, C. (2010). Peek a peak: A glance at statistics for quantitative label-free proteomics. *Expert Review of Proteomics*, *7*(2), 249–261. https://doi.org/10.1586/epr.09.107
265. Porro, D., Gasser, B., Fossati, T., Maurer, M., Branduardi, P., Sauer, M., & Mattanovich, D. (2011). Production of recombinant proteins and metabolites in yeasts: When are these systems better than bacterial production systems? *Applied Microbiology and Biotechnology*, *89*(4), 939–948. https://doi.org/10.1007/s00253-010-3019-z
266. Portig, I., Pankuweit, S., Lottspeich, F., & Maisch, B. (1996). Identification of stress proteins in endothelial cells. *Electrophoresis*, *17*(4), 803–808. https://doi.org/10.1002/elps.1150170431
267. Posch, A. (2014). Sample preparation guidelines for two-dimensional electrophoresis. *Archives of Physiology and Biochemistry*, *120*(5), 192–197. https://doi.org/10.3109/13813455.2014.955031

268. Potvin, G., Ahmad, A., & Zhang, Z. (2012). Bioprocess engineering aspects of heterologous protein production in Pichia pastoris: A review. *Biochemical Engineering Journal*, *64*, 91–105. https://doi.org/10.1016/j.bej.2010.07.017
269. Price, V., Mochizuki, D., March, C. J., Cosman, D., Deeley, M. C., Klinke, R., Clevenger, W., Gillis, S., Baker, P., & Urdal, D. (1987). Expression, purification and characterization of recombinant murine granulocyte-macrophage colony-stimulating factor and bovine interleukin-2 from yeast. *Gene*, *55*(2–3), 287–293. https://doi.org/10.1016/0378-1119(87)90288-5
270. Qiu, Y., & Michalak, M. (2009). Transcriptional control of the calreticulin gene in health and disease. *The International Journal of Biochemistry & Cell Biology*, *41*(3), 531–538. https://doi.org/10.1016/j.biocel.2008.06.020
271. Rabilloud, T. (1996). Solubilization of proteins for electrophoretic analyses. *Electrophoresis*, *17*(5), 813–829. https://doi.org/10.1002/elps.1150170503
272. Rabilloud, T. (2009). Membrane proteins and proteomics: Love is possible, but so difficult. *Electrophoresis*, *30 Suppl 1*, S174-180. https://doi.org/10.1002/elps.200900050
273. Rabilloud, T., Adessi, C., Giraudel, A., & Lunardi, J. (1997). Improvement of the solubilization of proteins in two-dimensional electrophoresis with immobilized pH gradients. *Electrophoresis*, *18*(3–4), 307–316. https://doi.org/10.1002/elps.1150180303
274. Rabilloud, T., Chevallet, M., Luche, S., & Lelong, C. (2010). Two-dimensional gel electrophoresis in proteomics: Past, present and future. *Journal of Proteomics*, *73*(11), 2064–2077. https://doi.org/10.1016/j.jprot.2010.05.016
275. Raymond, C. K., Bukowski, T., Holderman, S. D., Ching, A. F., Vanaja, E., & Stamm, M. R. (1998). Development of the methylotrophic yeast Pichia methanolica for the expression of the 65 kilodalton isoform of human glutamate decarboxylase. *Yeast (Chichester, England)*, *14*(1), 11–23. https://doi.org/10.1002/(SICI)1097-0061(19980115)14:1<11::AID-YEA196>3.0.CO;2-S
276. Reggiori, F., & Klionsky, D. J. (2013). Autophagic processes in yeast: Mechanism, machinery and regulation. *Genetics*, *194*(2), 341–361. https://doi.org/10.1534/genetics.112.149013
277. Rep, M., Krantz, M., Thevelein, J. M., & Hohmann, S. (2000). The transcriptional response of Saccharomyces cerevisiae to osmotic shock. Hot1p and Msn2p/Msn4p are required for the induction of subsets of high osmolarity glycerol pathway-dependent genes. *The Journal of Biological Chemistry*, *275*(12), 8290–8300. https://doi.org/10.1074/jbc.275.12.8290
278. Reynolds, J. A., & Tanford, C. (1970). Binding of Dodecyl Sulfate to Proteins at High Binding Ratios. Possible Implications for the State of Proteins in Biological Membranes*. *Proceedings of the National Academy of Sciences of the United States of America*, *66*(3), 1002–1007.
279. Robinson, A. S., Bockhaus, J. A., Voegler, A. C., & Wittrup, K. D. (1996). Reduction of BiP levels decreases heterologous protein secretion in Saccharomyces cerevisiae. *The Journal of Biological Chemistry*, *271*(17), 10017–10022. https://doi.org/10.1074/jbc.271.17.10017
280. Robinson, A. S., Hines, V., & Wittrup, K. D. (1994). Protein disulfide isomerase overexpression increases secretion of foreign proteins in Saccharomyces cerevisiae. *Bio/Technology (Nature Publishing Company)*, *12*(4), 381–384. https://doi.org/10.1038/nbt0494-381
281. Rocha, S. N., Abrahão-Neto, J., Cerdán, M. E., González-Siso, M. I., & Gombert, A. K. (2010). Heterologous expression of glucose oxidase in the yeast Kluyveromyces marxianus. *Microbial Cell Factories*, *9*, 4. https://doi.org/10.1186/1475-2859-9-4
282. Rolland, F., Winderickx, J., & Thevelein, J. M. (2002). Glucose-sensing and -signalling mechanisms in yeast. *FEMS Yeast Research*, *2*(2), 183–201. https://doi.org/10.1111/j.1567-1364.2002.tb00084.x
283. Rufo, N., Garg, A. D., & Agostinis, P. (2017). The Unfolded Protein Response in Immunogenic Cell Death and Cancer Immunotherapy. *Trends in Cancer*, *3*(9), 643–658. https://doi.org/10.1016/j.trecan.2017.07.002

284. Ruis, H., & Schüller, C. (1995). Stress signaling in yeast. *BioEssays: News and Reviews in Molecular, Cellular and Developmental Biology*, *17*(11), 959–965. https://doi.org/10.1002/bies.950171109
285. Sahara, T., Goda, T., & Ohgiya, S. (2002). Comprehensive expression analysis of time-dependent genetic responses in yeast cells to low temperature. *The Journal of Biological Chemistry*, *277*(51), 50015–50021. https://doi.org/10.1074/jbc.M209258200
286. Sakamoto, S., Ide, T., Tokiyoshi, S., Nakao, J., Hamada, F., Yamamoto, M., Grosby, J. A., Ni, Y., & Kawai, A. (1999). Studies on the structures and antigenic properties of rabies virus glycoprotein analogues produced in yeast cells. *Vaccine*, *17*(3), 205–218. https://doi.org/10.1016/s0264-410x(98)00196-0
287. Salazar, O. (2008). Bacteria and yeast cell disruption using lytic enzymes. *Methods in Molecular Biology (Clifton, N.J.)*, *424*, 23–34. https://doi.org/10.1007/978-1-60327-064-9_2
288. Samaraweera, B., Mahanama, A., Ahamad, A. Z., Wimalaratne, G. I., & Abeynayake, J. (2020). The laboratory investigation of a measles outbreak in the eve of its elimination in Sri Lanka. *Journal of Clinical Virology: The Official Publication of the Pan American Society for Clinical Virology*, *122*, 104230. https://doi.org/10.1016/j.jcv.2019.104230
289. Sambrook, J., & Russell, D. W. (2001). *Molecular cloning: A laboratory manual* (3rd. ed). Cold Spring Harbor Laboratory.
290. Samuel, D., Sasnauskas, K., Jin, L., Beard, S., Zvirbliene, A., Gedvilaite, A., & Cohen, B. (2002). High level expression of recombinant mumps nucleoprotein in Saccharomyces cerevisiae and its evaluation in mumps IgM serology. *Journal of Medical Virology*, *66*(1), 123–130. https://doi.org/10.1002/jmv.2120
291. Sanchez, Y., Taulien, J., Borkovich, K. A., & Lindquist, S. (1992). Hsp104 is required for tolerance to many forms of stress. *The EMBO Journal*, *11*(6), 2357–2364.
292. Sato, H., Yoneda, M., Honda, T., & Kai, C. (2012). Morbillivirus Receptors and Tropism: Multiple Pathways for Infection. *Frontiers in Microbiology*, *3*, 75. https://doi.org/10.3389/fmicb.2012.00075
293. Schlesser, A., Ulaszewski, S., Ghislain, M., & Goffeau, A. (1988). A second transport ATPase gene in Saccharomyces cerevisiae. *The Journal of Biological Chemistry*, *263*(36), 19480–19487.
294. Schmidt, F. R. (2004). Recombinant expression systems in the pharmaceutical industry. *Applied Microbiology and Biotechnology*, *65*(4), 363–372. https://doi.org/10.1007/s00253-004-1656-9
295. Schüller, C., Brewster, J. L., Alexander, M. R., Gustin, M. C., & Ruis, H. (1994). The HOG pathway controls osmotic regulation of transcription via the stress response element (STRE) of the Saccharomyces cerevisiae CTT1 gene. *The EMBO Journal*, *13*(18), 4382–4389.
296. Scorer, C. A., Buckholz, R. G., Clare, J. J., & Romanos, M. A. (1993). The intracellular production and secretion of HIV-1 envelope protein in the methylotrophic yeast Pichia pastoris. *Gene*, *136*(1–2), 111–119. https://doi.org/10.1016/0378-1119(93)90454-b
297. Shamovsky, I., Ivannikov, M., Kandel, E. S., Gershon, D., & Nudler, E. (2006). RNA-mediated response to heat shock in mammalian cells. *Nature*, *440*(7083), 556–560. https://doi.org/10.1038/nature04518
298. Shapiro, A. L., Viñuela, E., & Maizel, J. V. (1967). Molecular weight estimation of polypeptide chains by electrophoresis in SDS-polyacrylamide gels. *Biochemical and Biophysical Research Communications*, *28*(5), 815–820. https://doi.org/10.1016/0006-291x(67)90391-9
299. Sharma, K., Schmitt, S., Bergner, C. G., Tyanova, S., Kannaiyan, N., Manrique-Hoyos, N., Kongi, K., Cantuti, L., Hanisch, U.-K., Philips, M.-A., Rossner, M. J., Mann, M., & Simons, M. (2015). Cell type– and brain region–resolved mouse brain proteome. *Nature Neuroscience*, *18*(12), 1819–1831. https://doi.org/10.1038/nn.4160
300. Shaw, A. C., Røssel Larsen, M., Roepstorff, P., Holm, A., Christiansen, G., & Birkelund, S. (1999). Mapping and identification of HeLa cell proteins separated by immobilized pH-gradient two-dimensional gel electrophoresis and construction of a two-dimensional polyacrylamide gel electrophoresis database. *Electrophoresis*, *20*(4–5), 977–983.

https://doi.org/10.1002/(SICI)1522-2683(19990101)20:4/5<977::AID-ELPS977>3.0.CO;2-J
301. Shaw, M. M., & Riederer, B. M. (2003). Sample preparation for two-dimensional gel electrophoresis. *PROTEOMICS*, *3*(8), 1408–1417. https://doi.org/10.1002/pmic.200300471
302. Shevchenko, A., Tomas, H., Havlis, J., Olsen, J. V., & Mann, M. (2006). In-gel digestion for mass spectrometric characterization of proteins and proteomes. *Nature Protocols*, *1*(6), 2856–2860. https://doi.org/10.1038/nprot.2006.468
303. Shi, X., Karkut, T., Chamankhah, M., Alting-Mees, M., Hemmingsen, S. M., & Hegedus, D. (2003). Optimal conditions for the expression of a single-chain antibody (scFv) gene in Pichia pastoris. *Protein Expression and Purification*, *28*(2), 321–330. https://doi.org/10.1016/s1046-5928(02)00706-4
304. Shusta, E. V., Raines, R. T., Plückthun, A., & Wittrup, K. D. (1998). Increasing the secretory capacity of Saccharomyces cerevisiae for production of single-chain antibody fragments. *Nature Biotechnology*, *16*(8), 773–777. https://doi.org/10.1038/nbt0898-773
305. Sidrauski, C., & Walter, P. (1997). The transmembrane kinase Ire1p is a site-specific endonuclease that initiates mRNA splicing in the unfolded protein response. *Cell*, *90*(6), 1031–1039. https://doi.org/10.1016/s0092-8674(00)80369-4
306. Silberstein, S., Schlenstedt, G., Silver, P. A., & Gilmore, R. (1998). A role for the DnaJ homologue Scj1p in protein folding in the yeast endoplasmic reticulum. *The Journal of Cell Biology*, *143*(4), 921–933. https://doi.org/10.1083/jcb.143.4.921
307. Siso, M. I. G., Becerra, M., Maceiras, M. L., Vázquez, Á. V., & Cerdán, M. E. (2012). The yeast hypoxic responses, resources for new biotechnological opportunities. *Biotechnology Letters*, *34*(12), 2161–2173. https://doi.org/10.1007/s10529-012-1039-8
308. Slavov, N., Semrau, S., Airoldi, E., Budnik, B., & van Oudenaarden, A. (2015). Differential Stoichiometry among Core Ribosomal Proteins. *Cell Reports*, *13*(5), 865–873. https://doi.org/10.1016/j.celrep.2015.09.056
309. Slibinskas, R., Ražanskas, R., Zinkevičiūtė, R., & Čiplys, E. (2013). Comparison of first dimension IPG and NEPHGE techniques in two-dimensional gel electrophoresis experiment with cytosolic unfolded protein response in Saccharomyces cerevisiae. *Proteome Science*, *11*, 36. https://doi.org/10.1186/1477-5956-11-36
310. Slibinskas, R., Samuel, D., Gedvilaite, A., Staniulis, J., & Sasnauskas, K. (2004). Synthesis of the measles virus nucleoprotein in yeast Pichia pastoris and Saccharomyces cerevisiae. *Journal of Biotechnology*, *107*(2), 115–124. https://doi.org/10.1016/j.jbiotec.2003.10.018
311. Smith, J. D., Richardson, N. E., & Robinson, A. S. (2005). Elevated expression temperature in a mesophilic host results in increased secretion of a hyperthermophilic enzyme and decreased cell stress. *Biochimica et Biophysica Acta (BBA) - Proteins and Proteomics*, *1752*(1), 18–25. https://doi.org/10.1016/j.bbapap.2005.07.016
312. Smithies, O., & Poulik, M. D. (1956). Two-dimensional electrophoresis of serum proteins. *Nature*, *177*(4518), 1033. https://doi.org/10.1038/1771033a0
313. Sousa, M. J., Miranda, L., Côrte-Real, M., & Leão, C. (1996). Transport of acetic acid in Zygosaccharomyces bailii: Effects of ethanol and their implications on the resistance of the yeast to acidic environments. *Applied and Environmental Microbiology*, *62*(9), 3152–3157. https://doi.org/10.1128/aem.62.9.3152-3157.1996
314. Steinberg, T. H., Haugland, R. P., & Singer, V. L. (1996). Applications of SYPRO orange and SYPRO red protein gel stains. *Analytical Biochemistry*, *239*(2), 238–245. https://doi.org/10.1006/abio.1996.0320
315. Strayle, J., Pozzan, T., & Rudolph, H. K. (1999). Steady-state free Ca(2+) in the yeast endoplasmic reticulum reaches only 10 microM and is mainly controlled by the secretory pathway pump pmr1. *The EMBO Journal*, *18*(17), 4733–4743. https://doi.org/10.1093/emboj/18.17.4733
316. Strebel, P. M., Cochi, S. L., Hoekstra, E., Rota, P. A., Featherstone, D., Bellini, W. J., & Katz, S. L. (2011). A world without measles. *The Journal of Infectious Diseases*, *204 Suppl 1*, S1-3. https://doi.org/10.1093/infdis/jir111

317. Stromer, T., Ehrnsperger, M., Gaestel, M., & Buchner, J. (2003). Analysis of the interaction of small heat shock proteins with unfolding proteins. *The Journal of Biological Chemistry*, *278*(20), 18015–18021. https://doi.org/10.1074/jbc.M301640200
318. Sudbery, P. E., Gleeson, M. A., Veale, R. A., Ledeboer, A. M., & Zoetmulder, M. C. (1988). Hansenula polymorpha as a novel yeast system for the expression of heterologous genes. *Biochemical Society Transactions*, *16*(6), 1081–1083. https://doi.org/10.1042/bst0161081a
319. Supply, P., Wach, A., & Goffeau, A. (1993). Enzymatic properties of the PMA2 plasma membrane-bound H(+)-ATPase of Saccharomyces cerevisiae. *The Journal of Biological Chemistry*, *268*(26), 19753–19759.
320. Tahara, M., Bürckert, J.-P., Kanou, K., Maenaka, K., Muller, C. P., & Takeda, M. (2016). Measles Virus Hemagglutinin Protein Epitopes: The Basis of Antigenic Stability. *Viruses*, *8*(8), 216. https://doi.org/10.3390/v8080216
321. Takeda, M., Tahara, M., Nagata, N., & Seki, F. (2011). Wild-Type Measles Virus is Intrinsically Dual-Tropic. *Frontiers in Microbiology*, *2*, 279. https://doi.org/10.3389/fmicb.2011.00279
322. Taleuzzaman M, Ali S, Gilani SJ, Imam SS, & Hafeez A. (2015). Ultra Performance Liquid Chromatography (UPLC)—A Review.Ali S, Gilani SJ, Imam SS, Hafeez A. *Austin J Anal Pharm Chem*, *2*(6), 1056.
323. Tantipaiboonwong, P., Sinchaikul, S., Sriyam, S., Phutrakul, S., & Chen, S.-T. (2005). Different techniques for urinary protein analysis of normal and lung cancer patients. *Proteomics*, *5*(4), 1140–1149. https://doi.org/10.1002/pmic.200401143
324. Tarr, J. M., Young, P. J., Morse, R., Shaw, D. J., Haigh, R., Petrov, P. G., Johnson, S. J., Winyard, P. G., & Eggleton, P. (2010). A mechanism of release of calreticulin from cells during apoptosis. *Journal of Molecular Biology*, *401*(5), 799–812. https://doi.org/10.1016/j.jmb.2010.06.064
325. Tatsuo, H., Ono, N., Tanaka, K., & Yanagi, Y. (2000). SLAM (CDw150) is a cellular receptor for measles virus. *Nature*, *406*(6798), 893–897. https://doi.org/10.1038/35022579
326. Taylor, J., Anderson, N. L., Scandora, A. E., Willard, K. E., & Anderson, N. G. (1982). Design and implementation of a prototype Human Protein Index. *Clinical Chemistry*, *28*(4 Pt 2), 861–866.
327. Taylor, R. C., & Coorssen, J. R. (2006). Proteome resolution by two-dimensional gel electrophoresis varies with the commercial source of IPG strips. *Journal of Proteome Research*, *5*(11), 2919–2927. https://doi.org/10.1021/pr060298d
328. Tesfaw, A., & Assefa, F. (2014). Current Trends in Bioethanol Production by Saccharomyces cerevisiae: Substrate, Inhibitor Reduction, Growth Variables, Coculture, and Immobilization. *International Scholarly Research Notices*, *2014*, 532852. https://doi.org/10.1155/2014/532852
329. Tesniere, A., Apetoh, L., Ghiringhelli, F., Joza, N., Panaretakis, T., Kepp, O., Schlemmer, F., Zitvogel, L., & Kroemer, G. (2008). Immunogenic cancer cell death: A key-lock paradigm. *Current Opinion in Immunology*, *20*(5), 504–511. https://doi.org/10.1016/j.coi.2008.05.007
330. The, M., Tasnim, A., & Käll, L. (2016). How to talk about protein-level false discovery rates in shotgun proteomics. *Proteomics*, *16*(18), 2461–2469. https://doi.org/10.1002/pmic.201500431
331. Thiede, B., Höhenwarter, W., Krah, A., Mattow, J., Schmid, M., Schmidt, F., & Jungblut, P. R. (2005). Peptide mass fingerprinting. *Methods*, *35*(3), 237–247. https://doi.org/10.1016/j.ymeth.2004.08.015
332. Thim, L., Hansen, M. T., Norris, K., Hoegh, I., Boel, E., Forstrom, J., Ammerer, G., & Fiil, N. P. (1986). Secretion and processing of insulin precursors in yeast. *Proceedings of the National Academy of Sciences of the United States of America*, *83*(18), 6766–6770. https://doi.org/10.1073/pnas.83.18.6766
333. Thompson, D. A., Roy, S., Chan, M., Styczynsky, M. P., Pfiffner, J., French, C., Socha, A., Thielke, A., Napolitano, S., Muller, P., Kellis, M., Konieczka, J. H., Wapinski, I., &

Regev, A. (2013). Evolutionary principles of modular gene regulation in yeasts. *ELife*, *2*, e00603. https://doi.org/10.7554/eLife.00603
334. Timms, J., & Cramer, R. (2008). Difference Gel Electrophoresis. *Proteomics*, *8*, 4886–4897. https://doi.org/10.1002/pmic.200800298
335. Tiselius, A. & Uppsala universitet. (1930). *The moving boundary method of studying the electrophoresis of proteins*. Almqvist & Wiksell.
336. Torres-Sangiao, E., Leal Rodriguez, C., & García-Riestra, C. (2021). Application and Perspectives of MALDI–TOF Mass Spectrometry in Clinical Microbiology Laboratories. *Microorganisms*, *9*(7), 1539. https://doi.org/10.3390/microorganisms9071539
337. Totary-Jain, H., Naveh-Many, T., Riahi, Y., Kaiser, N., Eckel, J., & Sasson, S. (2005). Calreticulin Destabilizes Glucose Transporter-1 mRNA in Vascular Endothelial and Smooth Muscle Cells Under High-Glucose Conditions. *Circulation Research*, *97*(10), 1001–1008. https://doi.org/10.1161/01.RES.0000189260.46084.e5
338. Travers, K. J., Patil, C. K., Wodicka, L., Lockhart, D. J., Weissman, J. S., & Walter, P. (2000). Functional and genomic analyses reveal an essential coordination between the unfolded protein response and ER-associated degradation. *Cell*, *101*(3), 249–258. https://doi.org/10.1016/s0092-8674(00)80835-1
339. Tudisca, V., Simpson, C., Castelli, L., Lui, J., Hoyle, N., Moreno, S., Ashe, M., & Portela, P. (2012). PKA isoforms coordinate mRNA fate during nutrient starvation. *Journal of Cell Science*, *125*(21), 5221–5232. https://doi.org/10.1242/jcs.111534
340. Tufi, R., Panaretakis, T., Bianchi, K., Criollo, A., Fazi, B., Di Sano, F., Tesniere, A., Kepp, O., Paterlini-Brechot, P., Zitvogel, L., Piacentini, M., Szabadkai, G., & Kroemer, G. (2008). Reduction of endoplasmic reticulum Ca2+ levels favors plasma membrane surface exposure of calreticulin. *Cell Death and Differentiation*, *15*(2), 274–282. https://doi.org/10.1038/sj.cdd.4402275
341. Twyman, R., Cfe, P. D., & A, G. (2013). *Principles of Proteomics*. Garland Science.
342. Tyo, K. E., Liu, Z., Petranovic, D., & Nielsen, J. (2012). Imbalance of heterologous protein folding and disulfide bond formation rates yields runaway oxidative stress. *BMC Biology*, *10*, 16. https://doi.org/10.1186/1741-7007-10-16
343. Unlü, M., Morgan, M. E., & Minden, J. S. (1997). Difference gel electrophoresis: A single gel method for detecting changes in protein extracts. *Electrophoresis*, *18*(11), 2071–2077. https://doi.org/10.1002/elps.1150181133
344. van de Laar, T., Visser, C., Holster, M., López, C. G., Kreuning, D., Sierkstra, L., Lindner, N., & Verrips, T. (2007). Increased heterologous protein production by Saccharomyces cerevisiae growing on ethanol as sole carbon source. *Biotechnology and Bioengineering*, *96*(3), 483–494. https://doi.org/10.1002/bit.21150
345. van Ooyen, A. J. J., Dekker, P., Huang, M., Olsthoorn, M. M. A., Jacobs, D. I., Colussi, P. A., & Taron, C. H. (2006). Heterologous protein production in the yeast Kluyveromyces lactis. *FEMS Yeast Research*, *6*(3), 381–392. https://doi.org/10.1111/j.1567-1364.2006.00049.x
346. Vera, M., Pani, B., Griffiths, L. A., Muchardt, C., Abbott, C. M., Singer, R. H., & Nudler, E. (2014). The translation elongation factor eEF1A1 couples transcription to translation during heat shock response. *ELife*, *3*, e03164. https://doi.org/10.7554/eLife.03164
347. von der Haar, T., & McCarthy, J. E. G. (2002). Intracellular translation initiation factor levels in Saccharomyces cerevisiae and their role in cap-complex function. *Molecular Microbiology*, *46*(2), 531–544. https://doi.org/10.1046/j.1365-2958.2002.03172.x
348. Wang, Q., Groenendyk, J., & Michalak, M. (2015). Glycoprotein Quality Control and Endoplasmic Reticulum Stress. *Molecules*, *20*(8), 13689–13704. https://doi.org/10.3390/molecules200813689
349. Wangeline, M. A., & Hampton, R. Y. (2018). "Mallostery"—Ligand-dependent protein misfolding enables physiological regulation by ERAD. *Journal of Biological Chemistry*, *293*(38), 14937–14950. https://doi.org/10.1074/jbc.RA118.001808
350. Watarai, H., Inagaki, Y., Kubota, N., Fuju, K., Nagafune, J., Yamaguchi, Y., & Kadoya, T. (2000). Proteomic approach to the identification of cell membrane proteins. *Electrophoresis*, *21*(2), 460–464. https://doi.org/10.1002/(SICI)1522-2683(20000101)21:2<460::AID-ELPS460>3.0.CO;2-P

351. Wegner, G. H. (1990). Emerging applications of the methylotrophic yeasts. *FEMS Microbiology Reviews*, *7*(3–4), 279–283. https://doi.org/10.1111/j.1574-6968.1990.tb04925.x
352. Weinhandl, K., Winkler, M., Glieder, A., & Camattari, A. (2014). Carbon source dependent promoters in yeasts. *Microbial Cell Factories*, *13*, 5. https://doi.org/10.1186/1475-2859-13-5
353. Wen, D., Ding, M. X., & Schlesinger, M. J. (1986). Expression of genes encoding vesicular stomatitis and Sindbis virus glycoproteins in yeast leads to formation of disulfide-linked oligomers. *Virology*, *153*(1), 150–154. https://doi.org/10.1016/0042-6822(86)90016-4
354. Wieczorke, R., Krampe, S., Weierstall, T., Freidel, K., Hollenberg, C. P., & Boles, E. (1999). Concurrent knock-out of at least 20 transporter genes is required to block uptake of hexoses in Saccharomyces cerevisiae. *FEBS Letters*, *464*(3), 123–128. https://doi.org/10.1016/S0014-5793(99)01698-1
355. Wiersma, V. R., Michalak, M., Abdullah, T. M., Bremer, E., & Eggleton, P. (2015). Mechanisms of Translocation of ER Chaperones to the Cell Surface and Immunomodulatory Roles in Cancer and Autoimmunity. *Frontiers in Oncology*, *5*, 7. https://doi.org/10.3389/fonc.2015.00007
356. Wilkins, M. (2009). Proteomics data mining. *Expert Review of Proteomics*, *6*(6), 599–603. https://doi.org/10.1586/epr.09.81
357. Williams, D. B. (2006). Beyond lectins: The calnexin/calreticulin chaperone system of the endoplasmic reticulum. *Journal of Cell Science*, *119*(Pt 4), 615–623. https://doi.org/10.1242/jcs.02856
358. Wiśniewski, J. R., Zougman, A., Nagaraj, N., & Mann, M. (2009). Universal sample preparation method for proteome analysis. *Nature Methods*, *6*(5), 359–362. https://doi.org/10.1038/nmeth.1322
359. Wittmann-Liebold, B., Graack, H.-R., & Pohl, T. (2006). Two-dimensional gel electrophoresis as tool for proteomics studies in combination with protein identification by mass spectrometry. *PROTEOMICS*, *6*(17), 4688–4703. https://doi.org/10.1002/pmic.200500874
360. Woods, A. G., Sokolowska, I., Ngounou Wetie, A. G., Channaveerappa, D., Dupree, E. J., Jayathirtha, M., Aslebagh, R., Wormwood, K. L., & Darie, C. C. (2019). Mass Spectrometry for Proteomics-Based Investigation. In A. G. Woods & C. C. Darie (Eds.), *Advancements of Mass Spectrometry in Biomedical Research* (pp. 1–26). Springer International Publishing. https://doi.org/10.1007/978-3-030-15950-4_1
361. Xie, Y., & Varshavsky, A. (2001). RPN4 is a ligand, substrate, and transcriptional regulator of the 26S proteasome: A negative feedback circuit. *Proceedings of the National Academy of Sciences of the United States of America*, *98*(6), 3056–3061. https://doi.org/10.1073/pnas.071022298
362. Yadav, S., Srivastava, A., Biswas, S., Chaurasia, N., Singh, S. K., Kumar, S., Srivastava, V., & Mishra, Y. (2020). Comparison and optimization of protein extraction and two-dimensional gel electrophoresis protocols for liverworts. *BMC Research Notes*, *13*(1), 60. https://doi.org/10.1186/s13104-020-4929-1
363. Yamada, M., Hayatsu, N., Matsuura, A., & Ishikawa, F. (1998). Y′-Help1, a DNA Helicase Encoded by the Yeast Subtelomeric Y′ Element, Is Induced in Survivors Defective for Telomerase *. *Journal of Biological Chemistry*, *273*(50), 33360–33366. https://doi.org/10.1074/jbc.273.50.33360
364. Yanagi, Y., Takeda, M., Ohno, S., & Hashiguchi, T. (2009). Measles virus receptors. *Current Topics in Microbiology and Immunology*, *329*, 13–30. https://doi.org/10.1007/978-3-540-70523-9_2
365. Yu, H., Zhang, Y., Zhang, D., Lu, Y., He, H., Zheng, F., & Wang, M. (2017). Identification of a Ribose-Phosphate Pyrophosphokinase that Can Interact In Vivo with the Anaphase Promoting Complex/Cyclosome. *International Journal of Molecular Sciences*, *18*(4). https://doi.org/10.3390/ijms18040617

366. Yurimoto, H. (2009). Molecular basis of methanol-inducible gene expression and its application in the methylotrophic yeast Candida boidinii. *Bioscience, Biotechnology, and Biochemistry*, *73*(4), 793–800. https://doi.org/10.1271/bbb.80825
367. Zahrl, R. J., Gasser, B., Mattanovich, D., & Ferrer, P. (2019). Detection and Elimination of Cellular Bottlenecks in Protein-Producing Yeasts. In B. Gasser & D. Mattanovich (Eds.), *Recombinant Protein Production in Yeast* (pp. 75–95). Springer. https://doi.org/10.1007/978-1-4939-9024-5_2
368. Zaratiegui, M. (2017). Cross-Regulation between Transposable Elements and Host DNA Replication. *Viruses*, *9*(3), 57. https://doi.org/10.3390/v9030057
369. Zepeda, A. B., Pessoa, A., & Farías, J. G. (2018). Carbon metabolism influenced for promoters and temperature used in the heterologous protein production using Pichia pastoris yeast. *Brazilian Journal of Microbiology: [Publication of the Brazilian Society for Microbiology]*, *49 Suppl 1*, 119–127. https://doi.org/10.1016/j.bjm.2018.03.010
370. Zhang, K., & Kaufman, R. J. (2008). Identification and Characterization of Endoplasmic Reticulum Stress-Induced Apoptosis In Vivo. *Methods in Enzymology*, *442*, 395–419. https://doi.org/10.1016/S0076-6879(08)01420-1
371. Zhang, W., Qu, P., Li, D., Zhang, C., Liu, Q., Zou, G., Dupont-Rouzeyrol, M., Lavillette, D., Jin, X., Yin, F., & Huang, Z. (2019). Yeast-produced subunit protein vaccine elicits broadly neutralizing antibodies that protect mice against Zika virus lethal infection. *Antiviral Research*, *170*, 104578. https://doi.org/10.1016/j.antiviral.2019.104578
372. Zhou, J., Zhang, H., Liu, X., Wang, P. G., & Qi, Q. (2007). Influence of N-glycosylation on Saccharomyces cerevisiae morphology: A golgi glycosylation mutant shows cell division defects. *Current Microbiology*, *55*(3), 198–204. https://doi.org/10.1007/s00284-006-0585-5
373. Zhou, S., Bailey, M. J., Dunn, M. J., Preedy, V. R., & Emery, P. W. (2005). A quantitative investigation into the losses of proteins at different stages of a two-dimensional gel electrophoresis procedure. *Proteomics*, *5*(11), 2739–2747. https://doi.org/10.1002/pmic.200401178
374. Zhu, H., Bilgin, M., Bangham, R., Hall, D., Casamayor, A., Bertone, P., Lan, N., Jansen, R., Bidlingmaier, S., Houfek, T., Mitchell, T., Miller, P., Dean, R. A., Gerstein, M., & Snyder, M. (2001). Global analysis of protein activities using proteome chips. *Science (New York, N.Y.)*, *293*(5537), 2101–2105. https://doi.org/10.1126/science.1062191
375. Zinkevičiūtė, R., Bakūnaitė, E., Čiplys, E., Ražanskas, R., Raškevičiūtė, J., & Slibinskas, R. (2015). Heat shock at higher cell densities improves measles hemagglutinin translocation and human GRP78/BiP secretion in Saccharomyces cerevisiae. *New Biotechnology*, *32*(6), 690–700. https://doi.org/10.1016/j.nbt.2015.04.001

SUMMARY

SANTRUMPŲ SĄRAŠAS

2DE	dvikryptė elektroforezė
MS	masių spektrometrija
pI	izoelektrinis taškas
IEF	izoelektrinis fokusavimas
IPG	imobilizuotas pH gradientas
NEPHGE	nepusiausvyro pH gradiento elektroforezė
LC-MS^E	skysčių chromatografijos/masių spektrometrijos metodas su nuo duomenų nepriklausomos analizės nustatymais
ET	endoplazminis tinklas
ERAD	su endoplazminiu tinklu asocijuota baltymų degradacija
UPR-Cyto	citozolinis nesulankstytų baltymų atsakas
UPR	nesulankstytų baltymų atsakas
AN	amfolitai nešėjai
TVH	tymų viruso hemagliutinino baltymas
TVN	tymų viruso nukleokapsidės baltymas
CALR	žmogaus kalretikulino baltymas
RE	restrikcijos endonuklеazė
OD600	optinis tankis matuojamas 600 nm ilgio šviesos banga
NDS	natrio dodecilsulfatas
NDS-PAGE	natrio dodecilsulfato poliakrilamido gelio elektroforezė
DTT	ditiotreitolas
IAC	jodoacetamidas
APS	amoniopersulfatas
EDTA	etilendiamino tetraacto rūgštis
PMSF	fenilmetilsulfonilchloridas
Tris	trisaminometanas
TEMED	tetrametiletlendiaminas
H_2O MilliQ	itin aukšto švarumo vanduo
GAPDH	gliceraldehido 3-fosfato dehidrogenazė
kDa	kilodaltonai

MALDI TOF/TOF	matriksu asistuotos lazerinės desorbcijos/jonizacijos masių spektrometrijos metodas, jonų skrydžio laiko matavimo režime
FDR	klaidingų atradimų rodiklis
ACN	acetonitrilas
TFR	trifluoracto rūgštis
SC	skysčių chromatografija
SGD	*S. cerevisiae* genomo duombazė
YPD	mielių baltymų duombazė
HSR	karščio šoko atsakas
eEF1A	eukariotų transliacijos elongacijos faktorius
HSF1	karščio šoko faktorius 1

ĮVADAS

Mielės *S. cerevisiae* yra vienas dažniausiai naudojamų organizmų rekombinantinių baltymų produkcijai. Taip yra dėl to, jog šis organizmas yra vienas geriausiai ištyrinėtų eukariotinių organizmų (Duina *et al*., 2014), jį lengva ir nebrangu kultyvuoti, bei yra sukurta daugybė patogių molekulinių įrankių genetinėms manipuliacijoms (Mattanovich *et al*., 2012; Porro *et al*., 2011). Šiose mielėse yra gaminami svarbūs biofarmaciniai baltymai tokie, kaip Hepatito viruso subvienetų vakcinos (McAleer *et al*., 1984), hirudinas (Bischoff *et al*., 1989), insulinas (Thim *et al*., 1986), trambocitų kilmės augimo faktorius (Finnis *et al*., 1992), urato oksidazė (Leplatois *et al.,* 1992) bei makrofagų kolonijas stimuliuojantis faktorius (Price *et al.,* 1987).

Tačiau, rekombinantinių baltymų gamyba *S. cerevisiae* vis dar turi kliūčių, tokių, kaip neteisingas glikozilinimas, žema baltymų išeiga bei ūmus ląstelinis stresas (Mattanovich *et al.,* 2004, 2012), kurios trukdo sėkmingai dar platesnio spektro baltymų gamybai. Norint pašalinti efektyvios baltymų produkcijos kliūtis, reikalinga gilesnė ląstelinės mielių proteomos analizė. Deja, rekombinantinių baltymų sintezės įtaka mielių ląstelei yra ištyrinėta menkai. Tokio pobūdžio tyrimai gali padėti identifikuoti itin efektyvios arba atvirkščiai, nesėkmingos rekombinantinių baltymų biosintezės priežastis. Gauta informacija gali būti panaudota patobulintų mielių kamienų konstravimui arba sintezės kliūčių identifikavimui ir jų įveikimui. Proteominė analizė yra galingas įrankis palyginamuosiuose tyrimuose, nes ji tiesiogiai suteikia informaciją apie ląstelinių baltymų, kurie yra heterologinių baltymų biosintezės vykdytojai, kiekio ir gausumo pokyčius. Dvikrypte elektroforeze (2DE) pagrįsta proteominė analizė yra patikimas, greitas ir nebrangus metodas suteikiantis informaciją apie esminius tiriamų ląstelių proteomų pokyčius. Papildomos, masių spektrometrijos (MS) metodais pagrįstos analizės technikos, praturtina proteominio eksperimento duomenis skirtinga sinteze pasižymėjusių baltymų identifikacija, arba visų ląstelės baltymų analize leidžiančia išskirti net mažus proteomų pokyčius.

Darbo tikslas:

Pritaikyti dvikrypte elektroforeze ir masių spektrometrija pagrįstą proteominę analizę, rekombinantinių baltymų sintezės tyrimams mielėse *S. cerevisiae.*

Darbo uždaviniai:

1. Pasirinkti geriausiai veikiantį 2DE metodą, mielių *S. cerevisiae* ląstelių proteomos analizei, plačiame pH diapazone (pH 3–10).
2. Nustatyti mielių ląstelių kultūros augimo sąlygas, gerinančias TVH baltymo translokaciją; nustatyti ląstelinius baltymus, susijusius su pagerinta translokacija.
3. Atkurti amfolitų nešėjų ir gelių tirpalų sudėtį pirmos krypties NEPHGE pagrįstai 2DE, ir palyginti gautus gelius su anksčiau komerciškai prieinamais geliais.
4. Ištirti efektyvios žmogaus CALR baltymo sekrecijos poveikį, mielių *S. cerevisiae* ląstelinei proteomai.

Darbo naujumas

Šiame darbe pirmą kartą palyginti IPG ir NEPHGE pagrįsti 2DE metodai, bei įrodyta, jog NEPHGE 2DE metodas labiau tinkamas mielių proteomos analizei. Mums taip pat pavyko pagerinti neefektyvią TVH baltymo pirmtakų translokaciją į ET ir padidinti glikozilinto baltymo kiekį ~3 kartus. TVH ekspresuojančių ląstelių NEPHGE pagrįsta 2DE analizė, atlikta po karščio šoko taikymo, padėjo identifikuoti 15 ląstelinių baltymų-taikinių galimai susijusių su pagerėjusia baltymo translokacija. Šie baltymai-taikiniai gali būti panaudoti tolesniam mielių kamienų, su pagerinta baltymų translokacija į ET ar net nuslopintu citozoliniu nesulankstytų baltymų atsaku (UPR-Cyto), konstravimui. Šiame darbe taip pat pristatome atkurtą amfolitų nešėjų (AN) sudėtį NEPHGE pagrįstiems pirmos krypties baltymų atskyrimo geliams, kurie gali būti naudojami vietoje komerciškai nebeprieinamų gelių. Komercinių gelių sudėtis niekuomet nebuvo paviešinta, o originalus receptas NEPHGE pagrįstam IEF buvo publikuotas 1995 (Klose ir Kobalz, 1995), tad originaliai naudoti amfolitai nebegaminami. Visos šios kliūtys apsunkino atkūrimo procesą, bei suteikė svarbos ir naujumo mūsų publikuotam receptui.

Galiausiai, mes pristatome itin efektyvią (140 mg/L) heterologinio žmogaus CALR baltymo sekreciją mielėse *S. cerevisiae*. Netikėtai, NEPHGE 2DE ir LC-MS^E pagrįstos kiekybinės, CALR sekretuojančių bei kontrolinių ląstelių transformuotų tuščiu vektoriumi, analizės atskleidė, jog efektyvi CALR sekrecija neindukuoja jokio ląstelinio streso atsako bei sekrecinio kelio baltymų biosintezės pokyčių. Labai neįprasta, jog tokia aukšto lygio sekrecija ląstelės proteomą įtakoja tiek mažai. Tai gali reikšti, jog sėkminga sekrecija gali priklausyti nuo paties baltymo prigimtinių savybių ir suteikia pagrindą tolesniems, tokios sekrecijos mielėse *S. cerevisiae* tyrimams.

Darbo reikšmė

Kadangi šiame darbe parodome, jog NEPHGE pagrįsta 2DE yra labiau tinkamas 2DE metodas mielių proteomos analizei, o tirpalai reikalingi šiam metodui yra komerciškai nebeprieinami, mūsų publikuotas AN mišinio receptas turi didelę vertę visiems NEPHGE pagrįstos IEF įrangos naudotojams. Mūsų nustatytos efektyvesnės TVH baltymo translokacijos sąlygos ir identifikuoti baltymai-taikiniai, suteikia svarbią informaciją virusinių paviršinių glikobaltymų gamybai, kurie pastaraisiais metais vis dažniau naudojami, kaip subvienetų vakcinos *(*Gebauer *et al., 2019;* Lin *et al*., 2012; Zhang *et al*., 2019). Mūsų rezultatai apie CALR sekreciją mielėse siūlo, jog CALR gali būti lengvai sekretuojamas ne kažkokio specialaus mechanizmo pagalba, bet veikiau dėl pačiam baltymui būdingų savybių. Ši informacija gali būti svarbi aiškinantis šio baltymo sekrecijos mechanizmą žinduolių ląstelėse. Mūsų skelbiami proteominiai duomenys apie efektyvią CALR sekreciją yra svarbūs ir iš biotechnologinės pusės, nes suteikia informaciją apie bestresę, aukšto lygio žmogaus baltymų gamybą mielėse.

Ginamieji teiginiai:

1. NEPHGE pagrįsta 2DE yra tinkamesnis 2DE metodas mielių proteomos analizei plačiame pH diapazone (pH 3–10). IPG 3–10 (Invitrogen) 2DE metodas yra patikimas tik rūgštinių baltymų analizei, nes bazinėje 2D gelių pusėje rezultatai neatsikartoja. Tuo tarpu, NEPHGE pagrįstas metodas yra tinkamas analizuoti baltymus visame pI diapazone ir ypač efektyvus bazinių baltymų analizei.
2. TVH glikobaltymo kiekis ir translokacijos efektyvumas padidėja ~3 kartus, kai karščio šokas taikomas didesnio tankio ląstelių kultūroms su tolesne rekombinantinio baltymo sinteze 37 °C temperatūroje. Atlikus palyginamąją proteominę analizę, identifikuoti 15 skirtinga biosinteze pasižymėję ląsteliniai baltymai galimai susiję su pagerėjusia TVH translokacija.
3. Atkurtas AN mišinys ir gelių tirpalai NEPHGE pagrįstam pirmos krypties baltymų atskyrimui, pasižymi geresniu atsikartojamumu ir gali būti naudojami vietoje komerciškai nebeprieinamų gelių tirpalų.
4. Aukšto lygio rekombinantinio CALR baltymo sekrecija mielėse įtakoja mielių ląstelių proteomą labai silpnai, neapkrauna ląstelės sekrecinio aparato ir nesukelia jokio akivaizdaus ląstelinio streso. CALR sintezė turi tik nežymų poveikį struktūrinių ribosomos baltymų, dalyvaujančiu baltymų transliacijoje, sintezei.

1. MEDŽIAGOS IR TYRIMO METODAI

1.1. MEDŽIAGOS

1.1.1. Plazmidės

pFGG3 – tuščias kontrolinis vektorius (konstravimas aprašytas Slibinskas *et al*., 2004);
pFGG3-MeH – indukuojamai TVH baltymo, sukeliančio UPR-Cyto streso atsaką mielėse, produkcijai (konstravimas aprašytas (Ciplys *et al*., 2011));
pFGG3-MeN – indukuojamai TVN baltymo produkcijai, kuri nesukelia streso atsako mielėse, naudota kontrolei (konstravimas aprašytas (Slibinskas *et al*., 2004));
pFGAL7-CRT – indukuojmai žmogaus CALR baltymo sintezei bei sekrecijai. pFGAL7 vektorius buvo gautas iš pFGG3 vektoriaus (Slibinskas *et al*., 2004) iškerpant GAL10/PYK1 promotorių su SmaI ir XbaI restrikcijos endonukleazėmis (RE). Stipresnę genų raišką sąlygoja vienintelio GAL7 promotoriaus reguliuojama transkripcija. Genas, koduojantis pilno ilgio laukinio tipo žmogaus CALR baltymo pirmtaką (GenBank prieigos nr. M84739 kopijinės DNR sekai ir UniProtKB prieigos nr. P27797 aminorūgščių sekai) buvo susintetintas GenScript. Šis genas buvo įklonuotas į mielių raiškos vektorių pFGAL7, kur genų raiška reguliuojama galaktoze indukuojamo mielių *GAL7* geno promotoriaus, naudojant BcuI RE. DNR manipuliacijos buvo atliktos pagal standartines procedūras (Sambrook ir Russell, 2001). *CALR* geno seka pFGAL7-CRT vektoriuje buvo patvirtinta Sangerio sekvenavimo metodu.

1.1.2. Mielių *S. cerevisiae* kamienai

Kamienas AH22 pasirinktas naudoti šios disertacijos eksperimentuose, nes jis rutiniškai naudojamas mūsų laboratorijoje bei autorė yra su juo gerai susipažinusi. Tai yra gerai ištirtas laboratorinis kamienas su pilnai nusekvenuotu genomu.
Kamienas BY4741 naudotas tik, kaip kontrolė eksperimente su deleciniu BY4741 ΔSOD1 kamienu.
AH22 (*MATa leu2-3 leu2-112 his4-519 can1 [KIL-o]*);
BY4741 (*MATa his3Δ1 leu2Δ0 met15Δ0 ura3Δ0*);
BY4741 ΔSOD1 (*MATa his3Δ1 leu2Δ0 met15Δ0 ura3Δ0 ΔSOD1*) (Mielių mutantų kolekcija);

1.1.3. Kultūrų auginimo terpės

Kieta YEPD – mielių ekstraktas 1 %, peptonas 2 %, gliukozė 2 %, agar-agaras 2 %;
YEPD – mielių ekstraktas 1 %, peptonas 2 %, gliukozė 2 %;
YEPG – mielių ekstraktas 1 %, peptonas 2 %, galaktozė 2.5 %;

1.1.4. Buferiniai tirpalai ir kiti reagentai

Ardymo buferis: 50 mM natrio fosfato (pH 7,2), 5 mM EDTA, 1 mM, PMSF.
Stiklo rutuliukai 0,5 mm diametro (BioSpec Products Inc., JAV);
Bredfordo reagentas („Roti-NanoQuant", Carl Roth GmbH.);
Gliukozės koncentracijos nustatymo rinkinys (Enzytec *fluid* D-Glucose, ThermoFisher Scientific);
Etanolio koncentracijos nustatymo rinkinys (Enzytec *fluid* Ethanol, ThermoFisher Scientific);
2×NDS-PAGE pavyzdžių buferis: 125 mM Tris (trishidroksimetilaminometanas)-HCl (pH 6,8), 20 % glicerolio, 8 % natrio dodecil sulfato (NDS), 150 mM ditiotreitolo (DTT), 0,01 % bromfenolio mėlio.
4 % koncentruojančio gelio tirpalas: 24,9 % 0,5 M Tris-HCl (pH 6,8), 0,1 % NDS 10 % (svoris/tūris), 10 % Akrilamido 40 % (37,5:1), 34,9 % H_2O MilliQ, 0,1 % APS 10 % (amonio persulfatas), 0.01 % TEMED (*N*,*N*,*N*′,*N*′-Tetrametiletano-1,2-diaminas).
10 % frakcionuojančio gelio tirpalas (kultūros augimo terpių analizei, Western baltymų hibridizacijai): 24,9 % 1,5 M Tris-HCl (pH 8,8), 0,1 % NDS 10 % (svoris/tūris), 24,9 % Akrilamido 40 % (37,5:1), 50 % H_2O MilliQ, 0,1 % APS 10 %, 0,01 % TEMED.
12 % frakcionuojančio gelio tirpalas (antrai 2DE krypčiai): 24,9 % 1,5 M Tris-HCl (pH 8,8), 0,1 % NDS 10 % (svoris/tūris), 30 % Akrilamido 40 % (37,5:1), 44,9 % H_2O MilliQ, 0,1 % APS 10 %, 0,01 % TEMED.
NDS-PAGE buferis: 25mM Tris, 190 mM glicino (pH 8,3 25°C), 0,1 % NDS (svoris/tūris).
Gelių fiksavimo tirpalas: 50 % etanolio, 40 % H_2O MilliQ, 10 % acto rūgšties.
Coomassie brilliantinis mėlis R-250: 50 % etanolis, 10 % acto rūgštis, 0.1 % Coomassie brilliantinis mėlis R-250 (CBB R-250), 40 % H_2O MilliQ.
Gelių plovimo tirpalas: 5 % etanolis, 12,5 % acto rūgštis H_2O MilliQ.
Gelių saugojimo tirpalas: 7 % acto rūgštis H_2O MilliQ.
Denatūruojantis IEF buferis: 7 M šlapalas, 2 M tiošlapalas, 2 % CHAPS detergentas, 1 % amfolitų (pH 3–10, Pharmalyte, GE Healthcare), 0,002 %

Bromfenolio mėlio ir 75 mM DTT (ditiotreitolas) (dedamas prieš pat naudojimą).

Katodinis buferis NEPHGE pirmos krypties izoelektriniam fokusavimui: 20 g glicerolio ir 216 g šlapalo ištirpinta 170 ml distiliuoto vandens, iki 380 ml tūrio; tada pridėta 20 ml etilendiamino; tirpalas ruoštas kaitinant iki 40°C ant šildančios maišyklės.

Anodinis buferis NEPHGE pirmos krypties izoelektriniam fokusavimui: 72g šlapalo ištirpinta 300 ml distiliuoto vandens, iki 380 ml tūrio; tada pridėta 20 ml fosforo rūgšties.

Pusiausvyrinimo buferis: 125 mM of Tris-H3PO4 (pH 6,8), 40 % glicerolio, 3 % NDS.

1.1.5. Amfolitai

Servalyt (pH 2–11) (Serva), Pharmalyte (pH 5–8) (SigmaAldrich), Pharmalyte pH (4–6,5) (SigmaAldrich), Ampholyte aukštos rezoliucijos (pH 6–9) (Carl Roth), Ampholyte aukštos rezoliucijos (pH 3–10) (Carl Roth).

1.2. TYRIMO METODAI

1.2.1. Mielių kamienų transformacija

Prieš tai paminėtos plazmidės buvo naudotos transformuoti *S. cerevisiae* kamienus naudojant įprastą cheminės transfromacijos LiCl metodą (Sambrook ir Russell, 2001).

1.2.2. Ląstelių kultūrų auginimo ir temperatūrinės sąlygos

1.2.2.1. Mielių ląstelių, naudotų palyginamiesiems proteominiams eksperimentams, auginimo sąlygos

S. cerevisiae ląstelių kultūros buvo auginamos aeruojant 100 ml purtymui skirtose kolbose, 20 ml YEPD terpės su 5 mM formaldehido. TVH, CALR baltymų sintezė indukuota pakeičiant auginimo terpę į YEPG terpę su galaktoze. *S. cerevisiae* ląstelės transformuotos plazmidėmis su tymų viruso H ir N genais, žmogaus CALR genu ar tuščiu kontroliniu vektoriumi, buvo inokuliuotos į YEPD terpę su 5 mM formaldehido, augintos per naktį ir tuomet re-inokuliuotos į šviežią YEPD terpę su 5 mM formaldehido iki 0,05 OD_{600}. Ląstelių kultūros augintos 21 valandą iki terpės pakeitimo, ir dar 16–21 valandą po to, 30 °C purtant 220 rpm greičiu. Nucentrifūguotos ląstelės užšaldytos tolesniam saugojimui –70 °C.

1.2.2.2. Mielių ląstelių, naudotų TVH translokacijos gerinimo eksperimente, auginimo bei karščio šoko sąlygos

S. cerevisiae ląstelių kultūros buvo auginamos aeruojant 100 ml purtymui skirtose kolbose, 20 ml YEPD terpės su 5 mM formaldehido. TVH sintezė indukuota pakeičiant auginimo terpę į YEPG terpę su galaktoze. Karščio šokas, perkeliant ląsteles į 42 °C vandens vonią 2 min ir toliau auginant 37 °C purtyklėje 220 rpm greičiu iki TVH gamybos pabaigos, buvo taikytas skirtingais kultūros augimo momentais, prieš ir po TVH sintezės indukcijos. Manipuliacijų "37 °C–30 °C" atveju, kultyvavimas 37 °C po karščio šoko buvo vykdytas 3 valandas, ir tuomet kultūros perkeltos atgal į 30 °C iki TVH sintezės pabaigos. Bent viena kontrolė, kuomet ląstelės augintos standartinėje 30 °C temperatūroje, buvo įtraukta į visus nepriklausomus eksperimentus.

Augimo kreivės nustatymui, ląstelės sintetinančios TVH baltymą buvo auginamos nuo OD 0,05 30 °C purtant 220 rpm greičiu, 72 val. Kas 2 val buvo matuotas optinis tankis, bei imti mėginiai gliukozės bei etanolio koncncetracijoms nustatyti.

Tam, kad įvertinti karščio šoko įtaką TVH translokacijai skirtinguose ląstelių kultūros tankiuose, kultūroms buvo atliekamas karščio šokas, bei jos buvo perkeliamos į 37 °C penkios valandos iki indukcijos, bei augintos tokioje temperatūroje iki TVH sintezės pabaigos.

1.2.3. Kultūros terpės mėginių paruošimas ir NDS-PAGE.

Kultūros terpė sumaišyta lygiomis dalimis su 2×NDS-PAGE pavyzdžių buferiu ir virta 8–10 min. Paruošti mėginiai užnešti į 10 % NDS-PAGE gelio, po 16 µl į šulinėlį. Geliai fiksuoti 15 min fiksavimo tirpalu ir dažyti 25 min su Coomassie briliantinio mėlio R-250 tirpalu.

1.2.4. Mielių ląstelių lizatų mėginių paruošimas ir NDS-PAGE.

10–20 mg mielių ląstelių buvo nucentrifūguotos į 1,5 ml mėgintuvėlį. Ląstelės praplautos distiliuotu vandeniu ir suspenduotos 10 tūrių ardymo buferio. Ląstelės suardytos pridedant apytiksliai lygų tūrį stiklo rutuliukų (0,5 mm diametro) ir purtant maksimaliu greičiu 8 kartus po 30 s, bei atvėsinant ledo vonioje 30 s po kiekvieno ardymo. Pridėtas 2×NDS-PAGE pavyzdžių buferio tūris lygus naudotam ardymo buferio tūriui, ir mėginys virtas 10 min. 4 µl (iki 20 µg baltymų) paruošto grubaus ląstelių lizato mėginio buvo užnešta į 10 % NDS poliakrilamido gelį, tuomet leista NDS-PAGE buferyje, fiksuota ir dažyta taip pat, kaip minėta anksčiau.

1.2.5. Ląstelių mėginių paruošimas 2DE

300–500 mg ląstelių buvo nucentrifūguotos, išplautos, surinktos į stiklinį mėgintuvėlį bei užšaldytos –80 °C. Po saugojimo, ląstelės perkeltos į ledo vonią ir resuspenduotos 3–10 tūriuose (tūris/svoris) (priklausomai nuo eksperimento) denatūruojančio IEF buferio. Ląstelės lizuotos pridedant dvigubą tūrį stiklo rutuliukų, nei buvo naudota ląstelių, ir purtant maksimaliu greičiu 16 kartų po 30 s, po kiekvieno karto atvėsinant ląsteles 10 s ledo vonioje, bei 30 s ant stalo. Ląstelių nuolaužos buvo pašalintos centrifūguojant 16000×*g* greičiu, 15 min, 16 °C temperatūroje, bei persiurbiant nuskaidrintą lizatą į naują mėgituvėlį. Mėginių koncentracijos išmatuotos modifikuotu Bredfordo metodu (Roti-Nanoquant, Carl Roth GmbH), bei suvienodintos skiedžiant IEF buferiu. Mėginiai saugoti –80 °C.

Naudotas IEF buferis buvo tinkamas abiems 2DE metodams naudotiems šios disertacijos rezultatams gauti, atsižvelgiant į gamintojų rekomendacijas.

1.2.6. NEPHGE gelių tirpalų gaminimas

Kiekvienas amfolitų nešėjų (AN) mišinys buvo sukurtas su siauro ir plataus pH spektro amfolitais komerciškai prieinamais tuo metu, kurie sudarė nelinijinį pH gradientą. Mūsų atkurtą “Naujo mišinio” AN mišinį sudarė: Servalyt (pH 2–11) (Serva) – 1 dalis; Pharmalyte (pH 5–8) (SigmaAldrich) – 2 dalys; Pharmalyte (pH 4–6,5) (SigmaAldrich) – 3 dalys; Ampholyte aukštos rezoliucijos (pH 6–9) (Carl Roth) – 1 dalis; Ampholyte aukštos rezoliucijos (pH 3–10) (Carl Roth) – 1 dalis; viso 8 dalys. Šis AN mišinys buvo naudotas pagaminti du esminius NEPHGE gelių tirpalus – skirstantįjį ir “dangtelio” gelius, aprašytus (Klose ir Kobalz, 1995).

1.2.7. Pirmos krypties NEPHGE gelių užpylimas

Skirstantysis ir “dangtelio” geliai buvo užpilti vienas po kito vertikaliame įrenginyje skirtame užpilti dvisluoksnius vamzdelio formos gelius pirmos krypties baltymų atskyrimui. Skirstantysis gelis sudaro 2/3, o “dangtelio” gelis nuo 1/10 iki 1/20 stiklinio vamzdelio tūrio. Likusi dalis paliekama mėginio užnešimui. 8 cm ilgio IEF geliui (11 cm vamzdelio forma) užpilti reikia 500 µl skirstomojo gelio su 12 µl 0,8 % APS ir 100 µl “dangtelio” geliui su 2,5 µl 0,8 % APS (visi tirpalai prieš naudojimą degazuojami). Užpylus abu sluoksnius, pradinė “dangtelio” gelio polimerizacija vyksta paliekant gelius stingti 30 min kambario temperatūroje. Vėliau, gelio forma išimama iš stovo bei, kad gelis nedehidratuotų, uždedamas

lašas distiliuoto vandens vamzdelio viršuje, mėginio užnešimo pusėje bei vamzdelio formos galai apvyniojami vašku ir paliekami pilnai polimerizuotis 72 valandas kambario temperatūroje. WITA gamintojo geliai buvo pilami taip pat, tik naudojant komerciškai prieinamus standartizuotus gelių tirpalus.

1.2.8. Pirma 2DE kryptis

1.2.8.1. Pirmos krypties baltymų atskyrimas naudojant IPG juosteles

IPG juostelės (ZOOM juostelės (pH 3–10NL), Invitrogen) buvo naudotos IEF Invitrogen ZOOM IPGRunner sistemoje. 50 arba 100 µg baltymų iš grubaus mielių ląstelių lizato, buvo atskiesta iki 155 µl su IEF buferiu ir užnešta ant IPG juostelės rehidratacijai per naktį. Kitą dieną, ZOOM IPGRunner Mini-Cell Sistema buvo surinkta ir paleistas IEF naudojant "PowerEase 500 Power Supply" (Invitrogen) srovės šaltinį laikantis sąlygų: 200 V 20 min; 350 V 10 min; 500 V 4 val. Paskutinis žingsnis buvo aukštenio voltažo - 2000 V 2 val ("Consort EV233" aparatu), pagal gamintojo rekomendacijas. Sufokusuotos IPG juostelės buvo saugomos -80 °C. Juostelės buvo nupusiausvyrintos prieš pat antros krypties baltymų skirstymą, inkubuojant pusiausvyrinimo buferyje su redukuojančiais (75mM DTT) ir alkilinančiais (125 mM 2-jodoacetamidas (IAC)) reagentais (inkubuota abiejuose po 15 min).

1.2.8.2. Pirmos krypties baltymų atskyrimas naudojant NEPHGE vamzdelio formos gelius

Po pilnos polimerizacijos, pirmos krypties baltymų atskyrimas vamzdelio formos geliuose buvo vykdytas vertikaliame elektroforezės aparate (Klose ir Kobalz, 1995). Apatinė prietaiso talpa buvo užpildyta 400 ml degazuoto katodinio buferio. Vamzdeliai su geliais buvo įtaisyti aparate taip, kad jų galai būtų pasinėrę į katodinį buferį, ir tuomet pašalintas vandens kamštis. 80–200 µg ląstelių lizatų mėginių buvo sumaišyti su pašildytu (iki 50 °C) amfolitų fosfatiniu buferiu su agaroze, santykiu 4:1, bei nedelsiant užnešti į anodinę vamzdelių pusę nepaliekant oro burbulų. Ant mėginio viršaus papildomai užnešta po 10 µl mėginį stabilizuojančio užlajos tirpalo (O'Farrell *et al*., 1977) ir palikta sustingti 5–10 min. Po to, 400 ml degazuoto anodinio buferio supilta į viršutinę aparato talpą panardinant vamzdelius su geliais. Pirmos krypties elektroforezės leidimo sąlygos: 100 V 75 min; 200 V 75 min; 400 V 75 min; 600 V 75 min; 800 V 10 min; 1000 V 5 min. Pasibaigus elektroforezei, cilindro formos geliai buvo švelniai išstumti iš vamzdelių į plastikinius lovelius, švirkšto pagalba. Tuomet geliai buvo paruošti antros

kryptiems atskyrimui inkubuojant tris kartus po 15 min pusiausvyrinimo buferyje su 75 mM DTT, bei tris kartus po 15 min tame pačiame buferyje su 125 mM IAC. Nupusiausvyrinti geliai buvo saugomi –80 °C iki antros krypties leidimo.

1.2.9. Antros krypties baltymų atskyrimas NDS-PAGE

Baltymai antroje kryptyje buvo atskirti standartine NDS-PAGE elektroforeze, 11 % arba 12 % (svoris/tūris) poliakrilamido geliuose naudojant Minigel-Twin aparatus (Biometra). IPG juostelės arba NEPHGE cilindro formos geliai buvo švelniai perkelti iš saugojimo lovelių ant koncentruojančio poliakrilamidinio gelio viršaus ir užlieti 0,5 % (svoris/tūris) išlydytos agarozės tirpalu. Sustingus agarozei, antros krypties baltymų skirstymas vykdytas sąlygomis: 15 mA geliui (~100 V) ~ 15 min (kol dažas pasiekia skirstomąjį gelį); 30 mA geliui (įtampa palaipsniui užkyla iki 200 V limito) maždaug 1 val, arba kol Bromofenolio dažas pasiekia gelio apačią ir išeina į buferį.
NDS-PAGE geliai buvo fiksuojami 1 val švelniai siūbuojant kambario temperatūroje bei nudažyti Kumasi mėliu R-250 per naktį siūbuojant kambario temperatūroje. Kitą dieną, geliai buvo paveikti dažą išimančiu tirpalu siūbuojant 1 val, bei toliau inkubuojami saugojimo tirpale jį periodiškai pakeičiant iki kol dažas išsiplaus iš gelio.

1.2.10. Gelių skenavimas ir vaizdų analizė

1.2.10.1. Vienos krypties NDS-PAGE ir Vestern baltymų hibridizavimo membranų vaizdinė analizė

Visi vienkrypčiai geliai buvo skenuoti ImageSanner III (GE Healthcare) skeneriu naudojant tuščią filtrą, permatomu režimu bei 300 dpi rezoliucija. Densitometrinė vienkrypčių gelių analizė buvo atlikta ImageQuant TL (GE Healthcare) programa su standartiniais nustatymais.
Baltymų juostelių intensyvumo reikšmės buvo normalizuotos pagal atitinkamą užnešimo kontrolės (GAPDH) arba kontrolės (30 °C) juostelių intensyvumą Vestern baltymų membranose.
Norint įvertinti TVH glikobaltymo kiekį translokacijos eksperimente, dviejų ~75 kDa juostelių, atitinkančių glikozilintą TVH baltymą (taškuotos rodyklės 3 Paveiksle), tūriai buvo susumuoti. Didžioji ~65 kDa juostelė nebuvo įtraukta į skaičiavimus, nes ji atstovauja neperkeltą į ET, neglikozilintą TVH pirmtaką lokalizuotą citozolyje (Ciplys *et al.,* 2011). Glikozilinto TVH tūriai, visuose analizuotuose variantuose buvo palyginti su kontrolinių mėginių, gautų iš ląstelių pastoviai augintų 30 °C, tūriais. Kadangi TVH glikobaltymo ir

neglikozilinto pirmtako santykis keitėsi tirtose skirtingose sąlygose, mes taip pat paskaičiavome translokacijos efektyvumą. Jis pateiktas glikozilinto TVH procentais, nuo viso TVH aptikto tame pačiame mėginyje.

1.2.10.2. 2DE gelių analizė

Visi dvikrypčiai geliai buvo skenuoti ImageSanner III (GE Healthcare) skeneriu naudojant tuščią filtrą, permatomu režimu bei 300 dpi rezoliucija. Gelių, užpiltų su mūsų "Nauju mišiniu" ir "WITA" komerciniais tirpalais, vaizdai buvo analizuoti BioRad PDQuest 8.0.1 2-D analizės programa pagal gamintojo rekomendacijas. Lyginant visus gelius vieną su kitu, buvo paskaičiuotas koreliacijos koeficientas (r). Pirsono koreliacijos koeficientas matuoja linijinę dviejų kintamųjų asocijaciją, ir kinta nuo –1 iki +1, o r=1 reiškia stiprią linijinę asocijaciją (Kirch, 2008).
Visi kiti dvikrypčių gelių vaizdai buvo analizuoti ImageMaster 2D Platinum 7.0 programa (GE Healthcare). Baltymų taškai buvo aptikti automatiškai naudojant tuos pačius parametrus visiems geliams. Artefaktiniai taškai, bei dulkės (dažniausiai prie gelių kraštų) buvo rankiniu būdu pašalintos iš kiekvieno gelio. Tuomet buvo vykdyta palyginamoji gelių vaizdų analizė, bei geliai lyginti tarpusavyje atskirose grupėse ir tarp grupių. Skirtinga ląstelinių baltymų sintezė buvo įvertinta suskaičiuojant kiekio pokytį – to paties taško tūrio, išreikšto procentais, pokytis kartais tarp gelių. Mūsų pasirinkta slenkstinė pokyčio riba buvo 1,5 karto (0,58 log2FC) – visuose eksperimentuose buvo laikoma, jog baltymų taškų, kurių tūris gelyje padidėjo arba sumažėjo 1,5 karto, sintezė skiriasi.

1.2.11. Baltymų nustatymas

Baltymų nustatymas MALDI-TOF/TOF ir LC-MS^E metodais buvo atliktas, Biochemijos instituto Proteomikos centre (Gyvybės mokslų centras, Vilniaus universitetas, Vilnius, Lietuva).

1.2.11.1. Mėginio paruošimas ir baltymų nustatymas MALDI-TOF/TOF masių spektrometrijos metodu

Iš gelio išpjauti baltymų taškai minimi skyriuose 2.1. ir 2.2. buvo identifikuoti naudojant tripsino – peptidų masių pirštų antspaudų metodą (Hellman *et al.*, 1995). Baltymų taškai buvo išpjauti iš gelio ir susmulkinti 1×1 mm gabalėliais. Gelio gabalėliai buvo nublukinti 200 µl 25 mM amonio bikarbonato 50 % acetonitrilo (ACN) tirpale, dehidratuoti ACN ir inkubuoti su 40 µl 10 ng/µl tripsino tirpalo 25 mM amonio bikarbonate per naktį 37 °C

temperatūroje. Kitą dieną, peptidai ekstrahuoti su 2 × 100 µl 5 % trifluoracto rūgštimi (TFR), liofilizuoti ir ištirpinti 3 µl 0,1 % TFR, 50 % ACN tirpale. Mėginiai buvo užnešti ant 384 šulinėlių MALDI plokštelės. 0,5 µl mėginio buvo užlieti 0,5 µl matrikso (alpha-ciano-4-hidroksicinnamono rūgštis, 4 mg/ml 50 % ACN su 0,1 % TFR).

Baltymai buvo identifikuoti matriksu asistuotos lazerinės desorbcijos/jonizacijos (MALDI) masių spektrometrija, naudojant 4800 MALDI TOF/TOF masių spektrometrą (AB/Sciex). Peptidų masių spektrai buvo gauti reflektoriaus teigiamų jonų režimu, 800–4000 Da m/z diapazone, 400 lazerio šūvių buvo susumuoti kiekvienam mėginiui su ±50 ppm masės tikslumu. MS/MS spektrai dominuojantiems peptidams buvo gauti pozityviame režime, bei jonų susidūrimų energija buvo nustatyta iki 1 keV, 500 lazerio šūvių buvo surinkta kiekvienam spektrui su ±0,1 Da masės tikslumu. Baltymai nustatyti TrEMBL duombazėje (3-23-10 laidos) naudojant Mascot algoritmą.

1.2.11.2. Mėginio paruošimas ir baltymų nustatymas LC-MS^E metodu, nuo duomenų nepriklausomos analizės (angl., Data-Independent Aquisition, DIA) režimu

Baltymų taškai išpjauti iš gelių, tačiau identifikuoti LC-MS^E (Skyrius 2.4.) buvo paruošti pagal (Shevchenko *et al.*, 2006).
Visos mielių proteomos mėginiai buvo suskaldyti tripsinu pagal FASP protokolą aprašytą (Wiśniewski *et al*., 2009). Mėginiai buvo atskiesti 8 M šlapalu, tada du kartus praplauti šlapalu ir alkilinti 50 mM jodoacetamidu (GE Healthcare Life Sciences). Baltymų koncentratoriai buvo du kartus išplauti šlapalu ir du kartus su 50 mM NH_4HCO_3. Baltymai skaldyti TPCK tripsinu 20233 (Thermo Scientific) per naktį. Po to, peptidai surinkti iš koncentratorių centrifūguojant 14000 ×*g* 10 min ir papildomai eliuoti 20 % CH_3CN. Eliucijos frakcijos sumaišytos, nurūgštintos 10 % CF_3COOH ir liofilizuotos vakuminėje centrifūgoje. Liofilizuoti peptidai ištirpinti 0,1 % skruzdžių rūgštyje.

Skysčių chromatografija (SC) buvo atlikta naudojant Waters Acquity itin aukšto našumo SC sistema (Waters Corporation). Peptidų atskyrimui buvo naudota ACQUITY UPLC HSS T3 250 mm analitinė kolonėlė. Duomenys buvo gauti naudojant Synapt G2 masių spektrometrą ir Masslynx 4.1 programinę įrangą (Waters Corporation) pozityvių jonų režime naudojant nuo duomenų nepriklausomą įgijimą (*angl., Data-Independent Aquisition (DIA)*), susietą su jonų judrumo atskyrimu (*angl., ion mobility separation, IMS, UDMSE*) (Distler *et al*., 2014). Žvalgomąjam nuskaitymui, masės rėžiai buvo

50–2,000 Da, su 0,8 s nuskaitymo laiku. Neapdoroti duomenys yra prieinami MassIVE saugykloje, identifikacinis kodas MSV000088879. Jie taip pat buvo visuotinai pakoreguoti naudojant dvigubai įkrautą [Glu1]-fibrinopeptido B (m/z 785.8426; $[M^{+2H}]^{2+}$) joną ir 0,25 Da tolerancijos langą. Neapdoroti duomenys buvo apdirbti ProteinLynx Global SERVER (PLGS) versija 3.0.1 (Waters Corporation, UK) Apex3D ir Pep3D algoritmais, norint sugeneruoti pirmtakų masių sąrašus ir asocijuotų jonų produktų masių sąrašus tolesnei baltymų identifikacijai ir kiekybiniam įvertinimui. Smailių sąrašai buvo sugeneruoti naudojant šiuos parametrus: (i) žemos energijos slenkstis buvo nustatytas iki 150 skaičiavimų, (ii) pakeltos energijos slenkstis buvo 50 skaičiavimų, (iii) intensyvumo slenkstis buvo nustatytas iki 750 skaičiavimų. Paieška duomenų bazėse buvo vykdyta PLGS paieškos varikliu naudojant automatinę peptidų ir fragmentų toleranciją, minimaliai 1 fragmentų jonų atitikmenį per peptidą, bei 3 per baltymą, klaidingų atradimų rodiklis (*angl., False Discovery Rate, FDR*) < 4%. Kaip karpanti proteazė buvo naudotas tripsinas, buvo toleruojama vieno praleisto kirpimo klaidų darymo riba. Cisteinų karbamidometilinimas buvo nustatytas, kaip fiksuota modifikacija, o metioninų oksidacija, buvo nustatyta, kaip variabili modifikacija. Baltymų nustatymui buvo naudotos UniprotKB/SwissProt *S. cerevisiae* duombazės (2020-09-24) su jaučio tripsinu (TRY1_BOVIN). Kiekybinis baltymų be etikečių (*angl., label-free*) nustatymas buvo vykdytas naudojant TOP3 metodą. TOP3 intensyvumas buvo apskaičiuotas, kaip vidutinis trijų geriausiai besijonizuojančių peptidų vidurkis, naudojant ISOQuant (Kuharev *et al*., 2015). Maksimalus nustatytas baltymų nustatymo klaidingų atradimų vidurkis (*angl., FDR*) buvo 1%. Prieš skaičiuojant baltymų raiškos pokytį kartais, duomenys buvo Log2 transformuoti. Baltymų raiškos pokyčio log2 bei p-reikšmės buvo apskaičiuotos naudojant Bayes algoritmą iš limma Bioconductor paketo. Suskaičiuotos p-reikšmės yra Benjamini-Hochberg procedūra pakoreguoti klaidingų atradimų vidurkiai.

2. REZULTATAI IR JŲ APTARIMAS

Šio darbo rezultatai pristatomi keturiuose atskiruose skyriuose pagal atlikto darbo eiliškumą. Pirmame skyriuje pristatomas IPG ir NEPHGE pirmos krypties baltymų atskyrimo technikų palyginimas dvikryptės elektroforezės eksperimente tiriant UPR-Cyto ląstelinį atsaką sukeltą TVH baltymo gamybos mielėse *S. cerevisiae*. Sekančiame skyriuje, aprašomas karščio šoko poveikis TVH baltymo translokacijai. Trečiajame skyriuje supažindinama su AN mišinio, bei gelių tirpalų skirtų NEPHGE 2DE atkūrimo rezultatais, o ketvirtajame skyriuje bus pristatomi žmogaus CALR baltymo aukšto lygio sekrecijos, palyginamosios proteominės analizės rezultatai.

2.1. IPG ir NEPHGE pirmos krypties baltymų atskyrimo technikų palyginimas dvikryptės elektroforezės eksperimente tiriant UPR-Cyto ląstelinį atsaką sukeltą TVH baltymo sintezės *S. cerevisiae* mielėse

Šio tyrimo tikslas buvo tiesiogiai palyginti IPG ir NEPHGE pirmos krypties baltymų atskyrimo technikas 2DE, naudojant tuos pačius mėginius bei identiškas antros krypties leidimo sąlygas. Pirmos krypties atskyrimui IPG juostelėmis, mes pasirinkome Invitrogen "ZOOM IPGRunner" sistemą. Ši mini gelio 2DE sistema pasižymi paprastumu, nedidele kaina, o IEF gelio ilgis (7 cm), bei pavyzdžių buferis suderinami su "WITAvision" NEPHGE 2DE sistema. Yra žinoma, kad komerciškai prieinamų IPG juostelių baltymų atskyrimo rezoliucija gali ženkliai skirtis, priklausomai nuo gamintojo (Taylor ir Coorssen, 2006). Reiktų pabrėžti, jog mūsų rezultatai reprezentuoja tik Invitrogen IPG 2DE juosteles.

Anksčiau atlikti IPG ir NEPHGE technikų palyginimai, buvo atlikti analizuojant ištisas proteomas (Nawrocki *et al*., 1998; Nowalk *et al*., 2006). Šiame darbe, mes atlikome skirtingos baltymų sintezės proteominį tyrimą, naudodami abejas IEF technikas plačiame (pH 3–10) pH diapazone, tiriant UPR-Cyto ląstelinio streso atsaką *S. cerevisiae* mielėse. Gauti rezultatai buvo palyginti su mūsų ankstesnio, to paties fenomeno, tyrimo rezultatais gautais naudojant Invitrogen siauro pH diapazono (pH 4–7) IPG juosteles (Ciplys *et al*., 2011). Mūsų rezultatai rodo, jog NEPHGE 2DE metodas yra tinkamesnis metodas bazinių baltymų analizei bei ryškiausias to įrodymas, yra stipriai bazinio baltymo Sis1p kiekio pokyčio nustatymas NEPHGE 2DE, bet ne IPG 2DE. Rūgštiniame pH diapazone abi šios technikos pasirodė lygiavertės su kai kuriais specifiniais privalumais bei trūkumais. Mes tikimės, jog šis mūsų atliktas tyrimas leis kitiems mokslininkams lengviau pasirinkti tinkamiausią 2DE sistemą proteominiams eksperimentams.

Pastaba: IPG 2DE buvo atlikta E. Čiplio; gelių analizę atliko R. Slibinskas; statistinę analizę atliko R. Ražanskas; NEPHGE 2DE atliko disertacijos autorė.

2.1.1. Protokolų apžvalga

Tie patys ląstelių lizatų mėginiai iš mielių gaminančių TVH arba TVN baltymus, bei kontrolinių ląstelių (transformuotų tuščiu pFGG3 vektoriumi), buvo sufokusuoti plačiame pH diapazone (pH 3–10) IPG (Invitrogen) juostelėse bei NEPHGE pirmos krypties geliuose, užpiltuose pagal gamintojo (WITA) rekomendacijas. Po nupusiausvyrinimo, juostelės bei vamzdelio formos geliai buvo perkelti ant NDS-PAGE antros krypties gelių ir leisti identiškomis sąlygomis "Biometra" sistemoje. Antros krypties NDS-PAGE su tolesniais gelių dažymo, skenavimo bei vaizdų analizės žingsniais, buvo vykdyta identiškai. Todėl, pagrindinis skirtumas tarp IPG ir NEPHGE pagrįstos 2DE, buvo pirmos krypties izoelektrinis fokusavimas, bei šiek tiek skirtingas pusiausvyrinimo protokolas (IPG juostelės buvo nupusiausvyrintos po, o NEPHGE geliai prieš, šaldymą –70 °C). Tai leido tiesiogiai palyginti pirmos krypties IPG ir NEPHGE technikas, nes visi kiti parametrai, sąlygos bei mėginiai buvo vienodi abiejuose eksperimentuose.

2D gelių vaizdų pavyzdžiai pademonstruoti paveiksluose 1 ir 2, o bendra kiekybinė IPG ir NEPHGE metodais atskirtų baltymų analizė bei šių duomenų bandomasis palyginimas su konkrečiu biologiniu eksperimentu (Ciplys *et al*., 2011) apibendrintas 1 lentelėje.

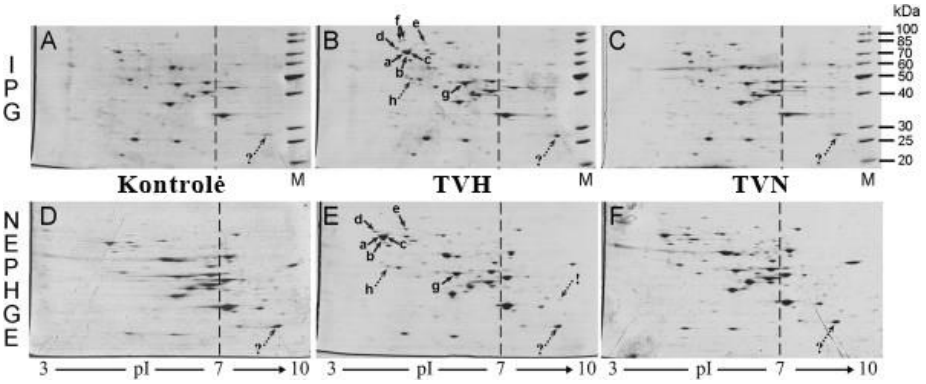

1. Paveikslas Mielių lizatų 2DE naudojant IPG (A-C) ir NEPHGE (D-F) technikas, užnešus standartinį baltymų kiekį. Mielių ląstelių lizatų, transformuotų kontroliniu tuščiu vektoriumi, bei gaminančių TVH ir TVN baltymus, mėginiai buvo užnešti ant IPG juostelių (50 µg baltymų kiekvienai juostelei) ir NEPHGE gelių (30 µg baltymų kiekvienam geliui). Apytikslės pI reikšmės sužymėtos paveikslo apačioje (pH 3–10 gradientas naudotas abiem atvejais).

Brūkšniuotos linijos žymi apytikslę neutralaus pI 7,0 ribą, kuri atskiria rūgštinius (kairėje pusėje pI < 7) ir bazinius (dešinėje pusėje, pI > 7) baltymų taškus. Baltymų molekulinio svorio standartai (M) užnešti į IPG 2DE gelius, jų masės pažymėtos dešinėje paveikslo pusėje (kDa). Rodyklės rodo į baltymų taškus aprašytus 8 lentelėje. Vientisos rodyklės žymi taškus identifikuotus mūsų ankstesniame darbe (Ciplys *et al*., 2011), tuo tarpu punktyrinės rodyklės žymi taškus identifikuotus MS šiame darbe. Kiekybinė kiekvieno pažymėto taško analizė pateikta 1 lentelėje.

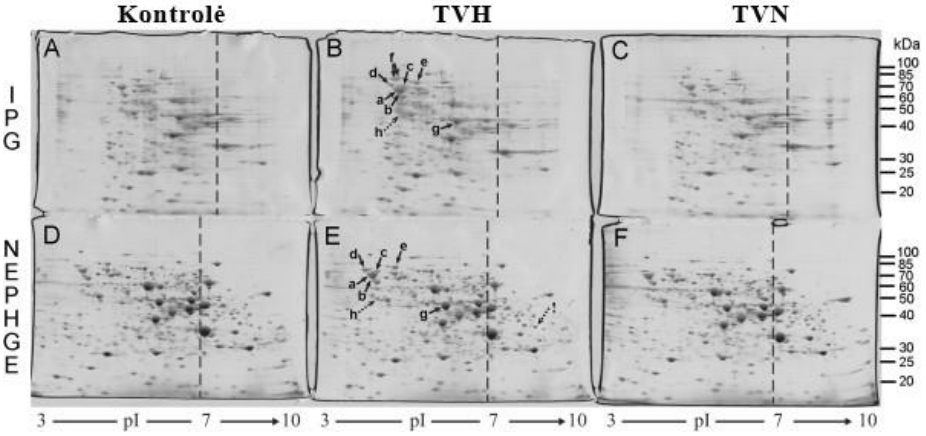

2. Paveikslas. Mielių lizatų 2DE naudojant IPG (A-C) ir NEPHGE (D-F) technikas, užnešus dvigubą baltymų kiekį. Mielių ląstelių lizatų, transformuotų kontroliniu tuščiu vektoriumi, bei gaminančių TVH ir TVN baltymus, mėginiai buvo užnešti ant IPG juostelių (100 µg baltymų kiekvienai juostelei) ir NEPHGE gelių (100 µg baltymų kiekvienam geliui). Paveiksle pateikiamas originalus vienos visų variantų replikos vaizdas (visi geliai skenuoti paraleliai tuo pačiu metu). Legenda tokia pati, kaip 1 Paveiksle.

1 Lentelė. Kiekybinė skirtinga sinteze pasižymėjusių baltymų analizė 2DE metodu, naudojant plataus (pH 3–10) (šis darbas) bei siauro (pH 4–7) (ankstesnis darbas (Ciplys *et al*., 2011)) diapazono 2DE platformas.

Nr.[1]	Nr.[2]		IPG 4–7[4]	IPG 3–10[5]		NEPHGE 3–10[6]	
				Standartinis[5]	Dvigubas[5]	Standartinis[5]	Dvigubas[5]
a	1	SSA1/2	2.4 ± 0.2	1,6 ± 0,1	1,6 ± 0,4	2,6 ± 0,3	2,0 ± 0,2
b	2	SSA1/2					
c	3	SSA4					
d	4	KAR2	3.8 ± 0.4	2,7 ± 0,5	1,8 ± 0,4	9,0 ± 3,1	2,5 ± 0,2
e	5	SSE1	2.3 ± 0.2	1,4 ± 0,3	1,8 ± 0,7	2,2 ± 0,8	1,7 ± 0,1
f	6	HSC82	2.1 ± 0.3	2,0 ± 0,2	2,1 ± 1,0	- -	- -
g	6	HSP82					
	7	ENO2	1.5 ± 0.2	1,4 ± 0,3	1,1 ± 0,2	1,3 ± 0,2	1,1 ± 0,1
h	N.I.[7]	SSA1/2[7]	2.2 ± 0.3	1,5 ± 0,1	1,1 ± 0,1	1,6 ± 0,3	2,1 ± 0,4
?[8]	N.A.	GPM1	N.A.	2,2 ± 1,3	0,7 ± 0,2	1,3 ± 0,3	1,0 ± 0,1
![8]	N.A.	SIS1	N.A.	- -	- -	2,6 ± 0,4	2,2 ± 0,2

[1] Raidės žymi baltymus pasižymėjusius skirtinga sinteze šiame eksperimente (Paveikslai 1 ir 2).

[2]Tie patys baltymų taškai sužymėti skaičiais ankstesniame darbe (Ciplys *et al*., 2011).

[3]Baltymo pavadinimas iš *Saccharomyces* genomo (SGD) bei mielių baltymų (YPD) duombazių. Taškai 1 ir 2 žymi panašių baltymų Ssa1 ir Ssa2 (97% identiškumas) mišinį, nežinomu santykiu (žiūrėti (Ciplys *et al*., 2011)).

[4]Ląstelinių baltymų skirtingos raiškos pokytis kartais TVH gaminančiose bei kontrolinėse ląstelėse, nustaytas ankstesnio tyrimo metu naudojant pH4–7 IPG 2DE sistemą (Invitrogen) (Ciplys *et al*., 2011).

[5]Tų pačių baltymų baltymų sintezės pokytis kartais, nustatytas iš nepriklausomų eksperimentų atliktų šiame darbe naudojant pH3–10 IPG juosteles (Invitrogen); ~50 µg mielių ląstelių lizato baltymų buvo užnešta ant IPG juostelių standartinio eksperimento metu, bei ~100µg buvo užnešta dvigubo eksperimento metu.

[6]Tų pačių baltymų sintezės pokytis kartais, nustatytas iš nepriklausomų eksperimentų atliktų šiame darbe naudojant pH3–10 NEPHGE pirmos krypties gelius (WITAvision); ~30 µg mielių ląstelių lizato baltymų buvo užnešta ant NEPHGE gelių standartinio eksperimento metu, bei ~100 µg buvo užnešta dvigubo eksperimento metu.

[7]Neidentifikuotas (N.I.) taškas praeito eksperimento metu, nes padidintas šio baltymo kiekis buvo rastas tik ląstelėse gaminančiose TVH, bet ne TVN baltymą (biosintezės pokytis kartais TVH/kontrolinėse ląstelėse nustatytas IPG4–7 sistema, čia pateikiamas iš nepublikuotų duomenų).

[8]? ir ! žymi bazinius baltymų taškus (pI > 7), kurie nebuvo analizuoti ankstesnio eksperimento metu pH4–7 platforma (N.A. – neištirtas). Nepriklausomai nuo to, taškas "?" rodė netikrą raiškos pokytį ("artefaktą") IPG sistemoje (nepatikimi sintezės pokyčiai matomi dėl didelio klaidų diapazono), šiame tyrime jis identifikuotas, kaip fosfoglicerato mutazė 1 (Gpm1p). Baltymas Sis1p šiame darbe identifikuotas naudojant NEPHGE 2DE sistemą, bei nebuvo aptiktas naudojant IPG 2DE metodą.

2.1.2. Baltymų taškų atsikartojamumas

Palyginamojo proteominio 2DE pagrįsto eksperimento metu geliai buvo dažomi Kumasi mėliu, kuris nepasižymi aukšta skiriamąja geba, todėl kai standartinio eksperimento metu užnešėme po 50 μg baltymų ant IPG juostelių (pagal gamintojo rekomendacijas), bei po 30 μg baltymų ant NEPHGE gelių (dėl mėginio užnešimo tūrio apribojimų) mums pavyko išskirti tik apie 100 baltymų taškų gelyje (žiūrėti 1 Paveikslą). Kadangi šis rezultatas neleido kokybiškai įvertinti pokyčių ląstelės proteomoje, eksperimentą pakartojome užnešant dvigubą baltymų kiekį (~100 μg). Atskirtų baltymų kiekis geliuose ženkliai padidėjo – aptikome apie 400 baltymų taškų IPG 2DE geliuose, bei apie 500 taškų NEPHGE 2DE geliuose (žiūrėti 2 Paveikslą).

Užneštų ir aptiktų baltymų taškų palyginimas atskleidė, jog IPG 2DE geliuose matomas 1/3 baltymų praradimas. IPG atveju prarandami daugiausiai baziniai baltymai. Ir nors rūgštinių baltymų kiekis yra panašus IPG ir NEPHGE variantuose, NEPHGE 2DE geliuose aptinkama dvigubai daugiau bazinių baltymų.

IPG metodas taip pat nepasižymi duomenų atsikartojamumu – skirtinguose eksperimentuose yra pametami skirtingi baltymai, bei tik pusė bazinių baltymų (~44 % standartinio, bei ~51 % dvigubo kiekio eksperimentuose) atsikartoja. Taigi apibendrinus, IPG metodu galima kiekybiškai įvertinti tik ~50 % baltymų. Tuo tarpu, NEPHGE metodas pasižymi beveik 90 % atsikartojamumu bazinėje pusėje. Rūgštinėje gradiento pusėje standartinio kiekio eksperimente IPG metodas pasirodė geriau – atsikartojo >80 % baltymų, tačiau padidinto baltymų kiekio eksperimente, NEPHGE metodas efektyviai atskyrė baltymus ir rūgštinėje pusėje, kas padidino jo bendrą baltymų taškų atsikartojamumą iki ~87 %, lyginant su ~68 % IPG 2DE. Taip pat, prastas baltymų taškų fokusas IPG gelių rūgštinėje pusėje rodo, jog IPG juostelės galimai buvo perkrautos.

2.1.3. Baltymų taškų kokybė bei pirmos krypties gelių talpa

Visų analizuotų 2DE gelių baltymų taškų kokybė buvo įvertinta atsižvelgiant į jų formą, bei išlenktumą naudojantis vaizdų analizės programa ImageMaster 2D Platinum 7.0 (GE Healthcare). Standartinio eksperimento metu, IPG 2DE geliai pasižymėjo geresnės kokybės taškais rūgštinėje pusėje, o NEPHGE 2DE – bazinėje pusėje. Užnešus padidintą baltymų kiekį, šis rezultatas drastiškai pasikeitė, nes IPG 2DE geliuose ženkliai padidėjo prastos kokybės baltymų taškų, o NEPHGE 2DE geliuose baltymų taškų bendra kokybė pakilo. Tai dar kartą patvirtina, jog IPG geliai yra perkraunami užnešus padidintą baltymų kiekį. Tuo tarpu, naudojant NEPHGE 2DE metodą, 100 μg užneštų baltymų kiekis yra beveik optimalus patikimam aukštos kokybės taškų atskyrimui. Atsižvelgiant į IPG juostelių ir NEPHGE gelių tūrius, galima teigti, jog NEPHGE geliai turi ~5 kartus didesnę baltymų talpą.

2.1.4. Bendras IPG ir NEPHGE pagrįstų 2DE metodų palyginimas

Atsižvelgiant į visus gautus duomenis, NEPHGE pagrįstas 2DE metodas atrodo pranašesnis sudėtingų baltymų mišinių analizei plačiame pH diapazone (pH 3–10). IPG pagrįsta 2DE yra pranašesnė atskiriant nedidelį kiekį baltymų rūgštinėje pusėje, tačiau prastai atskiria bazinius baltymus. Akivaizdu, kad atliekant IPG 2DE su standartiniu baltymų kiekiu, atskirtų baltymų skaičius yra per žemas, norint tyrinėti sudėtingus baltymų mišinius, o užnešus padidintą kiekį IPG juostelės perkraunamos, prarandama dalis baltymų, bei suprastėja baltymų taškų kokybė. Tuo tarpu, NEPHGE metodas geriau atskiria ne tik bazinius baltymus užnešus nedidelį jų kiekį, bet ir yra visokeriopai pranašesnis analizuojant didesnį baltymų kiekį dėl žymiai didesnės baltymų talpos, bei geresnės baltymų taškų rezoliucijos. Šie duomenys leidžia teigti, jog NEPHGE pagrįsta 2DE yra labiau tinkamas metodas mielių proteomos analizei. Ryškiausias to pavyzdys yra, jog NEPHGE pagrįsta 2DE atskleidė pasikartojančią ir statistiškai reikšmingą, smarkiai bazinio bei labai negausaus baltymo Sis1p, dalyvaujančio UPR-Cyto atsake skirtingą sintezės lygį, o IPG pagrįsta 2DE analizė to nesugebėjo. Akivaizdu, kad tokių sudėtingų baltymų mėginių, kaip proteomos, analizei, yra būtinas jautrus metodas pasižymintis atsikartojamumu tam, kad suteiktų kuo daugiau vizualinės informacijos apie visus ląstelinius baltymus. Mūsų rezultatai rodo, jog NEPHGE pagrįsta 2DE ir yra tam tinkamas metodas.

2.2. Karščio šokas esant didesniam ląstelių kultūros tankiui pagerina tymų viruso hemagliutinino baltymo translokaciją *S. cerevisiae*

Nors *S. cerevisiae* mielės yra plačiai naudojamos rekombinantinių baltymų gamybai bei sugeba atlikti potransliacines baltymų modifikacijas, tačiau žmogaus virusų paviršinių glikoproteinų bei kitų sudėtingų žinduolių baltymų sintezė šiame modeliniame organizme vis dar yra labai apsunkinta. Ankstesniais tyrimais buvo parodyta, kad aktyvaus TVH baltymo gamyba mielėse *S. cerevisiae* yra neefektyvi dėl butelio kaklelio efekto baltymo pirmtakų translokacijoje į ET, bei UPR-Cyto atsako indukcijos. UPR-Cyto ląstelinis streso atsakas indukuoja baltymų susijusiu su karščio šoko atsaku, sintezę (Ciplys *et al*., 2011). Temperatūra reguliuojamų šaperonų aktyvavimas siūlo, kad pati kultūros auginimo temperatūra gali turėti įtakos rekombinantinių baltymų gamybai. Aplinkos pokyčiai, tokie, kaip temperatūra, maisto medžiagos, oksidacija, pH bei osmoliariškumas, įprastai indukuoja drastiškus daugelio mielių genų raiškos pokyčius (Causton *et al*., 2001). Potencialiai, bet kurios iš šių sąlygų gali būti panaudotos įtakoti rekombinantinio baltymo biosintezę. Šio darbo tikslas buvo pagerinti TVH translokaciją *S. cerevisiae* mielėse, keičiant kultūros augimo sąlygas.

Rekombinantinis TVH yra patogus modelis translokacijos į mielių ET efektyvumui įvertinti. Sintetinamas mielėse, šis baltymas randamas neglikozilinto pirmtako (~65 kDa), bei N glikozilinto TVH baltymo (~75 kDa) formose, kurias lengva atskirti Vestern baltymų hibridizacijos metodu. Neglikozilinti TVH pirmtakai yra lokalizuoti citozolyje, kur kartu su citozoliniais mielių baltymais formuoja netirpius agregatus (Ciplys *et al*., 2011), tuo tarpu glikozilintas TVH baltymas atstovauja baltymą translokuotą į ET (Čiplys *et al*., 2011). Tokiu būdu, TVH glikobaltymo kiekis rodo translokacijos apkrovą, o N-glikozilinto TVH santykis su visu TVH baltymo kiekiu, rodo translokacijos efektyvumą.

Šiame darbe mes tyrėme karščio šoko bei ląstelių kultūros tankio įtaką rekombinantinio TVH translokacijai. Karščio šoko taikymas didesnio tankio ląstelių kultūrai, su tolesne baltymo biosinteze 37 °C, pagerino tiek translokacijos efektyvumą, tiek TVH glikobaltymo kiekį 3 kartus. Toliau sekė NEPHGE pagrįsta 2DE analizė siekiant identifikuoti gausius ląstelinius baltymus, kurių sintezės pokyčiai koreliuoja su pagerėjusia TVH translokacija į ET. Tolesniam rekombinantinių baltymų gamybos mielėse gerinimui, identifikuoti 15 ląstelinių baltymų-taikinių

2.2.1. Karščio šoko bei ląstelių kultūros tankio įtaka rekombinantinio TVH baltymo translokacijai į mielių ET

Šiame darbe naudota galaktoze indukuojama raiškos sistema suteikia platų langą pasirinkti karščio šoko taikymo laiką, bei trukmę. Mes taikėme

karščio šoką įvairiais laiko momentais prieš rekombinantio baltymo sintezės indukciją, o tuomet perkeldavome ląstelių kultūrą į 37 °C tolesniam auginimui. Didžiausią glikozilinto TVH kiekio padidėjimą nustatėme, kuomet karščio šoką atlikome 5 valandos iki TVH sintezės indukcijos, bei toliau ląsteles auginome 37 °C. Tokios sąlygos padidino glikozilinto, į ET translokuoto TVH kiekį 3 kartus, lyginant su kontrolinėmis ląstelėmis nuolatos augintomis 30 °C. Kitos karščio šoko taikymo sąlygos parodė silpnesnį efektą, o mielių ląstelių perkėlimas į 20 °C, vietoje 37 °C, sumažino glikozilinto TVH kiekį 4-5 kartus. Duomenų apie aukštesnių temperatūrų įtaką rekombinantinių baltymų sintezei yra labai mažai, tačiau buvo parodyta, kad pakelta temperatūra padidino hipertermofilinio fermento kiekį iki 440 % *S. cerevisiae* ląstelėse (Smith *et al.,* 2005). Mes manome, kad teigiamas karščio šoko efektas rekombinantinių baltymų gamybai nebuvo pastebėtas, nes tyrimai daugumoje buvo atliekami ankstyvojoje ar vidurinėje logaritminio augimo fazėse, kuriose glikozilinto TVH kiekis taip pat nepadidėjo.

Temperatūrinių eksperimentų metu mes pastebėjome, kad glikozilinto TVH kiekio padidėjimui įtakos turi ne tik karščio šokas, bet ir tai kokiame ląstelių kultūros tankyje jis buvo taikytas. Šis pastebėjimas atskleidė, jog ne tik karščio šoko taikymo trukmė, bet ir mielių kultūros augimo fazė gali turėti įtakos translokacijos efektyvumui.

Tam, kad nustatyti mūsų naudojamų mielių kamieno augimo fazes, mes išmatavome kultūros optinį tankį, gliukozės bei etanolio koncentracijas bei sudarėme augimo kreives. Tuomet įvairiose kultūros augimo fazėse taikėme anksčiau atrinktas karščio šoko sąlygas, ir radome, kad karščio šokas pagerina TVH translokaciją didesnio tankio kultūrose. Santykinis glikozilinto TVH kiekis padidėjo 3 kartus, kuomet karščio šokas buvo taikytas vėlyvosiose gliukozės ir etanolio fazėse.

Glikozilinto TVH baltymo santykinio kiekio lyginimas su kontrolinėmis ląstelėmis augintomis 30 °C, neapima neglikozilinto TVH baltymo kiekio įvertinimo. Todėl, mes taip pat įvertinome translokacijos efektyvumą, kaip santykį tarp glikozilinto ir bendro TVH kiekio. Apibendrinus, karščio šokas pagerina TVH translokaciją didesniuose kultūros tankiuose. Tačiau, translokacijos efektyvumas ne visuomet koreliavo su glikozilinto TVH kiekio padidėjimu. Translokacijos efektyvumas padidėjo 2 kartus vėlyvojoje gliukozės fazėje, bei tik ~25 % vėlyvojoje etanolio fazėje, nors šiame taške fiksuotas didžiausias glikozilinto TVH kiekis. Didžiausias translokacijos efektyvumas buvo stebėtas diauksinės kaitos fazėje, tačiau šiam rezultatui įtakos turėjo bendras neglikozilintos TVH formos kiekio sumažėjimas.

Literatūroje aprašomas panašus efektas, kur karščio šoko atsakas (*angl. Heat Shock Response, HSR*) pagerino heterologinio baltymo sekreciją *S. cerevisiae* (Hou *et al.*, 2013). Straipsnio autoriai stipriai padidino mutantinio *HSF1* geno, kuris konstitutyviai aktyvuoja karščio šoko atsaką ląsteles auginant 30 °C, raišką ir tai ženkliai pagerino heterologinės α-amilazės išeigą. Mūsų rezultatai rodo, kad viena iš priežasčių kodėl karščio šoko atsakas pagerina baltymų sekreciją, gali būti padidėjęs translokacijos greitis. Tai sutampa su anksčiau publikuotais įrodymais, kad karščio šoko atsakas palengvina naujų polipeptidų translokaciją į ET (Liu ir Chang, 2008). Žinoma, mūsų taikytas karščio šokas skiriasi nuo konstitutyvaus karščio šoko atsako (Hou *et al.*, 2013), tačiau abi studijos rodo, kaip karščio šokas gali būti pritaikytas norint pagerinti heterologinių baltymų biosintezę *S. cerevisiae* mielėse.

Atrinkę karščio šoko taikymo sąlygas, kurios lėmė didžiausią glikozilinto TVH kiekį, atlikome papildomą nepriklausomą eksperimentą, leidusį patvirtinti gautus rezultatus (3 Paveikslas).

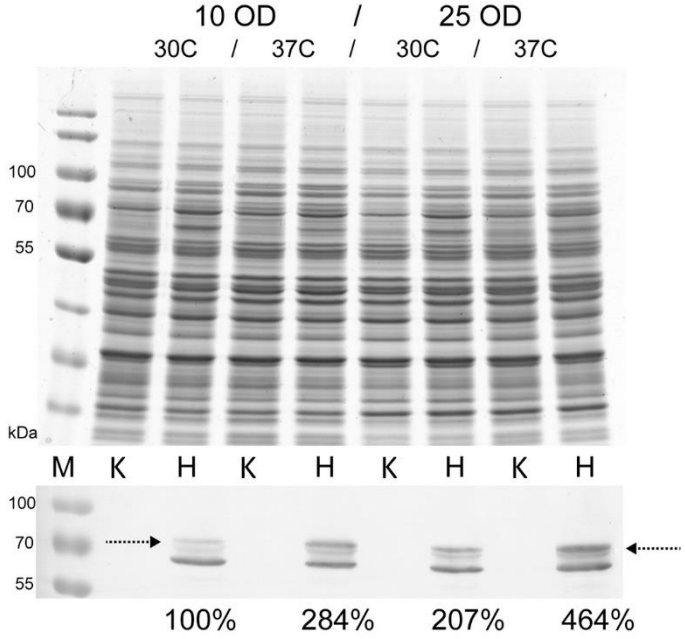

3 Paveikslas. Rezultatų patvirtinimas papildomu nepriklausomu eksperimentu. Grubūs ląstelių, gaminančių TVH (H) baltymų bei kontrolinių ląstelių transformuotų tuščiu vektoriumi (K), lizatai buvo analizuoti NDS-PAGE (viršuje) ir Western baltymų hibridizavimo (apačioje) metodais. Kolbos su ląstelių subkultūromis gautomis iš tos pačios pradinės kultūros buvo augintos paraleliai iki 10 arba 25 OD_{600} kultūros tankių. Tuomet ląstelių kultūros buvo perkeltos į karščio šoko sąlygas (42 °C 2 min) ir toliau augintos 5 valandas 37 °C iki kultūros augimo terpės keitimo. Pakeitus terpę ląstelės toliau augintos 37 °C iki TVH sintezės pabaigos. TVH kiekis "10 OD 30 °C" ląstelėse buvo prilygintas 100 %, ir nuo jo skaičiuotas TVH kiekio pokytis kitose sąlygose.

2.2.2. Ląstelinių baltymų, kurių kiekio pokyčiai koreliuoja su pagerinta TVH translokacija, identifikavimas

Norint nustatyti, kurie ląsteliniai baltymai gali būti susiję su efektyvesne TVH translokacija, mes atlikome palyginamąją, IPG ir NEPHGE 2DE pagrįstą, proteominę analizę. Šiam tikslui norėjome išanalizuoti mielių ląstelių kultūros augimo sąlygas, kuomet TVH translokacija yra pati efektyviausia, bei sąlygas kuomet translokacija neefektyvi, kas leistų nustatyti stipriausius pokyčius proteomoje. Mes nustatėme, kad kuomet mielių ląstelių kultūra buvo perkeliama į 20 °C vėlyvojoje diauksinės kaitos fazėje, su tolesne indukcija ir auginimu toje pačioje temperatūroje, TVH translokacija buvo beveik pilnai nuslopinta. Glikozilinto TVH kiekis buvo 80 kartų didesnis, o o translokacija 60 kartų efektyvesnė tarp ląstelių augintų 20 °C ir 37 °C. Šis drastiškas pokytis leido mums išanalizuoti gausių mielių baltymų proteomą, kai TVH translokacija buvo „įjungta“ arba „išjungta“.

Abiejomis 2DE technikomis buvo analizuoti viso devyni eksperimentiniai variantai (mielės gaminančios TVH, TVN, bei transformuotos tuščiu vektoriumi, kiekvienas variantas augintas 20 °C, 30 °C ir 37 °C). Pasirinktomis sąlygomis apie 20 % gausiausių ląstelinių baltymų taškų, pasižymėjo skirtingu sintezės lygiu. NEPHGE pagrįsta 2DE patikimiau atskyrė baltymų taškus, todėl baltymai buvo identifikuojami iš šiuo metodu gautų gelių. Lyginant „įjungta“/“išjungta“ sąlygas, tripsinizuotų peptidų masių pirštų antspaudų metodu (*angl. tryptic peptide mass fingerprinting*), buvo identifikuota 40 baltymų taškų. Atmetus dalinai degraduotas formas, izoformas bei mažai tikėtinus baltymus, likę ~15 ląstelinių baltymų buvo pasirinkti, kaip galimai susiję su pagerėjusia TVH translokacija. Remiantis literatūra, keturi iš jų laikomi pagrindiniais taikiniais. Nors šiame tyrime kiekybiškai analizavome tik gausius ląstelinius baltymus, mes manome, kad stipri virusinių baltymų gamyba turėtų būti lydima ir palyginamai stipresne ląstelinių baltymų sinteze. Taip pat, ypač gausūs ląsteliniai baltymai tarnauja, kaip biologinių procesų žymenys bei parodo galimus mechanizmus susijusius su heterologinių baltymų translokacija abiejose ET membranos pusėse.

Pirmasis karščio šoko paveiktas ir TVH translokaciją pagerinantis, gali būti pats translokacijos mechanizmas. Iš visų identifikuotų galimai susijusių su TVH translokacija baltymų, Kar2/BiP yra pats gausiausias padidintos biosintezės (>3 kartus) baltymas. Yra gerai žinoma, kad nesulankstytų baltymų atsako (UPR) neturinčiose ire1D ląstelėse, Kar2p yra būtinas baltymų translokacijai į mielių ET ir atlieka kritinę rolę palengvindamas baltymų translokaciją karščio šoko atsako metu (Liu ir Chang, 2008). Tačiau, vienas

Kar2p gali tik dalinai pagelbėti karščio šoko atsako įtakojamam ET streso slopinimui (Hou *et al.,* 2014). Tikėtina, jog norint stipriai pagerinti rekombinantinių baltymų translokaciją, reiktų kartu padidinti ir ET ko-šaperonų raišką.

Kiti stipria skirtinga sinteze pasižymintys galimi baltymai-taikiniai buvo didieji citozoliniai Hsp90 ir Hsp110 šeimų šaperonai. Padidėjusi Hsp104p šaperono gamyba gali užtikrinti didesnę termotolerancijią ir kartu atsparumą daugeliui ląstelinio streso formų (Sanchez *et al.,* 1992). Šis šaperonas taip pat reikalingas karščiu denatūruotų baltymų konformaciniam taisymui mielių ET (Hänninen *et al.,* 1999). Galima šio šaperono rolė baltymų translokacijoje gali išryškinti Hsp104p sąsają su baltymų perlankstymo mechanizmu ET.

Dar vienas svarbus identifikuotas baltymas-taikinys galimai susijęs su pagerėjusia TVH translokacija yra Tef1p, dar žinomas kaip eukariotų transliacijos elongacijos faktorius 1 (eEF1A). Tai yra pirmasis ląstelinis baltymas dalyvaujantis naujai susintetintų baltymų pirmtakų kokybės kontrolėje, po jų paleidimo iš ribosomos (Hotokezaka *et al.,* 2002). Ankstesniame mūsų darbe, mes parodėme, kad eEF1A tiesiogiai sąveikauja su TVH baltymo pirmtakais ir formuoja didelius, disulfidiniais ryšiais sujungtus multimerus (Ciplys *et al.,* 2011). Žinduolių ląstelėse karščio šoko metu šis transkripcijos faktorius yra būtinas karščio šoko transkripcijos faktoriaus 1 (*angl. Heat-Shock Factor, HSF1*) aktyvacijai (Shamovsky *et al.,* 2006), bei dalyvauja visame karščio šoko atsako procese nuo transkripcijos iki transliacijos (Vera *et al.,* 2014). Jei mielėse šis transkripcijos faktorius funkcionuoja panašiai, jis gali padėti TVH pirmtakų translokacijai į ET, pateikdamas translokuoti tinkamus TVH polipeptidus bei koordinuodamas karščio šoko atsaką, kuris palengvina translokacijos procesą slopindamas ET stresą.

Šio tyrimo metu identifikuoti baltymai-taikiniai turėtų būti toliau nagrinėjami genų inžinerijos metodais.

2.3. NEPHGE metodo atkūrimas

2DE yra patikimas aukštos rezoliucijos metodas leidžiantis analizuoti visą baltymų rinkinį ar proteomą, įskaitant baltymų izoformas bei po-transliaciškai modifikuotus baltymus (Rabilloud, 2009). Nors NEPHGE pagrįsta 2DE yra ne taip plačiai naudojamas, bei daugiau rankų darbo reikalaujantis metodas negu IPG pagrįsta 2DE, jis vis dar naudojamas specializuotose laboratorijose. NEPHGE 2DE metodo sugebėjimas geriau atskirti bazinius baltymų taškus, lyginant su IPG 2DE, yra panaudojamas

funkcinės proteomikos eksperimentuose plačiame pH diapazone, bei eksperimentuose dirbant su stipriai baziniais baltymais (Bjarnadóttir ir Flengsrud, 2014; Kreipke *et al*., 2007). Nors atnaujintas NEPHGE 2DE protokolas buvo aprašytas 1995 metais Klose ir Kobalz (Klose ir Kobalz, 1995), jis komercializuotas daug vėliau WITA GmbH įmonės (Wittmann-Liebold *et al*., 2006), kuomet buvo sukurta „WITAvision“ 2DE sistema. Deja, ši kompanija nutraukė savo veiklą, o šios įrangos naudotojai neteko galimybės įsigyti reikiamų reagentų. Iš anksto paruoštų gelių tirpalų neprieinamumas, dar labiau sumažino šio metodo naudojimą, todėl mums atrodė svarbu atkurti AN sudėtį pirmos krypties geliuose bei paviešinti ją kitiems šio metodo naudotojams. AN sudėtis, WITA GmbH pardavinėjamuose IEF geliuose niekuomet nebuvo paviešinta, o atkurti originalią AN sudėtį paskelbtą Klose ir Kobalz taip pat buvo iššūkis dėl daugumos tuo metu naudotų amfolitų gamybos nutraukimo. Nepaisant to, čia mes pristatome atkurtą AN sudėtį NEPHGE pagrįstai 2DE, kuri rodo stiprią koreliaciją su anksčiau komerciškai prieinamais geliais.

Mūsų atkurto AN „Naujojo mišinio“ sudėtis pirmos krypties NEPHGE geliams aprašyta skyriuje Tyrimo metodai.

2.3.1. Atkurtų NEPHGE gelių pirmos krypties atskyrimui palyginimas su komerciniais „WITA“ geliais

Toliau, mes palyginome pirmos krypties gelius pagamintus su mūsų „Naujuoju mišiniu“ bei komercinius, užpiltus naudojant „WITA“ gelių tirpalus (4 Paveikslas). Šiame eksperimente mėginys, leidimo nustatymai bei antros krypties procedūros buvo atliktos taip pat identiškai. Mes išanalizavome dėl statistinio patikimumo triplikuotus 2DE gelius naudodami PDQuest (BioRad) 2-D analizės programinę įrangą. Pirsono koreliacijos koeficiento (r) tarp gelių apskaičiavimui, sulyginome visus šešis gelius tarpusavyje.

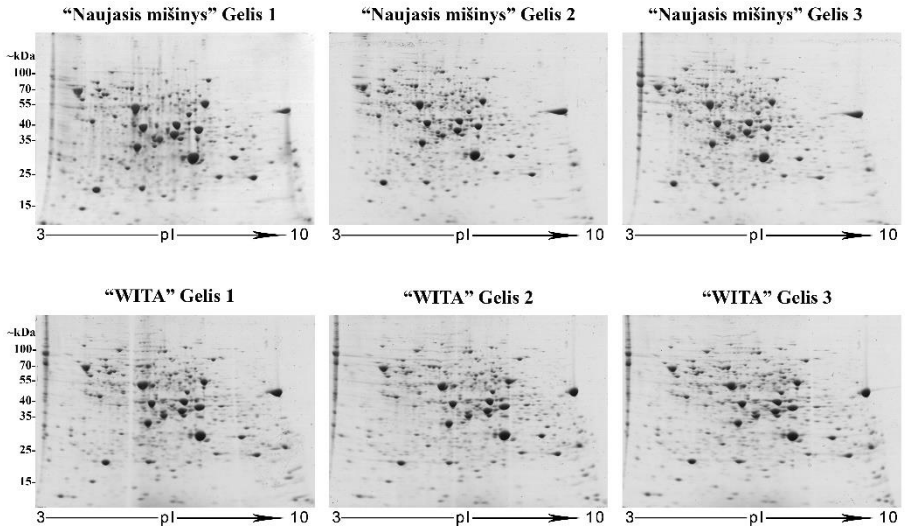

4 Paveikslas. To paties mėginio (80 µg *S. cerevisiae* AH22 kamieno, transformuoto pFGG3 vektoriumi, lizatas) baltymų atskyrimo 2DE triplikacija, naudojant mūsų atkurtą "Naująjį mišinį" arba komercinius "WITA" tirpalus, NEPHGE pagrįstam pirmos krypties IEF. Atskirtų baltymų pI diapazonas sužymėtas gelių apačiose, kairėje sužymėtos apytikslės molekulinės masės, kDa.

Visi geliai rodė stiprią teigiamą koreliaciją ($r > 0,7$) tarpusavyje, su mažais nuokrypiais. Gelių grupės, pagamintos su "WITA" tirpalais, viduje, koreliacija svyravo nuo 0,81 iki 0,85, o tarp gelių pagamintų su mūsų "Naujuoju mišiniu" koreliacijos koeficientas buvo truputį didesnis ir svyravo nuo 0,87 iki 0,9. Lyginant gelius tarp šių dviejų grupių, koreliacijos koeficientas buvo žemesnis (r=0,71–0,77), nei grupių viduje (r=0,87–0,9 ir r=0,81–0,85). To buvo galima tikėtis turint omenyje, jog AN sudėtis geliuose greičiausiai yra skirtinga, nes "WITA" gelių sudėtis niekuomet nebuvo paviešinta. Truptį geresnė koreliacija tarp "Naujojo mišinio" gelių perša išvadą, jog atsikartojamumas tarp techninių replikų taip pat geresnis. Nors koreliacija tarp "WITA" ir mūsų atkurto recepto gelių nėra ideali, jie vis tiek rodo stiprią teigiamą koreliaciją. Todėl mes manome, jog mūsų atkurtas AN mišinys bei gelių tirpalų sudėtis NEPHGE pirmos krypties baltymų atskyrimui gali būti pilnai naudojamas proteominiuose 2DE pagrįstuose eksperimentuose, vietoje komerciškai nebeprieinamų tirpalų. Atskirtų baltymų taškų skaičius taip pat buvo labai panašus – apie 800 atskirtų baltymų taškų mūsų "Naujojo mišinio" (vidutiniškai 795 taškai) ir "WITA" (vidutiniškai 807 taškai) geliuose.

Siekiant ištestuoti mūsų atkurtą NEPHGE pirmos krypties gelių sudėtį, mes panaudojome juos palyginamąjam proteominiam eksperimentui

analizuojančiam rekombinantinio žmogaus CALR baltymo sekreciją iš mielių *S. cerevisiae* (Skyrius 2.4.).

2.4. Palyginamoji aukšto lygio rekombinantinio žmogaus CALR baltymo sekrecijos mielėse *S. cerevisiae* analizė

Žmogaus CALR baltymas yra ET šaperonas, kuris taip pat turi ir ekstraląstelinių funkcijų. Įvairūs streso faktoriai gali sukelti šio baltymo sekreciją iš žinduolių ląstelės, nors tikslus mechanizmas, kaip tai įvyksta nėra aiškus. Mielės *S. cerevisiae* sekretuoja šį baltymą labai efektyviai ir šios sekrecijos analizė gali padėti išaiškinti, kaip CALR išeina iš eukariotinės ląstelės. Šio tyrimo tikslas buvo atlikti palyginamąją, CALR sekretuojančių mielių *S. cerevisiae* bei kontrolinių mielių ląstelių transformuotų tuščiu vektoriumi, visos proteomos analizę pasitelkiant NEPHGE pagrįstą 2DE bei LC-MS^E identifikuojant ląstelinius baltymus galimai susijusius su CALR sekrecija.

Šiame proteominiame eksperimente lygindami CALR sekretuojančias bei kontrolines ląsteles transformuotas tuščiu vektoriumi, kiekybiškai įvertinome baltymų gausą iš 2DE gelių pagamintų su mūsų atkurtu AN mišiniu, bei kiekybiškai įvertinome visus LC-MS^E metodu identifikuotus peptidus esančius pilnuose proteomos mėginiuose, naudodami beetiketį TOP3 metodą. Nustatėme, jog efektyvi CALR sekrecija neindukuoja nei ląstelinio streso nei sekrecinio kelio baltymų raiškos, ir tik truputį padidina energijos bei maisto medžiagų poreikį *S. cerevisiae* mielėse.

2.4.1. Rekombinantinio žmogaus CALR baltymo biosintezė bei sekrecija *S. cerevisiae*

Siekiant gauti mėginius palyginamajam 2DE eksperimentui, mes *S. cerevisiae* AH22 mielių kamiene transformuotame plazmide nešančia šio baltymo geną, indukavome pilno ilgio žmogaus rekombinantinio CALR baltymo pirmtako su natyvia signaline seka, sintezę. Mielių ląstelių kultūrai esant diauksinės kaitos fazėje baltymo sintezės indukcija buvo gauta pakeičiant augimo į terpę į YEPG. Densitometrinė NDS-PAGE kultūros terpės analizė atskleidė, jog 18 val po rekombinantinio baltymo gamybos indukcijos, brandaus CALR baltymo išeiga yra 138 mg iš 1 L kultūros augimo terpės (120–160 mg/L ribose). Augimo fazės, kuomet CALR sekrecija buvo efektyviausia, nustatymui, densitometriškai įvertinome kultūros terpės mėginius imtus kas tris valandas nuo baltymo sintezės indukcijos. Išmatavę santykinius CALR juostelių tūrių pokyčius nustatėme, jog didžiausias CALR kiekio pokytis terpėje atsiranda tarp 0 ir 3, bei tarp 3 ir 6 valandų (~2,8 karto)

po indukcijos. Mes galvojome, jog tais laiko momentais, kai CALR sekrecija buvo efektyviausia, ląstelinių baltymų padedančių jai vykti gausa irgi turi būti didesnė. Mėginiai 2DE paimti 3 ir 6 valandos po CALR raiškos indukcijos.

Gautas 138 mg/L sekrecijos titras du kartus viršijo mūsų seniau publikuotus rezultatus, kuomet rekombinantinio žmogaus CALR baltymo išeiga buvo 60–66 mg iš 1 L kultūros terpės, jo geno raišką reguliuojant PGK1 ir pFGADH1 promotoriais *S. cerevisiae* mielėse (Čiplys *et al*., 2015, 2021). Nors naudoti promotoriai skyrėsi, mielių kamienas, kultūros auginimo terpės bei auginimo sąlygos buvo identiškos, kas leidžia mums tiesiogiai lyginti šių eksperimentų rezultatus. Šį sekretuojamo CALR kiekio padidėjimą lėmė indukuojamas promotorius, bei tai, jog indukcija buvo vykdyta didesniame ląstelių kultūros tankyje, o tai leido ląstelėms efektyviai augti iki jų augimą potencialiai apsunkinančios baltymo sintezės fazės (Weinhandl *et al*., 2014).

Efektyvi CALR sekrecija mielėse gali būti sąlygota ir paties baltymo savybių – yra parodyta, jog CALR būdingas mažesnis viduląstelinis sulaikymas, lyginant su kitais panašiai sekretuojamais ET šaperonais BiP ir ERp57 (Čiplys *et al*., 2013, 2014, 2015). Dar viena efektyvios CALR sekrecijos priežastis gali būti žema laisvo Ca^{2+} koncentracija mielių ET. Žmonėse ET Ca^{2+} išeikvojimas indukuoja CALR sekreciją (Peters ir Raghavan, 2011), o mielių ET yra 10-100 kartų mažiau laisvo Ca^{2+} (Strayle *et al*., 1999), lyginant su žmogaus ET.

Aukštas sekrecijos titras taip pat ženkliai priklauso nuo baltymo stabilumo. Neseniai mūsų grupės publikuotame tyrime, kuriame buvo analizuoti 50-ies CALR baltymo mutantų sekrecijos titrai, stabilumas bei kiti parametrai *S. cerevisiae*, buvo parodyta, kad vieno taško mutantai, kurie pasižymėjo žemesniais sekrecijos titrais, taip pat pasižymėjo žemesniu stabilumu (Čiplys *et al*., 2021). Tokiu būdu, mūsų gauta itin efektyvi 138 mg/L CALR sekrecija įrodo, kad šis rekombinantinis baltymas yra labai stabilus bei teisingai sulankstytas.

2.4.2. Palyginamoji, 2DE pagrįsta, CALR sekretuojančių ir kontrolinių ląstelių analizė

Lygindami CALR sekretuojančių bei kontrolinių ląstelių mėginių 2DE gelius, 3 ir 6 valandų po baltymo sintezės indukcijos augimo taškuose (užnešta 200 µg mielių *S. cerevisiae* AH22 kamieno sekretuojančio CALR baltymą arba transformuoto tuščiu vektoriumi, lizato), gavome iš viso 811 skirtingų baltymų taškų, iš kurių 734 sutapo visuose geliuose. Įvertinę skirtinga sinteze pasižyminčių baltymų taškų kiekio pokytį kartais, bei statistinį pokyčio reikšmingumą (Stjudento *t*-testas), mes radome, kad 35 taškai rodė statistiškai

patikimą (p-reikšmė < 0,05) kiekio pokytį ir tik 8 iš jų pasižymėjo itin statistiškai patikimu (p-reikšmė < 0,01) kiekio pokyčiu. Deja, dauguma jų buvo labai smulkūs bei neryškūs arba jų pozicijos buvo gelių kraštuose, todėl jie buvo netinkami išpjovimui ir identifikavimui.

Papildoma baltymų taškų duomenų analizė DESeq2 išskyrė 11-a labiausiai statistiškai patikimų baltymų taškų, kurie atitiko mūsų 1,5 karto slenkstinį kiekio pokytį. 8-i iš jų (nr. 749–756), kurie pasižymėjo didžiausiu kiekio pokyčiu kartais (4 Paveikslas), mums buvo patys įdomiausi, bei tai buvo tie patys statistiškai patikim skirtingu sintezės lygiu pasižymėję baltymai nustatyti Stjudento t-testu.

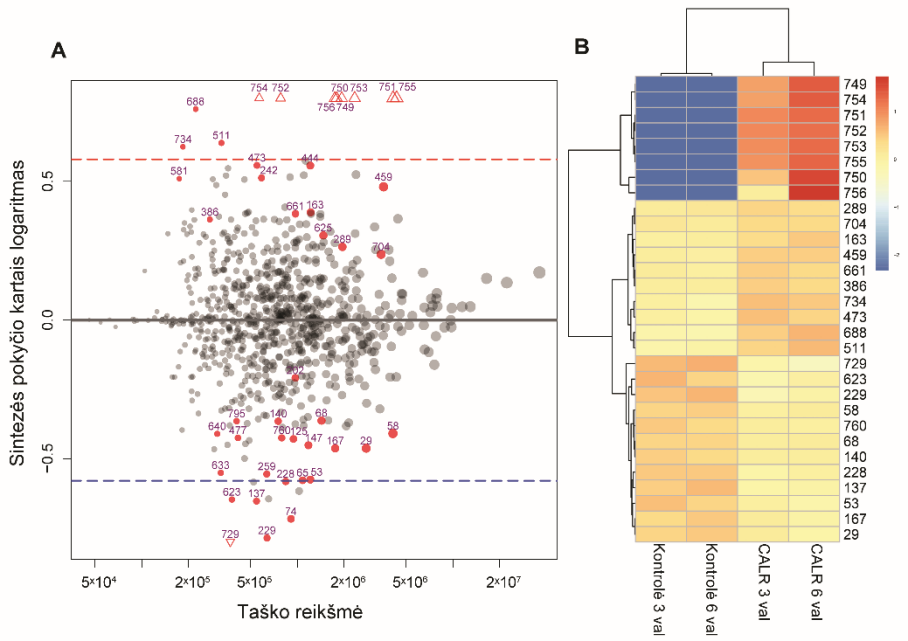

4 Paveikslas. Skirtingu kiekiu pasižymėjusių baltymų taškų NEPHGE 2DE pagrįsto, CALR sekretuojančių ir kontrolinių ląstelių palyginimo, reprezentacija. Baltymų taškai 749–756 rodo labiausiai reikšmingą kiekio pokytį. A – MA brėžinys (log santykio (M) bei vidutinio vidurkio (A) skalių brėžinys)-baltymų taškų vidutinio sintezės lygio (x-ašis) priklausomybė nuo log2 kiekio pokyčio kartais (y-ašis) po DeSeq2 analizės, atspindinti skirtingos baltymų sintezės stiprumą. Stipria skirtinga sinteze pasižymėję baltymų taškai, su aukščiausiu kiekio pokyčiu kartais, pažymėti raudonais trikampiais. Punktyrinės linijos atspindi 0,58 log2 pokyčio kartais slenksčius: mėlyna linija žymi sumažėjusios sintezės slenkstį, o raudona linija žymi padidėjusios baltymų sintezės CALR mėginiuose, slenkstį. Taškai su numeriu žymi baltymus, kurių sintezės pokytis buvo statistiškai reikšmingas (p-reikšmė ≤ 0,05), raudoni taškai žymi baltymus su pakoreguota p-reikšme DeSeq2 analizėje (padj ≤ 0,1). B – 30 baltymų taškų su žemiausia p-reikšme, šilumos žemėlapio reprezentacija. Spalvos intensyvumas žymi kiek taško vertė yra didesnė (raudona) arba mažesnė (mėlyna) nei vidurkis.

Minėti taškai 749–756, pasižymėję statistiškai reikšmingiausiu sintezės pokyčiu buvo pasirinkti LC-MS^E identifikacijai. Taškai 751–756 buvo identifikuoti, kaip žmogaus CALR baltymas (Prisijungimo nr. P27797, įrašas CALR_HUMAN, MW 48111, pI 4,09, Calreticulin OS=*Homo sapiens*). Vienas taškas atitinka brandų CALR baltymą, kurio molekulinė masė yra ~46 kDa, o kitas taškas atitinka pilno ilgio netranslokuotą baltymo pirmtaką su nepažeistu signaliniu peptidu, kurio molekulinė masė yra ~48 kDa. Identifikuotų peptidų sekų analizė atskleidė, jog taškai identifikuoti, kaip CALR, bet esantys skirtingose MW ir pI pozicijose, yra CALR degradacijos produktai. Analizuotų peptidų sekos atitiko *N*-galinę, *C*-galinę bei centrinę CALR baltymo dalis, tokie rezultatai galimi tik vykstant baltymo degradacijai.

Šie duomenys rodo, jog nepaisant efektyvios pilno ilgio CALR sekrecijos, ląstelės viduje vistiek vyksta degradacija. Degradavusio ir nepažeisto CALR baltymo kiekiai ląstelėje atrodo labai panašūs, o tai reiškia, jog degradacija nėra nežymi. CALR degradacijos produktai nėra sekretuojami ir turi būti metabolizuoti ląstelėje. Kol kas mes nežinome į kokį degradacijos kelią dalis CALR baltymo patenka, bet efektyvi sekrecija leidžia manyti, jog degradacija neturi negatyvaus poveikio ląstelei.

Taškai 749–750 buvo identifikuoti, kaip mielių citozolinė superoksido dismutazė (SOD1) (Prisijungimo nr.: P00445, įrašas SODC_YEAST, MW 15844, pI 5,5708, Superoxide dismutase [Cu-Zn] OS=*Saccharomyces cerevisiae*). Dėl labai mažo atstumo nuo šių taškų, nustatėme ir šalia esantį tašką, kuris pasirodė esantis tas pats SOD1 baltymas, nors nepasižymėjo kiekio pokyčiu. Kiekio pokyčiu pasižymėję taškai 749 ir 750 buvo rasti tik CALR sekretuojančių mielių mėginiuose. Panašu, jog taškai atsirandantys šalia pagrindinio SOD1 taško yra šio baltymo izoformos, tačiau kol kas neaišku, kaip jų atsiradimas susijęs su CALR sekrecija. CALR sintezė deleciniame ΔSOD1 kamiene nesutrikdė sekrecijos, lyginant su sinteze motininiame kontroliniame BY4741 kamiene, o tai rodo, jog SOD1 nėra būtinas CALR sekrecijai mielėse.

Nepaisant to, atsirandantys SOD1 izoformų taškai neturi įtakos pagrindinio SOD1 taško tūriui, o tai gali reikšti bendrą šio baltymo kiekio padidėjimą ląstelėje. Heterologinių baltymų sintezė mielėse generuoja didelius kiekius aktyvių deguonies formų (*angl. Reactive Oxygen Species, ROS*), bei indukuoja ląstelinį oksidacinį stresą (Martínez *et al*., 2016). Tai atsitinka arba šaperonams lankstant padidintos sintezės baltymus ir formuojant disulfidinius ryšius (Tyo *et al*., 2012) arba mitochondrijoms gaminant didelius kiekius ATP šiam procesui vykti (Haynes *et al*., 2004). Tai gali paaiškinti SOD1 kiekio padidėjimą CALR sekretuojančiose ląstelėse.

2DE pagrįsta proteominė analizė visumoje atstovauja tik nedidelę analizuojamos proteomos dalį – tik gausius baltymus, kurie rodo tik didelio laipsnio pokyčius proteomoje ir dažniausiai turi biologinę reikšmę (Twyman *et al*., 2013). Ši analizė mums taip pat suteikia vizualinį analizuojamos proteomos kontekstą – lengvą būdą nustatyti kiek ląstelės yra paveiktos rekombinantinio baltymo raiškos. Šio tyrimo atveju, 2DE pagrįsta proteominė analizė parodė labai žemo laipsnio gausių baltymų kiekio pokytį. Baltymų taškų raštai ir intensyvumai varijavo labai nedaug tarp CALR sekretuojančių ir kontrolinių mielių ląstelių mėginių, su minėtų 8 taškų išimtimi.

2.4.3. Palyginamoji, LC-MS^E pagrįsta, CALR sekretuojančių bei kontrolinių ląstelių analizė

Jeigu NEPHGE pagrįsta 2DE analizė buvo limituota tik gausių baltymų reprezentacija, LC-MS^E metodas leido mums ištyrinėti didelę dalį CALR sekretuojančių bei kontrolinių ląstelių proteomų. Buvo atlikta palyginamoji tripsinu skaldyto pilno baltymų mėginio analizė. Šio eksperimento metu analizavome baltymų mėginį paimtą 3 valandos po CALR sintezės indukcijos bei kontrolinį mėginį gautą iš ląstelių transformuotų tuščiu vektoriumi. Biologinės ir metodologinės variacijos įvertinimui triplikavome tuos pačius mėginius. Iš viso mums pavyko identifikuoti 1726 unikalius baltymus, iš kurių 1574 buvo rasti visuose mėginiuose. Identifikuotų baltymų skaičius sudarė apie trečdalį visos haploidinių mielių proteomos (de Godoy *et al*., 2008; Ho *et al.,* 2018). Pasirinkus slenkstines ribas (raiškos pokytis kartais ≥1,5 (0,58log2 raiškos pokytis), $p < 0,01$, FDR < 0,05) iš visų 1574 baltymų, tik 20 atitiko mūsų nusistatytus kriterijus.

Iš atrinktų 20 baltymų, dalis buvo aptikta tik vienoje ar kitoje mėginių grupėje (tik CALR sekretuojančių arba tik kontrolinių ląstelių mėginiuose). 9 baltymai buvo neaptikti kontroliniuose mėginiuose ir aptikti tik CALR sekretuojančiuose mėginiuose. Kiti 4 buvo neaptikti CALR mėginiuose. 60S ribosominiai baltymai L17-B, L26-A, L15-B, ribozės fosfato pirofosfokinazė 2 (KPR2), citochromo c oksidazės polipeptidas 5B (COX5b), nuo cAMP priklausoma 3-io tipo baltymų kinazė (KAPC) ir heksozių transporteris 15 (HXT15) nebuvo aptikti kontroliniuose mėginiuose. 3-hidroksi-3-metilglutaril kofermento A reduktazė (HMDH2) ir Y' elemento nuo ATP priklausoma helikazė YIL177C buvo neaptiktos CALR sekretuojančių mielių mėginiuose. Turint omenyje, jog visi paminėti baltymai yra esminiai ląstelės bazinių funkcijų palaikymui, mes laikėme jų neaptikimą viename mėginyje ir aptikimą kitame, kaip padidėjusią sintezę.

Didžioji dalis baltymų, kurie pasižymėjo skirtinga sinteze CALR sekretuojančių mielių mėginiuose lyginant su kontrole, buvo atsakingi už baltymų transliaciją, energiją, nukleotidų, aminorūgščių bei riebalų metabolizmą. Baltymų, susijusių su centriniu anglies metabolizmu, baltymų lansktymu ar pernešimu, kurie sudarė pagrindinius skirtinga sinteze pasižymėjusius baltymus aptiktus atliekant panašius palyginamuosius proteominius tyrimus analizuojančius mielių *Pichia pastoris* su padidinta ksilanazės A gamyba (Lin *et al.,* 2013) bei mielių *Schizosaccharomyces pombe* gaminančių α-gliukozidazės maltazę (Hung *et al.,* 2016) proteomas, kiekio pokyčių neaptikome. Kartu su skirtingais funkciniais baltymų profiliais, stipriai skiriasi ir rekombinantinių baltymų sintezės įtakotų ląstelinių baltymų skaičius. *S. pombe* mielių gaminančių α-gliukozidazės maltazę proteomos analizė atskleidė, jog pakito 30–40 ląstelinių baltymų gamyba, o *Pichia pastoris* mielėse su padidinta ksilanazės A produkcija, buvo stebimi šimtų ląstelinių baltymų sintezės pokyčiai, tame tarpe ir visų UPR žymenų. Sąlyginai nedidelis skaičius skirtingu kiekiu pasižymėjusių baltymų rastų šiame darbe tik patvirtina, jog CALR sintezė bei sekrecija mielėse neindukuoja didelių pokyčių proteomoje.

Didžiausią nuostabą kelią tai, jog nepavyko rasti jokių su sekreciniu keliu susijusių baltymų, kurie būtų pasižymėję kiekio pokyčiais. Mes tikėjomės, jog su tokia aukšto lygio CALR sekrecija, bent vieno sekrecinio kelio mechanizmo baltymų sintezė taip pat turėtų būti padidėjusi. Kaip buvo minėta anksčiau, yra nežinoma kaip tiksliai CALR palieka žinduolių ląsteles. Pagrinde, šio baltymo patekimas į išorę būna sukeltas ET destabilizacijos arba ląstelinio streso (Kielbik *et al.,* 2021), kuris sąlygoja UPR atsiradimą. Vis dėlto, neradome jokių ląstelinio streso, sukelto CALR sekrecijos iš mielių ląstelių, įrodymų. Mielėms gaminančioms rekombinantinius baltymus yra normalu patirti tam tikrą stresą, dažniausiai susijusį su baltymų lankstymu ir sekrecija (Gasser *et al*., 2008; Mattanovich *et al*., 2004). Neefektyvi baltymų translokacija į ET sukelia baltymų pirmtakų akumuliaciją citozolyje, indukuoja UPR-Cyto ir formuoja netirpius baltymų agregatus (Ciplys *et al*., 2011). Neefektyvus arba neteisingas baltymų lankstymas sukelia UPR ET-e (Kauffman *et al*., 2002), kuris yra tiesiogiai susijęs su baltymų ET-asocijuotu baltymų degradacijos (*angl. ER-Associated protein Degradation,* (ERAD)) keliu (Hiller *et al*., 1996) ir oksidaciniu stresu (Gasser *et al*., 2008). Bendrai, ląstelinio streso žymenys gali būti naudojami nustatyti kokį stresą patiria ląstelė. Pavyzdžiui, UPR-Cyto atveju stebima padidėjusi citozolinių Hsp70, Hsp90, Hsp110 šeimų, karščio šoko šaperonų gamyba (Ciplys *et al*., 2011), o esant UPR streso atsakui, stebima ET baltymų BiP ir PDI skirtinga sintezė (Kauffman *et al*., 2002; Mattanovich *et al*., 2004). Yra žinoma, jog ET

baltymas BiP nukreipia neteisingai sulankstytus baltymus į ERAD dregradacijos kelią (Nishikawa *et al*., 2001). Tai, jog mes neradome jokių BiP baltymo kiekio pokyčių leidžia manyti, jog CALR sekretuojančiose ląstelėse nėra aktyvaus UPR, bei CALR degradacija nėra ERAD pasekmė. Taip pat, mes nenustatėme jokių kitų ET ar citozolinių ERAD komponentų, kaip Der1p, Der3p/Hrd1p, Hrd3p ar Sec61p, kiekio pokyčių (Bordallo *et al*., 1998; Hampton *et al*., 1996; Knop *et al*., 1996; Pilon M *et al*., 1997). Taipogi, nepastebėjome jokio ląstelių sekretuojančių CALR augimo sutrikimų, kas dažniausiai yra ląstelinio streso požymis. Ląstelinių baltymų nebuvimas kultūros augimo terpėje taip pat atmeta apoptozės galimybę.

Apibendrinus, aukšto lygio rekombinantinio žmogaus CALR baltymo sekrecija *S. cerevisiae* mielėse buvo daugumoje paremta baltymų transliacijos mechanizmų persitvarkymu bei nedideliais, ląstelinių baltymų atsakingų už energiją ir metabolizmą, kiekio pokyčiais. Kitų reikšmingų sekrecinio kelio baltymų kiekio pokyčių nebuvimas rodo, jog normalioje būsenoje, mielių sekrecinis aparatas yra pakankamas palaikyti aukšto lygio CALR sekreciją. Atrodo, kad tokia lengvos sekrecijos savybė turėtų būti labiau būdinga natūraliai sekreciniam baltymui, o ne viduląsteliniam ET šaperonui. Norint įsigilinti į šią netipinę CALR sekreciją, reikalingi tolesni darbai, pavyzdžiui atliekant panašius tyrimus su natūraliai sekreciniais žmogaus ar mielių baltymais. Palyginamieji proteominiai tyrimai gali padėti atskleisti specifinius itin efektyvios rekombinantinių baltymų sekrecijos mechanizmus eukariotinėse ląstelėse ir galbūt paaiškinti dvilypę CALR prigimtį, kuris yra ir sekretuojama ektraląstelinė molekulė ir viduląstelinis ET šaperonas.

IŠVADOS

1. Plačiame pH 3–10 diapazone, NEPHGE pagrįsta 2DE yra tinkamesnis metodas mielių proteomos analizei, nei IPG pagrįsta 2DE.
2. Karščio šokas taikytas didesnio tankio ląstelių kultūrai bei tolesnė baltymo sintezė 37 °C temperatūroje, tris kartus padidina translokacijos efektyvumą ir TVH glikobaltymo kiekį. NEPHGE pagrįstos 2DE metodu buvo identifikuoti kiekio pokyčiais pasižymėjusių 15 ląstelinių baltymų, kurie galimai yra susiję su pagerėjusia TVH baltymo translokacija.
3. Atkurtas AN "Naujasis mišinys" ir gelių tirpalai NEPHGE pagrįstai 2DE, pasižymi geresniu atsikartojamumu ir gali būti naudojami proteomikos eksperimentuose vietoje komerciškai nebeprieinamų tirpalų.
4. Efektyvi rekombinantinio žmogaus CALR sekrecija neapsunkina mielių sekrecijos aparato, sukelia tik nedidelius pokyčius ląstelės proteomoje ir nesukelia jokio akivaizdaus ląstelinio streso. Pagrindiniai baltymai, kurių sintezė pakito buvo struktūriniai ribosomų baltymai dalyvaujantys baltymų transliacijoje.

LITERATŪROS SĄRAŠAS

1. Bischoff, R., Clesse, D., Whitechurch, O., Lepage, P., & Roitsch, C. (1989). Isolation of recombinant hirudin by preparative high-performance liquid chromatography. *Journal of Chromatography*, *476*, 245–255. https://doi.org/10.1016/s0021-9673(01)93873-7
2. Bjarnadóttir, S. G., & Flengsrud, R. (2014). Affinity chromatography, two-dimensional electrophoresis, adapted immunodepletion and mass spectrometry used for detection of porcine and piscine heparin-binding human plasma proteins. *Journal of Chromatography. B, Analytical Technologies in the Biomedical and Life Sciences*, *944*, 107–113. https://doi.org/10.1016/j.jchromb.2013.11.004
3. Bordallo, J., Plemper, R. K., Finger, A., & Wolf, D. H. (1998). Der3p/Hrd1p Is Required for Endoplasmic Reticulum-associated Degradation of Misfolded Lumenal and Integral Membrane Proteins. *Molecular Biology of the Cell*, *9*(1), 209–222. https://doi.org/10.1091/mbc.9.1.209
4. Causton, H. C., Ren, B., Koh, S. S., Harbison, C. T., Kanin, E., Jennings, E. G., Lee, T. I., True, H. L., Lander, E. S., & Young, R. A. (2001). Remodeling of yeast genome expression in response to environmental changes. *Molecular Biology of the Cell*, *12*(2), 323–337. https://doi.org/10.1091/mbc.12.2.323
5. Čiplys, E., Aučynaitė, A., & Slibinskas, R. (2014). Generation of human ER chaperone BiP in yeast Saccharomyces cerevisiae. *Microbial Cell Factories*, *13*, 22. https://doi.org/10.1186/1475-2859-13-22
6. Čiplys, E., Paškevičius, T., Žitkus, E., Bielskis, J., Ražanskas, R., Šneideris, T., Smirnovas, V., Kaupinis, A., Tester, D. J., Ackerman, M. J., Højrup, P., Michalak, M., Houen, G., & Slibinskas, R. (2021). Mapping human calreticulin regions important for structural stability. *Biochimica Et Biophysica Acta. Proteins and Proteomics*, *1869*(11), 140710. https://doi.org/10.1016/j.bbapap.2021.140710
7. Ciplys, E., Samuel, D., Juozapaitis, M., Sasnauskas, K., & Slibinskas, R. (2011). Overexpression of human virus surface glycoprotein precursors induces cytosolic unfolded protein response in Saccharomyces cerevisiae. *Microbial Cell Factories*, *10*, 37. https://doi.org/10.1186/1475-2859-10-37
8. Čiplys, E., Sasnauskas, K., & Slibinskas, R. (2011). Overexpression of human calnexin in yeast improves measles surface glycoprotein solubility. *FEMS Yeast Research*, *11*(6), 514–523. https://doi.org/10.1111/j.1567-1364.2011.00742.x
9. Čiplys, E., Žitkus, E., Gold, L. I., Daubriac, J., Pavlides, S. C., Højrup, P., Houen, G., Wang, W.-A., Michalak, M., & Slibinskas, R. (2015). High-level secretion of native recombinant human calreticulin in yeast. *Microbial Cell Factories*, *14*. https://doi.org/10.1186/s12934-015-0356-8
10. Čiplys, E., Žitkus, E., & Slibinskas, R. (2013). Native signal peptide of human ERp57 disulfide isomerase mediates secretion of active native recombinant ERp57 protein in yeast Saccharomyces cerevisiae. *Protein Expression and Purification*, *89*(2), 131–135. https://doi.org/10.1016/j.pep.2013.03.003
11. de Godoy, L. M. F., Olsen, J. V., Cox, J., Nielsen, M. L., Hubner, N. C., Fröhlich, F., Walther, T. C., & Mann, M. (2008). Comprehensive mass-spectrometry-based proteome quantification of haploid versus diploid yeast. *Nature*, *455*(7217), 1251–1254. https://doi.org/10.1038/nature07341
12. Distler, U., Kuharev, J., Navarro, P., Levin, Y., Schild, H., & Tenzer, S. (2014). Drift time-specific collision energies enable deep-coverage data-independent acquisition proteomics. *Nature Methods*, *11*(2), 167–170. https://doi.org/10.1038/nmeth.2767
13. Duina, A. A., Miller, M. E., & Keeney, J. B. (2014). Budding yeast for budding geneticists: A primer on the Saccharomyces cerevisiae model system. *Genetics*, *197*(1), 33–48. https://doi.org/10.1534/genetics.114.163188
14. Finnis, C., Goodey, A., Courtney, M., & Sleep, D. (1992). Expression of recombinant platelet-derived endothelial cell growth factor in the yeast Saccharomyces cerevisiae. *Yeast (Chichester, England)*, *8*(1), 57–60. https://doi.org/10.1002/yea.320080106

15. Gasser, B., Saloheimo, M., Rinas, U., Dragosits, M., Rodríguez-Carmona, E., Baumann, K., Giuliani, M., Parrilli, E., Branduardi, P., Lang, C., Porro, D., Ferrer, P., Tutino, M. L., Mattanovich, D., & Villaverde, A. (2008). Protein folding and conformational stress in microbial cells producing recombinant proteins: A host comparative overview. *Microbial Cell Factories*, *7*(1), 11. https://doi.org/10.1186/1475-2859-7-11
16. Gebauer, M., Hürlimann, H. C., Behrens, M., Wolff, T., & Behrens, S.-E. (2019). Subunit vaccines based on recombinant yeast protect against influenza A virus in a one-shot vaccination scheme. *Vaccine*, *37*(37), 5578–5587. https://doi.org/10.1016/j.vaccine.2019.07.094
17. Hampton, R. Y., Gardner, R. G., & Rine, J. (1996). Role of 26S proteasome and HRD genes in the degradation of 3-hydroxy-3-methylglutaryl-CoA reductase, an integral endoplasmic reticulum membrane protein. *Molecular Biology of the Cell*, *7*(12), 2029–2044. https://doi.org/10.1091/mbc.7.12.2029
18. Hänninen, A. L., Simola, M., Saris, N., & Makarow, M. (1999). The cytoplasmic chaperone hsp104 is required for conformational repair of heat-denatured proteins in the yeast endoplasmic reticulum. *Molecular Biology of the Cell*, *10*(11), 3623–3632. https://doi.org/10.1091/mbc.10.11.3623
19. Haynes, C. M., Titus, E. A., & Cooper, A. A. (2004). Degradation of Misfolded Proteins Prevents ER-Derived Oxidative Stress and Cell Death. *Molecular Cell*, *15*(5), 767–776. https://doi.org/10.1016/j.molcel.2004.08.025
20. Hellman, U., Wernstedt, C., Góñez, J., & Heldin, C. H. (1995). Improvement of an 'In-Gel' digestion procedure for the micropreparation of internal protein fragments for amino acid sequencing. *Analytical Biochemistry*, *224*(1), 451–455. https://doi.org/10.1006/abio.1995.1070
21. Hiller, M. M., Finger, A., Schweiger, M., & Wolf, D. H. (1996). ER Degradation of a Misfolded Luminal Protein by the Cytosolic Ubiquitin-Proteasome Pathway. *Science*, *273*(5282), 1725–1728. https://doi.org/10.1126/science.273.5282.1725
22. Ho, B., Baryshnikova, A., & Brown, G. W. (2018). Unification of Protein Abundance Datasets Yields a Quantitative Saccharomyces cerevisiae Proteome. *Cell Systems*, *6*(2), 192-205.e3. https://doi.org/10.1016/j.cels.2017.12.004
23. Hotokezaka, Y., Tobben, U., Hotokezaka, H., Van Leyen, K., Beatrix, B., Smith, D. H., Nakamura, T., & Wiedmann, M. (2002). Interaction of the eukaryotic elongation factor 1A with newly synthesized polypeptides. *The Journal of Biological Chemistry*, *277*(21), 18545–18551. https://doi.org/10.1074/jbc.M201022200
24. Hou, J., Österlund, T., Liu, Z., Petranovic, D., & Nielsen, J. (2013). Heat shock response improves heterologous protein secretion in Saccharomyces cerevisiae. *Applied Microbiology and Biotechnology*, *97*(8), 3559–3568. https://doi.org/10.1007/s00253-012-4596-9
25. Hou, J., Tang, H., Liu, Z., Österlund, T., Nielsen, J., & Petranovic, D. (2014). Management of the endoplasmic reticulum stress by activation of the heat shock response in yeast. *FEMS Yeast Research*, *14*(3), 481–494. https://doi.org/10.1111/1567-1364.12125
26. Hung, C.-W., Klein, T., Cassidy, L., Linke, D., Lange, S., Anders, U., Bureik, M., Heinzle, E., Schneider, K., & Tholey, A. (2016). Comparative Proteome Analysis in Schizosaccharomyces pombe Identifies Metabolic Targets to Improve Protein Production and Secretion *. *Molecular & Cellular Proteomics*, *15*(10), 3090–3106. https://doi.org/10.1074/mcp.M115.051474
27. Kauffman, K. J., Pridgen, E. M., Doyle, F. J., Dhurjati, P. S., & Robinson, A. S. (2002). Decreased protein expression and intermittent recoveries in BiP levels result from cellular stress during heterologous protein expression in Saccharomyces cerevisiae. *Biotechnology Progress*, *18*(5), 942–950. https://doi.org/10.1021/bp025518g
28. Kielbik, M., Szulc-Kielbik, I., & Klink, M. (2021). Calreticulin—Multifunctional Chaperone in Immunogenic Cell Death: Potential Significance as a Prognostic Biomarker in Ovarian Cancer Patients. *Cells*, *10*(1), 130. https://doi.org/10.3390/cells10010130
29. Kirch, W. (Ed.). (2008). Pearson's Correlation Coefficient. In *Encyclopedia of Public Health* (pp. 1090–1091). Springer Netherlands. https://doi.org/10.1007/978-1-4020-5614-7_2569

30. Klose, J., & Kobalz, U. (1995). Two-dimensional electrophoresis of proteins: An updated protocol and implications for a functional analysis of the genome. *Electrophoresis*, *16*(6), 1034–1059. https://doi.org/10.1002/elps.11501601175
31. Knop, M., Finger, A., Braun, T., Hellmuth, K., & Wolf, D. H. (1996). Der1, a novel protein specifically required for endoplasmic reticulum degradation in yeast. *The EMBO Journal*, *15*(4), 753–763.
32. Kreipke, C. W., Morgan, R., Roberts, G., Bagchi, M., & Rafols, J. A. (2007). Calponin phosphorylation in cerebral cortex microvessels mediates sustained vasoconstriction after brain trauma. *Neurological Research*, *29*(4), 369–374. https://doi.org/10.1179/016164107X204684
33. Kuharev, J., Navarro, P., Distler, U., Jahn, O., & Tenzer, S. (2015). In-depth evaluation of software tools for data-independent acquisition based label-free quantification. *PROTEOMICS*, *15*(18), 3140–3151. https://doi.org/10.1002/pmic.201400396
34. Leplatois, P., Le Douarin, B., & Loison, G. (1992). High-level production of a peroxisomal enzyme: Aspergillus flavus uricase accumulates intracellularly and is active in Saccharomyces cerevisiae. *Gene*, *122*(1), 139–145. https://doi.org/10.1016/0378-1119(92)90041-m
35. Lin, G.-J., Deng, M.-C., Chen, Z.-W., Liu, T.-Y., Wu, C.-W., Cheng, C.-Y., Chien, M.-S., & Huang, C. (2012). Yeast expressed classical swine fever E2 subunit vaccine candidate provides complete protection against lethal challenge infection and prevents horizontal virus transmission. *Vaccine*, *30*(13), 2336–2341. https://doi.org/10.1016/j.vaccine.2012.01.051
36. Lin, X., Liang, S., Han, S., Zheng, S., Ye, Y., & Lin, Y. (2013). Quantitative iTRAQ LC–MS/MS proteomics reveals the cellular response to heterologous protein overexpression and the regulation of HAC1 in Pichia pastoris. *Journal of Proteomics*, *91*, 58–72. https://doi.org/10.1016/j.jprot.2013.06.031
37. Liu, Y., & Chang, A. (2008). Heat shock response relieves ER stress. *The EMBO Journal*, *27*(7), 1049–1059. https://doi.org/10.1038/emboj.2008.42
38. Martínez, J. L., Meza, E., Petranovic, D., & Nielsen, J. (2016). The impact of respiration and oxidative stress response on recombinant α-amylase production by Saccharomyces cerevisiae. *Metabolic Engineering Communications*, *3*, 205–210. https://doi.org/10.1016/j.meteno.2016.06.003
39. Mattanovich, D., Branduardi, P., Dato, L., Gasser, B., Sauer, M., & Porro, D. (2012). Recombinant protein production in yeasts. *Methods in Molecular Biology (Clifton, N.J.)*, *824*, 329–358. https://doi.org/10.1007/978-1-61779-433-9_17
40. Mattanovich, D., Gasser, B., Hohenblum, H., & Sauer, M. (2004). Stress in recombinant protein producing yeasts. *Journal of Biotechnology*, *113*(1), 121–135. https://doi.org/10.1016/j.jbiotec.2004.04.035
41. Nawrocki, A., Larsen, M. R., Podtelejnikov, A. V., Jensen, O. N., Mann, M., Roepstorff, P., Görg, A., Fey, S. J., & Larsen, P. M. (1998). Correlation of acidic and basic carrier ampholyte and immobilized pH gradient two-dimensional gel electrophoresis patterns based on mass spectrometric protein identification. *Electrophoresis*, *19*(6), 1024–1035. https://doi.org/10.1002/elps.1150190618
42. Nishikawa, S. I., Fewell, S. W., Kato, Y., Brodsky, J. L., & Endo, T. (2001). Molecular chaperones in the yeast endoplasmic reticulum maintain the solubility of proteins for retrotranslocation and degradation. *The Journal of Cell Biology*, *153*(5), 1061–1070. https://doi.org/10.1083/jcb.153.5.1061
43. Nowalk, A. J., Nolder, C., Clifton, D. R., & Carroll, J. A. (2006). Comparative proteome analysis of subcellular fractions from Borrelia burgdorferi by NEPHGE and IPG. *Proteomics*, *6*(7), 2121–2134. https://doi.org/10.1002/pmic.200500187
44. O'Farrell, P. Z., Goodman, H. M., & O'Farrell, P. H. (1977). High resolution two-dimensional electrophoresis of basic as well as acidic proteins. *Cell*, *12*(4), 1133–1141. https://doi.org/10.1016/0092-8674(77)90176-3
45. Peters, L. R., & Raghavan, M. (2011). Endoplasmic reticulum calcium depletion impacts chaperone secretion, innate immunity, and phagocytic uptake of cells. *Journal of*

Immunology (Baltimore, Md.: 1950), *187*(2), 919–931. https://doi.org/10.4049/jimmunol.1100690
46. Pilon M, Schekman R, & Romisch K. (1997). Sec61p mediates export of a misfolded secretory protein from the endoplasmic reticulum to the cytosol for degradation. *The EMBO Journal*, *16*(15), 4540–4548. https://doi.org/10.1093/emboj/16.15.4540
47. Porro, D., Gasser, B., Fossati, T., Maurer, M., Branduardi, P., Sauer, M., & Mattanovich, D. (2011). Production of recombinant proteins and metabolites in yeasts: When are these systems better than bacterial production systems? *Applied Microbiology and Biotechnology*, *89*(4), 939–948. https://doi.org/10.1007/s00253-010-3019-z
48. Price, V., Mochizuki, D., March, C. J., Cosman, D., Deeley, M. C., Klinke, R., Clevenger, W., Gillis, S., Baker, P., & Urdal, D. (1987). Expression, purification and characterization of recombinant murine granulocyte-macrophage colony-stimulating factor and bovine interleukin-2 from yeast. *Gene*, *55*(2–3), 287–293. https://doi.org/10.1016/0378-1119(87)90288-5
49. Rabilloud, T. (2009). Membrane proteins and proteomics: Love is possible, but so difficult. *Electrophoresis*, *30 Suppl 1*, S174-180. https://doi.org/10.1002/elps.200900050
50. Sambrook, J., & Russell, D. W. (2001). *Molecular cloning: A laboratory manual* (3rd. ed). Cold Spring Harbor Laboratory.
51. Sanchez, Y., Taulien, J., Borkovich, K. A., & Lindquist, S. (1992). Hsp104 is required for tolerance to many forms of stress. *The EMBO Journal*, *11*(6), 2357–2364.
52. Shamovsky, I., Ivannikov, M., Kandel, E. S., Gershon, D., & Nudler, E. (2006). RNA-mediated response to heat shock in mammalian cells. *Nature*, *440*(7083), 556–560. https://doi.org/10.1038/nature04518
53. Shevchenko, A., Tomas, H., Havlis, J., Olsen, J. V., & Mann, M. (2006). In-gel digestion for mass spectrometric characterization of proteins and proteomes. *Nature Protocols*, *1*(6), 2856–2860. https://doi.org/10.1038/nprot.2006.468
54. Slibinskas, R., Ražanskas, R., Zinkevičiūtė, R., & Čiplys, E. (2013). Comparison of first dimension IPG and NEPHGE techniques in two-dimensional gel electrophoresis experiment with cytosolic unfolded protein response in Saccharomyces cerevisiae. *Proteome Science*, *11*, 36. https://doi.org/10.1186/1477-5956-11-36
55. Slibinskas, R., Samuel, D., Gedvilaite, A., Staniulis, J., & Sasnauskas, K. (2004). Synthesis of the measles virus nucleoprotein in yeast Pichia pastoris and Saccharomyces cerevisiae. *Journal of Biotechnology*, *107*(2), 115–124. https://doi.org/10.1016/j.jbiotec.2003.10.018
56. Smith, J. D., Richardson, N. E., & Robinson, A. S. (2005). Elevated expression temperature in a mesophilic host results in increased secretion of a hyperthermophilic enzyme and decreased cell stress. *Biochimica et Biophysica Acta (BBA) - Proteins and Proteomics*, *1752*(1), 18–25. https://doi.org/10.1016/j.bbapap.2005.07.016
57. Strayle, J., Pozzan, T., & Rudolph, H. K. (1999). Steady-state free Ca(2+) in the yeast endoplasmic reticulum reaches only 10 microM and is mainly controlled by the secretory pathway pump pmr1. *The EMBO Journal*, *18*(17), 4733–4743. https://doi.org/10.1093/emboj/18.17.4733
58. Taylor, R. C., & Coorssen, J. R. (2006). Proteome resolution by two-dimensional gel electrophoresis varies with the commercial source of IPG strips. *Journal of Proteome Research*, *5*(11), 2919–2927. https://doi.org/10.1021/pr060298d
59. Thim, L., Hansen, M. T., Norris, K., Hoegh, I., Boel, E., Forstrom, J., Ammerer, G., & Fiil, N. P. (1986). Secretion and processing of insulin precursors in yeast. *Proceedings of the National Academy of Sciences of the United States of America*, *83*(18), 6766–6770. https://doi.org/10.1073/pnas.83.18.6766
60. Twyman, R., Cfe, P. D., & A, G. (2013). *Principles of Proteomics*. Garland Science.
61. Tyo, K. E., Liu, Z., Petranovic, D., & Nielsen, J. (2012). Imbalance of heterologous protein folding and disulfide bond formation rates yields runaway oxidative stress. *BMC Biology*, *10*, 16. https://doi.org/10.1186/1741-7007-10-16
62. Vera, M., Pani, B., Griffiths, L. A., Muchardt, C., Abbott, C. M., Singer, R. H., & Nudler, E. (2014). The translation elongation factor eEF1A1 couples transcription to translation during heat shock response. *ELife*, *3*, e03164. https://doi.org/10.7554/eLife.03164

63. Weinhandl, K., Winkler, M., Glieder, A., & Camattari, A. (2014). Carbon source dependent promoters in yeasts. *Microbial Cell Factories*, *13*, 5. https://doi.org/10.1186/1475-2859-13-5
64. Wiśniewski, J. R., Zougman, A., Nagaraj, N., & Mann, M. (2009). Universal sample preparation method for proteome analysis. *Nature Methods*, *6*(5), 359–362. https://doi.org/10.1038/nmeth.1322
65. Wittmann-Liebold, B., Graack, H.-R., & Pohl, T. (2006). Two-dimensional gel electrophoresis as tool for proteomics studies in combination with protein identification by mass spectrometry. *PROTEOMICS*, *6*(17), 4688–4703. https://doi.org/10.1002/pmic.200500874
66. Zhang, W., Qu, P., Li, D., Zhang, C., Liu, Q., Zou, G., Dupont-Rouzeyrol, M., Lavillette, D., Jin, X., Yin, F., & Huang, Z. (2019). Yeast-produced subunit protein vaccine elicits broadly neutralizing antibodies that protect mice against Zika virus lethal infection. *Antiviral Research*, *170*, 104578. https://doi.org/10.1016/j.antiviral.2019.104578

TRUMPOS ŽINIOS APIE DISERTANTĘ

Šios disertacijos autorė, disertantė Rūta Zinkevičiūtė, 2012 metais baigė molekulinės biologijos bakalauro studijas Vilniaus universiteto Gamtos mokslų fakultete ir gavo K. Jankevičiaus stipendiją už geriausią biotechnologijų krypties bakalauro darbą. 2014 metais baigė molekulinės biologijos magistro studijas Vilniaus universiteto Gamtos mokslų fakultete, bei jai buvo įteiktas *Magna Cum Laude* diplomas su aukščiausiu pagyrimu. Nuo 2014 iki 2018 metų studijavo biochemijos krypties doktorantūrą Biotechnologijos institute (vėliau Vilniaus universiteto Biotechnologijos institute). Nuo 2009 metų dirba Biotechnologijos instituto Eukariotų genų inžinerijos skyriuje. Pradėjusi nuo laboratorinės praktikos, šiuo metu yra jaunesnioji mokslo darbuotoja. Lygiagrečiai, nuo 2013 metų dirba bioinžiniere biotechnologijų įmonėje UAB Baltymas. Yra šešių mokslinių straipsnių su tarptautiniu citavimo indeksu koautorė, pristačiusi savo darbus dviejose konferencijose. Sėkmingai vadovavusi dviejų studenčių baigiamiesiems darbams, dalyvavusi septyniuose moksliniuose projektuose bei aktyviai vykdanti mokslo populiarinimo veiklą.

ACKNOWLEDGEMENTS

I would like to thank my colleagues from the department of Eukaryote Gene Engineering, Institute of Biotechnology and my supervisor Rimantas Slibinskas PhD, for scientific support and critical remarks during the preparation of this thesis.

I am also very grateful for all the co-authors of publications for their enormous input in our shared published work.

I would especially like to thank my family and friends Neringa Macijauskaitė, Lina Aitmanaitė PhD and Evelina Zagorskaitė PhD for their constant support during long thesis writing process.

A special mention goes to Vykintas Jauniškis for inexhaustible motivation and drive to achieve more.

APPENDIX: LIST OF PUBLICATIONS (1, 2, 3)

The results of this thesis were presented in following publications and conferences.

Publications:

1. Slibinskas, R., Ražanskas, R., **Zinkevičiūtė, R**., & Čiplys, E. (2013). Comparison of first dimension IPG and NEPHGE techniques in two-dimensional gel electrophoresis experiment with cytosolic unfolded protein response in *Saccharomyces cerevisiae*. *Proteome Science, 11*, 36. https://doi.org/10.1186/1477-5956-11-36.
2. **Zinkevičiūtė, R**., Bakūnaitė, E., Čiplys, E., Ražanskas, R., Raškevičiūtė, J., & Slibinskas, R. (2015). Heat shock at higher cell densities improves measles hemagglutinin translocation and human GRP78/BiP secretion in *Saccharomyces cerevisiae*. *New Biotechnology*, *32*(6), 690–700. https://doi.org/10.1016/j.nbt.2015.04.001.
3. **Zinkevičiūtė, R**., Ražanskas, R., Kaupinis, A., Macijauskaitė, N., Čiplys, E., Houen, G., & Slibinskas, R. (2022). Yeast Secretes High Amounts of Human Calreticulin without Cellular Stress. *Current Issues in Molecular Biology*, *44*(5), 1768–1787. https://doi.org/10.3390/cimb44050122.

Conferences:

1. **R. Zinkevičiūtė**, R. Slibinskas, E. Čiplys, E. Bakūnaitė. Proteomic analysis of the impact of cell culture growth conditions to heterologous measles hemagglutinin protein expression in yeast *Saccharomyces cerevisiae*. 14th international conference of Lithuanian Biochemical Society, "Young biochemistry" symposium, Druskininkai, Lithuania, 2016. 06. 28-30.
2. **R. Zinkevičiūtė**. Restoration of the NEPHGE two-dimensional electrophoresis method. 43rd FEBS Congress, Prague, Czech Republic, 2018. 07. 07-12.

NOTES

Vilniaus universiteto leidykla
Saulėtekio al. 9, III rūmai, LT-10222 Vilnius
El. p. info@leidykla.vu.lt, www.leidykla.vu.lt
bookshop.vu.lt, journals.vu.lt
Tiražas 13 egz.